

## INFORMATION TO USERS

This manuscript has been reproduced from the microfilm master. UMI films the text directly from the original or copy submitted. Thus, some thesis and dissertation copies are in typewriter face, while others may be from any type of computer printer.

**The quality of this reproduction is dependent upon the quality of the copy submitted.** Broken or indistinct print, colored or poor quality illustrations and photographs, print bleedthrough, substandard margins, and improper alignment can adversely affect reproduction.

In the unlikely event that the author did not send UMI a complete manuscript and there are missing pages, these will be noted. Also, if unauthorized copyright material had to be removed, a note will indicate the deletion.

Oversize materials (e.g., maps, drawings, charts) are reproduced by sectioning the original, beginning at the upper left-hand corner and continuing from left to right in equal sections with small overlaps.

Photographs included in the original manuscript have been reproduced xerographically in this copy. Higher quality 6" x 9" black and white photographic prints are available for any photographs or illustrations appearing in this copy for an additional charge. Contact UMI directly to order.

ProQuest Information and Learning  
300 North Zeeb Road, Ann Arbor, MI 48106-1346 USA  
800-521-0600

UMI<sup>®</sup>



**University of Alberta**

Functional Analysis of the Copper-Transporting P-type ATPase, ATP7B, Defective in  
Wilson Disease.

By

John Richard Forbes



A thesis submitted to the Faculty of Graduate Studies and Research in partial fulfilment  
of the requirements for the degree of Doctor of Philosophy

in

Medical Science-Medical Genetics

Edmonton, Alberta

Spring 2000.



National Library  
of Canada

Acquisitions and  
Bibliographic Services

395 Wellington Street  
Ottawa ON K1A 0N4  
Canada

Bibliothèque nationale  
du Canada

Acquisitions et  
services bibliographiques

395, rue Wellington  
Ottawa ON K1A 0N4  
Canada

*Your file Votre référence*

*Our file Notre référence*

The author has granted a non-exclusive licence allowing the National Library of Canada to reproduce, loan, distribute or sell copies of this thesis in microform, paper or electronic formats.

The author retains ownership of the copyright in this thesis. Neither the thesis nor substantial extracts from it may be printed or otherwise reproduced without the author's permission.

L'auteur a accordé une licence non exclusive permettant à la Bibliothèque nationale du Canada de reproduire, prêter, distribuer ou vendre des copies de cette thèse sous la forme de microfiche/film, de reproduction sur papier ou sur format électronique.

L'auteur conserve la propriété du droit d'auteur qui protège cette thèse. Ni la thèse ni des extraits substantiels de celle-ci ne doivent être imprimés ou autrement reproduits sans son autorisation.

0-612-59959-0

**Canada**

**University of Alberta**

**Library Release Form**

**Name of Author:** John Richard Forbes

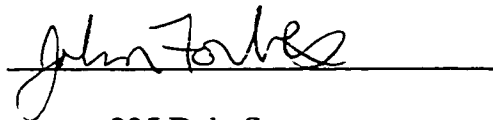
**Title of Thesis:** Functional analysis of the copper transporting P-type ATPase, ATP7B, defective in Wilson disease.

**Degree Type:** Doctor of Philosophy

**Year this Degree Granted:** 2000

Permission is hereby granted to the University of Alberta Library to reproduce single copies of this thesis and to lend or sell such copies for private, scholarly, or scientific research purposes only.

The author reserves all other publication and other rights in association with the copyright in this thesis, and except as hereinbefore provided, neither the thesis nor any substantial portion thereof may be printed or otherwise reproduced in any material form whatever without the author's prior written permission.

A handwritten signature in cursive script, reading "John Forbes", is written over a horizontal line.

235 Daly St.  
Palmerston, Ontario.  
Canada.  
N0G 2P0

Date submitted to FSGR:

Jan 31/2000

**University of Alberta**

**Faculty of Graduate Studies and Research**

The undersigned certify that they have read, and recommend to the Faculty of Graduate Studies and Research for acceptance, a thesis entitled "Functional Analysis of the Copper-Transporting P-type ATPase, ATP7B, Defective in Wilson Disease" submitted by John Richard Forbes in partial fulfilment of the requirements for the degree of Doctor of Philosophy in Medical Science-Medical Genetics.



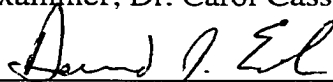
Supervisor, Dr. Diane W. Cox



Examiner, Dr. Joseph Casey



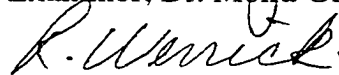
Examiner, Dr. Carol Cass



Examiner, Dr. David Eide



Examiner, Dr. Moira Glerum



Examiner, Dr. Rachel Wevrick

January 28, 2000

Date signed by supervisor.

## **DEDICATION**

To Megan:  
For her boundless love and support.  
I could not have made it without you.

## **ABSTRACT**

Wilson disease (WD) is a disorder of copper transport leading to hepatic copper accumulation. The protein defective is ATP7B, a copper transporting P-type ATPase expressed primarily in the liver. ATP7B is localised to the trans-Golgi network of hepatocytes, where it transports copper into cuproenzymes such as ceruloplasmin. Under conditions of elevated hepatic copper, ATP7B redistributes to vesicles and mediates biliary copper efflux.

Described in this thesis is the development of an assay for ATP7B function based on complementation of its yeast orthologue, Ccc2p. ATP7B is able to replace Ccc2p in yeast, allowing growth on iron-limited medium. This assay was used to analyse the functional effect of WD mutations in ATP7B. WD mutations can be distinguished from rare normal variants.

Several WD mutations did not significantly affect ATP7B function.

Immunofluorescence microscopy was employed to determine the effect of these WD mutations on ATP7B localisation and copper-dependent trafficking. Two mutant ATP7B proteins which, with normal function in our assay, were mislocalised to the endoplasmic reticulum, but retained partially normal localisation and trafficking. These proteins may therefore mediate limited copper efflux and incorporation of copper into ceruloplasmin. One functional mutant ATP7B protein was localised to the Golgi network but could not redistribute in response to copper. This protein may be capable of copper incorporation into ceruloplasmin, but poorly mediate copper efflux. From these data, a likely biological mechanism which can explain in part the biochemical variability observed in WD patients is proposed.

ATP7B has an N-terminal domain containing six copper-binding subdomains.

The functional consequences of mutations and deletions in the copper-binding domain of ATP7B have been determined by the yeast complementation assay. Only a single copper binding subdomain close to the transmembrane channel is necessary for copper transport. The N-terminal two or three subdomains are not sufficient for transport which suggests that the six subdomains are not functionally redundant. Based on these data, the copper-binding domain of ATP7B is proposed to be functionally divided such that the subdomains close to the channel are involved in copper transport. The remaining N-terminal most subdomains may be involved in triggering copper-dependent redistribution.

## **ACKNOWLEDGEMENTS**

I thank my supervisor, Dr. Diane Cox, for over five years of tireless supervision (Do you sleep?). Despite her tremendous workload as the chair of the new Department of Medical Genetics, and head of an internationally known lab, she always made time to ensure that the needs of her students were met. Diane has been (and is) an incredible teaching resource and inspiration. Besides her tremendous scientific knowledge, she gave me invaluable insight into the inner workings of the scientific community as a whole.

I thank members of Dr. B. Sarkar's laboratory, in particular Michael DiDonato for shared data and great discussions about things copper related. Michael and I had a fantastic collaborative relationship allowing us to create many useful resources for both of our laboratories.

I thank all members of the Cox laboratory that I have known before and during my Ph. D training for much entertainment as well as scientific insight. In particular, I would like to thank past members Adam Chen, Gordon Thomas, Richard Wintle, Barbara Byth, and Pete Bull who gave me the foundations of my bench science training, not to mention a nasty, cynical and outspoken attitude (Rich!). I would also like to thank Gloria Hsi for her technical help as a summer student. I would like to thank Manoj Nanji for great discussions and more than a few beers.

I would like to thank members of my supervisory committee at the U. of A., Joe Casey, Moira Glerum, and Rachel Wevrick, along with my committee at the U. of T., Roderick McInnes, Emil Pai, and Brian Robinson, for keeping me on track, in focus, and providing much useful advice and discussion.

I thank Morrie Manolson (U. of T.) for training in basic yeast handling methods (rock climbing as well). I would like to thank Danial Yuan (N.I.H) for providing knockout plasmids with which I made my yeast strains. And I would like to thank Gregory Lee (U.B.C.), and members of the H.S.L.A.S. animal facility at the U. of A. for dealing with the rabbits during antibody production. I would also like to thank Hubert Eng, Megan Blacker, and Darren Cikaluk for advice regarding immunofluorescence.

Support from the Medical Research Council of Canada, and the Faculty of Graduate Studies and Research is gratefully acknowledged, and much appreciated.

## **TABLE OF CONTENTS**

<b>CHAPTER 1: INTRODUCTION</b> .....	<b>1</b>
1A) AIMS OF THESIS AND HYPOTHESES.....	2
1B) HUMAN COPPER HOMEOSTASIS AND RELATED DISORDERS.....	2
1B-1) Overview of human copper homeostasis.....	3
1B-2) Menkes Disease.....	5
1B-3) Wilson Disease.....	6
1B-4) Aceruloplasminemia: a role for ceruloplasmin in iron uptake.....	9
1C) CPX-TYPE ATPASES: COPPER TRANSPORTING P-TYPE ATPASES.....	11
1C-1) P-type ATPases.....	12
1C-2) CPx-type ATPases.....	13
1C-3) Structure and metal binding properties of Cys-box copper-binding domains.....	16
1C-4) Copper transport by CPx-type ATPases.....	20
1D) CELLULAR COPPER HOMEOSTASIS AND THE ROLE OF CPX-TYPE ATPASES IN YEAST.....	22
1D-1) Copper uptake.....	22
1D-2) Copper detoxification.....	25
1D-3) Intracellular copper trafficking.....	26
1D-4) High affinity iron uptake: a role for CPx-type ATPases.....	27
1E) HEPATIC COPPER HOMEOSTASIS AND THE ROLE OF CPX-TYPE ATPASES IN MAMMALS.....	30
1E-1) Cellular copper uptake.....	30
1E-2) Hepatic copper pools.....	32
1E-3) Copper detoxification: metallothioneins.....	33
1E-4) Hepatic copper efflux and the role of ATP7B.....	34
1E-5) Copper induced intracellular trafficking of ATP7B.....	36
1F) OUTLINE OF THESIS.....	41
<b>CHAPTER 2: DEVELOPMENT OF REAGENTS AND METHODS</b> .....	<b>43</b>
2A) INTRODUCTION.....	44
2B) MATERIALS AND METHODS.....	45
2B-1) General molecular-biology techniques.....	45
2B-2) Construction of <i>ATP7B</i> cDNA.....	46
2B-3) cDNA constructs for ATP7B fusion proteins.....	47
2B-4) SDS-PAGE and immunoblotting.....	47
2B-5) Expression of fusion proteins in <i>E. coli</i> .....	48
2B-6) Production of rabbit polyclonal antibodies against ATP7B.....	49
2B-7) Affinity purification of ATP7B antibodies.....	50

2B-8) Yeast strains and transformation. ....	51
2B-9) Construction of Yeast expression Vectors. ....	52
2B-10) Yeast complementation assay.....	53
2B-11) Fet3p oxidase assay.....	53
2B-12) Yeast protein preparation. ....	54
<b>2C) RESULTS</b> .....	<b>54</b>
2C-1) Construction of <i>ATP7B</i> cDNA. ....	54
2C-2) Expression of <i>ATP7B</i> fusion proteins in <i>E. coli</i> . ....	56
2C-3) Production and affinity purification of <i>ATP7B</i> rabbit polyclonal antibodies. ....	56
2C-4) Expression of <i>ATP7B</i> in yeast. ....	61
2C-5) Yeast complementation assay for <i>ATP7B</i> . ....	61
<b>2D) DISCUSSION.</b> .....	<b>67</b>
<b>CHAPTER 3: FUNCTIONAL ANALYSIS OF WILSON DISEASE MUTATIONS.</b> .....	<b>70</b>
<b>3A) INTRODUCTION.</b> .....	<b>71</b>
<b>3B) MATERIALS AND METHODS.</b> .....	<b>72</b>
3B-1) Yeast strains. ....	72
3B-2) Site-directed mutagenesis.....	72
3B-3) Expression vectors. ....	74
3B-4) Complementation assay and Fet3p oxidase assay. ....	74
3B-5) Polyclonal antibodies against <i>ATP7B</i> . ....	75
3B-6) Yeast protein preparations and immunoblotting. ....	75
<b>3C) RESULTS.</b> .....	<b>75</b>
3d) <b>DISCUSSION.</b> .....	<b>81</b>
<b>CHAPTER 4: SUBCELLULAR LOCALIZATION OF <i>ATP7B</i> MUTANT PROTEINS.</b> .....	<b>85</b>
<b>4A) INTRODUCTION.</b> .....	<b>86</b>
<b>4B) MATERIALS AND METHODS.</b> .....	<b>87</b>
4B-1) Cell culture and antibodies.....	87
4B-2) Transient transfection.....	88
4B-3) Indirect immunofluorescence microscopy. ....	88
<b>4C) RESULTS.</b> .....	<b>89</b>
4C-1) Specificity of antibodies.....	89
4C-2) Copper-induced trafficking of <i>ATP7B</i> . ....	89
4C-3) Localisation of <i>ATP7B</i> WD mutant proteins. ....	94

4D) DISCUSSION. ....	100
<b>CHAPTER 5: ANALYSIS OF THE ATP7B COPPER-BINDING DOMAIN.....</b>	<b>105</b>
5A) INTRODUCTION.....	106
5B) MATERIALS AND METHODS. ....	107
5B-1) Yeast strains. ....	107
5B-2) Expression constructs.....	107
5B-3) Complementation assay and oxidase assay.....	108
5B-4) Polyclonal antibodies against ATP7B. ....	108
5B-5) Protein preparations and immunoblotting.....	108
5C) RESULTS. ....	109
5D) DISCUSSION. ....	116
<b>CHAPTER 6: CONCLUSIONS AND FUTURE DIRECTIONS. ....</b>	<b>121</b>
6A) ATP7B AND WILSON DISEASE. ....	123
6A-1) Effect of WD mutations on ATP7B: mutation or normal variant? .....	123
6A-2) Allelic variation in <i>ATP7B</i> relating to WD biochemical phenotype: insight into normal copper homeostasis. ....	125
6B) ROLE OF THE ATP7B COPPER-BINDING DOMAIN. ....	130
6B-1) Requirement for the copper-binding domain of ATP7B for copper transport. .....	130
6B-2) Requirement of the copper-binding domain of ATP7B for copper dependent trafficking. ....	133
6B-3) Proposed mechanisms of ATP7B copper-binding domain function. ....	135
6C) CONCLUSIONS. ....	138
<b>BIBLIOGRAPHY.....</b>	<b>139</b>
<b>APPENDIX. ....</b>	<b>157</b>

## **LIST OF TABLES**

<b>Table 3-1:</b> Growth rates of yeast strains expressing WD mutant <i>ATP7B</i> proteins.....	80
<b>Table 4-1:</b> Summary of localisation and functional data for <i>ATP7B</i> Wilson disease mutant proteins.....	97
<b>Table 5-1:</b> Growth rates of yeast expressing <i>ATP7B</i> copper-binding domain proteins. ....	112
<b>Table A-1:</b> Primers used for amplification of <i>ATP7B</i> cDNA. ....	157
<b>Table A-2:</b> Primers used for amplification of <i>ATP7B</i> fusion protein DNA constructs. ....	157
<b>Table A-3:</b> Mutagenic primers used to create WD mutant <i>ATP7B</i> cDNA constructs. ....	158
<b>Table A-4:</b> Mutagenic primers used to create <i>ATP7B</i> copper-binding domain cDNA constructs. ....	159
<b>Table A-5:</b> Primers used for construction of <i>ATP7B</i> deletion constructs. ....	159

## **LIST OF FIGURES**

<b>Figure 1-1: Overview of human copper homeostasis</b> .....	4
<b>Figure 1-2: Predicted model of ATP7B</b> .....	14
<b>Figure 1-3: Yeast copper and iron homeostasis</b> .....	23
<b>Figure 1-4: Mammalian hepatic copper efflux mediated by ATP7B</b> .....	39
<b>Figure 2-1: Schematic of ATP7B cDNA construction</b> .....	55
<b>Figure 2-2: Example of nickel-affinity purification of 6xHis-tagged Pept3 fusion protein expressed in <i>E. coli</i></b> .....	57
<b>Figure 2-3: Antiserum specificity</b> .....	59
<b>Figure 2-4: Example of column affinity purification procedure (anti-ATP7B.C10)</b> .....	60
<b>Figure 2-5: Example of screening for singlecopy expression construct integrations</b> .....	62
<b>Figure 2-6: Expression of ATP7B in yeast</b> .....	63
<b>Figure 2-7: Complementation of <i>ccc2</i> mutant yeast by ATP7B</b> .....	65
<b>Figure 3-1: Location of WD mutations within the predicted transmembrane domain of ATP7B</b> .....	73
<b>Figure 3-2: Complementation of <i>ccc2</i> mutant yeast by WD mutants</b> .....	76
<b>Figure 3-3: Complementation of <i>ccc2</i> mutant yeast by WD mutants</b> .....	77
<b>Figure 3-4: Growth rates of yeast strains in iron-limited medium</b> .....	79
<b>Figure 4-1: Specificity of antibodies</b> .....	90
<b>Figure 4-2: Copper-dependent subcellular localisation of ATP7B transiently expressed in HeLa cells</b> .....	92
<b>Figure 4-3: Copper-induced redistribution of ATP7B transiently expressed in CHO cells</b> .....	93
<b>Figure 4-4: Copper-induced redistribution of ATP7B Wilson disease mutant proteins transiently expressed in CHO cells</b> .....	95
<b>Figure 4-5: Copper-induced redistribution of ATP7B Wilson disease mutant proteins transiently expressed in CHO cells</b> .....	96
<b>Figure 4-6: Copper-induced redistribution of ATP7B Wilson disease mutant proteins transiently expressed in CHO cells</b> .....	98
<b>Figure 4-7: Localisation of ATP7B Wilson disease mutant proteins transiently expressed in HeLa cells</b> .....	99

<b>Figure 5-1: ATP7B expression constructs.</b> .....	110
<b>Figure 5-2: Complementation of <i>ccc2</i> mutant yeast by ATP7B copper-binding domain mutation series 1 constructs.</b> .....	111
<b>Figure 5-3: Complementation of <i>ccc2</i> mutant yeast by ATP7B copper-binding domain mutation series 2 constructs.</b> .....	113
<b>Figure 5-4: Complementation of <i>ccc2</i> mutant yeast by ATP7B copper-binding domain deletion series constructs.</b> .....	115
<b>Figure 6-1: Role of the copper-binding domain in copper transport by ATP7B</b> .....	136

## LIST OF SYMBOLS AND ABBREVIATIONS.

$A_{600}$	absorbance at 600 nm
AMCA-S	7-amino-3-((((succinimidyl)oxy)carbonyl)methyl)-4-methylcoumarin-6-sulfonic acid
ATP	adenosine 5'-triphosphate
BCA	bicinchoninic acid
BCS	bathocuproine disulfonate
bp	base-pair
BSA	bovine serum albumin
C-terminal	carboxy-terminal
cDNA	complementary deoxyribonucleic acid
CHO	Chinese hamster ovary
cMOAT	canalicular multi-organic anion transporter
ConA	concanavalin A
Cp	ceruloplasmin
dATP	deoxyadenosine 5'-triphosphate
dCTP	deoxycytidine 5'-triphosphate
dGTP	deoxyguanosine 5'-triphosphate
DNA	deoxyribonucleic acid
DTT	dithiothrietol
dTTP	deoxythymidine 5'-triphosphate
<i>E. coli</i>	<i>Escherichia coli</i>
<i>E. hirae</i>	<i>Enterococcus hirae</i>
$E_1$	enzyme intermediate 1
$E_1P$	enzyme intermediate 1 phosphorylated
$E_2$	enzyme intermediate 2
$E_2P$	enzyme intermediate 2 phosphorylated
ECL	enhanced chemiluminescence
EDTA	Ethylenediaminetetraacetic acid
FITC	fluorescein isothiocyanate
g	gram
GAPDH	glyceraldehyde-3-phosphate dehydrogenase
HA	haemagglutinin
HEPES	4-(2-Hydroxyethyl)-1-piperazineethanesulfonic acid
IgG	immunoglobulin G
IPTG	isopropylthio- $\beta$ -D-galactoside
kb	kilobase
kDa	kiloDalton
$K_m$	Michaelis constant
L	litre
LB	Luria broth
LEC	Long-Evans cinnamon
M	molar
MD	Menkes disease
MES	2-[N-morpholino]ethanesulfonic acid

mg	milligram
mL	milliLitre
<i>Mo</i>	mouse mottled locus
<i>Mo</i> <sup>Bl</sup>	blotchy allele of mottled locus
<i>Mo</i> <sup>Br</sup>	brindled allele of mottled locus
mRNA	messenger ribonucleic acid
MT	metallothionein
N-terminal	amino-terminal
NHS	N-hydroxysuccinimide
nm	nanometre
NMR	nuclear magnetic resonance
NTA	nitrilotriacetic acid
OHS	occipital horn syndrome
oligo-d(T)	oligomeric deoxythymidine
PBS	phosphate buffered saline
PBST	PBS with Tween-20 detergent
PCR	polymerase chain reaction
PGK	phosphoglycerate kinase
PVDF	polyvinylidene difluoride
RT-PCR	reverse transcriptase-PCR
<i>S. cerevisiae</i>	<i>Saccharomyces cerevisiae</i>
SDS	sodium dodecyl sulfate
SDS-PAGE	SDS poly-acrylamide gel electrophoresis
SOD1	superoxide dismutase 1
TBE	Tris-Borate-EDTA
TBS	Tris buffered saline
TBST	TBS with Tween-20 detergent
Tris	tris(hydroxymethyl)aminomethane
µg	microgram
µL	microLitre
µM	micromolar
V·Hr	volt-hour
WD	Wilson disease
WGA	wheat-germ agglutinin
xg	times gravity
YNB	yeast nitrogen base

**CHAPTER 1**

**INTRODUCTION**

## 1A) AIMS OF THESIS AND HYPOTHESES.

The general aim of this thesis was to use structure/function analysis of ATP7B to aid in elucidating its biochemical and physiologic function. Specific goals were as follows:

1) To study the effect of selected, genetically identified Wilson disease mutations on ATP7B function and intracellular localisation, in order to gain insight into the normal function of ATP7B, the molecular pathogenesis of Wilson disease, and as an aid to discriminate true Wilson disease missense mutations from rare normal variants.

Hypothesis: Changes in the function and intracellular localisation of ATP7B, due to allelic variation, can explain in part the variable biochemical features observed in Wilson disease patients.

2) To study the role of the ATP7B copper-binding domain with respect to the putative copper transport function of ATP7B. Hypothesis: The copper-binding domain of ATP7B is essential for its function as a copper transporter.

## 1B) HUMAN COPPER HOMEOSTASIS AND RELATED DISORDERS.

Copper is an essential element required for life, due to its use as a cofactor in many proteins (Danks, 1995; Uauy *et al.* 1998). For example, cytochrome-*c*-oxidase is a mitochondrial inner membrane protein complex, containing three copper atoms between two subunits. This protein is a key enzyme which catalyses the reduction of oxygen to water, and utilises the free energy of the reaction to contribute to the proton gradient required for respiration. Superoxide dismutase (SOD1) requires copper as a catalytic cofactor in order to convert superoxide anion to hydrogen peroxide as the first step in protection against cellular free radical damage. Other proteins requiring copper as a cofactor include lysyl-oxidase (collagen and elastin cross-linking), dopamine- $\beta$ -monooxygenase (converts dopamine to norepinephrine), and ceruloplasmin (ferroxidase).

Copper is a potent cellular toxin capable of catalysing reduction/oxidation reactions (Bremner, 1998). Copper can generate hydroxyl radicals and hydrogen peroxide via the Haber-Weiss reaction *in vitro* and has been shown to generate hydroxyl radicals in rat livers *in vivo*. The consequences of hydroxyl radical production *in vivo* include lipid peroxidation, DNA strand breakage and base oxidation, mitochondrial damage leading to reduced efficiency of respiration, and protein damage.

Maintenance of proper copper homeostasis is a biological process essential for living organisms. Disruption of this balance in mammals leads to disease. A general overview of mammalian copper homeostasis and disorders related to perturbations in this process will be discussed in the following section.

### **1B-1) Overview of human copper homeostasis.**

The average adult human body contains approximately 70 to 100 mg of copper (Danks, 1995; Linder *et al.* 1998; Wapnir, 1998). Copper levels depend on a balance between dietary copper absorption and copper excretion. Dietary copper intake is approximately 1-2 mg daily, and approximately half of this is absorbed (Linder *et al.* 1998). A large amount of copper is secreted from the digestive tract, but the majority (about 4.5 mg) is reabsorbed. Bile is the main route of copper elimination since copper excreted in the bile is not readily reabsorbed. Net copper elimination via the bile is normally equal to net copper absorption. The two generally increase or decrease simultaneously depending on available copper, thereby maintaining normal copper levels in the body. There is normally negligible urinary copper excretion.

Copper is absorbed in the small intestine of rodents and presumably humans as well (Fig. 1-1) (Wapnir, 1998). Analysis of the distribution of newly absorbed radiotracer copper in rats and humans has been performed by several groups (Danks, 1995; Linder *et al.* 1998). Newly absorbed copper rapidly enters the bloodstream bound to albumin, transcuprein, and small peptides (Linder *et al.* 1998). Within 2 to 6 hr. nearly all newly absorbed copper has accumulated in the liver, probably delivered by albumin or transcuprein. The liver is the homeostatic control point governing levels of copper in the body. Most newly absorbed copper entering the liver reappears in the bile for excretion, except for the trace amount delivered to plasma. Starting 4 hours following absorption and lasting for several days, copper appears in the plasma bound to ceruloplasmin. Ceruloplasmin carries over 80% of copper in the plasma and changes in plasma copper levels are usually associated with changes in ceruloplasmin concentration. Serum copper concentrations are normally 11-24  $\mu\text{M}$  in adults and ceruloplasmin concentrations are usually 200-400 mg/L (Danks, 1995). The remaining plasma copper remains bound predominantly to albumin, with some bound to transcuprein, peptides, or amino acids (low picomolar range) (Linder *et al.* 1998).

Copper is found in other organs, including the kidney and brain, within two hours of intestinal absorption, and increases over time during the phase in which liver copper is decreasing and reappearing in plasma ceruloplasmin (Danks, 1995; Linder *et al.* 1998). Ceruloplasmin has been suggested to be the major donor of copper to other tissues (Linder *et al.* 1998; Frieden *et al.* 1976). Consistent with this hypothesis, ceruloplasmin is able to donate copper to cells in culture (Percival *et al.* 1990). Additionally, radioactive tracer copper contained in ceruloplasmin that was infused intravenously into rats at a physiologic concentration, resulted in tracer copper accumulation in all tissues examined (Linder *et al.* 1998; Frieden *et al.* 1976).

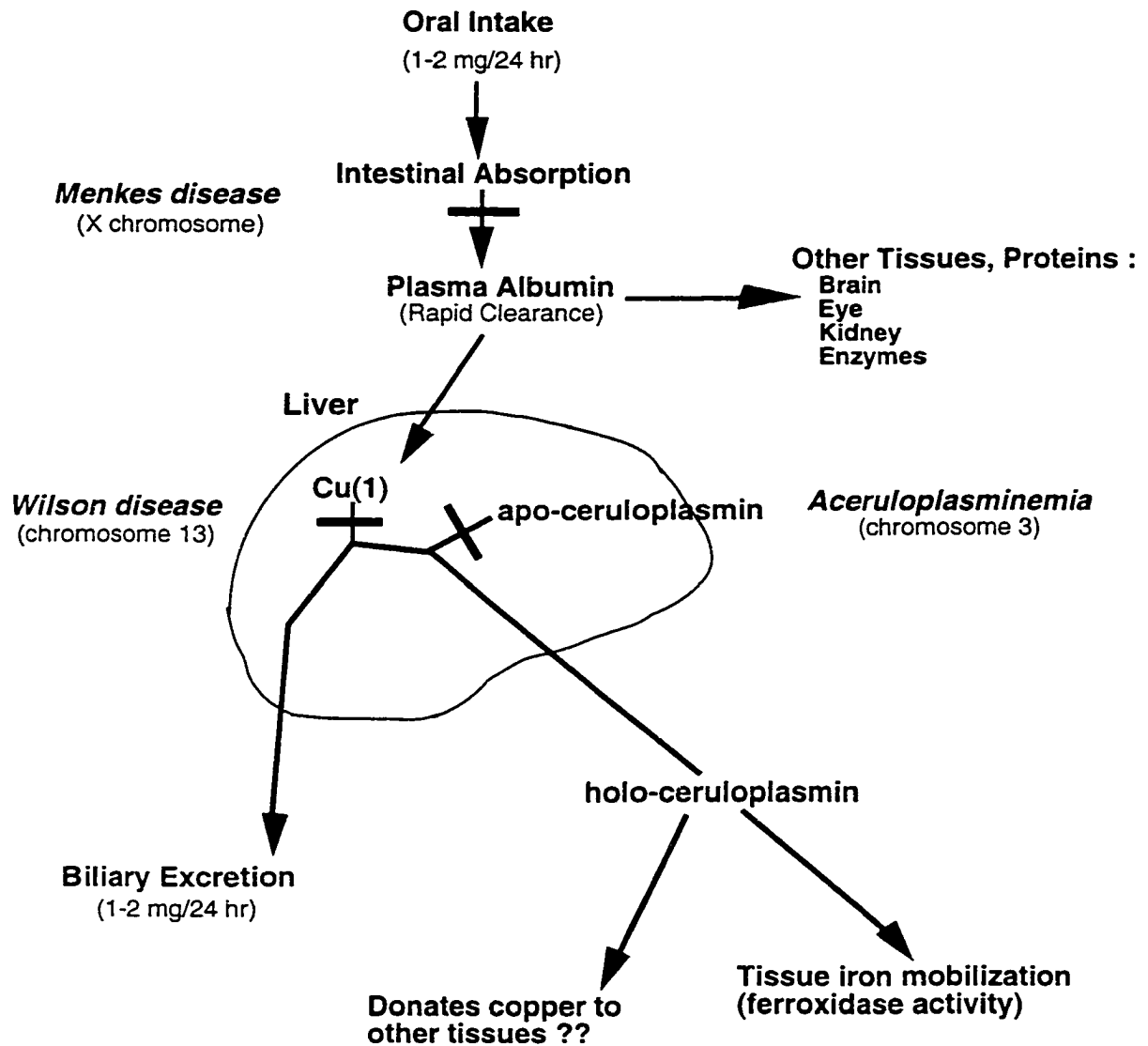


**Figure 1-1: Overview of human copper homeostasis.**

There are three major diseases that arise from perturbations of the primary copper homeostasis pathways just described. Menkes disease is a defect in intestinal copper absorption leading to copper deficiency. Wilson disease is a defect in biliary copper excretion and copper incorporation into ceruloplasmin leading to hepatic copper overload. Aceruloplasminemia is a defect in ceruloplasmin biosynthesis leading to iron accumulation in several tissues. These will be described in turn, focusing on Wilson disease. Discovery of the genes for these diseases has greatly advanced the understanding of human (mammalian) copper homeostasis.

### **1B-2) Menkes Disease.**

Menkes disease (MD) is an inherited X-linked recessive copper deficiency leading to severe disease and death usually in early childhood (Danks, 1995; Mercer, 1998; Tumer *et al.* 1999). Patients with classical MD are developmentally delayed and exhibit neurodegeneration. Developmental delay is thought to be due to reduced activity of copper dependent enzymes such as dopamine- $\beta$ -monooxygenase required for brain development, and to reduction of cytochrome-c-oxidase activity. Patients exhibit hypopigmentation due to loss of copper dependent tyrosinase enzyme activity, and suffer from hypothermia due to reduced cytochrome-c-oxidase activity. One of the defining features of MD is distinctive brittle hair with a corkscrew like appearance called pili torti. Other symptoms of MD include bone, skin, connective tissue, and arterial abnormalities due to defective collagen cross-linking mediated by the copper dependent enzyme lysyl-oxidase. Patients with MD usually die by the age of three or four. Treatment of patients using copper-histidine can increase hepatic copper levels, restore circulating plasma copper levels, and give some improvement in physical health, thereby greatly extending the lifespan of Menkes patients if treatment begins soon after birth. However, copper histidine does not seem to effect neurodegeneration or brain copper levels.

A major allelic variant of MD is known as occipital horn syndrome (OHS) (Danks, 1995; Mercer, 1998; Tumer *et al.* 1999). This is a mild form of MD characterised by connective tissue abnormalities such as hyperelastic skin, skeletal abnormalities, hernias, bladder diverticula, and aortic aneurysms, all due to reduced lysyl oxidase activity as a result of somatic copper deficiency. OHS patients may have mild developmental delay, but far less severe than in classical MD.

Biochemical features of MD are characteristic of body wide copper deficiency (Danks, 1995; Mercer, 1998; Tumer *et al.* 1999). These include reduction of liver copper, and consequently reduced serum copper, due to reduced copper incorporation into ceruloplasmin. However copper levels in the duodenal mucosa, where copper is thought

to be absorbed, is 2-3 fold higher than the maximum seen in normal individuals. Copper absorption in the intestine is normal, suggesting that there is a defect in copper transport out of the intestinal epithelium and into the circulation leading to somatic deficiency. Consistent with this hypothesis, orally administered radioactive copper is poorly absorbed in MD patients but radioactive copper given to the patients intravenously is handled normally by the liver. An additional diagnostic feature of MD is that patient fibroblasts in culture accumulate high levels of copper due to defective copper efflux compared with that of normal controls.

The gene for MD was identified in 1993 by positional cloning (Vulpe *et al.* 1993; Mercer *et al.* 1993; Chelly *et al.* 1993). Sequencing of the cDNA revealed a predicted protein characteristic of a copper transporting P-type ATPase (gene: *ATP7A*; protein: ATP7A), consistent with the defect of intestinal copper transport seen in MD. ATP7A is expressed in all tissues except for the liver. The protein is thought to mediate intestinal copper uptake into the circulation as well as copper efflux from cells in peripheral tissues as a mechanism of copper homeostasis. ATP7A may also be involved in copper incorporation into cuproenzymes in peripheral tissues. There have been many *ATP7A* mutations identified in MD patients (Tumer *et al.* 1999). Approximately 90% of known mutations are predicted to prevent ATP7A protein production thereby causing the severe disease seen in most patients. These mutations include chromosomal aberrations, gross gene deletions, frameshift insertion/deletions, nonsense mutations, and splice site mutations. The few missense mutations or small in frame deletions observed are typically found in patients with OHS.

There is a mouse model for MD known as the Mottled mouse that shares the symptoms of MD found in humans (Mercer, 1998; Tumer *et al.* 1999). There are approximately 30 mutations in *Atp7a* that lead to the mottled (*Mo*) phenotype, nine of which have been characterised. Different alleles of the mottled locus lead to mice with different phenotypic severity. For example the Brindled mouse (*Mo*<sup>Br</sup>) has a 6 bp gene deletion and a phenotype consistent with classical MD. The Blotchy mouse (*Mo*<sup>Bl</sup>) has a splice site mutation that interferes with normal splicing leading to reduced mRNA levels and has a phenotype consistent with OHS.

### **1B-3) Wilson Disease.**

Wilson disease (WD) is an autosomal recessive disorder of hepatic copper transport mapped to chromosome 13q14.3. WD affects approximately 1 in 30,000 individuals (Danks, 1995; Cox *et al.* 1998). WD clinical presentation is highly variable making diagnosis difficult (Cox *et al.* 1998). Age of onset varies from less than 5 years to

greater than 50 years. Patients may have chronic or fulminant liver disease, neurologic disorder with or without liver involvement, purely psychiatric illness, or isolated acute hemolysis. The major presentation of WD is hepatic. Patients with hepatic WD exhibit jaundice, non-specific malaise perhaps accompanied by nausea, anorexia, and chronic hepatitis. Patients may have fulminant hepatic failure with encephelopathy and couagulopathy. Acute intravascular hemolysis usually accompanies hepatic failure. Renal damage may also occur and urinary copper excretion is greatly elevated. Patients with predominantly hepatic disease may also have mild neurologic symptoms. Hepatic presentation of WD usually begins in childhood as early as three years of age but may not manifest itself until 50 years of age.

The neurologic form of WD is typically found in patients in their second or third decades of life but can occur in children as early as 6 years old (Danks, 1995; Cox *et al.* 1998). Intellect is usually not impaired. Patients with neurologic WD may have movement disorders or rigid dystonia. Movement disorders tend to occur earlier in life than dystonia. Patients with movement disorders can exhibit poor co-ordination, tremors, and loss of motor control. Patients with spastic dystonia exhibit rigidity and gait disturbance, drooling, swallowing difficulty, a mask like facies, and dysarthria. Patients with neurologic WD have hepatic involvement, including copper accumulation and reduced plasma ceruloplasmin levels, but often do not show clinical evidence of liver damage. It is unknown why liver disease does not occur in some patients.

Psychiatric disorders may occur in as many as 20% of WD patients (Danks, 1995; Cox *et al.* 1998). Symptoms commonly include depression. Other psychiatric symptoms include aggressive, antisocial behaviour, or neurotic behaviour including phobias or compulsion.

A distinctive feature of patients with WD is the presence of ocular Kayser-Fleischer rings due to copper deposition in Descemet's membrane of the cornea (Danks, 1995; Cox *et al.* 1998). This is sometimes easily visible but frequently requires careful slit lamp examination. Kayser-Fleischer rings may be absent in patients with hepatic disease.

The main biochemical feature of WD is hepatic copper accumulation due to impaired biliary copper efflux (Danks, 1995; Cox *et al.* 1998). Normal adults typically have 20-50  $\mu\text{g}$  copper per gram dry liver whereas WD patients have greater than 250  $\mu\text{g/g}$ . Copper also accumulates in the kidney, brain, and cornea. Serum holo-ceruloplasmin levels, and consequently serum copper levels, are greatly reduced. Apo-ceruloplasmin biosynthesis is normal in WD patients, but copper incorporation into the protein during biosynthesis is impaired. Some patients with WD have borderline or

normal ceruloplasmin levels and therefore may not be easily distinguished from carriers or normal individuals by ceruloplasmin measurements alone.

WD is effectively treated with chelating agents (Danks, 1995; Cox *et al.* 1998). Penicillamine treatment removes copper from the body by greatly increasing urinary copper excretion. Penicillamine does not appear to remove hepatic copper, however it does induce hepatic metallothionein production, which may have a protective effect against hepatic damage (McQuaid *et al.* 1992; McArdle *et al.* 1989; Danks, 1995; Cox *et al.* 1998). Penicillamine treatment can have severe side effects including nephrotic syndrome, anaemia, and pyridoxine deficiency, to name a few, and can initially worsen neurologic symptoms in some cases perhaps by inducing copper deficiency in the brain (Danks, 1995; Cox *et al.* 1998). Another commonly used chelating agent is trientine, which also increases urinary copper excretion. Trientine is less potent than penicillamine, but is less toxic, and therefore trientine is often used as a long-term replacement for penicillamine. Thiomolybdate is also a chelation therapy for WD. This is a very potent chelator, the only one capable of removing copper from the liver for urinary excretion. It also prevents absorption of intestinal copper. Thiomolybdate may be too potent to be used for long-term treatment but may be used for initial copper reduction in patients.

Orally administered zinc has been useful as a treatment for WD (Danks, 1995; Cox *et al.* 1998). Zinc induces metallothioneins in the intestine, presumably sequestering copper and thereby reducing copper absorption. Zinc treatment has some adverse side effects, but has been used effectively, particularly following a period of chelation.

The gene for WD (gene: *ATP7B*; protein: ATP7B) has been cloned by positional cloning in our laboratory and by another group (Tanzi *et al.* 1993; Bull *et al.* 1993). *ATP7B* encodes a predicted protein characteristic of copper transporting P-type ATPases, which has 57% amino acid identity to *ATP7A*. Amino acid conservation between *ATP7B* and *ATP7A* is much greater within putative functional domains (see section 1C-1 and 1C-2) (Bull *et al.* 1993). *ATP7B* is expressed primarily in liver and kidney, and to a lesser extent in the brain, consistent with the WD phenotype. *ATP7A* and *ATP7B* have distinct tissue expression profiles leading to the distinct phenotypes of Menkes and WD. Over 150 mutations have been found in the *ATP7B* gene of WD patients (for reference see the Human Genome Organisation Wilson disease database <http://www.medgen.med.ualberta.ca/database.html>). The spectrum of known mutations is completely different than that of *ATP7A* (Danks, 1995; Cox *et al.* 1998). The majority of known mutations in *ATP7B* (51%) are single-base pair missense mutations, which are rare in *ATP7A* (2%) (Cox *et al.* 1999). The remaining *ATP7B* mutations include nonsense, splice site, and

small insertion/deletions mutations sometimes resulting in frameshifts. No gross gene deletions of *ATP7B* have been observed (common in *ATP7A*). Differences in the observed mutation spectrum of *ATP7A* and *ATP7B* may be artifactual since WD mRNA or genomic structure are not routinely screened for abnormalities in patients. Most mutations are very rare in the population and consequently most patients are compound heterozygotes. One mutation, His1069Glu, is found in up to 30% of patients of European descent and in homozygous form is associated with relatively high (9-10 years) but variable age of onset (Thomas *et al.* 1994). The Arg778Leu mutation is commonly found in Asian populations and is associated with severe early onset hepatic disease in homozygotes (Nanji *et al.* 1997). Generally, WD patients compound heterozygous for mutations such as frameshifts, and nonsense mutations predicted to destroy the protein have an early age of disease onset (average 7.2 years) (Cox *et al.* 1999). Patients compound heterozygous for missense mutations predicted to be less severe, typically have an older age of onset (average 16.8 years) (Cox *et al.* 1999). The extreme phenotypic variation among Wilson disease patients may be explained in part by allelic heterogeneity of the *ATP7B* gene.

There are two rodent models of WD, the LEC rat and the toxic milk mouse (Wu *et al.* 1994; Theophilos *et al.* 1996). Both rodents exhibit hepatic copper accumulation due to reduced biliary copper excretion and reduced copper incorporation into ceruloplasmin. The LEC rat has a large deletion removing 25% of the *Atp7b* coding region (Wu *et al.* 1994), and the toxic milk mouse has a single amino acid substitution in the predicted eighth transmembrane segment of *Atp7b* (Theophilos *et al.* 1996). The toxic mutation appears to render *Atp7b* non-functional as its phenotype is identical to a recently described *Atp7b* knockout mouse (Buiakova *et al.* 1999).

#### **1B-4) Aceruloplasminemia: a role for ceruloplasmin in iron uptake.**

The ceruloplasmin gene maps to chromosome 3q24 (Danks, 1995). An autosomal recessive disorder of ceruloplasmin biosynthesis in which there is no circulating ceruloplasmin is known as aceruloplasminemia (Harris *et al.* 1998; Yoshida, 1999; Harris *et al.* 1995). Patients with this disease have slowly developing neurologic disorders caused by progressive neurodegeneration of the retina and basal ganglia with an age of onset from 38-65 years. Initial symptoms in patients include movement disorders such as ataxic gait, speech slurring, and bletherospasm. Patients may initially exhibit mental disturbance, or intellectual impairments. Full blown disease develops slowly and includes dementia similar to Huntington disease, and Parkinsonian symptoms including dystonia, choreic movements, facial grimacing, and oral dyskinesia. All patients develop

non-insulin dependent diabetes mellitus sometimes without neurologic symptoms. Retinal pigment degeneration may also occur.

The main biochemical features of aceruloplasminemia are massive iron accumulation in the liver, pancreas, and brain, particularly the basal ganglia and retina (Harris *et al.* 1998; Yoshida, 1999; Harris *et al.* 1995). There is no circulating ceruloplasmin and consequently serum copper levels are reduced. Although hepatic iron accumulation is observed, which can be equal to that seen in hemochromatosis, there is no clinical evidence of liver disease. Aceruloplasminemia can be treated by the chelating agent desferroxamine, which promotes iron excretion and can ameliorate some of the disease symptoms.

Known mutations (total of six) in the ceruloplasmin gene are all frameshift insertion/deletions or nonsense mutations predicted to result in premature truncation of the protein (Harris *et al.* 1998; Yoshida, 1999). Most patients are compound heterozygotes. These data are consistent with the absence of plasma ceruloplasmin seen in patients.

The discovery of inherited aceruloplasminemia has helped elucidate the biological role of ceruloplasmin protein (Harris *et al.* 1995). Interestingly, since there is no apparent defect in copper homeostasis in aceruloplasminemia patients (Harris *et al.* 1995) it seems unlikely that ceruloplasmin plays a role in human copper transport as has been proposed (Linder *et al.* 1998; Frieden *et al.* 1976). Instead ceruloplasmin appears to play a key role in iron homeostasis (Harris *et al.* 1995; Frieden *et al.* 1976). Ceruloplasmin is a heavily glycosylated, serum, multicopper (six atoms) containing oxidase protein capable of oxidising several substrates such as primary amines and has ferroxidase activity capable of oxidising Fe(II) to Fe(III) (Frieden *et al.* 1976; Harris *et al.* 1998). Early studies in animals suggested a role for ceruloplasmin in the mobilisation of iron from cellular stores, into the plasma for transport to other tissues, under conditions of iron depletion (Frieden *et al.* 1976). Recent molecular studies have confirmed these data. A ceruloplasmin gene disruption has been made in mice (Harris *et al.* 1999). Harris *et al.* (1999) have shown that in the absence of circulating ceruloplasmin (Cp), Cp<sup>-/-</sup> mice exhibit severe tissue iron storage, especially in the liver and spleen, as seen in patients with aceruloplasminemia. Since initial iron uptake, tissue distribution, and plasma iron turnover appeared normal in Cp<sup>-/-</sup> mice, it was postulated that slow, but progressive, parenchymal iron accumulation was due to defective cellular efflux. Consistent with this hypothesis, hepatic iron efflux was found to be impaired while uptake appeared normal. Further experimentation revealed that iron given to Cp<sup>-/-</sup> mice in the form of heat damaged red blood cells, was not recycled out of the reticuloendothelial system and into

new red blood cells as normal, leading to progressive iron accumulation in this compartment (uptake was normal). Continued phlebotomy of the mutant mice led to anaemia, as stored iron was not released from the reticuloendothelial system for the formation of new red blood cells. Similarly, there was no release of stored iron from the livers of  $Cp^{-/-}$  mice in response to phlebotomy, as seen in control mice. Infusion of holo-ceruloplasmin into  $Cp^{-/-}$  mice corrected these defects, releasing iron from the both the liver and reticuloendothelial system. Together these data suggest a role for ceruloplasmin in iron efflux from cells with mobilisable stores, particularly the liver and reticuloendothelial system.

There is little iron storage observed in patients with WD probably since holo-ceruloplasmin levels are rarely completely abolished. (Harris *et al.* 1998; Cox *et al.* 1999; Cox *et al.* 1998). Holo-ceruloplasmin levels 1-5 % of normal, appear to be sufficient for normal iron metabolism (Frieden *et al.* 1976; Harris *et al.* 1998). Holo-ceruloplasmin production in Wilson disease patients may be due to extrahepatic ceruloplasmin biosynthesis, or diffusional copper loading of apo-ceruloplasmin in heavily copper loaded livers, or to allelic variation in the ATP7B gene (Chapter 3,4,6)(Harris *et al.* 1998; Yoshida, 1999). Alternatively, iron storage may be overlooked if not specifically assayed in WD patients. Over-treatment of WD patients with copper chelators may reduce or eliminate circulating holo-ceruloplasmin, leading to iron storage.

### **1C) CPX-TYPE ATPASES: COPPER TRANSPORTING P-TYPE ATPASES.**

Cloning and sequencing of the genes encoding the proteins defective for MD and WD (ATP7A and ATP7B respectively) revealed predicted structures very similar to each other (57% identity), and to a class of integral membrane proteins known as P-type ATPases (Vulpe *et al.* 1993; Mercer *et al.* 1993; Chelly *et al.* 1993; Tanzi *et al.* 1993; Bull *et al.* 1993). P-type ATPases (or  $E_1E_2$ -ATPases) are so named because of their ability to bind and hydrolyse ATP forming a phosphoenzyme intermediate. P-type ATPases are inhibited by vanadate, and undergo conformational changes during ATP hydrolysis (MacLennan *et al.* 1997). Much experimentation has been done on the structure and function of mammalian P-type ATPase proteins. In particular, the  $Ca^{2+}$  transporter of the sarco(endo)plasmic reticulum continues to be extensively studied, and is used as a general model for the function and structure of P-type ATPases. Indeed, studies performed on this protein and others revealed extensive conservation of basic structure and mechanism among P-type ATPase proteins such as the  $Ca^+/H^+$ -,  $Na^+/K^+$ -, or  $H^+/K^+$ -transporters (MacLennan *et al.* 1997). The  $Ca^{2+}$ -ATPase has been used as a model to describe the putative structure and function copper-transporting P-type ATPases.

Copper-transporting P-type ATPases, including ATP7A and ATP7B, have been proposed to be part of a subgroup, designated CPx-type ATPases, due to conserved sequence features found among heavy-metal transporters from many prokaryotic and eukaryotic species which suggests common function (Soligo *et al.* 1996).

### 1C-1) P-type ATPases.

The mechanistic aspects of transport by P-type ATPases have been studied in detail and are briefly described as follows using the reaction cycle of the  $\text{Ca}^{2+}$ -ATPase as an example (MacLennan *et al.* 1997). The resting intermediate of the protein is designated  $E_1$ . Two calcium ions bind to the  $E_1$  protein, followed by binding of ATP. ATP is hydrolysed, resulting in phosphorylation of a nearby aspartate residue forming the  $E_1\text{P}(\text{Ca}_2)$  intermediate. The hydrolysis of ATP and phosphorylation of  $E_1$  depends on both calcium binding sites being occupied. At this point in the reaction cycle, the calcium ions become occluded within the protein, no-longer accessible to solvent from either side of the membrane. A rate-limiting conformational change occurs forming the  $E_2\text{P}$  intermediate. This affinity of this intermediate for calcium is reduced by three orders of magnitude, allowing calcium to dissociate from the enzyme such that calcium transport through the membrane is achieved. Dissociation of the calcium ions triggers spontaneous hydrolysis of  $E_2\text{P}$ , liberating inorganic phosphate, and resulting in conformational changes that return the protein to its  $E_1$  state to begin the transport cycle anew. In proteins such as the  $\text{Na}^+/\text{K}^+$ -ATPase, that co-transport different ions in opposite directions, hydrolysis of the  $E_2\text{P}$  intermediate is triggered by binding of the co-transport ion, causing a conformational change back to  $E_1$  that results in translocation of the ion across the membrane (Skou *et al.* 1992).

The  $E_2\text{P}$  intermediate of P-type ATPases can be biochemically distinguished from the  $E_1\text{P}$  intermediate (MacLennan *et al.* 1997). The phosphate bond of  $E_1\text{P}$  can react with ADP, whereas  $E_2\text{P}$  can only react with water. This fact has enabled the dissection of the P-type ATPase reaction mechanism, and has allowed detailed biochemical analysis of the effect of site-directed mutations on protein function. The transport mechanism just described can be used generally to describe P-type ATPases and is the likely mechanism by which CPx-type ATPases function.

Structural models of the  $\text{Ca}^{2+}$ -ATPase based on electron microscopy of protein crystals describe a large cytoplasmic head structure linked to a membrane domain (10 helices) by a narrow stalk (Green *et al.* 1993; Stokes *et al.* 1994). The functional domains of the  $\text{Ca}^{2+}$ -ATPases within this structure, have been extensively mapped by biochemical and molecular means. The following features are found in all P-type ATPases, including

ATP7B and other CPx-type ATPases (Fig. 1-2) (MacLennan *et al.* 1992; MacLennan *et al.* 1997; Solioz, 1998; Solioz *et al.* 1996; Bull *et al.* 1994; Petrukhin *et al.* 1994). The transduction domain, predicted to consist mostly of  $\beta$ -strand structures, is defined by a Thr-Gly-Glu-Ala (TGEA) sequence motif. Site-directed mutagenesis of certain residues within this domain of the  $\text{Ca}^{2+}$ -ATPase resulted in non-functional proteins trapped cycling between the  $E_1$  and  $E_1P$  intermediates. These mutant proteins were unable to go forward to the  $E_2P$  intermediate, suggesting that the transduction domain is involved in transducing the energy of ATP hydrolysis to conformational changes in the protein. A conserved Asp-Lys-Thr-Gly-Thr (DKTGT) motif is found in the cytoplasmic head structure. The aspartate (D) residue in this motif is phosphorylated forming the aspartyl-phosphate intermediate during the transport cycle of the  $\text{Ca}^{2+}$ -ATPase. An ATP-binding domain predicted to be a mixture of regularly alternating  $\beta$ -strands and  $\alpha$ -helices consistent with a nucleotide binding fold resides on the underside of the cytoplasmic head structure of the  $\text{Ca}^{2+}$ -ATPase and has a conserved Thr-Gly-Asp-Asn (TGDN) motif. Mutations in this region of the  $\text{Ca}^{2+}$ -ATPase result in a loss of ATP binding, ATP hydrolysis, or affect phosphorylation, possibly due to effects on ATP binding. The final conserved functional domain is the ATP-hinge region located between the ATP binding domain and the transmembrane domain. Mutations in this region of the  $\text{Ca}^{2+}$ -ATPase result in proteins with absent or slow transitions between phosphorylated intermediates, suggesting that it is involved in conformational changes.

### 1C-2) CPx-type ATPases.

Although absolute sequence homology among the P-type ATPase family is not high, there is striking similarity in the hydrophobicity profiles among them, suggesting the formation of a common core membrane domain topology with six membrane-spanning segments (Solioz, 1998; Petrukhin *et al.* 1994). The core consists of two predicted N-terminal membrane-spanning segments followed by the soluble transduction domain then two more predicted membrane-spanning segments. Next is the large, soluble domain which contains the ATP binding fold followed by two more predicted transmembrane segments. Outside of the core domain, CPx-type ATPases diverge from the topology of non-heavy metal transporting P-type ATPases. The overall hydrophobicity profile of CPx-type ATPases is consistent with a total of eight putative membrane-spanning segments. CPx-type ATPases have a large N-terminal domain, predicted to be soluble, that is joined to the core ATPase portion of the molecule by two additional predicted transmembrane segments making a total of four between the N-terminal domain and transduction domain of these proteins. There is no equivalent

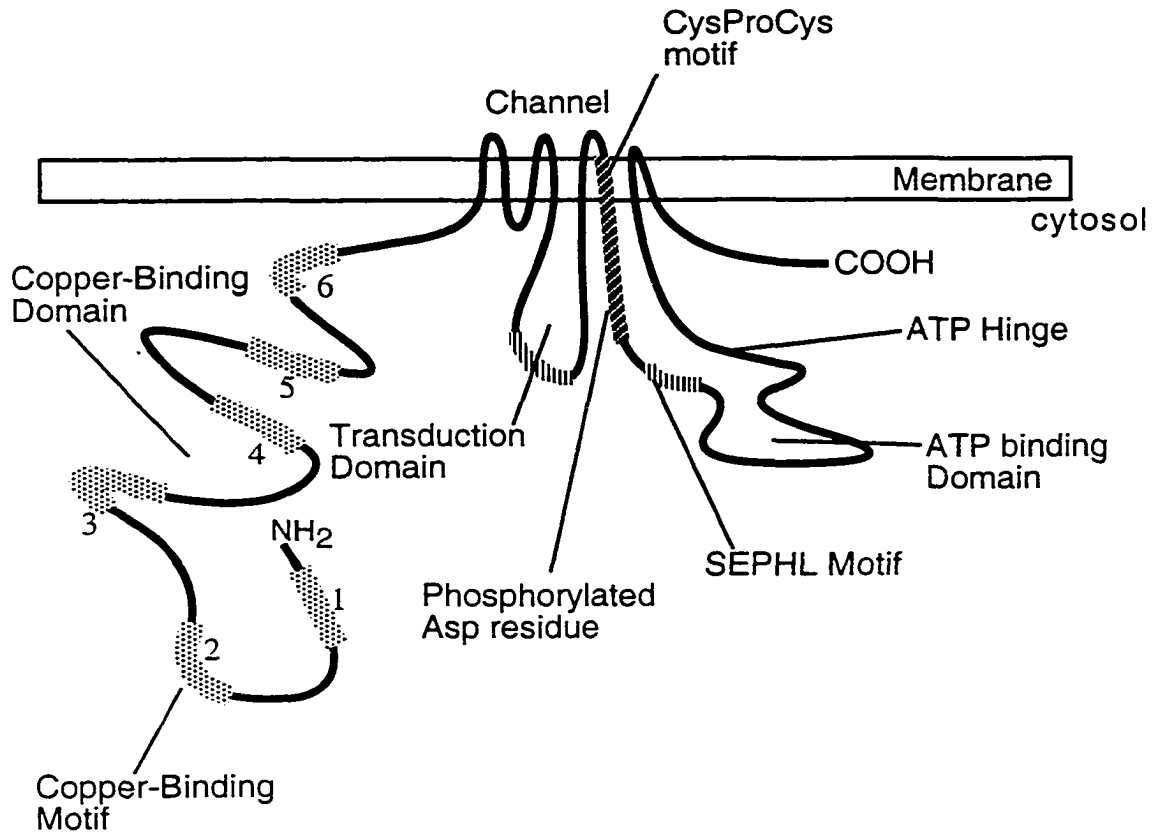


**Figure 1-2: Predicted Model of ATP7B.**

The topology of ATP7B was predicted from sequence data and must be considered putative.

predicted N-terminal structure on non-heavy metal transporting ATPases, which begin immediately with the ATPase core preceded by a very short soluble sequence. Instead, non-heavy metal P-type ATPase transporters typically have four additional C-terminal transmembrane segments added to the ATPase core, giving a predicted topology of 10 membrane spanning helices, which is supported by biochemical data (Green *et al.* 1993; MacLennan *et al.* 1997; Stokes *et al.* 1994). The transmembrane segments of ATP7B and ATP7A are predicted from sequence data alone, therefore the protein topology should be considered putative.

The most striking feature that distinguishes CPx-type ATPases from other P-type ATPases is the large N-terminal domain originally predicted to be a heavy metal-binding domain by virtue of homology with the bacterial mercury binding protein MerP and cadmium efflux protein CadA (Vulpe *et al.* 1993; Mercer *et al.* 1993; Chelly *et al.* 1993; Tanzi *et al.* 1993; Bull *et al.* 1993). Sequence alignments between putative copper-binding domains of ATP7B and ATP7A, with MerP and a number of bacterial CPx-type ATPases revealed a region of 42 amino acids with significant homology. This was designated the Cys-box (Solioz, 1998) and was predicted to contain the heavy-metal binding sites (Bull *et al.* 1994; Vulpe *et al.* 1993; Mercer *et al.* 1993; Chelly *et al.* 1993; Tanzi *et al.* 1993; Bull *et al.* 1993). The hallmark motif in the Cys-box is the absolutely conserved Gly-Met-X-Cys-X-X-Cys (GMxCxxC) sequence predicted to bind metal via the cysteine residues. ATP7A and ATP7B each contain six copies of Cys-box copper-binding motifs within their heavy metal binding domains. Each Cys-box is likely part of an individual subdomain, which together form the entire copper-binding domain. Bacterial CPx-type ATPases typically contain only one or two Cys-box motifs within a metal binding domain. A second type of putative copper-binding motif, designated the His-box, was also identified in bacterial CPx-type copper ATPases (Bull *et al.* 1994; Solioz, 1998). These domains are rich in histidine and methionine residues that are organised into loose repeats and predicted to bind copper.

The feature of CPx-type ATPases from which they were named, is the Cys-Pro-Cys/His (CPx) motif predicted to fall within the membrane domain of these proteins (Solioz *et al.* 1996). This motif is located in the predicted sixth transmembrane segment of all known CPx-type ATPases. Most, including ATP7A and ATP7B, contain the CPC motif. The CPH motif is found in a few bacterial proteins including CopB from *Enterococcus hirae* (Solioz, 1998). The proline residue is conserved in all P-type ATPases, and mutation of this residue in the Ca<sup>2+</sup>-ATPase resulted in a protein with reduced affinity for calcium binding (Solioz, 1998; Vilsen *et al.* 1989). In the Ca<sup>2+</sup>-ATPase the proline residue is part of the Val-Pro-Glu (VPE) motif. Biochemical data

from site-directed mutants of this motif identified the glutamine (E) residue as part of a high-affinity binding site for calcium ions (MacLennan *et al.* 1997; Clarke *et al.* 1989). On the basis of this biochemical data, the CPx motif is thought to be part of a copper-binding site within the membrane domain of CPx-ATPases to which copper is transiently bound during copper transport (Bull *et al.* 1994; Solioz, 1998). Interestingly, the CPH motif is found exclusively in proteins with the His-box copper-binding domain, whereas the CPC motif is found exclusively in proteins with Cys-Box copper-binding domains. This observation implies that copper may be transferred from the copper-binding domain to an equivalent CPx motif prior to translocation through the membrane.

The last sequence motif that distinguishes CPx-type ATPases from other P-type ATPases is Ser-Glu-His-Pro-Leu (SEHPL) motif found approximately 40 amino acids C-terminal to the putative phosphorylated aspartate residue (Solioz, 1998; Tanzi *et al.* 1993). This motif is not found in non-heavy metal P-type transporters. No functional data exists to help deduce the role of this motif.

### **1C-3) Structure and metal binding properties of Cys-box copper-binding domains.**

The structure and copper-binding properties of the copper-binding domains of ATP7B and ATP7A have begun to be biochemically characterised. The solution structure of the fourth copper-binding subdomain of ATP7A has been solved by NMR (Gitschier *et al.* 1998). This protein will be referred to as ATP7A.Cu4. ATP7A.Cu4 was expressed in *Escherichia coli* as a 72 amino acid polypeptide chosen on the basis of sequence alignments with the bacterial MerP mercury binding protein. The structure of the purified apo-protein was found to be very similar to the overall fold of MerP, consisting of a four-strand antiparallel  $\beta$ -sheet and two  $\alpha$ -helices forming an  $\alpha/\beta$ -sandwich. The linear order of the structural motifs is N- $\beta_1$ - $\alpha_A$ - $\beta_2$ - $\beta_3$ - $\alpha_B$ - $\beta_4$ -C. This basic fold is found in a number of functionally diverse proteins and is known as the "ferridoxin-like" structural domain. The metal binding residues were found in the loop between  $\beta_1$  and  $\alpha_A$  and in the apo-protein could not be well resolved, indicating that the structure was disordered. Addition of silver (Ag(I)) to the apo-protein resulted in no global structural changes. The metal binding loop however became ordered, binding a single silver atom in a linear arrangement between cysteine residues in the GMTCASC motif. For reference, the highly conserved metal binding residues were labelled Cys 14 and Cys 17 in this report, based on their linear order in the ATP7A.Cu4 protein analysed. The metal atom was bound in a surface pocket defined by Thr 13, Cys 14, Ser 16, and Cys 17. The residues Ile 21 and Phe 66, conserved in Cys-box motifs, pack directly against the metal binding Cys 17 residue. The conserved Leu 38 residue packs

underneath and against Cys 14. These residues are likely critical for metal binding being involved in correctly positioning the metal binding residues. In general, most of the absolutely conserved or conservatively substituted amino acids found in Cys-box motifs, outside of the metal binding residues themselves, were found within the hydrophobic core of ATP7A.Cu4 and are likely involved in defining the protein's overall fold. The highly conserved residues Gly 11 and Met 12, found at the end of  $\beta_1$  immediately preceding the metal binding loop, are likely involved in correctly positioning the metal binding loop. Met 12 was hypothesised to be a metal binding ligand, due to its sulphur moiety and close proximity to the conserved cysteine residues. Metal binding by Met 12 was not observed in the NMR structure of ATP7A.Cu4.

Recently the crystal structure of Atx1p, a small metallochaperone protein was solved by x-ray diffraction (Rosenzweig *et al.* 1999). Attempts to crystallise the protein with copper bound resulted in loss of the metal and therefore mercury was substituted for copper. This protein has sequence homology to Cys-box copper-binding subdomains found in CPx-type ATPases including the GMxCxxC motif, and was proposed to be essentially a soluble Cys-box metal binding domain (Lin *et al.* 1997). Consistent with this proposal, the overall fold and metal binding geometry of the mercury containing metal binding domain of Atx1p was conserved between MerP and ATP7A.Cu4 (Rosenzweig *et al.* 1999). Biophysical analysis of purified Atx1p with copper bound revealed one atom bound per protein molecule as Cu(I) (Pufahl *et al.* 1997). Copper bound to apo-Atx1p even in the presence of 20-fold excess concentrations of the copper chelating thiol reagent dithiothreitol (DTT) suggesting high affinity. The copper was bound entirely by sulphur containing residues in either a two or three co-ordinate geometry. Since the Atx1p copper-binding site contains only two cysteine residues, and mutagenesis of the only methionine residue did not change the observations, the third sulphur ligand was postulated to have been provided by exogenous DTT present in the analyte solution. These data suggest considerable structural conservation among Cys-box copper-binding domains and sub-domains.

The structure of the fourth ATP7A copper-binding subdomain solved by Gitschier *et al.* (1998) likely represents the prototypical fold of copper-binding sub-domains found in the copper-binding domains of CPx-type ATPases subject to a few caveats. There may be subtle differences between this structure, solved with silver bound, and a copper bound form of the protein. Silver was used instead of copper due to similar co-ordination chemistry compared with Cu(I), and because Ag(I) is more stable against oxidation in solution compared to Cu(I) facilitating metal loading (Gitschier *et al.* 1998). In hindsight, this precaution was probably not necessary as other studies showed that copper added to

the copper-binding domains of ATP7A and ATP7B as Cu(II) was reduced to Cu(I) when bound by the protein (Lutsenko *et al.* 1997; DiDonato *et al.* 1997). Additionally, recent biophysical studies comparing the structures of copper versus silver bound metallothioneins revealed differences in the manner in which the different metals were bound by these proteins (Bofill *et al.* 1999). These data suggested that copper and silver may not be entirely interchangeable. Finally, this study does not address the manner in which individual Cys-box subdomains fold in relation to each other to form a complete copper-binding domain consisting of multiple subdomains in ATP7B and ATP7A. An x-ray crystallographic or NMR study of the structure of the entire copper-binding domains, or at least several copper-binding subdomains, from these proteins with copper bound should address these issues.

Metal binding to the entire copper-binding domains of ATP7B and ATP7A has been studied. These proteins, referred to as ATP7B.Cu and ATP7A.Cu, were expressed in *E. coli* and purified. Neutron activation analysis determined a stoichiometry of 6.5-7.3 moles of copper per mole of ATP7B.Cu protein (DiDonato *et al.* 1997). By reaction with the copper chelator bicinchoninic acid (BCA) stoichiometries of 5.75 moles copper per mole ATP7B.Cu protein and 5.39 moles copper per mole ATP7A.Cu protein were obtained (Lutsenko *et al.* 1997). These data suggest that at least six atoms of copper can bind to the copper-binding domains of ATP7B and ATP7B with one atom occupying each of the six copper-binding subdomains. There are six cysteine residues outside of the copper-binding motifs in ATP7B.Cu, which may also participate in copper-binding (DiDonato *et al.* 1997). The copper bound to both proteins was in the Cu(I) form, even when added in Cu(II) form, as determined by spectroscopy and by reaction with Cu(I) specific indicators suggesting that it was reduced upon binding (Lutsenko *et al.* 1997; DiDonato *et al.* 1997). To assess the role of the conserved cysteine residues within ATP7B.Cu and ATP7A.Cu, fluorescent coumarin maleimide, which specifically reacts with cysteine residues was used (Lutsenko *et al.* 1997). The chemical probe was unable to react with the purified proteins following preincubation with copper, or following purification of the proteins from cells grown in the presence of added copper. Protection against maleimide was specific for copper, as cadmium could not prevent maleimide binding, and suggests that the cysteine residues were directly involved in copper-binding. Immobilised metal affinity chromatography was used to explore the specificity and relative affinities of the copper-binding domains for a variety of metals. In this technique chelating Sepharose or agarose resin in a column was charged with a variety of metals and the purified copper-binding domains were passed through to determine which metals the proteins could bind. Both the ATP7A.Cu and ATP7B.Cu could bind strongly to

copper charged resin (Lutsenko *et al.* 1997; DiDonato *et al.* 1997) and ATP7B.Cu could only be removed by treatment with high concentrations of copper chelator suggesting high affinity copper binding (DiDonato *et al.* 1997). Both proteins could weakly bind to zinc charged resins (Lutsenko *et al.* 1997; DiDonato *et al.* 1997). Lutsenko *et al.* (1997) found that ATP7A.Cu and ATP7B.Cu could not bind to cobalt or cadmium charged columns under the conditions used. DiDonato *et al.* (1997) found iron-charged resin was completely unable to bind ATP7B.Cu and established a relative order of heavy metal binding affinities for ATP7B.Cu of  $\text{Cu} \gg \text{Zn} > \text{Ni} > \text{Co}$  (DiDonato *et al.* 1997), based on the elution conditions required to remove bound ATP7B.Cu from the resin. These data suggest that the copper-binding domains of ATP7A and ATP7B are highly selective towards copper binding. To address further metal binding selectivity, DiDonato *et al.* (1997) employed competitive zinc blotting experiments. Radioactive zinc was incubated with membrane bound ATP7B.Cu in the presence of increasing concentrations of competitor metals and the relative amount of zinc bound was determined at each competitor concentration. Several metals, particularly Cd(II), Au(III), and Hg(II) had the highest affinity for ATP7B.Cu relative to zinc whereas Ni(II) and Mn(II) had little or no affinity. Copper, both Cu(I) and Cu(II), was the best competitor of zinc binding to ATP7B.Cu. At low concentrations of copper (up to 10  $\mu\text{M}$ ), copper reduced zinc binding (constant at 30  $\mu\text{M}$ ) by approximately 30%, which was comparable to the best of the other competitor metals at the same concentration. However, at copper concentrations exceeding 10  $\mu\text{M}$ , virtually all zinc binding was eliminated. All other heavy metals competed for zinc with a linear concentration dependence. These data were suggestive of selective and possibly cooperative copper binding to the copper-binding domain of ATP7B.

Copper binding by the copper-binding domain of ATP7A also appears to be cooperative (Jensen *et al.* 1999a). Based on equilibrium copper binding experiments using purified ATP7A.Cu protein, affinity for copper was found to increase as copper stoichiometry increased. A protein containing copper-binding subdomains one and two only also exhibited weak cooperativity for copper binding. The first copper-binding subdomain in isolation had a  $K_d = 39\text{--}46 \mu\text{M}$  (Jensen *et al.* 1999a; Jensen *et al.* 1999b), and the entire copper-binding domain had a  $K_d = 19 \mu\text{M}$  consistent with cooperative binding. Copper binding is not all or nothing. ATP7A.Cu had a basal affinity for copper that increased with copper binding. Increased copper binding affinity was accompanied by conformational changes in ATP7A.Cu measured by circular dichroism spectroscopy and quenching of tryptophan fluorescence as the copper binding stoichiometry increased.

The functional significance of the copper-binding domain of ATP7B, with respect to copper transport, will be discussed in Chapter 5 and 6 of this thesis.

#### **1C-4) Copper transport by CPx-type ATPases.**

The first copper transporting CPx-type ATPase shown to be capable of directly transporting copper was the CopB ATPase of *E. hirae*, which contains two His-box copper-binding sub-domains in its N-terminal copper-binding domain. The protein was able to transport copper into native membrane vesicles only under strongly reducing conditions using dithiothreitol (maximal transport at 5 mM DTT) indicating that copper was transported in the Cu(I) form (Solioz *et al.* 1995). Copper transport exhibited saturation kinetics dependent on copper concentration. Copper transport was dependent on ATP concentration and was inhibited by low concentrations of vanadate characteristic of P-type ATPases. Interestingly inhibition no longer occurred at high concentrations of vanadate. Refractory inhibition by vanadate is not seen in non-heavy metal transporting ATPases, which are completely inhibited at nanomolar vanadate concentrations (Skou *et al.* 1992). This observation remains unexplained but has been proposed to be related to vanadate oxidative chemistry in the highly reducing environment used for CopB transport. CopB was shown to be able to transport Ag(I) in a manner identical to copper. Purified CopB protein reconstituted into proteoliposomes was demonstrated to hydrolyse ATP and form a phosphorylated intermediate, another characteristic feature of P-type ATPases, when incubated with radioactive ATP in the presence of DTT (Wyler-Duda *et al.* 1996). Interestingly, neither phosphorylation nor ATP hydrolysis were strictly stimulated by copper addition. Both occurred in the absence of added copper and did not increase upon copper addition. Instead phosphorylation and ATPase activity were reduced, but not eliminated, by addition of a Cu(I) chelator suggesting a copper dependence of these activities. CopB phosphorylation and ATP hydrolysis were inhibited by vanadate in the same refractory manner seen for copper transport.

ATP7A expressed in stably transfected Chinese hamster ovary (CHO) cells has been shown to be capable of ATP dependent copper transport into isolated plasma membrane vesicles. ATP7A exhibited saturation kinetics dependent on copper concentration (Voskoboinik *et al.* 1998). Copper transport was dependent on DTT suggesting that transport of Cu(I), and was inhibited by vanadate. No refractory vanadate inhibition was observed as with CopB. Thiol reactive reagents inhibited copper transport consistent with a role for cysteine residues in copper transport in ATP7A. A phosphorylated ATP7A intermediate dependent on DTT, was demonstrated in membranes from stably transfected CHO cells (Solioz *et al.* 1997). As with CopB,

phosphorylation was not strictly stimulated by copper however phosphorylation was reduced by a Cu(I) chelator. Interestingly copper levels above 10  $\mu\text{M}$  inhibited phosphorylation. Vanadate was unable to inhibit ATP7A phosphorylation even at very high concentrations, and actually stimulated phosphorylation at concentrations of 100  $\mu\text{M}$ . Again, the anomalous vanadate mediated phosphorylation inhibition was believed to be caused by the oxidative chemistry of vanadate in the highly reducing reaction conditions used.

ATP dependent copper transport and formation of a phosphorylated intermediate support the idea that CopB and ATP7A are P-type ATPases. There remain many questions to be answered. First copper transport and phosphorylation was dependent on DTT. This data was interpreted to be a requirement for Cu(I) as the transport substrate. However, DTT is capable of binding copper and may influence the copper transport properties of these proteins, either stimulating transport by directly delivering copper for transport or reducing transport by establishing a copper binding equilibrium affecting the amount of copper available for transport (Solioz *et al.* 1995; Pufahl *et al.* 1997). Therefore copper transport experiments in the presence of a variety of different reducing agents including glutathione, which is a physiologic reducing agent and copper ligand, and ascorbate should be done to attempt to separate the requirement for copper reduction from a requirement for DTT. The physiologic form of copper for transport by ATP7A or CopB remains to be elucidated. A recent report suggests that there is essentially no free copper ion in eukaryotic cells, and instead copper is bound entirely to specific chaperone proteins (discussed in section 1C-3, 1D-2, and Chapter 5) (Rae *et al.* 1999). Eukaryotic metallochaperone proteins are likely the physiologic source of copper transport by ATP7A and ATP7B. Likewise, the small *E. hirae* copper chaperone, CopZ, may be required for copper delivery to CopB (Cobine *et al.* 1999). Therefore ionic copper may not represent the *in vivo* form of copper for transport.

The phosphorylation data obtained for CopB and ATP7A was anomalous compared to that seen for non-heavy-metal P-type ATPases. Phosphorylation was not stimulated by copper, and could only be reduced but not eliminated by copper chelators whereas phosphorylation of other P-type ATPases is absolutely substrate concentration dependent (Yamada *et al.* 1980). The reason for this difference is not clear but may have been related to the millimolar concentrations of DTT used in the experiments, or may have been due to copper contamination in the membrane preparations sufficient to stimulate maximal phosphorylation under the experimental conditions used.

Copper transport by ATP7B has not yet been directly demonstrated. Fet3p (see 1D-4) serves as a marker enzyme for the putative copper-transport function of Ccc2p, the

yeast orthologue of ATP7B, across an as yet unidentified post-Golgi membrane (Yuan *et al.* 1997). ATP7B is able to replace Ccc2p in yeast, delivering copper to Fet3p, demonstrating that it too is a putative copper-transporter (Hung *et al.* 1997; Iida *et al.* 1998; Forbes *et al.* 1998; Forbes *et al.* 1999). ATP-dependent copper uptake has been demonstrated in basolateral membranes of rat and human liver (Dijkstra *et al.* 1995; Dijkstra *et al.* 1996), and in Golgi membranes from rat hepatocytes (Bingham *et al.* 1996). However, these activities have not been specifically assigned to Atp7b. Recent reports have demonstrated that expression of ATP7B in Menkes patient fibroblast cell lines was able to reduce copper accumulation in these cells (La Fontaine *et al.* 1998; Payne *et al.* 1998b). Additionally, infusion of an adenovirus expressing human ATP7B into the LEC rat, a rodent model of WD, was able to restore ceruloplasmin biosynthesis and biliary copper efflux in the mutant rats (Terada *et al.* 1999; Terada *et al.* 1998). In light of these observations, together with the impaired hepatic copper efflux found in patients with WD in which ATP7B is mutated (Cox *et al.* 1998), ATP7B appears to be a copper transporter.

#### **1D) CELLULAR COPPER HOMEOSTASIS AND THE ROLE OF CPX-TYPE ATPASES IN YEAST.**

The cell biology of copper homeostasis has begun to be well characterised in yeast *Saccharomyces cerevisiae*, through extensive genetic and biochemical analysis. Due to functional conservation of proteins involved in copper transport with mammalian proteins, yeast can be used as a molecular model to decipher mammalian copper homeostasis at the cellular level. For this reason, yeast copper homeostasis will be described in some detail, in particular the role of Ccc2p, a yeast CPx-type copper transporter. Copper homeostasis in yeast is intimately associated with iron homeostasis. The role of Ccc2p is to provide a key link between iron and copper homeostasis (Fig. 1-3)

##### **1D-1) Copper uptake.**

Copper in the environment is typically found in oxidised, insoluble, forms that have limited bioavailability. Copper is usually transported into the yeast cell as the free ion not complexed to any extracellular ligands (Martins *et al.* 1998; Hassett *et al.* 1995). Prior to uptake, copper (and iron) is reduced primarily through the action of multi-spanning integral plasma membrane reductase proteins, Fre1p and Fre2p, to release the metal from extracellular ligands and increase bioavailability (Hassett *et al.* 1995; Georgatsou *et al.* 1997). Copper uptake is severely reduced in the absence of reductase activity, but can be restored in *fre1* mutant yeast by chemical reduction using ascorbate,

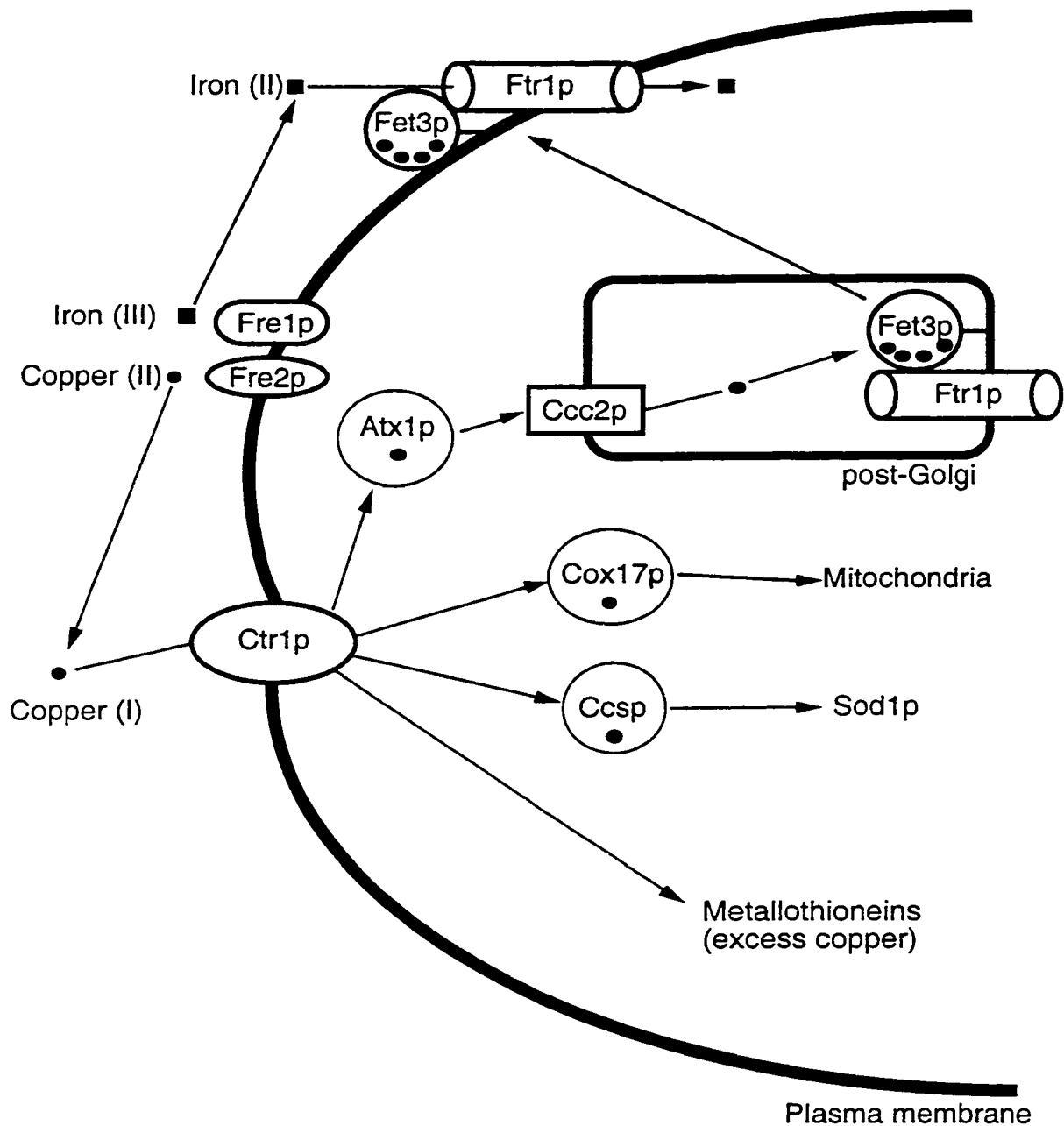


**Figure 1-3: Yeast copper and iron homeostasis.**

Iron and copper are reduced at the cell surface by Fre1p/Fre2p reductases. Copper is transported into the cytosol by Ctr1p high affinity transporter. Cytosolic copper is delivered to specific targets by cuprochaperones Atx1p, Cox17p, and Ccsp. Ccc2p delivers copper to Fet3p in a post-Golgi vesicular compartment. Fet3p is a multicopper oxidase required at the cell surface in association with Ftr1p to mediate high-affinity iron uptake. Most of these proteins have human counterparts with same function therefore this pathway also serves as a molecular model for mammalian copper homeostasis. Yeast proteins with know function are listed with their mammalian functional counterparts; Atx1p~ATOX1; Ccsp~Ccs; Cox17p~Cox17; Ccc2p~ATP7B/ATP7A; Fet3p~Ceruloplasmin; Ctr1p~Ctr1/Ctr2.

indicating that reduction is a key step preceding copper uptake (Hassett *et al.* 1995; Georgatsou *et al.* 1997). The primary protein responsible for high-affinity copper uptake in most yeast strains is Ctr1p (Dancis *et al.* 1994b; Dancis *et al.* 1994a). Ctr1p is localised to the plasma membrane, is predicted to contain 2-3 membrane-spanning helices, and is heavily glycosylated. Ctr1p has a domain containing 11 repeats of a histidine and methionine rich motif predicted to bind copper. Neither Ctr1p, nor its human counterpart, bear sequence similarity to known transport proteins making the mechanism of Ctr1p mediated copper transport difficult to deduce. On the basis of co-immunoprecipitation, and sucrose-gradient density centrifugation experiments, Ctr1p exists *in vivo* as at least a homodimer. High affinity copper uptake has an apparent  $K_m=1-4 \mu\text{M}$  that was absent in *ctr1* mutant yeast. Ctr1p was found to be copper specific, as copper uptake was not inhibited by Fe(II), Mn(II), Co(II), Ni (II), or Zn(II). Copper transport by Ctr1p remains to be demonstrated directly, and it is unclear if Ctr1p transports copper itself, or is part of a larger complex.

A second intracellular high-affinity copper transporter, Ctr3p, has been identified and was postulated to mediate copper uptake through an endocytic pathway (Knight *et al.* 1996). The *CTR3* gene is commonly disrupted by a Ty2 transposon insertion in the majority of laboratory yeast strains. Both *CTR1* and *CTR3* genes must be disrupted to abolish high-affinity copper uptake in yeast. Although either protein is sufficient for high-affinity copper uptake, both proteins are required for maximal copper uptake and cell growth under copper limited conditions

Copper uptake in yeast is tightly regulated in order to prevent toxic copper accumulation. *CTR1*, *CTR3*, and *FRE1* are co-ordinately regulated by the transcription factor Mac1p that transcribes these genes under conditions of copper starvation (Labbe *et al.* 1999; Yamaguchi-Iwai *et al.* 1997). *CTR1*, *CTR3*, and *FRE1* transcription is rapidly repressed by extracellular copper concentrations as little as  $1\mu\text{M}$ , via copper binding to Mac1p that prevents its binding to DNA (Labbe *et al.* 1999; Yamaguchi-Iwai *et al.* 1997; Pena *et al.* 1998). Besides being transcriptionally repressed by copper, Ctr1p is regulated post-translationally (Ooi *et al.* 1996). When cells were exposed to extracellular copper, Ctr1p was rapidly and specifically degraded at the plasma membrane through the action of a putative cell surface or periplasmic protease. Additionally, extracellular copper triggered the endocytosis of Ctr1p, resulting in the internalisation of Ctr1p to intracellular punctate structures. Co-ordinated transcriptional regulation of the copper uptake system, combined with proteolytic degradation and internalisation of Ctr1p in response to cytosolic copper levels, results in tight regulation of copper uptake. The copper demands of the cells are met while preventing copper overload. Copper levels in yeast cells appear

to be regulated exclusively by controlling uptake since no copper efflux systems have been identified.

### **1D-2) Copper detoxification.**

Yeast cells have means in addition to down-regulation of copper uptake to deal with copper toxicity. There are two proteins primarily responsible for resistance to copper: Cup1p and Crs5p, which are members of the eukaryotic metallothionein family of proteins (Culotta *et al.* 1994; Butt *et al.* 1984; Karin *et al.* 1984; Fogel *et al.* 1982). Yeast metallothioneins are low molecular weight, cysteine-rich proteins that are capable of binding heavy metals in polymetallic clusters (Jensen *et al.* 1996). These proteins exist to chelate and sequester heavy metal ions, preventing the toxic accumulation, and direct binding of metals to DNA, proteins, or lipids thereby protecting cells from metal-induced free radical damage. Yeast metallothioneins preferentially bind copper. Besides chelating metals, copper containing metallothioneins appear to have antioxidant activity *in vivo* (Tamai *et al.* 1993). Multicopy expression of metallothionein can suppress the oxidative stress sensitivity of *sod1* mutant yeast. In yeast, the copper-zinc superoxide dismutase protein Sod1p also plays a role in protecting cells against copper toxicity (Culotta *et al.* 1995). Overexpression of *SOD1* was able to suppress the copper-sensitive phenotype of *cup1* mutant yeast, even in anaerobic conditions, suggesting that is the copper-binding property of Sod1p, and not the oxygen free-radical scavenging activity, that is protective against copper.

The *CUP1*, *SOD1*, and *CRS5* genes are transcriptionally up regulated exclusively in response to cytosolic copper concentrations by the copper-specific Ace1p transcription factor (Culotta *et al.* 1994; Carri *et al.* 1991; Gralla *et al.* 1991; Thiele, 1988). Copper binding to Ace1p causes structural changes, which allow the metalloprotein to bind to specific regulatory elements in the promoters of *CUP1*, *SOD1*, and *CRS5*, inducing transcription of these genes (Culotta *et al.* 1994; Carri *et al.* 1991; Gralla *et al.* 1991; Furst *et al.* 1988). *CUP1* is dynamically regulated with components of the copper uptake pathway in response to copper (Pena *et al.* 1998). *CUP1* transcription is induced (by Ace1p) simultaneously with the transcriptional repression of the copper transporter *CTR3* (by Mac1p). Interestingly, *CUP1* transcription is not significantly induced in a *CTR1* deletion strain (Dancis *et al.* 1994a). The *ctr1* strain was copper resistant compared with wild-type, even at relatively high extracellular copper levels (>100  $\mu$ M), indicating that regulation of copper uptake is the primary means of preventing copper toxicity in yeast.

### 1D-3) Intracellular copper trafficking

Copper entering the cell is bound by a series of chaperone proteins that function to direct copper to specific and distinct cellular targets (Lin *et al.* 1997; Beers *et al.* 1997; Culotta *et al.* 1997). One such chaperone, Ccsp (originally called Lys7p; genetic locus *LYS7*), was found to be specifically required for copper delivery to Sod1p by directly interacting with its target protein (Culotta *et al.* 1997; Gamonet *et al.* 1998; Casareno *et al.* 1998). Another copper chaperone, Cox17p, has been shown to be required for delivery of copper to the mitochondria (Beers *et al.* 1997; Glerum *et al.* 1996). Atx1p was determined to be a copper chaperone protein involved in the high-affinity iron uptake pathway in yeast (Lin *et al.* 1997) to be discussed in the next section.

Through the study of Ccsp in yeast, an important paradigm for copper chaperone function as well as general eukaryotic copper cell biology has come to light (Rae *et al.* 1999). Rae *et al.* (1999) have found that purified Ccsp was capable of directly inserting copper into purified apo-Sod1p *in vitro*. Under the same experimental conditions, reconstitution of superoxide dismutase activity was also achieved by copper presented to Sod1p bound to glutathione or in Cu(I), or Cu(II) salt form. However, in the presence of bathocuproine disulfonate, a copper chelator, only Ccsp was able to effectively donate copper to Sod1p restoring its activity. These data led to the conclusion that Ccsp was not required for copper incorporation into Sod1p if sufficient pools of accessible copper exist, but that Ccsp was required for copper incorporation when free ionic copper levels were limited. While no active holo-Sod1p (apo-Sod1p was normal) could be detected in *lys7* mutant yeast, *in vivo* copper measurements indicated that the total cellular copper concentration remained unchanged compared with wild-type, suggesting that copper was inaccessible to apo-Sod1p. In the absence of Ccsp, Sod1p activity could only be restored *in vivo* by adding toxic levels of copper to the growth media, which increased cellular copper levels 100-fold compared to wild-type. Finally, kinetic and thermodynamic modelling of yeast cells, using copper concentrations measured *in vivo*, together with measured amounts of apo- and holo-SOD1p, estimated that under normal conditions there is less than one atom of free copper in a yeast cell (Rae *et al.* 1999). This amount of free copper is far too low to provide a significant supply to Sod1p, or other proteins. These data suggest that yeast cells possess tremendous copper chelation capacity, and that copper availability within a yeast cell is extremely restricted. While the major function of copper chaperones is to deliver copper to target proteins within the cell, another function of chaperones is to protect copper from random chelation and sequestration (e.g. by metallothioneins), such that copper can be adequately delivered to enzymes or organelles that require it. These data also suggest

that all copper transport processes within a yeast cell are entirely protein mediated, and that free copper ion is normally not a physiologic transport substrate. This model most likely applies to mammalian cells as well and is discussed in section 1E-2.

Copper chaperones have also been proposed to protect cells from toxicity by sequestering copper, however yeast cells lacking chaperones are not copper sensitive (Rae *et al.* 1999). The copper normally bound by a missing chaperone would likely be bound by metallothioneins.

#### **1D-4) High affinity iron uptake: a role for CPx-type ATPases.**

Interestingly, one of the first proteins identified as part of the high-affinity iron uptake system in yeast was the high-affinity copper transporter Ctr1p (Dancis *et al.* 1994b). Deletion of the *CTR1* gene abrogated both copper and iron uptake. Iron uptake was correctable by extracellular copper. Since Ctr1p did not directly transport iron, it appeared that copper was an essential co-factor required for iron uptake. The biochemical basis of copper requirement for iron uptake became clear when the *FET3* gene was discovered (Askwith *et al.* 1994). Disruption of *FET3* resulted in a mutant yeast strain lacking high-affinity iron uptake that was unable to grow on iron-limited medium, or on non-fermentable carbon source media, indicative of mitochondrial defects. These growth phenotypes could be corrected by addition of iron, but not copper, to the growth medium suggesting a role for Fet3p in iron uptake. Sequencing of the *FET3* gene revealed a predicted protein containing a single putative transmembrane domain that had limited sequence homology to members of the multi-copper oxidase proteins including laccase, ascorbate oxidase and ceruloplasmin.

Fet3p was localised by immunofluorescence microscopy to the yeast plasma membrane, consistent with a role in iron uptake (Stearman *et al.* 1996). Purified Fet3p is heavily glycosylated, and contains four atoms of copper (de Silva *et al.* 1997). The protein is capable of oxidising Fe(II) to Fe(III) *in vitro* as its preferred substrate. Fet3p can also oxidise organic substrates, including *p*-phenylenediamine and *o*-dianisidine, which are typically used as substrates for oxidase activity in *in vitro* assays (Stearman *et al.* 1996; Yuan *et al.* 1997; de Silva *et al.* 1997; Askwith *et al.* 1998). Fet3p depends on copper for activity, as no oxidase activity is present in apo-Fet3p, or in Fet3p with mutations in its putative copper-binding residues (Yuan *et al.* 1995; Askwith *et al.* 1998). Chloride ion is required by Fet3p, as an allosteric effector of copper binding *in vitro*, and *in vivo* dependent on the chloride delivered to it by the intracellular chloride channel protein Gef1p (Davis-Kaplan *et al.* 1998). Fet3p functions at the plasma membrane together with the iron permease protein Ftr1p, and the Cu(II)/Fe(III) reductase proteins

Fre1p and Fre2p, to mediate high-affinity iron uptake (Stearman *et al.* 1996; Askwith *et al.* 1998). The oxidase function of Fet3p is specifically required at the plasma membrane for iron uptake (Askwith *et al.* 1998). Mutant variants of Fet3p that have no *in vitro* oxidase activity, but are correctly localised to the plasma membrane, are unable to mediate high-affinity iron-uptake.

Ccc2p is required for copper incorporation into Fet3p *in vivo* (Yuan *et al.* 1995). Ccc2p is predicted to be a copper-transporting CPx-type ATPase with 31% and 29% amino acid identity to ATP7B and ATP7A respectively. Ccc2p has a putative N-terminal domain containing two Cys-box copper-binding subdomains. Disruption of the *CCC2* gene results in abrogation of high-affinity iron uptake, that is correctable by the addition of extracellular copper. The *ccc2* mutant yeast had no detectable Fet3p activity, but Fet3p activity could be restored *in vivo* by addition of copper to the growth medium, or *in vitro* by copper addition during protein preparation, indicating that the *ccc2* mutation affects copper incorporation into apo-Fet3p, but not apo-Fet3p biosynthesis. Defective iron uptake could be corrected by addition of extracellular copper in a *ccc2ctr1* double mutant, indicating that copper correction was independent of cytosolic copper, and was achieved by reconstitution of apo-Fet3p at the cell surface (Yuan *et al.* 1997). Additionally, copper added to growth medium could restore iron uptake to copper depleted yeast in the presence of cyclohexamide, which prevents *de novo* protein synthesis, further supporting that copper rescue was achieved by binding to pre-existing apo-Fet3p at the cell surface (Dancis *et al.* 1994b). These data support a role for Ccc2p in delivering copper to Fet3p within an intracellular compartment *in vivo*.

Biochemical and genetic experiments were utilised to determine the intracellular site of copper incorporation into Fet3p (Yuan *et al.* 1997). Ccc2p was localised by immunofluorescence microscopy, to punctate structures within the cell, characteristic of a late-Golgi protein. Incorporation of radioactive copper into Fet3p was monitored in a series of yeast mutants with temperature-sensitive defects in secretory protein trafficking (*sec* mutants). At the non-permissive temperature, copper incorporation into Fet3p was not seen in mutant cells with blocks in the secretory pathway preceding, or including, intra-Golgi transport (*sec23*, *sec18*, *sec7*, *sec21*, and *sec53*<sup>3</sup>). Copper incorporation into Fet3p was detected in cells with secretory blocks at stages involving transport or exocytosis of secretory vesicles (*sec4*, *sec1*). Fet3p biosynthesis was normal in all experiments. These data indicated that copper incorporation into Fet3p mediated by Ccc2p occurs in a late-Golgi, or post-Golgi, vesicular compartment. Ccc2p acts as the "lynch-pin" connecting the copper uptake pathway to the iron-uptake pathway in yeast.

There is no evidence to date suggesting that Ccc2p plays a role in cellular copper efflux as does ATP7B.

Copper is delivered to Ccc2p for transport into Fet3p by the copper chaperone Atx1p. The structure and metal binding properties of Atx1p have been described in section 1B-3. Deletion of the *ATX1* gene resulted in a mutant yeast deficient for high-affinity iron uptake, and copper incorporation into Fet3p was abolished (Lin *et al.* 1997; Klomp *et al.* 1997). Subsequently, the mutant yeast cells were unable to grow on iron-limited medium unless supplemented with copper or iron (Lin *et al.* 1997). This phenotype is similar to *ccc2* mutant yeast, suggesting that the two proteins act in the same or parallel pathways. To distinguish these possibilities, overexpression of *ccc2* could suppress the *atx1* mutation, but *atx1* could not suppress the *ccc2* mutation suggesting that Atx1p acted before Ccc2p in a linear pathway involved in delivering copper to Fet3p. The *atx1* phenotype was less severe than the *ccc2* mutant phenotype as iron uptake was only 65-70% reduced in the *atx1* mutant yeast compared with wild-type, while disruption of *CCC2* results in complete loss of high-affinity iron uptake. Additionally, growth on iron-limited medium was restored at a far lower concentration of iron in the *atx1* mutant yeast strain compared with that required for rescue of the *ccc2* mutant yeast. These data suggested that Atx1p was not the only source of copper used by Ccc2p for transport. An *atx1end3* double mutant, defective for both Atx1p and for endocytosis, was shown to have a phenotype identical to *ccc2* mutant yeast. The *end3* mutation alone had no effect on high-affinity iron uptake suggesting that in the absence of Atx1p, Ccc2p can also utilise copper delivered from the endocytic pathway. Yeast two-hybrid analysis was used to show that Atx1p was capable of interacting directly with the copper-binding domain of Ccc2p in a copper-dependent manner leading to a proposed mechanism for copper transfer between the two proteins (Pufahl *et al.* 1997). This will be discussed in more detail in Chapter 5,6.

The entire iron uptake pathway, including *FRE1*, *FRE2*, *ATX1*, *CCC2*, *FET3*, and *FTR1*, is positively regulated by the transcription factor Aft1p in response to iron starvation (Lin *et al.* 1997; Yamaguchi-Iwai *et al.* 1995; Yamaguchi-Iwai *et al.* 1996). A possible exception to this is the *ATX1* gene (Lin *et al.* 1997). *ATX1* expression was increased in the *aft1*<sup>up</sup> mutant yeast strain in which Aft1p is non-responsive to iron resulting in constitutive expression of the iron uptake pathway in iron-replete yeast cells (Yamaguchi-Iwai *et al.* 1995; Yamaguchi-Iwai *et al.* 1996). These data indicate transcriptional activation of *ATX1* by Aft1p. However, the basal level of *ATX1* transcription was not affected in the *aft1* null mutant, and was not repressed by iron, indicating that other transcription factors may also control *ATX1* expression

independently of iron. *ATX1* transcription was not affected by copper levels or by mutations in the *MAC1* gene (section 1D-2).

### **1E) HEPATIC COPPER HOMEOSTASIS AND THE ROLE OF CPX-TYPE ATPASES IN MAMMALS.**

Although little is known about the molecular mechanisms of mammalian copper homeostasis, many of the proteins found in yeast cells are also found in mammalian cells. Therefore yeast have been a useful tool to help decipher the mammalian system (Fig. 1-3 serves for the mammalian system as well). In mammals, the liver is the homeostatic control point regulating copper levels. Much work has been done on physiologic copper homeostasis in cultured hepatocytes and livers from rats, and to a lesser extent using mice. Rodent hepatocytes, particularly those of the rat, will therefore serve as a model for description of mammalian hepatic copper homeostasis, focusing on the physiologic role of ATP7B.

#### **1E-1) Cellular copper uptake.**

Copper uptake by hepatocytes has been actively studied, but remains poorly understood. In polarised hepatocytes *in vivo*, copper uptake occurs at the basolateral plasma membrane in contact with the sinusoids (Ballatori, 1991). The net accumulation of copper by mouse and rat hepatocytes shows steady state kinetics, with a rapid linear phase of accumulation, followed by a plateau phase, where no net accumulation is observed due to the balancing effect of influx and efflux mechanisms (Bingham *et al.* 1994; Weiner *et al.* 1980; McArdle *et al.* 1988; Darwish *et al.* 1984; Schmitt *et al.* 1983). Copper uptake experiments done with copper pre-loaded or pre-depleted mouse hepatocytes indicate that the kinetics of copper uptake are unchanged in response to cytosolic copper levels (Darwish *et al.* 1983; McArdle *et al.* 1990). Copper uptake does not require new-protein synthesis (Weiner *et al.* 1980). These data suggest that copper uptake is not regulated by intracellular copper concentrations in rodent hepatocytes. In rat and mouse hepatocytes copper uptake appears to be saturable, and is not affected by ATP depletion (Schmitt *et al.* 1983; Bingham *et al.* 1994; Darwish *et al.* 1983; McArdle *et al.* 1988; McArdle *et al.* 1990). Pre-treatment of mouse hepatocytes with extracellular proteases reduced copper uptake (McArdle *et al.* 1988). These data suggest that copper uptake is protein mediated but not ATP dependent. Copper uptake in rat hepatocytes was stimulated by ascorbate, suggesting a role for copper reduction as has been described in yeast (Bingham *et al.* 1994). The molecular mechanisms of copper uptake in mammalian cells have not yet been elucidated. A human orthologue of the yeast *CTR1* gene, as well as a second similar putative copper transporter named *CTR2*, have been identified by

functional complementation of the yeast *ctr1* mutant (Zhou *et al.* 1997). The human and mouse genome projects may reveal orthologues of the yeast *FRE* genes. Future studies may determine if these proteins are involved in mammalian copper uptake.

The physiologic source of copper entering hepatocytes has not been defined with certainty. Hepatocytes in culture will effectively take up copper from any source offered including albumin, transcuprein, ceruloplasmin, and copper complexes such as copper-histidine and copper salts (Linder *et al.* 1998). There is virtually no free copper ion in the plasma *in vivo* (Ballatori, 1991). Size exclusion chromatography has been used to identify two rat serum fractions containing newly absorbed radioactive copper (Linder *et al.* 1998). Albumin was one of the fractions, and is considered to be the major carrier for newly absorbed plasma copper. Albumin has high affinity copper-binding sites in its N-terminus, and copper bound to albumin is readily imported by cultured hepatocytes. However, copper is normally distributed in the Nagase rat, which has no plasma albumin (Vargas *et al.* 1994). There are no identified binding sites on hepatocytes for albumin (Linder *et al.* 1998). Therefore it has been hypothesised that copper bound to albumin represents a passive, and readily exchangeable pool of plasma copper that can be released to other carriers for actual cell uptake (Linder *et al.* 1998). Histidine is a trace component of human plasma, and is proposed to mobilise copper from albumin as a source of copper for uptake by hepatocytes (Linder *et al.* 1998). Histidine itself does not carry a significant amount of serum copper (Linder *et al.* 1998). Biochemical data support this hypothesis (Darwish *et al.* 1984). Albumin inhibits uptake of ionic copper by hepatocytes by reducing the concentration of free copper. Addition of histidine was capable of relieving this inhibition. Copper was imported into hepatocytes from a copper-histidine complex in equilibrium with copper-albumin. Although copper-histidine was the transport substrate, histidine itself was not imported concurrently with copper suggesting that copper ion is transferred to a transport protein prior to uptake. Linder *et al.* (1998) propose that since the rate of copper dissociation from albumin is slow in the presence of histidine, this route of copper uptake by hepatocytes is not likely sufficient *in vivo*.

The other major carrier of newly absorbed copper in rat serum identified by size-exclusion chromatography was a protein termed transcuprein (Linder *et al.* 1998). This protein eluted from the column with an apparent molecular mass of 270 kDa. Transcuprein protein remains to be fully characterised or its cDNA cloned. Copper bound to transcuprein rapidly exchanges with albumin bound copper. Transcuprein has therefore been suggested to donate copper to hepatocyte transporters, facilitate copper exchange from albumin to hepatocyte transporters, or directly import copper into hepatocytes by binding a hypothetical receptor. Transcuprein is not universally accepted

as a copper carrier, since the protein's existence cannot be confirmed by all investigators who have made an attempt (Danks, 1995).

### **1E-2) Hepatic copper pools.**

The intracellular pool of copper in hepatocytes remains to be fully elucidated. Early studies done by fractionation of hepatocyte or liver homogenates suggest that most cellular copper was bound to proteins, predominantly metallothionein (Weiner *et al.* 1980; Bingle *et al.* 1992; Narthey *et al.* 1987; Freedman *et al.* 1989; Baerga *et al.* 1992). The predominance of metallothioneins may be somewhat artifactual (Farrell *et al.* 1993). A study was performed showing that exogenous metallothionein, added to cell homogenates containing low levels of endogenous metallothionein, resulted in a shift in copper distribution to the added protein. These data suggested that during cell homogenisation, endogenous metallothioneins could remove copper from other ligands, or bind copper from disrupted intracellular compartments, thereby skewing the observed copper distribution. This caveat aside, the majority of copper in hepatocytes appears to be protein-associated. This observation is consistent with the studies in yeast showing that there is essentially no free ionic copper in yeast cells (Rae *et al.* 1999) and suggests that copper transport processes in mammalian cells are also entirely protein mediated. Mammalian functional orthologues of the yeast copper chaperones Atx1p, Ccsp, and Cox17p have been identified and are able to functionally replace their yeast counterparts suggesting that the molecular mechanisms of intracellular copper trafficking by metallochaperones are conserved in mammals (Klomp *et al.* 1997; Culotta *et al.* 1997; Amaravadi *et al.* 1997). Glutathione has been suggested to be involved in the transfer of copper stored in protein bound form, particularly in metallothionein, to other intracellular sites (Ballatori, 1991). However, metallothionein itself does not act as an intracellular pool of copper as yeast or mice lacking metallothioneins have no defects in copper transport (Palmiter, 1998). However under conditions of copper overload, when metallothioneins are highly induced, glutathione may mobilise copper from metallothionein for copper efflux by ATP7B, perhaps via ATOX1, or cMOAT (Dijkstra *et al.* 1996; Houwen *et al.* 1990).

Despite most copper being found in cytosolic protein fractions of hepatocyte extracts, a significant portion is found in membrane enclosed intracellular compartments, especially the lysosomes, as revealed by cell fractionation experiments, and experiments on whole cells using x-ray microprobes, or copper stains, in normal, copper-loaded, or WD livers (Bingle *et al.* 1992; Freedman *et al.* 1989; Baerga *et al.* 1992; Narthey *et al.* 1987; Fuentealba *et al.* 1989a; Fuentealba *et al.* 1989b; Stockert *et al.* 1986; Haywood *et al.* 1985;

Vaux *et al.* 1985). Lysosomal copper accumulation tends to appear later than cytosolic copper accumulation in chronically copper-loaded rat livers. Lysosomal copper has been reported to be bound to polymeric aggregates, of partially degraded, or oxidised metallothionein, suggesting that lysosomal copper may be derived from autophagocytosis of excess cytoplasmic metallothionein under conditions of copper loading (Klein *et al.* 1998; Danks, 1995).

### **1E-3) Copper detoxification: metallothioneins.**

Mammalian metallothionein proteins are small cysteine-rich proteins that utilise cysteine repeats to bind heavy-metals such as zinc, copper, and cadmium, in polynuclear thiolate clusters (Palmiter, 1998; Dameron *et al.* 1998). In mice there are four genes in a cluster on chromosome 8; MT I and MT II genes are expressed ubiquitously during all stages of development and are involved in metal detoxification (Palmiter, 1998). MT III is primarily neuronally expressed, and MT IV is expressed in squamous epithelium cells but the role of these proteins is unclear (Palmiter, 1998). In humans there are at least 16 metallothionein genes in a cluster on chromosome 16 (Palmiter, 1998). Mammalian metallothioneins can bind a variety of metals, whereas yeast metallothioneins bind copper preferentially (Palmiter, 1998; Dameron *et al.* 1998). The primary role of metallothioneins is thought to be the sequestration and detoxification of metals. Mammalian cells expressing excess metallothioneins are cadmium resistant (Palmiter, 1998; Dameron *et al.* 1998). Selection for cadmium resistance results in cells with an amplification of the entire metallothionein locus. Mice lacking both MT I and MT II genes are cadmium sensitive, but are only marginally sensitive to copper or zinc (sensitive only to large dietary doses). Metallothioneins only appear to be required for zinc detoxification in the absence of zinc efflux proteins (Palmiter, 1998). Similarly, metallothioneins are required for copper detoxification only when cellular copper efflux by ATP7A is impaired (Kelly *et al.* 1996). Thus, efflux is thought to be the primary mechanism of copper resistance in mammalian cells. Metallothioneins likely form a second line of defence when efflux mechanisms are overloaded. Metallothioneins are probably required for protection against cadmium toxicity because there are no identified mammalian cadmium efflux mechanisms (Palmiter, 1998). As in yeast, mammalian metallothioneins are thought to be involved in protection against free radicals (Palmiter, 1998). The metal-thiolate clusters in metallothionein are readily oxidised *in vitro*, and mouse cells that over-produce metallothioneins are resistant to chemically induced oxidative damage. Conversely, mouse cells lacking metallothioneins are more sensitive to oxidative stress.

In mice, metallothioneins MT I, and MT II are up-regulated in response to heavy-metals, particularly copper, cadmium, and zinc (Palmiter, 1998; Dameron *et al.* 1998). These genes are also induced by oxidative stress, and by cytokines perhaps to protect the host cells against free radicals generated by leukocytes during defence against invading pathogens. Consistent with these observations, metallothionein promoters have 5' metalloregulatory elements (MRE) that are occupied by transcription factors in response to heavy-metals. One such regulatory protein, MTF-1, has been identified in mice (Westin *et al.* 1988; Radtke *et al.* 1993). Homozygous deletion of MTF-1 results in no expression of the MT I or MT II genes and enhances sensitivity of the mutant embryonic stem cells to cadmium (Gunes *et al.* 1998; Heuchel *et al.* 1994). Knock-out mice generated from MTF-1 stem cells die *in utero*. Metallothionein I/II knockout mice are viable and healthy under normal conditions suggesting that MTF-1 regulates more than just the metallothionein genes.

#### **1E-4) Hepatic copper efflux and the role of ATP7B.**

Biliary copper excretion is the major route of copper efflux from the hepatocyte, and regulation of whole-body copper homeostasis occurs via this pathway (Ballatori, 1991; Linder *et al.* 1998). Copper is transported from the plasma to the bile in a transcellular pathway (Ballatori, 1991). Very little copper enters the bile in a paracellular manner as seen for metals such as magnesium. Copper efflux from isolated rat hepatocytes has a rate approximately equal to uptake, and obeys saturation kinetics, suggestive of a facilitated transport system (Darwish *et al.* 1984). In rat livers *in vivo*, there appear to be two routes of copper transport out of hepatocytes. One involves ceruloplasmin, and the other copper transport into the bile (Ballatori, 1991).

Most copper transported out of the liver and into the circulating plasma is bound to ceruloplasmin (Linder *et al.* 1998; Ballatori, 1991). Copper is incorporated into apo-ceruloplasmin within the trans-Golgi network of hepatocytes (Sato *et al.* 1991; Terada *et al.* 1998; Murata *et al.* 1995). Holo-ceruloplasmin is then secreted out of the basolateral membranes into the plasma (Linder *et al.* 1998; Ballatori, 1991). Copper incorporation into ceruloplasmin involves ATP7B. Patients with WD carrying defective ATP7B variants have impaired copper incorporation into ceruloplasmin (Cox *et al.* 1998). The LEC rat, a model for WD in which *Atp7b* is partially deleted, has normal synthesis, but defective copper incorporation, into apo-ceruloplasmin resulting in the secretion of inactive apo-ceruloplasmin (Terada *et al.* 1998; Murata *et al.* 1995; Wu *et al.* 1994; Yamada *et al.* 1993a). Adenoviral mediated re-introduction of human ATP7B into LEC rat livers *in vivo* results in the restoration of copper incorporation into apo-ceruloplasmin,

and re-emergence of active protein in the serum (Terada *et al.* 1998). As discussed in sections 1B-1 and 1B-4, plasma ceruloplasmin has been suggested to be a donor of copper to tissues, and its ferroxidase activity appears to be required for normal iron transport. The role of ceruloplasmin in mammalian iron homeostasis is analogous to the role of Fet3p in yeast iron uptake. Thus, it appears that in both yeast and humans, and likely all eukaryotes, that a CPx-type ATPase delivering copper to a ferroxidase enzyme, is a key and highly conserved aspect of normal cellular iron homeostasis.

The majority of copper efflux out of mammalian hepatocytes, and subsequently out of the body, is via the bile (Linder *et al.* 1998; Ballatori, 1991). The chemical form of copper in the bile has been extensively investigated (Ballatori, 1991). In the bile, copper is complexed to a vast array of ligands, including amino acids, peptides (including glutathione), proteins (including ceruloplasmin and metallothionein), and bile salts. Hepatic metallothionein induction can lower biliary copper excretion by sequestering the metal, but does not otherwise play a major role in copper efflux (Palmiter, 1998; Ballatori, 1991). Ceruloplasmin found in the bile is likely due to recycling by hepatocytes of ageing, deglycosylated, asialoceruloplasmin from the serum by endocytosis, followed by lysosomal degradation and exocytosis (Schilsky *et al.* 1994).

Two routes of copper efflux across the canalicular membrane are proposed (Ballatori, 1991). One suggested mechanism is that copper is transported into the bile bound to glutathione. Chemical depletion of hepatic and biliary glutathione in rat livers was found to result in decreased biliary copper, which suggested that copper efflux was linked to glutathione transport (Alexander *et al.* 1980). The role of glutathione transport related to copper efflux was later examined in the Groningen Yellow (GY) rat, a rat model which shows defective transport of glutathione into the bile, due to a defect in the ATP-dependent canalicular glutathione conjugate transporter protein cMOAT (Dijkstra *et al.* 1996; Houwen *et al.* 1990). These studies revealed two phases of biliary copper efflux in the rat; a rapid phase, sensitive to glutathione depleting chemicals that was absent in the GY rat, and a slow phase, independent of glutathione, not affected in the GY rat. The slow phase of transport was responsible for the majority of copper efflux, and the GY rat did not accumulate hepatic copper. These studies led to the conclusion that glutathione-dependent copper transport does occur but is not the major route of biliary copper efflux. Similar studies were done using the Eisai hyperbilirubinemic mutant rat, which is defective for biliary glutathione efflux, and similar conclusions were drawn (Sugawara *et al.* 1999; Sugawara *et al.* 1996). Finally, studies have shown that glutathione-dependent biliary copper excretion is only significant when rats are injected with copper intravenously (Dijkstra *et al.* 1997). Glutathione-dependent copper efflux does not appear

to be significant when rats are fed copper in the diet. The majority of biliary copper efflux found in the slow, glutathione-independent phase, was attributed to ATP7B (Dijkstra *et al.* 1997). This hypothesis is likely correct but remains to be directly demonstrated.

The second route of hepatic copper efflux appears to involve the lysosomes (Ballatori, 1991). As described in section 1D-2, a significant part of cellular copper is found within the lysosomal compartment in copper-loaded rat hepatocytes. Studies on rats that were acutely or chronically copper loaded, showed increased accumulation of copper in hepatic lysosomes, combined with increased numbers, and altered morphology perhaps due to copper induced membrane damage. (Gross *et al.* 1989; Harada *et al.* 1993). Copper efflux from copper loaded rats was associated with lysosomal enzyme secretion. Chemical stimulation of secretion of lysosomal contents out of the cell, simultaneously increased copper efflux and lysosomal enzyme secretion from copper loaded rats, whereas only lysosomal enzyme secretion was stimulated in control animals (Gross *et al.* 1989). These results, combined with subcellular copper distribution data, support a role for lysosomal copper efflux in rats.

Studies on the LEC rat support a role for lysosomes in biliary copper efflux, and link the process to ATP7B (Yamada *et al.* 1993b; Schilsky *et al.* 1994; Yamada *et al.* 1993a). LEC rats, which lack *Atp7b*, had normal rates of hepatic copper uptake, accumulated substantial amounts of hepatic copper, but showed impaired delivery of copper into subcellular fractions particularly the lysosomes. Biliary copper efflux was impaired. Lysosomal exocytosis was normal in the LEC rats, but no copper efflux occurred via this pathway. Lysosomal copper accumulation, and biliary copper excretion, could be restored in the LEC rat *in vivo*, by adenoviral mediated expression of human *ATP7B* in the liver (Terada *et al.* 1999). Overexpression of *ATP7B* in human hepatoblastoma cells resulted in resistance to copper but not zinc or cadmium, and increased copper accumulation in subcellular organelles (Schilsky *et al.* 1998). These data clearly implicate *ATP7B* in biliary copper efflux at the molecular level, and support a role for lysosomes in the process. The molecular aspects of copper efflux by *ATP7B* are discussed in the next section.

#### **1E-5) Copper induced intracellular trafficking of ATP7B.**

Studies involving the LEC rat clearly established a role for *ATP7B* in ceruloplasmin biosynthesis and biliary copper efflux. How these processes are linked within a hepatocyte by a single protein remained unclear. Studies to determine the localisation of *ATP7B* protein revealed an interesting observation (Hung *et al.* 1997). In

HepG2 hepatoblastoma cells, endogenous ATP7B protein was found to be localised to the trans-Golgi network, utilising immunofluorescence microscopy and cell fractionation experiments. When copper was added to the growth medium, ATP7B redistributed from the trans-Golgi to a cytoplasmic vesicular compartment. The effect was copper concentration dependent occurring within 15 min. (faster than ATP7B biosynthesis) at a minimum concentration of 40  $\mu\text{M}$  added extracellular copper. Redistribution was specific for copper, as zinc, cadmium, iron, or cobalt had no effect. Copper had no quantitative or qualitative effect on ATP7B, indicating that ATP7B is not regulated by copper levels. Copper-dependent redistribution was reversible by copper chelation indicating that ATP7B is recycled back to the trans-Golgi in the absence of copper. Copper-induced redistribution and recycling occurred in the absence of new protein synthesis, indicating that the localisation changes were not the result of new protein repopulating one compartment. Copper-dependent redistribution and recycling of ATP7B are continuous processes, copper levels only change the observable steady-state localisation. Copper-dependent relocation from the trans-Golgi network to cytoplasmic vesicles was later shown to occur in primary rat hepatocytes, and was observed in liver sections from copper-loaded rats, indicating that copper-dependent ATP7B redistribution is a physiologically relevant process *in vivo* (Schaefer *et al.* 1999a). Furthermore, in liver sections from copper loaded rats, ATP7B-containing vesicles were found throughout the cytoplasm, but concentrated near membranes adjacent to bile canaliculi, suggesting that these vesicles were involved in biliary copper efflux. ATP7B has also been localised to the mitochondria (Lutsenko *et al.* 1998)

New data favour an endosomal pathway over a lysosomal pathway for vesicular ATP7B-dependent copper efflux. The end-point of ATP7B copper-induced trafficking has been recently identified. Immunogold electron microscopy, performed on normal mouse cells, localised ATP7B to the late endosomal compartment in the presence of high copper concentrations (J. Mercer, personal communication). The late endosome compartment is a major protein sorting compartment involved in sorting proteins bearing mannose-6-phosphate using the mannose-6-phosphate receptor (MPR) (Kornfield, 1992). The MPR delivers proteins such as lysosomal enzymes from the trans-Golgi network, to the endosomal compartment, and is then recycled back to the trans-Golgi for reutilization. Proteins newly delivered to the late endosomes by the MPR are sorted further then delivered to the appropriate compartment. The late endosomes also sort endocytosed proteins destined for degradation by the lysosomes, and eventually fuse with the lysosomes forming a hybrid organelle (Kornfield, 1992; Mullock *et al.* 1998).

In human and rat liver sections, ATP7B was found to be localised to vesicles found in close association with the bile canalicular plasma membrane (Schaefer *et al.* 1999a; Schaefer *et al.* 1999b). These ATP7B vesicles also contained some Golgi markers (TGN38), which is consistent with an endosomal compartment since many proteins such as GLUT4, furin, and TGN38 cycle between the plasma membrane and trans-Golgi network through the endosomes (Wei *et al.* 1998; Mallet *et al.* 1999). In both rat and human liver sections a small proportion of ATP7B was found in the canalicular plasma membrane (Schaefer *et al.* 1999a; Schaefer *et al.* 1999b). ATP7B found in the plasma membrane may be due to fusion of ATP7B and copper-containing endosome derived vesicles with the plasma membrane during copper efflux by vesicle exocytosis. Consistent with this mechanism, ATP7B contains a C-terminal di-leucine motif, which is involved in recycling proteins from the plasma membrane to the late endosomes (Calvo *et al.* 1999). These data are fully consistent with earlier findings that implicate lysosomes in ATP7B dependent copper efflux. The late endosomes and lysosomes are functionally related cellular compartments that are not easily distinguished biochemically or histologically from each other (Gruenberg *et al.* 1995). Therefore it is possible that early studies implicating the lysosomes in copper efflux may not have had sufficient resolution to differentiate the two compartments.

These data combined with the data described section 1B-4 allow a mechanism by which ATP7B can deliver copper to ceruloplasmin within the trans-Golgi network, while still excreting copper out of the cell and into the bile (Fig. 1-4) (Forbes *et al.* 1998; Schaefer *et al.* 1999a). Under normal conditions, ATP7B resides mostly in the trans-Golgi network of hepatocytes, where it can deliver copper for incorporation into apo-ceruloplasmin. Holo-ceruloplasmin trafficks through the secretory pathway, for delivery to the plasma. Excess copper triggers ATP7B movement into vesicles, where it functions to remove copper from cytosolic ligands, and transport it into endosomal vesicles, for eventual delivery into the bile by exocytosis. Post-translational redistribution of ATP7B in response to copper occurs much faster than new-protein synthesis and processing could occur (Hung *et al.* 1997), allowing the cells to respond very rapidly to excess copper. The presence of multiple small ATP7B-containing vesicles throughout the cytoplasm would hypothetically result in a large surface area for copper uptake. A vesicular copper efflux mechanism is therefore more efficient than an entirely canalicular membrane localised efflux system involving ATP7B, since in polarised hepatocytes, the canalicular membrane surface is limited. If ATP7B was restricted to canalicular membranes, copper entering the cell from the basolateral cell surface, would have to diffuse through the entire cell volume before encountering ATP7B for efflux, leaving ample time to cause

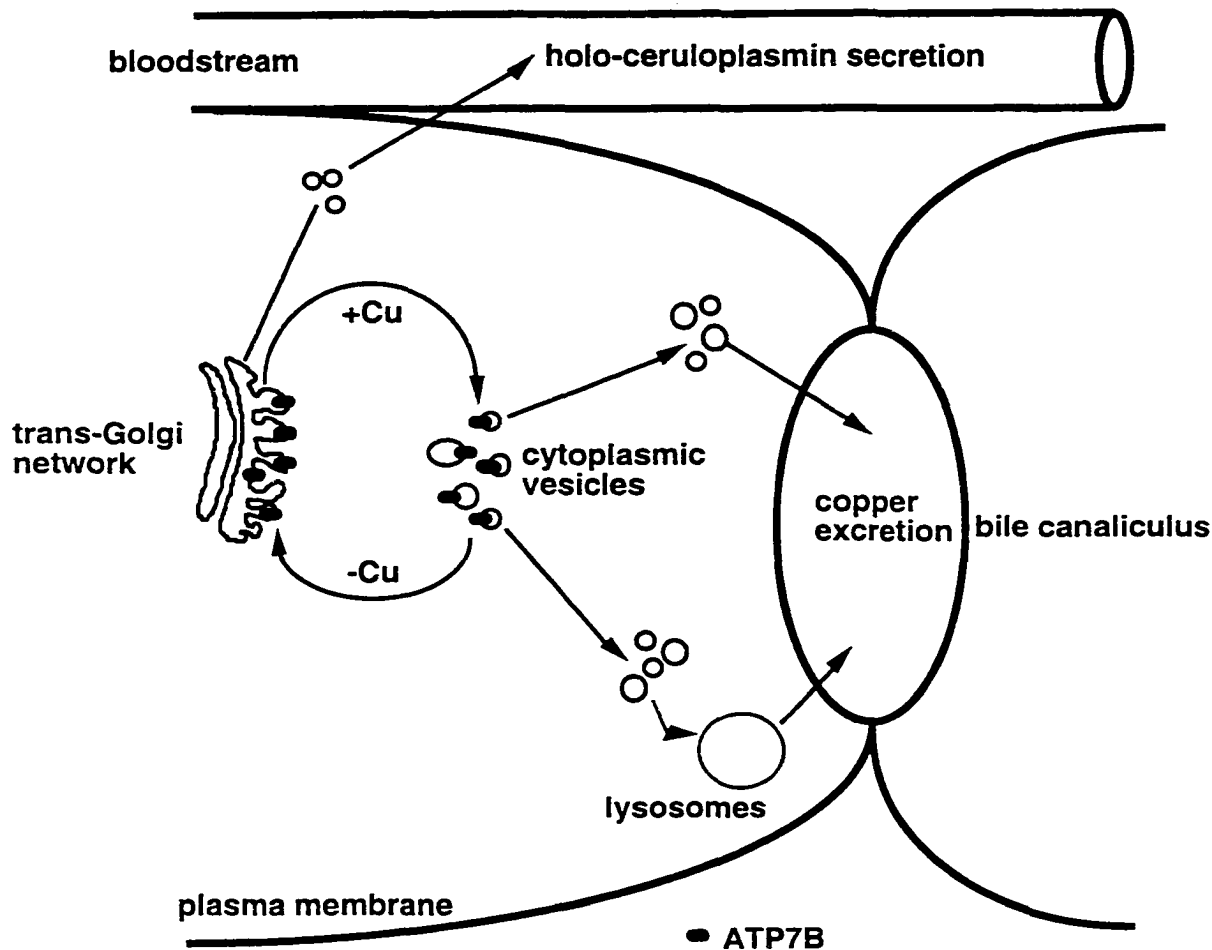


**Figure 1-4: Mammalian hepatic copper efflux mediated by ATP7B.**

ATP7B has a steady state localisation to the trans-Golgi network of hepatocytes under low copper conditions, where it incorporates copper into apo-ceruloplasmin during biosynthesis. Copper addition causes redistribution of ATP7B steady-state localization to a cytoplasmic vesicular compartment (probably endosomal). Presumably, ATP7B transports copper into this compartment for biliary efflux by endocytosis. Copper containing vesicles may be sorted directly to the canalicular plasma membrane for copper excretion into the bile. Alternatively, copper containing vesicles may be routed to the lysosomes prior to biliary excretion. Removal of excess copper triggers ATP7B redistribution back to the trans-Golgi network.

cellular damage. Copper within vesicles would be rapidly sequestered away from sensitive cellular components minimising oxidative damage if actual efflux could not be immediately achieved. Additionally, movement of ATP7B out of the Golgi network before large amounts of copper accumulates would prevent oxidative damage of proteins and lipids within this critical compartment.

Studies on the Bedlington terrier model of canine copper toxicosis may provide a biochemical mechanism to explain how copper contained in cytoplasmic vesicles is transported into the bile for excretion. Bedlington terriers accumulate large amounts of hepatic copper reminiscent of WD, however, molecular studies have ruled out genetic defects in *CTR1*, *CTR2*, *ATP7B*, or *ATOX1* genes as the basic defect in canine copper toxicosis (Daganais *et al.* 1999; van de Sluis *et al.* 1999). Consistent with normal ATP7B function, Bedlington terriers accumulate large amounts of hepatic copper within intracellular lysosomes and holo-ceruloplasmin biosynthesis and secretion is normal (Owen *et al.* 1982; Hultgren *et al.* 1986). These data suggest that the canine defect in hepatic copper efflux occurs at some point downstream of ATP7B dependent copper-transport into cytoplasmic vesicles/lysosomes. Perhaps copper containing vesicles within the endosomal compartment are not properly sorted, and therefore do not reach the plasma membrane by exocytosis for copper excretion resulting in excess lysosomal copper accumulation. Alternatively, there may be a defect in lysosomal exocytosis that prevents copper excretion.

Another avenue to elucidate the mechanism of ATP7B dependent vesicular/lysosomal copper efflux may come through the study of hereditary cholestasis. Since bile is the main route of copper elimination in humans, cholestatic diseases such as primary biliary cirrhosis, or extrahepatic biliary atresia can lead to hepatic copper accumulation (Beshgetoor *et al.* 1998; Danks, 1995). Two genes involved in hereditary cholestasis, *FIC1* and *PFIC2*, encoding P-type and ABC-cassette ATPase transport proteins respectively, have been identified and are thought to be involved in hepatic bile acid transport (Strautnieks *et al.* 1998; Bull *et al.* 1998). Patients with mutations in these genes accumulate hepatic copper. Presumably, ATP7B is functioning normally in these cholestasis patients suggesting a link between bile acid transport and copper efflux that may be revealed through biochemical study of the *PFIC2* and *FIC1* proteins.

The molecular mechanism of copper-dependent trafficking by ATP7B remains to be elucidated. Work on ATP7A revealed a copper-dependent trafficking event similar to ATP7B in most respects except that ATP7A moves from the trans-Golgi network to the plasma membrane following copper stimulation (Petris *et al.* 1996). Molecular studies on ATP7A have revealed that a C-terminal di-leucine motif is required for localisation of the

protein to the trans-Golgi network (Petris *et al.* 1998; Francis *et al.* 1999). ATP7A proteins with mutations in this motif were localised entirely to the plasma membrane, and could not recycle back to the trans-Golgi network in response to copper depletion suggesting that the motif was involved in retrieval of ATP7A from the plasma membrane. The mutant proteins could still mediate copper efflux, suggesting that the di-leucine is not involved in transport function, and that the plasma membrane is the site of ATP7A dependent copper efflux from the cell. A similar leucine-containing motif is present in ATP7B, which may provide a similar function, perhaps by interacting with a protein component of the secretory pathway.

A Golgi localisation signal was also identified in the third transmembrane segment of ATP7A (Francis *et al.* 1998). Deletion of exon 10 of ATP7A, resulted in localisation of the mutant protein, which lacked transmembrane segments three and four, to the endoplasmic reticulum. Fusion of the sequence encoding transmembrane segment three to a marker protein, resulted in localisation of the fusion protein to the Golgi, whereas sequences encoding transmembrane segment seven or eight, resulted in localisation of the fusion proteins to the endoplasmic reticulum, or plasma membrane, respectively. From these data the authors concluded that a Golgi targeting signal is present in transmembrane segment three of ATP7A. There is no extensive sequence conservation, besides hydrophobicity, between transmembrane segment three of ATP7A and ATP7B. If there is indeed a targeting signal in transmembrane 3 of ATP7A, it may be a conformational motif that could be conserved in ATP7B. Perhaps copper binding to ATP7A, causes conformational changes in the transmembrane domain, that mask the putative Golgi localisation motif, and allow movement to the plasma membrane.

## 1F) OUTLINE OF THESIS

The remainder of this thesis describes work done towards achieving the goals stated in section 1A. Chapter 2 is a methods chapter that describes the development of methods and resources, particularly antibodies and the yeast complementation assay, needed to perform the experiments described in subsequent chapters. Chapter 3 describes use of yeast complementation to analyse the effect of WD mutations on ATP7B function. Chapter 4 describes use of immunohistochemistry to determine the effect of WD mutations, for which we have functional data, on the subcellular localisation of ATP7B in mammalian cells. The role of the copper-binding domain of ATP7B, with respect to copper transport function, was analysed by functional assay of ATP7B copper-binding domain mutant proteins using yeast complementation. These data are described in Chapter 5. Chapter 6 summarises my data and puts it into the context of WD pathology,

ATP7B function, and mammalian copper homeostasis. All experiments were performed by J. Forbes unless specifically noted.

## **CHAPTER 2**

### **DEVELOPMENT OF REAGENTS AND METHODS.**

Methods and data discussed in this chapter have been published in the following publications:

Forbes, J.R., Hsi, G. and Cox, D.W. (1999) Role of the copper-binding domain in the copper transport function of ATP7B, the P-type ATPase defective in Wilson disease. *J.Biol.Chem.*, **274**:12408-12413.

Forbes, J.R. and Cox, D.W. (1998) Functional characterisation of missense mutations in ATP7B: Wilson disease mutation or normal variant? *Am.J.Hum.Genet.*, **63**:1663-1674.

DiDonato, M., Narindrasorasak, S., Forbes, J.R., Cox, D.W. and Sarkar, B. (1997) Expression, purification and metal binding properties of the N-terminal domain from the Wilson Disease putative Cu-transporting ATPase (ATP7B). *J.Biol.Chem.*, **272(52)**:32279.

Gloria Hsi (University of Alberta) contributed to sequencing and assembly of ATP7B expression constructs.

Michael DiDonato performed structural studies on the copper-binding domain of ATP7B with the assistance of Suree Narindrasorasak in Dr. Bibuhendra Sarkar's laboratory at the University of Toronto. Michael DiDonato contributed purified ATP7B copper-binding domain fusion protein for use in antibody production and purification described in this thesis.

Polyclonal antisera against the C-terminus of ATP7B were prepared in rabbits by Dr. Gregory Lee at the University of British Columbia. Polyclonal antisera against the N-terminal domain of ATP7B were prepared in rabbits by technicians of the Health Sciences Laboratory Animal Services at the University of Alberta.

## 2A) INTRODUCTION.

In order to study the function of ATP7B protein several resources were first required: a cDNA encoding the full-length ATP7B polypeptide, a heterologous expression system, antibodies to detect the expressed ATP7B, and an assay to measure the function of ATP7B. This chapter describes the development of these resources.

Specific antibodies against a protein of interest are a valuable resource. These can be used for many experiments including detection of expressed recombinant proteins in heterologous systems, distribution of proteins in tissues by immunohistochemistry, determination of the subcellular localisation of proteins in cells, and characterisation of protein-protein interactions by co-immunoprecipitation strategies (Harlow *et al.* 1988). Preparation of rabbit polyclonal antibodies against ATP7B fusion proteins was the method chosen to pursue. This approach was taken over other possible methods since polyclonal antibodies tend to have a high affinity for the antigen, and generally recognise both sequential and conformational epitopes (Harlow *et al.* 1988). These attributes usually result in antibodies that are useful for a wide range of experimental methods, especially when affinity purified to reduce, or eliminate, non-specific binding. In contrast, monoclonal antibodies are often low affinity, and recognise only a single epitope. Therefore they may not recognise the target protein if the epitope is disrupted or hidden (e.g. fixed cells or tissues) or be suitable for experiments such as immunoprecipitation, for which a high epitope binding affinity is required (Harlow *et al.* 1988). Therefore monoclonal antibodies may only be useful for a limited number of experiments making them potentially a less versatile reagent than polyclonal antibodies. Tagging of recombinant proteins by addition of sequences encoding known epitopes from proteins such as haemagglutinin or c-myc is also a viable means of detecting proteins expressed in a heterologous system (Harlow *et al.* 1988). This method has the advantage that sequence tagging can be done rapidly by molecular means, and antibodies against a variety of epitopes are commercially available. Protein specific antibodies, however, are a more versatile reagent that can detect native proteins, either endogenous or transfected, in tissues or cell lines, which cannot be done with epitope tags.

Yeast, *S. cerevisiae*, was chosen as both a heterologous expression system, and as means to develop a functional assay for ATP7B. Yeast can typically perform most post-translational modifications used by higher eukaryotes, can express proteins at high levels, and are readily manipulated by genetic means, making them an ideal system for heterologous expression of mammalian proteins (Bradley, 1990). More importantly, the copper-transport pathways in yeast have been well characterised genetically and

biochemically, as described in Chapter 1. In *ccc2* mutant yeast cells, which lack the Ccc2p copper transport function, copper is not incorporated into apo-Fet3p resulting in complete arrest of high-affinity iron uptake (Yuan *et al.* 1995). I made the hypothesis that ATP7B could replace Ccc2p in yeast, complementing the high-affinity iron uptake deficiency of the *ccc2* mutant yeast. This hypothesis proved to be correct, and subsequently complementation of the *ccc2* mutant yeast strain by ATP7B was exploited as an assay to study the function of ATP7B and ATP7B mutant proteins.

## **2B) MATERIALS AND METHODS.**

### **2B-1) General molecular-biology techniques.**

For analysing or purifying cloned cDNA fragments, plasmid DNA was digested with the appropriate restriction enzymes in buffers provided by the manufacturer (New England Biolabs, Boehringer Mannheim, Promega, Gibco/Life Technologies). Digested DNA was separated on agarose gels containing ethidium bromide, in Tris-borate-EDTA (TBE) buffer (Ausubel *et al.* 1998). The required cDNA fragment was cut from the gel, and/or the gel was photographed. DNA from gel slices was purified using the QiaQuick method according to the manufacturer's protocol (Qiagen).

cDNA ligations were carried out using T4 DNA ligase, in the buffer provided by the manufacturer (Gibco/ Life Technologies. New England Biolabs). Chemically competent DH5 $\alpha$  *E. coli* cells (Life Technologies) and carbenicillin selection were used for transformations and plasmid propagation according to the manufacturer's protocols. Alternatively, transformations were done by electroporation into XL-1Blue *E. coli* cells (Stratagene) using cells prepared as described (Ausubel *et al.* 1998). Electroporation conditions were as follows: 50  $\mu$ L of cells were placed in a sterile 2mm gap electroporation cuvette (BTX) with 1-2  $\mu$ L of ligation mixture. The mixture was subjected to electroporation with 2500 V, 200  $\Omega$  resistance, and 25  $\mu$ F capacitance using a BioRad electroporator. Immediately following electroporation, 1 mL of Luria-Broth (LB), or SOC, medium (Difco) was added to the cuvette, and the cells were incubated for 30 min. to 1 hr at 37°C, prior to plating on LB-agar with carbenicillin selection. *E. coli* strains were propagated in liquid LB medium (Difco), or solid LB medium made by adding 2% (w/v) Bacto-Agar (Difco) containing 100  $\mu$ g/mL carbenicillin. All DNA minipreps were prepared from 5 mL of *E. coli* culture using the QiaPrep-Spin Mini kits according to manufacturer's protocol (Qiagen).

Polymerase chain reaction (PCR) amplification was carried out as follows. Either 0.5-1 unit of *Taq* (Roche) or *pfu* (Stratagene) polymerase was used in the buffer provided by the manufacturer. Reaction mix consisted of reaction buffer, 2 mM each of dATP,

dCTP, dTTP, and dGTP nucleotides, 1.5 mM magnesium chloride, 50 ng of each oligonucleotide primer, and template DNA. Reactions were typically performed in a 25  $\mu$ L total volume, and the reaction mixtures were overlaid with a drop of mineral oil. Typical reaction conditions were as follows: 2 min. 95°C denaturation, followed by 15-35 cycles of 30 sec. 95°C denaturation, 30 sec. 55-58°C primer annealing, then 72°C extension. Extension time was altered depending on the size of the desired amplicon. For *Taq* polymerase, 1 min. per 2 kilobase (kb) of sequence was used, and for *pfu* polymerase, 2 min. per kb of sequence was used.

### **2B-2) Construction of *ATP7B* cDNA.**

Total human liver RNA was obtained from Dr. Roderick McInnes's laboratory at the Hospital for Sick Children (Toronto, Ontario). Subsequently, this was used as template for reverse transcription, using murine molony leukaemia virus reverse transcriptase, according to the manufacturers protocol (Pharmacia). Random hexamer primers, diluted ten fold from the manufacturers stock to allow larger fragment sizes, were used to reverse transcribe cDNA for amplification of the two 5' most cDNA fragments. The remaining reverse transcription reactions were performed using oligo-d(T) primers. cDNA obtained by this method, was used as a template for PCR amplification, using *pfu* polymerase, of five overlapping fragments containing the 4.395 kb coding region of *ATP7B*. Primers were chosen such that unique restriction sites were present near the ends of each cDNA fragment, facilitating construction of the full-length cDNA. Primers are listed in the appendix (Table A-1). A 5' Bam HI site was added to the PCR primer sequence immediately preceding the initiating ATG codon, for use in cloning into expression vectors. Following PCR, DNA fragments were adenylated by incubation with 1 unit of *Taq* polymerase for 10 min. at 72°C, to allow cloning with T/A-cloning vectors (Promega, Invitrogen). The two 5' cDNA fragments encoding the copper-binding domain, proved to be unstable when transformed into bacteria, resulting in plasmid mutation and rearrangements. This instability was corrected by the addition of 100  $\mu$ M copper sulphate to the culture medium. Each fragment was sequenced (Sequenase, Amersham) according to the manufacture's protocol to ensure sequence fidelity. Correct cDNA fragments were gel-purified and the full-length cDNA was constructed by ligating the fragments together. The final cDNA construct was cloned into pUC19 using the 5' Bam HI site and a 3' Sal I site from the polylinker of the Promega T/A vector. The full-length *ATP7B* plasmid was isolated from two large scale bacterial cultures using ion exchange chromatography (Mega-Prep columns, Qiagen)

according to the manufacturer's protocol. This plasmid stock was used as the source of *ATP7B* cDNA for all subsequent experiments.

### **2B-3) cDNA constructs for ATP7B fusion proteins.**

For the purpose of raising antibodies against ATP7B, antigenic regions were predicted using the method of Hopp and Woods (Hopp *et al.* 1981). Three fusion proteins were initially chosen; Pept1 (residues 179-262) between copper-binding motifs two and three, Pept2 (residues 292-364) between copper-binding motifs 3 and 4, and Pept3 (residues 1375-1465) corresponding to the C-terminal end of ATP7B. These polypeptides represented the most hydrophilic regions of ATP7B, and shared limited sequence identity with ATP7A such that they were predicted not to cross-react. DNA fragments encoding these polypeptides were amplified by PCR from cosmids containing the *ATP7B* genomic sequence using the primers shown in the Appendix (Table A-2). An in-frame Nde I restriction site was incorporated into each 5' primer, and a Bam HI restriction site into each 3' primer to allow cloning into the expression vector. PCR was carried out with *Taq* polymerase (Roche). The DNA fragments were cloned directly into a PCR cloning vector (T/A vector, Invitrogen). Individual clones were then sequenced to ensure sequence fidelity (Sequenase, Amersham). Correct DNA fragments were removed from the cloning vector by restriction enzyme digest using Bam HI and Nde I. Gel purified DNA fragments were ligated in-frame into the *E. coli* expression vector pET-16b (Novogen) using corresponding restriction sites in the vector polylinker. This vector expresses proteins as an N-terminal 6xHistidine fusion (His-tag) under control of an inducible T7/Lac promoter.

An expression construct encoding the N-terminal copper-binding domain of *ATP7B* was also made. The cDNA construct encoding amino acid residues 1-649 was made using the two 5' most cDNA fragments generated during construction of the full-length *ATP7B* cDNA. This cDNA incorporated a 5' Bam HI site and a 3' Sal I site for cloning into bacterial expression vectors.

### **2B-4) SDS-PAGE and immunoblotting.**

Sodium dodecyl sulphate polyacrylamide gel electrophoresis (SDS-PAGE) was performed using the discontinuous method of Laemmli (Laemmli, 1970). Reagents were prepared as described in Current Protocols (Ausubel *et al.* 1998). SDS-PAGE was performed using a 4% polyacrylamide (37.5:1 acrylamide:bis-acrylamide) stacking gel. 15% polyacrylamide separating gels were used for bacterial fusion proteins. Yeast cell protein extracts containing full-length ATP7B protein were electrophoresed on 7.5% separating gels. Protein was mixed with Laemmli loading buffer (Laemmli, 1970)

containing 50 mM dithiothreitol (DTT) and heated for 5 minutes at 100°C (bacterial fusion proteins) or at 75-85°C (full-length ATP7B protein) and loaded onto gels. Gels were typically electrophoresed in Mini-gel format on the Mini-Protean 2 apparatus (BioRad). Proteins in the gel were visualised by staining with Coomassie blue as described in Current Protocols (Ausubel *et al.* 1998).

For immunoblot experiments, proteins in unstained SDS-PAGE gels were transferred electrophoretically to polyvinylidene difluoride (PVDF) membrane using either the Mini-Protean 2 apparatus, or Protean 2Xi apparatus with plate electrodes (BioRad). Bacterial proteins were transferred for approximately 250 volt-hours (V·hr) in Towbin buffer (Towbin *et al.* 1979) containing 20% methanol. Yeast or mammalian cell extract containing full-length ATP7B protein was transferred for 450 V·hr in Towbin buffer (Towbin *et al.* 1979) containing 15% methanol and 0.01% SDS. Immunoblotting was performed as follows. Membranes were blocked with 5% milk powder in Tris-buffered saline (TBS, 100 mM Tris-HCl pH 7.5, 150 mM NaCl) for 30 min.- 1 hr. The membranes were washed 2 x 5 min. with TBS containing 0.1% Tween -20 (TBST). Membranes were incubated with primary antibodies in TBST for 1 to three hr. (antibodies and dilutions detailed in the appropriate sections or figures). Membranes were then rinsed twice with TBST followed by 3 x 5 min. washes in the same. Secondary antibodies were horseradish peroxidase conjugated goat anti-rabbit antibodies (Pierce Chemical) incubated for approximately 1 hr. in TBST. The membranes were rinsed 3x in TBST, and then washed 4 x 5 min. in the same. Bound antibodies were detected by enhanced chemiluminescence (ECL) using Supersignal substrate (Pierce Chemical) or in later experiments using Supersignal Ultra (Pierce Chemical) substrate with reduced concentrations of antibodies. ECL was detected by exposure to autoradiography film (Fuji).

### **2B-5) Expression of fusion proteins in *E. coli*.**

For expression of His-tagged fusion proteins, the complete expression vectors were transformed into the chemically competent *E. coli* BL21(DE3) strain according to manufacturers protocol (Novogen). To test for fusion protein expression, 5 mL overnight cultures of bacteria grown in 2xYT medium with carbenicillin (100 µg/mL), were used to inoculate fresh 5 mL cultures at a 1 in 10 dilution. Cells were grown at 37°C for one hour prior to induction with 1 mM isopropylthio-β-D-galactoside (IPTG). Protein was expressed for 3 hours following induction. Bacterial protein from 1 ml of pelleted culture was analysed by SDS-PAGE after cell lysis by boiling in sample buffer. Alternatively, cell pellets were resuspended in buffer and disrupted by sonication prior to SDS-PAGE.

Pept1 and Pept2 were very poorly expressed in *E. coli* under all expression conditions attempted. Therefore only Pept3 (C-terminal tail of ATP7B) was used in subsequent experiments.

For large-scale expression of Pept3 protein, a 50 mL culture was grown overnight at 37°C to saturation in 2xYT medium containing carbenicillin (100 µg/mL). This culture was inoculated into 500 mL of the same medium, and after 3 hours growth at 37°C, protein expression was induced by addition of IPTG to a final concentration of 1 mM. Protein was expressed for 4 hours. The culture was divided in half, chilled, and *E. coli* cells collected by centrifugation. The cell pellets were frozen at -70°C prior to protein purification. The purification procedure was based on one described in Current Protocols (Ausubel *et al.* 1998). The basic buffer used for the purification procedure was 20 mM Tris-HCl pH 7.9, 0.5 M NaCl. Pept3 protein was entirely insoluble and was therefore purified by nickel-affinity chromatography under denaturing conditions. Cell pellets were resuspended in buffer containing 6 M guanidine-HCl (lysis buffer), and lysed by a cycle of freezing and thawing, followed by 1 hr of gentle agitation at room temperature. The lysate, cleared of insoluble material and genomic DNA by centrifugation, was loaded onto a 2.5 mL bed volume column of nitrilotriacetic acid (NTA)-sepharose (Qiagen) charged with nickel, that was equilibrated with lysis buffer. Protein was allowed to bind to the column. The column was then re-equilibrated with buffer containing 8 M urea as denaturant instead of guanidine-HCl. Urea was used as the denaturant in all subsequent buffers. Protein bound to the affinity columns was washed in a stepwise fashion with 10 column volumes of buffer containing 20 mM, 40 mM, 60 mM, 100 mM, then 250 mM imidazole. Column fractions were analysed by SDS-PAGE and gel staining with Coomassie blue. Fractions containing pure fusion protein were combined, and dialysed extensively against 20 mM Tris-HCl pH 7.9, 0.5 M NaCl, to remove the urea. Protein was quantified using the Bradford assay (BioRad) with bovine serum albumin (BSA) as the standard.

The N-terminal copper-binding domain of ATP7B was expressed and purified as described by DiDonato *et al.* (1997).

#### **2B-6) Production of rabbit polyclonal antibodies against ATP7B.**

For production of polyclonal antiserum against the C-terminal polypeptide of ATP7B, the purified and dialysed Pept3 protein was lyophilised. Lyophilised protein was resuspended, conjugated to keyhole limpet haemocyanin (KLH), and injected into rabbits by Dr. Gregory Lee at the University of British Columbia.

For production of polyclonal antibodies against the copper-binding domain of ATP7B, purified glutathione-S-transferase (GST) fusion protein, containing the ATP7B copper-binding domain, was obtained in lyophilised form from Michael DiDonato (Hospital for Sick Children). Once obtained, the lyophilised protein was redissolved in sterile phosphate buffered saline (PBS, 4.3 mM Na<sub>2</sub>HPO<sub>4</sub>, 1.4 mM KH<sub>2</sub>PO<sub>4</sub>, 2.7 mM KCl, 137 mM NaCl) containing 2% SDS. For each of two rabbits (New Zealand White, Vandermeer Rabbits) used, one mL of protein solution was emulsified with an equal volume of Freund's complete adjuvant (Sigma Chemical). This mixture was injected into the rabbits using one 0.5 mL intramuscular injection, and four 0.25 mL subcutaneous injections. A total of approximately 375 µg of protein was injected each time. The injections were repeated three weeks later using Freund's incomplete adjuvant (Sigma Chemical). A second booster injection was performed 10 days later. Three weeks later the rabbits were anaesthetised, exsanguinated, and then euthanised. Antiserum was collected by centrifugal removal of clotted red blood cells. Antisera obtained 10 days after each injection were titred against ATP7B protein expressed in yeast by immunoblotting. Animal housing, and animal handling, was done by technicians of the Health Sciences Laboratory Animal Services at the University of Alberta in accordance with the guidelines published by the Health Sciences Animal Welfare committee.

#### **2B-7) Affinity purification of ATP7B antibodies.**

Initial affinity purification of the Pept3 antiserum was performed as follows (Harlow *et al.* 1988). Pept3 fusion protein (250 µg) was electrophoresed on 15% SDS-PAGE gels in a single lane made using a preparative gel comb. Protein was electrophoretically transferred to PVDF membrane, stained with Ponceau S reagent. The antigen band was cut out and rinsed free of stain with distilled water. Several antigen containing membrane strips were blocked with 3% BSA in PBS containing 0.1% Tween-20 (PBST). Strips were then incubated overnight at 4°C with 500 µL of rabbit antiserum diluted in PBST. Strips were washed extensively with PBST and bound antibodies eluted with 50 mM glycine pH 2.7. The eluate was neutralised with Tris buffer and concentrated using a Centricon-30 (Amicon) ultrafiltration device. The final antibodies, designated anti-ATP7B.C10, were made to 1xPBS and 0.1% BSA for storage at -20°C.

Later experiments used an affinity column method. Seven milligrams of Pept3 fusion protein, were coupled to a 5 mL gel-volume N-hydroxysuccinimide (NHS)-activated sepharose column (Hi-trap, Pharmacia) according to the manufacturers protocol. Coupling buffer consisted of 0.2 M NaHCO<sub>3</sub>, 0.5 M NaCl, and 100 mM guanidine-HCl to maintain solubility of the fusion protein. One mL of rabbit antiserum

was diluted to 5 mL in TBS, and then applied to the affinity column. After three hours incubation at room temperature, the column was washed extensively with TBS, and the bound antibodies eluted with six column volumes of Gentle Ab/Ag Elution buffer (Pierce Chemical) collected in 5 mL fractions. Fractions containing the antibodies were identified spectroscopically by measuring absorbance at 280 nm. Pooled antibody-containing fractions were dialysed against TBS, and concentrated using a Centricon-30 ultrafiltration device (Amicon) with a 30 kDa molecular weight cut-off. The concentrated antibodies were stored in TBS buffer containing 0.1% BSA, 0.1% thimerosal (as preservative), and 40% glycerol. The purified antibodies were designated "anti-ATP7B.C10".

For purification of antibodies against the copper-binding domain of ATP7B, 10 mg of fusion protein, in which the GST fusion domain was enzymatically cleaved as described by DiDonato *et al.* (1997) was obtained from Michael DiDonato (University of Toronto). Subsequently, the copper-binding domain fusion protein was coupled to a NHS-activated sepharose column in an identical fashion to the Pept3 fusion protein except that the protein was prepared in coupling buffer without added denaturant. Two mL of antiserum was used for the affinity purification and was done as described for anti-ATP7B.C10. The purified antibodies are designated "anti-ATP7B.N60". Following each experiment, the affinity columns were washed extensively with TBS, sealed, and then stored at 4°C containing TBS with 0.1% thimerosal as preservative.

#### **2B-8) Yeast strains and transformation.**

The wild-type strain used in all experiments was the vacuolar protease deficient *S. cerevisiae* strain BJ2168 (*MATa pep4-3 prc1-407 prb1-1122 ura3-52 trp1 leu2*) (Zubenko *et al.* 1980) obtained from Dr. Morrie Manolson at the University of Toronto (Toronto, Canada). Gene disruption plasmids p $\Delta$ fet3 (A. Dancis, unpublished) and E5-URA3.4 (Yuan *et al.* 1995) were obtained from Dr. Danial Yuan at the NIH (Bethesda, MD, U.S.A). Once obtained, these plasmids were used to make the yeast mutants *fet3* and *ccc2*, lacking functional *FET3* and *CCC2* genes, by transformation of BJ2168 with p $\Delta$ fet3 and E5-URA3.4 respectively. Prior to transformation, p $\Delta$ fet3 was linearised by digestion with Xho I and Xba I, and E5-URA3.4 was linearised by digestion with Bam HI and Not I. The linearised plasmids were ethanol precipitated, pelleted and then transformed into yeast. Integrations were selected on synthetic dextrose (SD) medium, made from 0.17% yeast nitrogen base without glucose or ammonium sulphate (Difco), supplemented with all amino acids except uracil, 2% glucose, and 0.5% ammonium sulphate (Kaiser *et al.* 1994). Solid SD medium, in petri dishes, was made by adding 2%

Bacto agar (Difco) to the liquid SD medium. Several single transformant colonies were isolated and streaked again onto selective medium. These transformants were plated on SD medium using non-fermentable glycerol carbon source instead of glucose either unsupplemented, or supplemented with 500  $\mu$ M copper sulphate, or 1 mM ferrous ammonium sulphate to confirm that the metal-dependent respiration deficiency phenotype of the new mutant strains was the same as was previously described (Yuan *et al.* 1995; Kaiser *et al.* 1994). All yeast transformations were performed using a modified lithium acetate method (Elble, 1992; Kaiser *et al.* 1994).

### **2B-9) Construction of Yeast expression Vectors.**

For high level expression of ATP7B in yeast, cDNAs were liberated from pUC19 vector by restriction digest, gel-purified, then ligated into a multicopy 2 $\mu$  replication origin vector pG3 (Schena *et al.* 1991) using Bam HI and Sal I restriction sites. pG3 vector was obtained from Dr. Morrie Manolson at the University of Toronto (Toronto, Canada). This vector utilises a strong, constitutive, glyceraldehyde-3-phosphate dehydrogenase (GAPDH) promoter, a phosphoglycerate kinase (PGK) terminator and polyadenylation sequence, and a tryptophan selectable marker. Using pG3 as starting material, a singlecopy integrating vector named pG4 was derived. The pG3 2 $\mu$  origin of replication, carried on a single Eco RI fragment, was removed by restriction enzyme digestion. The vector lacking its yeast origin of replication was gel-purified and ligated to form pG4. ATP7B cDNAs were cloned into pG4 as for pG3.

Expression vectors were transformed into yeast and transformants selected on SD medium made as described in section 2B-8 but containing uracil and lacking tryptophan. Single-colonies were restreaked onto selective medium to ensure clonality. Prior to transformation, pG4 constructs were linearised by digestion with Xba I, which targets the integration to the yeast *trp1* locus, and then ethanol precipitated. Genomic DNA from yeast strains carrying pG4 constructs was isolated as described in Current Protocols (Ausubel *et al.* 1998). This DNA was analysed by Southern blotting to confirm that the constructs were correctly integrated as a singlecopy. Five  $\mu$ g of genomic DNA was restriction enzyme digested with Bam HI (which cuts once within the expression construct) and electrophoresed for approximately 500 V·hr on a 0.6% agarose gel. Southern blotting was performed using alkaline transfer from the gels onto Hybond-N+ membrane as described by the manufacturer (Amersham). ATP7B cDNA was labelled with  $^{32}$ P (Amersham) by random priming using a T7 Quickprime kit according to the manufacturers protocol (Pharmacia). For singlecopy integrations, a single high molecular weight band was visible following autoradiography (BioMax MS film, Kodak). If

multicopy integrations occurred, a second band equal to the combined size of ATP7B cDNA and the expression vector was visible (approx. 9 kb for full-length ATP7B constructs).

#### **2B-10) Yeast complementation assay.**

Base assay medium consisted of 0.17% (w/v) yeast nitrogen base lacking iron, copper, glucose, and ammonium sulphate (Bio-101), and supplemented with all amino acids except tryptophan (Kaiser *et al.* 1994), 50 mM MES buffer pH 6.1, 2% (w/v) glucose, and 0.5% (w/v) ammonium sulphate. Iron-limited medium was base assay medium containing 1 mM ferrozine (an iron specific chelator), 50  $\mu$ M ferrous ammonium sulphate, and 1  $\mu$ M copper sulphate. Iron-limited medium was supplemented to 500  $\mu$ M copper sulphate or 350  $\mu$ M ferrous ammonium sulphate to make copper or iron-sufficient control media respectively. For the plating assay, solid media was made containing 2% Bacto agar (Difco). Cells were prepared for plating assays in the following manner: stationary yeast cultures grown in standard SD liquid culture lacking tryptophan were washed with sterile ice-cold distilled water, resuspended in liquid iron-limited medium then grown to saturation overnight. These cultures were diluted to an optical density of  $A_{600}=0.1$  in 1 mL of sterile deionized water. Five  $\mu$ L of this cell suspension was streaked onto plates containing assay media. Cells were grown at 30°C and then photographed after 48 hours.

#### **2B-11) Fet3p oxidase assay.**

Fet3p oxidase activity was measured using a modified version of the assay described by Yuan *et al.* (1995). Cells were grown to mid-log phase at 30°C in SD media lacking tryptophan, iron, and copper, and supplemented with 50 mM MES buffer pH 6.1 and 0.1- 0.5  $\mu$ M copper sulphate. Buffer for homogenisation consisted of 25 mM HEPES-NaOH pH 7.4, 150 mM NaCl, and a protease inhibitor cocktail of 30  $\mu$ M leupeptin, 10  $\mu$ M pepstatin A, and 5  $\mu$ M aprotinin. Buffer was supplemented during homogenisation with 1 mM bathocuproine disulfonate (BCS, a copper chelator), and 1 mM ascorbate, to prevent copper loading of Fet3p during homogenisation, or 50  $\mu$ M CuSO<sub>4</sub> to reconstitute apo-Fet3p *in vitro* during homogenisation, as a positive control. Cells from 25 mL of culture were washed twice with ice-cold deionized water, once with 800  $\mu$ L of supplemented buffer, then resuspended in 200  $\mu$ L of the same. Cells were lysed by vortexing with glass beads (425-600 micron diameter, Sigma Chemical) for a total of 5 minutes (cycles of 30 sec. vortex, 1 min. on ice). Yeast membranes were recovered by addition of 800  $\mu$ L of buffer supplemented as above, and the supernatants were cleared of unbroken cells and heavy organelles by centrifugation for 30 sec. at

10,000 xg. This step was repeated once. Membranes were collected by centrifugation at 20,000 xg for 30 min., then washed with buffer containing 1 mM BCS. The final membrane pellet was made soluble in 100  $\mu$ L of buffer containing 1 mM BCS and 1 % Triton X-100. Insoluble material was removed by centrifugation at 20,000 xg for 20 min. Protein was quantified using the Enhanced Bradford assay (Pierce Chemical). Thirty  $\mu$ g of soluble membrane proteins were dissolved in Laemmli loading buffer (Laemmli, 1970) lacking DTT and run on 7.5% SDS-PAGE gels without prior heating. Gels were equilibrated for 30 min. in 500 mL of oxidase buffer containing 100 mM sodium acetate pH 5.7, 10 % glycerol, 1 mM sodium azide and 0.05 % Triton X-100, followed by two further 15 min. incubations in 250 mL of the same buffer. Equilibrated gels were soaked in 20 mL/gel of buffer containing 100 mM sodium acetate pH 5.7, 0.5 mg/mL p-phenylenediamine dihydrochloride substrate, and 1 mM sodium azide for one hour in the dark. Gels were incubated overnight in the dark between cellophane sheets in a humidified box to develop bands of oxidase activity. All glassware and glass beads for cell disruption were washed extensively with copper free 1M hydrochloric acid (J.T. Baker, "Instra-Analysed" grade), and well rinsed with deionized water (Milli-Q, Millipore) to eliminate copper contamination.

### **2B-12) Yeast protein preparation.**

Yeast total cell protein extracts were prepared as follows: Homogenisation buffer consisted of 25 mM HEPES-NaOH pH 7.4, 150 mM NaCl, 1 mM DTT, and a protease inhibitor cocktail containing 30  $\mu$ M leupeptin, 10  $\mu$ M pepstatin A, 5  $\mu$ M aprotinin and 1 mM EDTA. Cells from 10 mL of stationary culture were washed twice with ice-cold distilled water, once with homogenisation buffer, and resuspended in 200  $\mu$ L of the same. Cells were broken by vortexing in the presence of acid washed glass beads (425-600 micron diameter, Sigma Chemical) for a total of 5 min. (cycles of 30 sec. vortex, 30 sec. on ice). The homogenate was centrifuged for 30 sec. at 10,000 xg to remove unbroken cells and heavy organelles. Protein content was estimated using the Enhanced Bradford Assay (Pierce Chemical).

## **2C) RESULTS**

### **2C-1) Construction of *ATP7B* cDNA.**

*ATP7B* cDNA was constructed by ligating together 5 overlapping fragments generated by RT-PCR (Fig. 2-1). The two fragments encoding the copper-binding domain proved to be unstable and prone to frequent deletion and mutation when grown in *E. coli*. Any expression of these fragments during growth was postulated to produce a

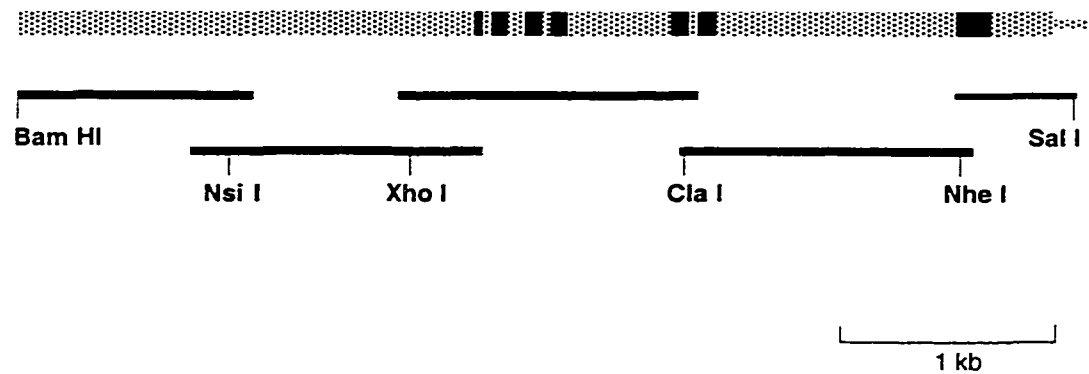


**Figure 2-1: Schematic of *ATP7B* cDNA construction.**

The *ATP7B* coding region is represented by the stipled line. Within the coding region, black bars represent the putative transmembrane segments. Black lines represent *ATP7B* cDNA fragments generated by RT-PCR. The cDNA fragments were joined at the indicated restriction enzyme sites to construct the full-length *ATP7B* coding region. Bam HI and Sal I sites were added during PCR.

polypeptide capable of binding copper, resulting in copper depletion within bacterial cells, such that only cells harbouring deleted or mutated cDNAs were capable of growth. Therefore, these clones were stabilised by supplementing the growth medium with copper sulphate. The full-length cDNA was ligated into pUC19 vector with the coding region in reverse orientation to the vector's *lacZ* promoter. *ATP7B* cDNA cloned in this manner was stable in *E. coli* without added copper. Another possibility would have been to use a low-copy bacterial vector to promote stability of the *ATP7B* cDNA (Fontaine *et al.* 1998). The complete cDNA was sequenced to ensure its fidelity prior to its use in further experiments.

### **2C-2) Expression of ATP7B fusion proteins in *E. coli*.**

Three fusion proteins were initially chosen for expression in bacteria; Pept1 between copper-binding motifs two and three, Pept2 between copper-binding motifs 3 and 4, and Pept3 corresponding to the C-terminal end of *ATP7B*. Pept1 was expressed very poorly in *E. coli*, and Pept2 expression could not be detected on SDS-PAGE gels stained with Coomassie blue. Pept1 and Pept2 expression could not be significantly improved by manipulating the expression conditions (done with the help of Elizabeth Whiting) and were not pursued further. Pept3 however was robustly expressed. Differential centrifugation experiments showed that Pept3 protein was contained entirely within bacterial inclusion bodies. As a result the protein purification was performed under denaturing conditions by nickel affinity chromatography as described in the materials and methods section of this chapter. The fusion protein eluted completely in wash buffer containing 100 mM imidazole (Fig. 2-2). There was little contamination by *E. coli* proteins and the protein was judged to be suitable for use generating rabbit polyclonal antibodies. The purified protein was dialysed extensively against Tris buffer to remove the urea. However in the absence of denaturant the protein precipitated into insoluble aggregates. The insoluble material was collected, lyophilised, and sent for use in production of antibodies at the Canadian Genetic Disease Network Hybridoma core facility.

A GST-fusion protein containing the entire N-terminal copper-binding domain of *ATP7B* was also prepared. The copper-binding domain fusion protein was expressed and purified by Michael DiDonato as described by DiDonato *et al.* (1997).

### **2C-3) Production and affinity purification of ATP7B rabbit polyclonal antibodies.**

Polyclonal antiserum against Pept3 fusion protein, was raised in rabbits by Dr. Gregory Lee, at the Canadian Genetic Disease Network Hybridoma core facility at the University of British Columbia (Vancouver, Canada). The antiserum obtained from Dr.

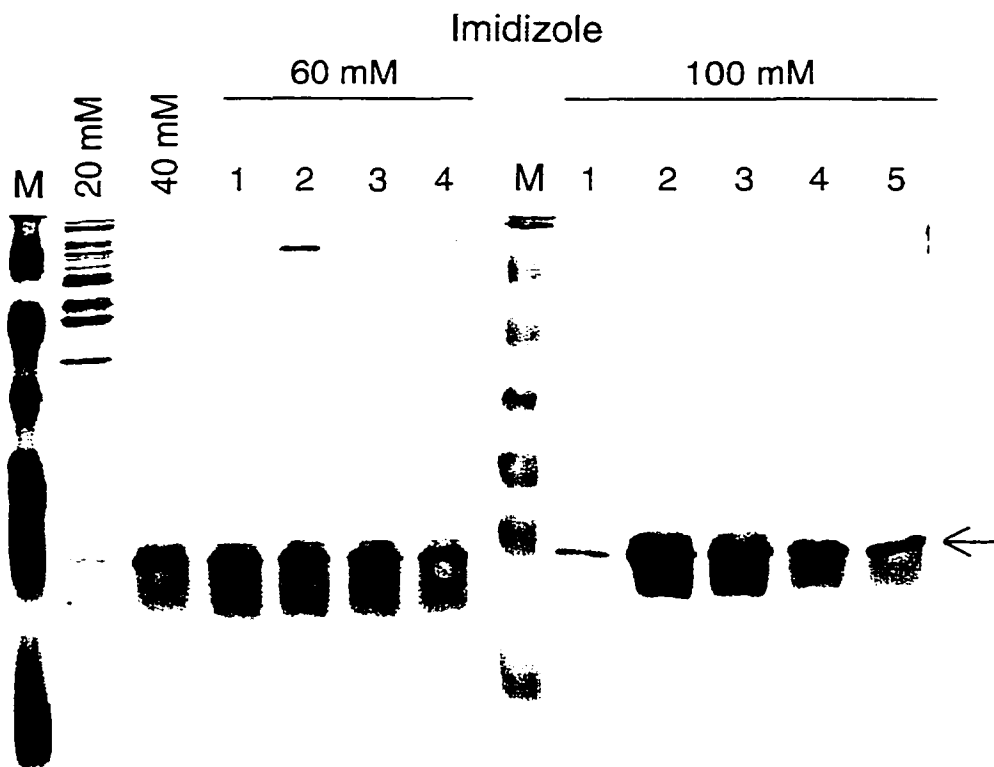


**Figure 2-2: Example of nickel affinity purification of 6xHis-tagged Pept3 fusion protein expressed in *E.coli*.**

SDS-PAGE gels of affinity column fractions were stained with Coomassie blue. Protein was bound to the column under denaturing conditions and washed with buffer containing increasing concentrations of imidazole. Imidazole concentrations and fraction numbers are indicated on the figure. Pept3 protein eluted in the 60 and 100 mM imidazole fractions. The arrow indicates the position of Pept3 protein. The molecular weight marker is indicated by "M".

Lee was analysed by immunoblotting. The antiserum recognised the Pept3 band while the pre-immune serum did not, indicating the antiserum was specific. The antiserum also recognised bands corresponding to bacterial proteins found as contaminants in the antigen preparation (Fig. 2-3), however these bands could be eliminated by diluting the antiserum. The antiserum was capable of recognising ATP7B protein expressed in yeast, while the pre-immune serum was not.

GST fusion protein containing the copper-binding domain of ATP7B was used to prepare polyclonal antibodies in rabbits. Antiserum from each of two rabbits, was tested by immunoblotting against ATP7B protein expressed in yeast. The antisera were able to detect ATP7B protein, while the pre-immune sera were not (Fig. 2-3).

While the antibodies were capable of recognising ATP7B protein, there was still considerable background binding therefore affinity purification of the antiserum was performed. Initial purification of the Pept3 antiserum was done by a membrane binding method as described in section 2B-7. This method had the advantage that it could be done with insoluble protein. Affinity purification of the Pept3 antiserum using this method resulted in a considerable improvement in antibody specificity. Background binding in bacterial extracts was eliminated and the purified antibodies recognised ATP7B protein expressed in yeast with little non-specific signal (Fig. 2-4).

While the membrane-based purification method was successful, the method is very inefficient and chemically harsh resulting in much loss of antibodies, and very likely selects for antibodies that bind strongly to denatured membrane bound protein, which may reduce the efficacy of the purified antibodies for techniques other than western-blotting. Therefore an alternative approach was established. Activated NHS-sepharose columns were obtained from Pharmacia. The NHS moiety reacts with amine functional groups on proteins resulting in covalent coupling of the protein to the sepharose beads in the column via a six carbon atom linker. This method has the advantage over other methods, for example CNBr coupling, because the reaction will work in the presence of guanidine-HCl denaturant (Pharmacia). Therefore, the Pept3 fusion protein was coupled to the column according to the manufacturers protocol in the presence of 0.1 M guanidine-HCl to maintain protein solubility. Protein binding to the column was complete; no Pept3 protein was found in the column flow through or wash fractions (Fig. 2-4). Purified ATP7B copper-binding domain protein from which the GST domain was enzymatically cleaved was bound to another NHS-sepharose column, as was Pept3 protein except that it was done under non-denaturing conditions. Again, the coupling reaction was complete.

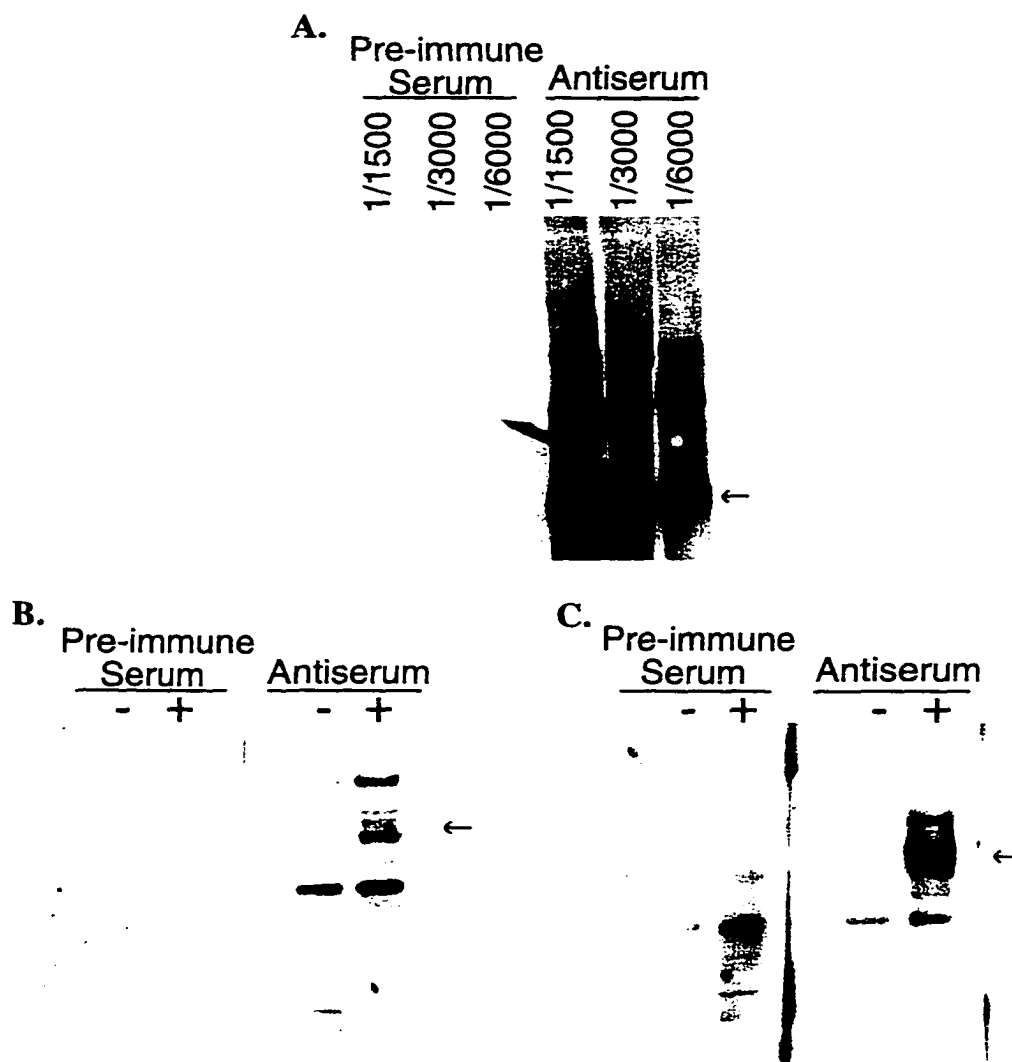


### Figure 2-3: Antiserum specificity.

**A,** Test-strips containing bacterially expressed Pept 3 protein were prepared and used for immunoblotting. Rabbit polyclonal antiserum against the C-terminus of ATP7B was able to detect bacterially expressed Pept3 fusion protein while the rabbit pre-immune was not. The dilutions used on each test strip are indicated. **B,** Rabbit H207 pre-immune and antiserum against the ATP7B copper binding domain (1/1000 dilution) **C,** Rabbit H208 pre-immune and polyclonal antisera against the ATP7B copper binding domain (1/1000) dilution. **B,C,** Test strips containing total cell protein extracts from control yeast (-), or yeast expressing ATP7B protein (+) were prepared, and used for immunoblotting. The antisera were able to detect ATP7B protein, but the pre-immune sera could not. Arrows indicate the expected protein band.

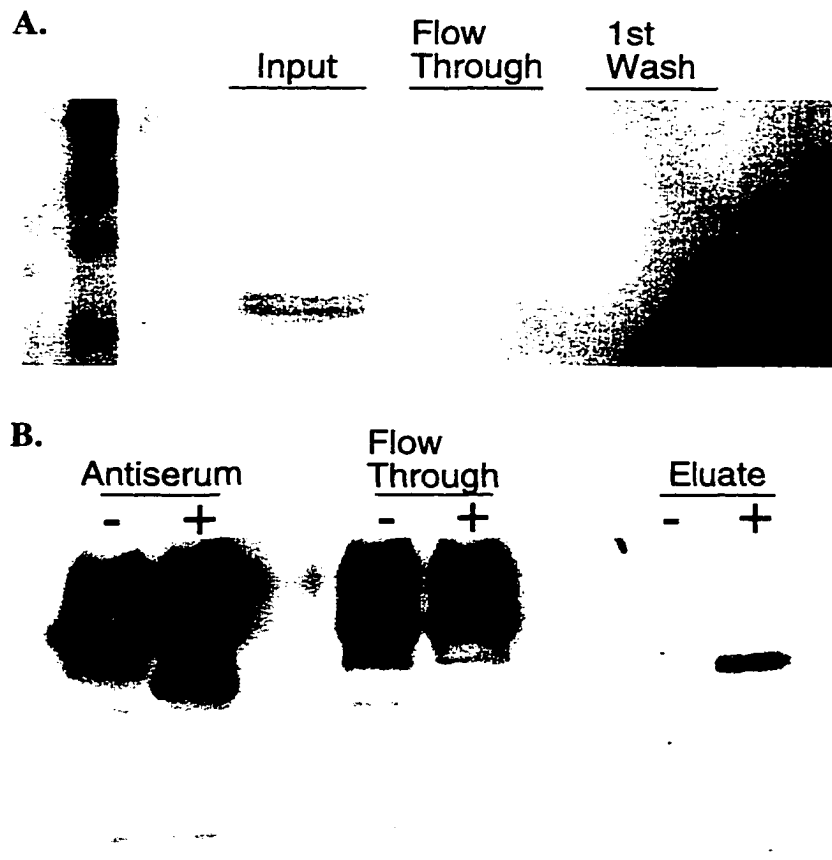


**Figure 2-4: Example of column affinity purification procedure (anti-ATP7B.C10).**

**A**, SDS-Page gel stained with Coomassie blue showing Pept3 fusion protein before, and after, coupling to the NHS-activated Sepharose column. **B**, Immunoblots (test strips) were performed on total protein extract from control yeast (-), or from ATP7B expressing yeast (+). The antiserum and column flow-through were used at equal final dilutions, estimated by volume correction, during immunodetection. The concentrated eluate and antiserum were used at 1/5000 dilutions.

The affinity columns were then used to purify ATP7B antisera. Pept3 antiserum or anti-copper-binding domain antiserum was bound to the appropriate columns, washed extensively, and then eluted. The resulting antibodies were mono-specific, able to detect ATP7B protein expressed in yeast as a single band without non-specific bands. The resulting antibodies could be used at a very high dilution (1/25,000 using Supersignal Ultra ECL substrate). In both cases binding of antibodies to the columns was complete. Column flow-through was unable to detect ATP7B protein expressed in yeast but still detected non-specific proteins (Fig. 2-4).

#### **2C-4) Expression of ATP7B in yeast.**

To express full-length ATP7B in yeast, the cDNA was cloned into two expression vectors: a multicopy vector pG3, and a singlecopy integrating vector pG4. These vectors were used so that the level of ATP7B expression, could be modulated by plasmid copy number. Singlecopy insertion of pG4 based constructs was confirmed by Southern blotting (Fig. 2-5). ATP7B expression in yeast protein extracts was analysed by immunoblotting using anti-ATP7B.C10 (Fig. 2-6). ATP7B protein produced in yeast migrates at approximately 175 kDa which, agrees well with the predicted molecular mass of 159 kDa for ATP7B. The multicopy vector produced approximately 30-fold more protein than the singlecopy vector as estimated by densitometry. ATP7B was found entirely in membrane pellets, consistent with its predicted integral membrane structure.

#### **2C-5) Yeast complementation assay for ATP7B.**

For complementation experiments, the yeast strain BJ2168, deficient for vacuolar proteases, was chosen as wild-type to minimise potential proteolysis during procedures, such as the oxidase assay, in which samples are not heated prior to electrophoresis. Mutant *fet3* and *ccc2* yeast were previously shown to be respiration deficient, due to defective iron uptake, and therefore unable to grow on non-fermentable carbon source medium (Yuan *et al.* 1995). Therefore the new BJ2168 derived *fet3* and *ccc2* yeast mutants were scored for phenotype by growth on glycerol based, non-fermentable carbon source medium, which tests for respiration competency (Kaiser *et al.* 1994). The *ccc2* mutant yeast were unable to grow on glycerol based medium unless supplemented with high levels of iron or copper. Similarly, the *fet3* mutant yeast were unable to grow on glycerol based medium unless supplemented with high levels of iron. The new transformants exhibited the correct phenotypes and were therefore judged to be suitable for complementation experiments.

The respiratory-deficient phenotype the *ccc2* mutant yeast was not severe allowing some growth to occur on glycerol-based media. Therefore this medium was



**Figure 2-5: Example of screening for singlecopy expression construct integrations.**

pG4 integrating vector based *ATP7B* expression constructs, were transformed into yeast as described in section 2B-9. The *ccc2* strain was transformed with empty expression vector. The other constructs in this figure are WD mutants described in Chapter 3. To analyse for singlecopy expression construct insertion, yeast genomic DNA was digested with Bam HI enzyme, and analysed by Southern blotting using *ATP7B* cDNA as probe. Bam HI digests the yeast genomic DNA and cuts once within the expression construct. A single copy insertion is detected as a large DNA band (> 12 kb) containing *ATP7B*, some vector, and a piece of yeast genomic DNA due to digestion and release of DNA fragments cut once within the integrated construct and again in the yeast genomic DNA at some point downstream of the construct. Multicopy integrations occur as tandemly arranged insertions, therefore digestion of tandemly arranged construct BamHI sites results in the release of construct DNA fragments. These are detected as approximately 9 kb bands by Southern blotting.

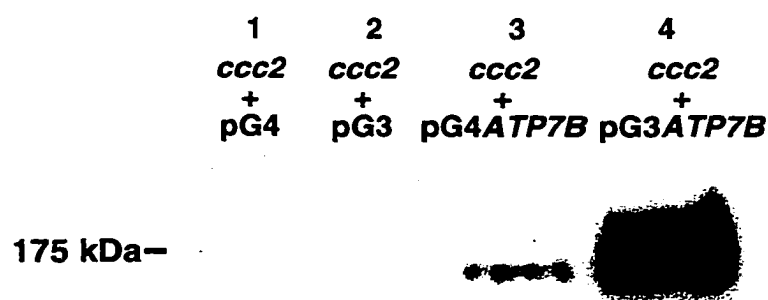


**Figure 2-6: Expression of ATP7B in yeast.**

ATP7B was expressed in *ccc2* mutant yeast and analyzed by immuno blotting. Analysis of 40  $\mu$ g total yeast protein was done by ECL using affinity purified rabbit polyclonal antibodies against the C-terminal 10 kDa fragment of ATP7B (anti-ATP7B.C10) at a 1/3000 dilution. Lanes 1 and 2 contain yeast protein from strains harbouring empty expression vector only. Lanes 3 and 4 contain yeast protein from strains harbouring the singlecopy (pG4) and multicopy (pG3) ATP7B expression constructs respectively. The multicopy vector produces approximately 30 fold more ATP7B protein than the single-copy vector as estimated by densitometry.

judged to be unsuitable for the detection of subtle differences in growth between normal and mutant ATP7B proteins in the complementation assay. Therefore the high-affinity iron uptake deficiency of the yeast mutant *ccc2* was exploited (Yuan *et al.* 1995; Stearman *et al.* 1996). In the absence of high-affinity iron uptake, *ccc2* mutant yeast are unable to grow on iron-limited medium. The iron-limited medium used, based on that reported by Stearman *et al.* (1997), contained 1 mM ferrozine (an iron specific chelator) and 50  $\mu$ M ferrous ammonium sulphate. The amount of copper added to the medium was chosen based on a report demonstrating the copper dependency of high-affinity iron uptake in yeast *ccc2ctr1* double mutants. Yeast *ccc2ctr1* mutants lack high-affinity copper uptake, and subsequently, lack high-affinity iron uptake (Dancis *et al.* 1994b; Yuan *et al.* 1995; Yuan *et al.* 1997). As a result no copper uptake and no copper incorporation into Fet3p occurs *in vivo*. Copper was shown to be able to overcome the *ccc2ctr1* mutant defect, restoring iron-uptake, in a concentration dependent manner by binding to Fet3p at the cell surface bypassing the requirement for Ctr1p and Ccc2p (Yuan *et al.* 1997). Copper up to 1  $\mu$ M in the medium did not affect Ctr1p/Ccc2p independent iron uptake and did not reconstitute Fet3p at the cell surface. Significant iron uptake was not observed until copper concentrations in the medium exceeded 5  $\mu$ M. Based on these observations, copper added to the growth media was limited to no more than 1  $\mu$ M in complementation assays so that iron dependent growth was dependent on Ccc2p (or ATP7B) mediated copper incorporation into apo-Fet3p *in vivo* during its biosynthesis.

Mutant *ccc2* yeast harbouring empty expression vectors were unable to grow on iron-limited medium (Fig. 2-7). Both singlecopy and multicopy expression of ATP7B were able to complement the *ccc2* mutation allowing the cells to grow (Fig. 2-7). Growth rescue of *ccc2* mutant yeast can be accomplished by addition of high concentrations of copper or iron to the iron-limited growth medium (Yuan *et al.* 1995; Stearman *et al.* 1996). Under these conditions, iron enters the cells by low-affinity pathways, or copper binds to apo-Fet3p at the cell surface, reconstituting its activity and restoring high-affinity iron uptake. All yeast strains tested were able to grow on culture plates containing either copper or iron-sufficient medium showing that the *ccc2* mutant strains containing vector are viable and that they exhibit the correct metal suppressible phenotype. Use of iron-limited medium as the assay medium resulted in a clear distinction between normal and mutant phenotypes and was therefore used in all subsequent complementation experiments.

Mutant *ccc2* yeast cells grown in standard SD medium, diluted, and plated directly onto assay medium could grow normally under iron-limited conditions. We found that transferring yeast cultures grown in SD medium to iron-limited medium for

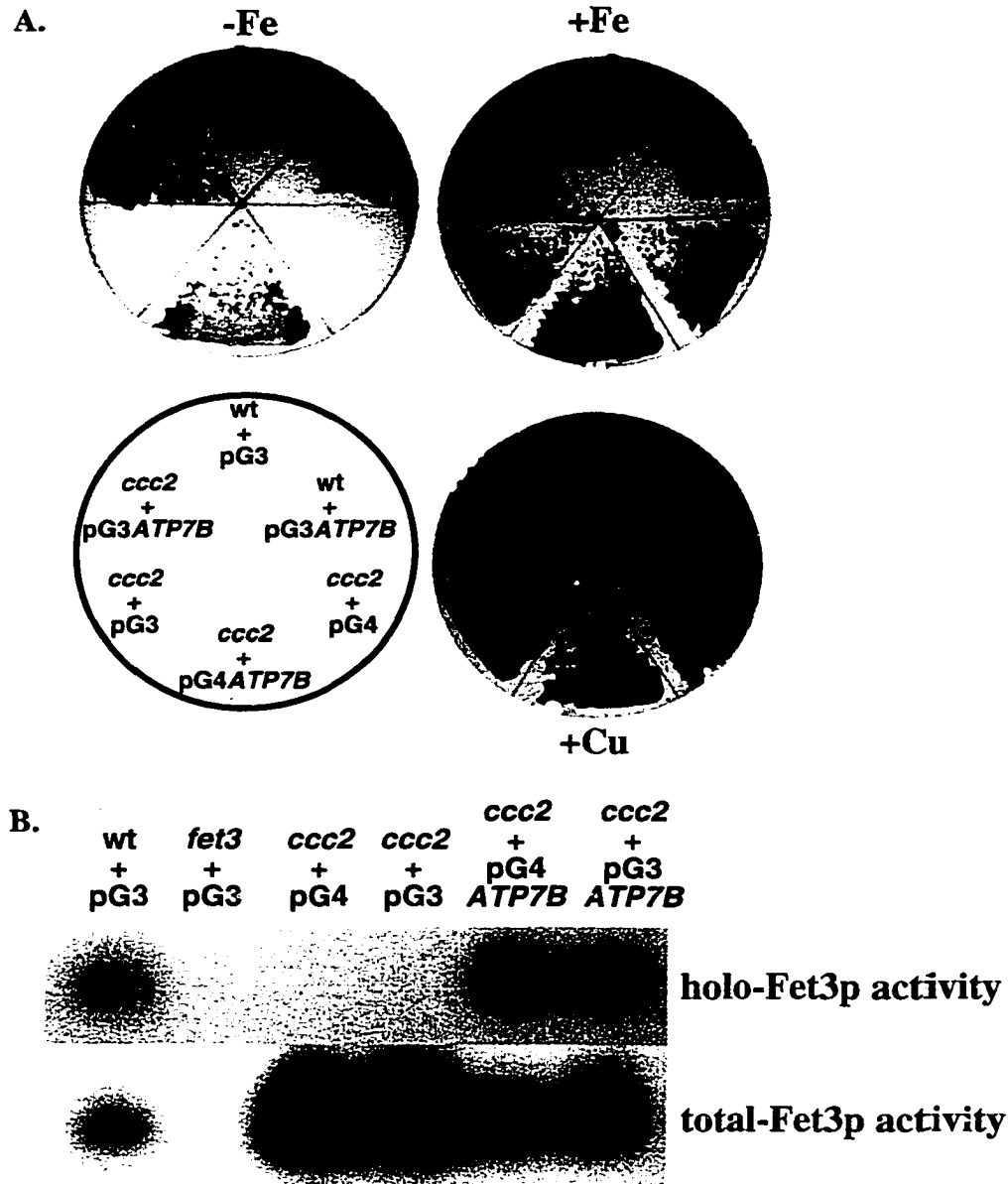


**Figure 2-7: Complementation of *ccc2* mutant yeast by ATP7B.**

ATP7B was expressed in *ccc2* mutant yeast from either a singlecopy (pG4) or multicopy vector (pG3). **A**, Plating assays were performed as described in 2B-10. **B**, Fet3p oxidase assays were performed as described in Chapter 2. Holo-Fet3p activity, Fet3p copper loaded *in vivo*, was detected by homogenising yeast in buffer containing the copper chelator BCS and the reducing agent ascorbate to prevent adventitious copper loading of apo-Fet3p during processing. Total-Fet3p activity, holo-Fet3p plus apo-Fet3p activity, was detected by homogenising yeast in the presence of copper to reconstitute apo-Fet3p *in vitro*.

overnight growth prior to the assay made the iron-dependent growth phenotype of *ccc2* mutant yeast apparent. These data suggest that yeast contain a significant store of intracellular iron, perhaps in mitochondria (Radisky *et al.* 1999; Babcock *et al.* 1997), that allows normal growth, for a time, if iron becomes limiting. Once these stores are depleted, growth under iron-limited conditions becomes dependent on high-affinity iron uptake.

Fet3p oxidase activity, dependent upon copper delivered to it by Ccc2p, serves as a marker enzyme for the putative copper transporting function of Ccc2p (Yuan *et al.* 1995). Gel based Fet3p oxidase assays were used to provide biochemical evidence that ATP7B can functionally replace Ccc2p *in vivo*. Holo-Fet3p activity is absent in BCS/ascorbate protein extracts from *ccc2* mutant yeast harbouring vector alone (Fig. 2-7). Expression of ATP7B in *ccc2* mutant yeast restores Fet3p activity *in vivo*. As positive control, Fet3p assays were performed on protein extracts from yeast homogenised in the presence of copper. Copper is able to reconstitute apo-Fet3p *in vitro*, restoring its oxidase activity such that total cellular Fet3p activity is detected. Although holo-Fet3p activity was absent in the *ccc2* strain, apo-Fet3p was still produced and capable of function (Fig. 2-7) as shown by the high level of copper reconstituted total-Fet3p activity in this strain. Total-Fet3p activity was notably much higher in the *ccc2* mutant protein extracts compared to those from wild-type or ATP7B expressing yeast strains. In the absence of holo-Fet3p synthesised *in vivo*, there is no high-affinity iron uptake in yeast. Under these conditions apo-Fet3p expression is induced to high levels detectable by copper reconstitution *in vitro*. In wild-type yeast and in yeast expressing normal ATP7B, there was little difference in holo- and total-Fet3p activity indicating little or no excess apo-Fet3p production. Therefore a high ratio of total-Fet3p to holo-Fet3p activity indicates an ATP7B mutant protein with absent or reduced function. These data show that ATP7B is able to functionally replace Ccc2p. ATP7B provides the putative copper transport activity required to deliver copper to Fet3p, thereby restoring the ability of *ccc2* mutant yeast to grow on iron-limited medium.

The pH of the media used to grow cells was critical especially for the Fet3p oxidase assay. Yeast SD medium is generally quite acidic, and becomes more acid as the yeast cultures grow. Most heavy metals including copper have enhanced solubility at acidic pH (Cotton *et al.* 1988), and copper is more bioavailable (Wapnir, 1998) at acidic pH. Fet3p was shown to require less copper for *in vitro* copper reconstitution at acidic compared to neutral pH (Davis-Kaplan *et al.* 1998). In standard SD medium trace levels of copper were able to reconstitute Fet3p at the cell surface resulting in normal Fet3p

activity the *ccc2* mutant yeast protein extracts. This was eliminated by adding 50 mM MES buffer pH 6.1 to the media as described by Stearman *et al.* (1997).

## 2D) DISCUSSION.

Resources for studying the biochemistry and cell-biology of ATP7B were created. Three polyclonal rabbit antisera were generated that specifically recognise full-length ATP7B expressed in yeast and/or bacterial derived ATP7B fusion proteins on immunoblots. Anti-ATP7B.N60 was capable of specific detection of endogenous ATP7B protein in HepG2 cells and ATP7B protein in transiently transfected HeLa cells or CHO cells by immunofluorescence (described in Chapter 4). ATP7B.C10 did not work in immunofluorescence experiments. An affinity purification method for use purifying ATP7B specific antibodies from the rabbit antisera was developed that resulted in significant improvements in antibody specificity. ATP7B from human liver protein extracts has not been unambiguously detected on immunoblots using either ATP7B.C10 or ATP7B.N60 antibodies. Several bands near the appropriate molecular weight were observed, but without a tissue panel for use as a control, ATP7B could not be identified with certainty. A mouse tissue protein immunoblot panel was prepared (Steven Moore, University of Alberta) and was probed with both anti-ATP7B.C10 and anti-ATP7B.N60 to determine if *Atp7b* protein expression paralleled its mRNA expression pattern (Steven Moore, University of Alberta). This experiment was unsuccessful perhaps due limited cross reactivity of our human directed antibodies with mouse protein, or due to insufficient *Atp7b* protein for detection with the reagents used. Despite the inability to unambiguously detect endogenous ATP7B in human liver (or mouse), these data confirms that both polyclonal antibodies are specific to ATP7B.

A full-length *ATP7B* cDNA was constructed. This resource can be used for heterologous protein expression, *in situ* hybridisation studies, and as template for site-directed mutagenesis and deletion analysis for the purpose of structure/function experiments. A protein expression system using the full-length *ATP7B* cDNA was developed in the yeast *Saccharomyces cerevisiae*. The system is capable of expression of functional ATP7B that could be used for direct biochemical studies. Protein expressed using the *ccc2* mutant yeast would be particularly useful for biochemical transport assays since the yeast orthologue of ATP7B, *Ccc2p*, was eliminated, therefore background CPx-type ATPase activity would be expected to be negligible.

A cDNA encoding the copper-binding domain of ATP7B was generated for use by Dr. Sarkar's laboratory at the Hospital for Sick Children in Toronto. This was used by Michael DiDonato to express and purify copper-binding domain protein, followed by

biochemical and biophysical characterisation. The results of this study were published by DiDonato *et al.* (1997) and are discussed in chapters 1 and 5 of this thesis.

A functional assay for ATP7B was developed, based on complementation of its yeast orthologue Ccc2p. As an assay for ATP7B, yeast complementation provides an elegant means to study protein function. The need for radioactive copper typically used in copper transport assay, which is extremely difficult to obtain, and is difficult to work with, due to its extremely short half-life and high energy particle emissions, is eliminated (Bingham *et al.* 1996; Dijkstra *et al.* 1996; Solioz *et al.* 1995; Bingham *et al.* 1994; Voskoboinik *et al.* 1998; Voskoboinik *et al.* 1999). ATP7B can apparently mediate wild-type levels of Fet3p activity and wild-type growth rate (Chapter 3) in iron-limited medium suggesting that ATP7B functions in yeast in a manner identical to Ccc2p. Copper incorporation into Fet3p appears to be directly mediated by Ccc2p (Yuan *et al.* 1995), or ATP7B, and therefore Fet3p serves as a marker of intracellular copper transport, although this statement has the caveat that there may be undiscovered proteins that mediate copper transfer between the proteins. Measuring growth rates of yeast strains in iron-limited medium is a sensitive assay that can detect functional differences between mutant ATP7B variants (Chapters 3 and 5). Copper incorporation into Fet3p by ATP7B appears to be the rate limiting step for iron-uptake and subsequent growth in iron-limited medium as all other proteins required for high-affinity uptake such as Fre1/2p, Ftr1p, and Fet3p are already induced and functioning under these conditions (Yamaguchi-Iwai *et al.* 1995; Stearman *et al.* 1996; Yamaguchi-Iwai *et al.* 1996). Additionally, due to extensive functional similarity of copper chaperones between yeast and mammals together with studies that show that copper within a cell is directed to the proper cellular target by specific chaperone proteins (Rae *et al.* 1999), yeast has the advantage that copper is likely delivered to ATP7B in a physiological form. Therefore, the assay is free from *in vitro* artifacts caused by using non-physiological forms of copper. Similar functional assays have been developed in parallel by other groups and were used to study ATP7A (Payne *et al.* 1998a), and ATP7B (Hung *et al.* 1997; Iida *et al.* 1998). Yeast based functional complementation assays have been developed for other mammalian membrane proteins such as NRAMP2 (Pinner *et al.* 1997) and CFTR (Teem *et al.* 1993) further demonstrating the utility of this type of assay.

Yeast complementation assays in general have certain limitations. Mutant proteins can only be judged by their relative ability to complement yeast mutants. Complementation cannot measure the exact change in protein activity, or give insight into the enzymology of proteins analysed. It may be that yeast requires only a fraction of normal ATP7B activity for complete Ccc2p replacement. Additionally, levels of ATP7B

protein may be higher than *Ccc2p* even when expressed from the singlecopy vector. Therefore the relative complementation capacity of mutant *ATP7B* proteins may be an underestimation of the degree to which copper transport activity is affected by a particular mutation. Another problem is that reduced or absent complementation could be due to either loss of protein activity or mislocalization of the mutant protein within the yeast cell. Since the cells appear to be saturated with *ATP7B* protein, reduced or absent ability of *ATP7B* mutant proteins to complement *ccc2* mutant yeast is likely the result of reduced copper transport function. However mislocalization of mutant proteins cannot be completely excluded. Additionally, mammalian proteins may be more stable or more rapidly degraded in yeast, compared with mammalian cells, due to differences in the folding environment, membrane composition, or protein processing (glycosylation, phosphorylation, etc.), thereby giving erroneous estimates on a particular mutations effect on protein activity. Similarly, important cofactor proteins or post-translational modifications, for targeting or regulation, may be absent in yeast. These caveats aside, yeast are an excellent prototypical model for eukaryotic copper homeostasis, and yeast complementation provides an excellent method to gain initial insight into the function of *ATP7B*.

### CHAPTER 3

#### **FUNCTIONAL ANALYSIS OF WILSON DISEASE MUTATIONS.**

Data presented in this chapter have been published in:

Forbes, J.R. and Cox, D.W. (1998) Functional characterisation of missense mutations in *ATP7B*: Wilson disease mutation or normal variant?  
*Am.J.Hum.Genet.*, **63**:1663-1674.

Gloria Hsi contributed to sequencing and assembly of the mutant *ATP7B* constructs described in this chapter.

### 3A) INTRODUCTION.

More than 150 mutations have been found in the *ATP7B* gene of WD patients (for reference see the Human Genome Organisation Wilson disease database <http://www.medgen.med.ualberta.ca/database.html>). Nonsense, frameshift, and splice site mutations are found throughout the gene. Missense mutations however, tend to be clustered within the putative ATP binding domain and membrane-spanning segments, supporting the importance of these structures for the proposed ATP-dependent copper transport function of *ATP7B*. A base-pair substitution generally is considered disease causing if it is not found on at least 50 normal chromosomes, if no other mutations can be detected, if the amino acid substitution is non-conservative, or if the substituted amino acid is conserved in functionally related proteins (e.g., *ATP7A*). There may be difficulty in distinguishing disease-causing missense mutations from rare normal variants not yet found on normal chromosomes, especially when the amino acid change appears to be conservative. Therefore, it is desirable to have a functional means to distinguish disease mutations from rare normal variants.

For diagnostic purposes, it is crucial to be sure whether or not a mutation is indeed disease causing. In the case of WD, early treatment is crucial to prevent irreversible liver damage, and conversely, many of the chelators used for treatment have adverse side effects; therefore misdiagnosis could be disastrous (Danks, 1995; Cox *et al.* 1998). Functional analysis of missense mutations is therefore an important adjunct to mutation screening in patients to confirm whether or not a mutation is likely to cause disease. The yeast complementation assay for *ATP7B* function described in Chapter 2 provides an ideal method to test putative mutations. It is relatively easy to perform, is sensitive, and can be used to assay a large number of mutant proteins in a short time (the advantages and disadvantages of complementation were discussed in Chapter 2D).

WD symptoms are highly variable (see section 1B-3), even in patients homozygous for the common northern European mutation H1069Q (Cox *et al.* 1999; Cox *et al.* 1998). However there is some correlation between WD disease severity and allelic variation of the *ATP7B* gene. Generally, WD patients compound heterozygous for mutations such as frameshifts, and nonsense mutations predicted to destroy the protein have a early age of disease onset (average 7.2 years) (Cox *et al.* 1999). Patients compound heterozygous for missense mutations predicted to be less damaging to *ATP7B* function typically have an later age of onset (average 16.8 years) (Cox *et al.* 1999). Environmental effects such as dietary copper intake may be a factor. Genetic background may also effect disease severity. For example, allelic differences in metallothionein and

superoxide dismutase genes between patients could alter the ability of tissues to cope with copper overload. Most WD mutations occur at low frequency, therefore most patients are compound heterozygotes (Cox *et al.* 1999; Cox *et al.* 1998). These factors combine to make genotype/phenotype correlations difficult. Determining the degree to which a missense mutation affects protein function will be helpful for interpreting the phenotype of patients, and give insight into the biochemical basis of WD variability.

After developing the yeast complementation assay, it was used to determine the degree to which selected WD associated mutations affect the function of ATP7B. Functional analysis was the first step taken to use WD mutations as a "biochemical probe" to gain insight into the molecular pathogenesis of WD, and the role of ATP7B in normal copper homeostasis. As a practical benefit of our yeast complementation assay, it was used to discriminate true WD causing mutations from rare normal variants by functional means as an aid to WD diagnosis. The WD mutations initially analysed were missense mutations within the predicted transmembrane domain of ATP7B (Fig. 3-1).

### **3B) MATERIALS AND METHODS.**

#### **3B-1) Yeast strains.**

Yeast strains used were as described in section 2B-8.

#### **3B-2) Site-directed mutagenesis.**

Mutant *ATP7B* cDNAs were made using the QuickChange method (Stratagene) starting with the normal *ATP7B* cDNA described in Chapter 2. To create mutations, two complementary oligonucleotide primers carrying the desired codon changes were synthesised. Primers were made so that approximately 10 bases of matched normal sequence flanked the mutated codon. Mutagenic primers are listed in the Appendix (Table A-3). Location of the mutations within the putative structure of ATP7B is shown in Figure 3-1. The number of bases was varied so that the annealing temperature of the primer pairs were above 68°C according to the formula provided by the QuickChange kit manufacturer (Stratagene). The site-directed mutagenesis was carried out as follows: Twenty ng of *ATP7B* cDNA was used as template together with 500-750 ng of each mutagenic primer, 2.5 units of *pfu* polymerase, 2.5 mM of each dCTP, dATP, dGTP, and dTTP in the manufacturers buffer at a total volume of 50 µL. The reaction mixtures were temperature cycled as follows: 95°C for one min. as an initial denaturation step, followed by twenty cycles of 30 sec. at 95°C denature, 1 min. at 55°C primer annealing, 17 min. at 68°C polymerase extension. Following the temperature cycling procedure, 20 units of the methylation sensitive restriction enzyme Dpn I was added to the reaction mixture and

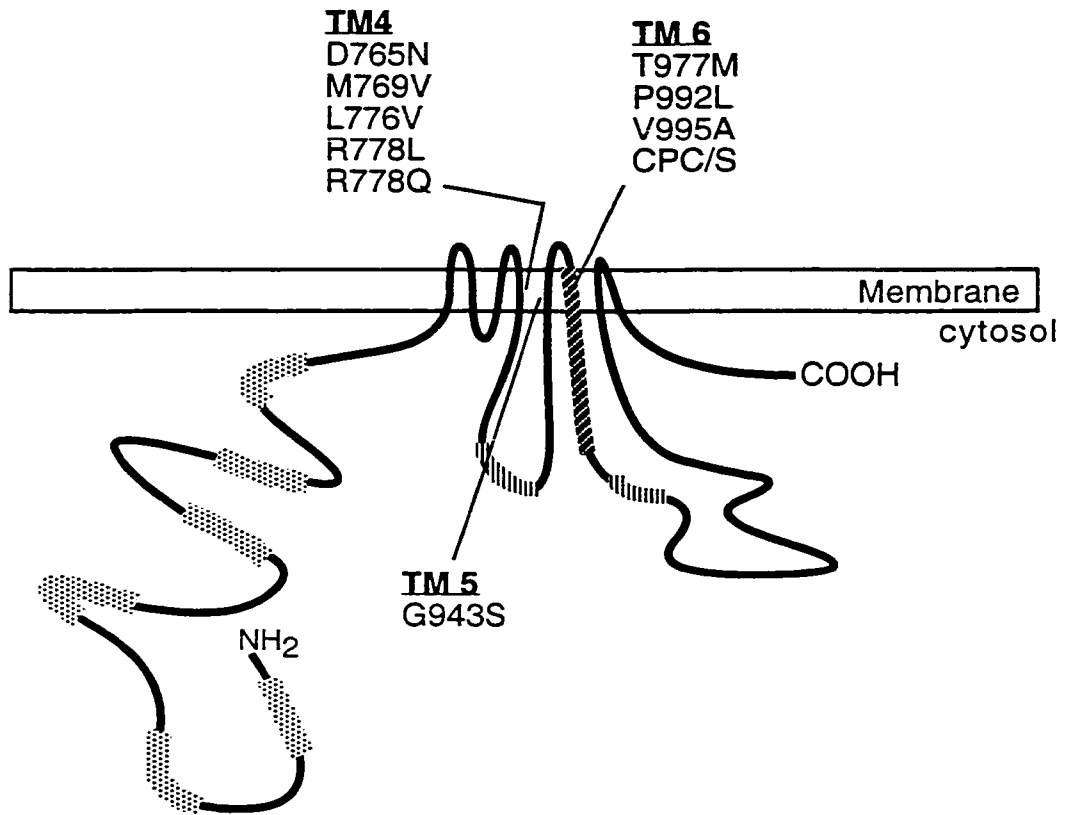


**Figure 3-1: Location of WD mutations within the predicted transmembrane domain of ATP7B.**

Mutations are grouped according to the transmembrane (TM) segment in which they are located.

incubated for approximately 2 hr. at 37°C to destroy the template plasmid. The digested DNA was transformed into chemically competent XL-1Blue *E. coli* according to the manufacturers protocol. Plasmid DNA isolated from individual mutated colonies were confirmed to contain the desired mutation by DNA sequencing (ThermoSequenase, Amersham) according to the manufacturers protocol. Mutated fragments were sequenced in the region between unique restriction sites in the ATP7B sequence to ensure there were no secondary mutations surrounding the desired mutation. Correct, mutated fragments were removed from the plasmid that underwent mutagenesis by restriction enzyme digestion and agarose gel purification, and then ligated back into a complementarily prepared, unmanipulated, cDNA to create the final mutant constructs. Construction of mutant ATP7B constructs was aided by technical assistance from Gloria Hsi who performed some sequencing and mutant construct assembly.

### **3B-3) Expression vectors.**

Yeast expression vectors were described in section 2B-9. Mutant ATP7B cDNA clones were liberated from pUC19 vector by Bam HI and Sal I digestion and then agarose gel purified. The cDNA fragments were ligated into pG3 and pG4 expression vectors and transformed into *ccc2* mutant yeast as described in section 2B-9. Yeast genomic DNA was isolated from pG4 strains and analysed by Southern blotting as described in section 2B-9 to ensure that all integrations were singlecopy.

### **3B-4) Complementation assay and Fet3p oxidase assay.**

The assays were performed as described in sections 2B-10 and 2B-11. To measure the heat shock response of *ccc2* mutant yeast expressing ATP7B mutant proteins, cells prepared and plated as described for the complementation assay were grown at 37°C for 48 hrs. prior to photography. To measure the growth rates of yeast strains expressing ATP7B mutant proteins, saturated yeast cultures grown overnight in SD medium at 30°C were pelleted and resuspended in iron-limited medium and then grown again overnight. These cells were pelleted and resuspended in fresh iron-limited medium. This was used to inoculate cultures at an optical density of  $A_{600} = 0.1$ . Cultures were grown at 30°C for 24 hours while growth was monitored spectroscopically at times 0, 3, 6, 12, and 24 hrs. Growth rates were calculated from the linear exponential growth phase between 3 and 12 hours after inoculation. Average rates were calculated from four independent experiments.

### 3B-5) Polyclonal antibodies against ATP7B.

The antibodies used were anti-ATP7B.C10, prepared as described in section 2B-6. Affinity purification was carried out using the membrane-based method, as described in section 2B-7.

### 3B-6) Yeast protein preparations and immunoblotting.

Yeast protein preparations and transfers were done as described in sections 2B-4 and 2B-12. Immunoblotting was performed using anti-ATP7B.C10 as primary antibody at a 1/3,000 dilution. Secondary antibody was horseradish peroxidase conjugated goat anti-rabbit antibodies at a dilution of 1/10,000 (Pierce Chemical). Bound antibodies were detected by ECL, using Supersignal substrate (Pierce Chemical).

## 3C) RESULTS.

Site-directed mutagenesis was used to create mutations in the *ATP7B* cDNA corresponding to those found in the predicted transmembrane segments of ATP7B from WD patients (Fig. 3-1). Five proposed disease-causing mutations were made: Asp765Asn (D765N), Arg778Leu (R778L), Arg778Gln (R778Q), Gly943Ser (G943S), and Pro992Leu (P992L). Two mutations, Met769Val (M769V) and Leu(776)Val (L776V), originally designated as possible mutations due to the conservative nature of the amino acid substitutions were made, as well as two proposed normal variants Thr977Met (T977M) and Val995Ala (V995A) (Thomas *et al.* 1994). The cysteines (C) of the CPC motif in predicted transmembrane segment six were mutated to serine (mutant construct designated CPC/S). These mutant ATP7B proteins were expressed in *ccc2* mutant yeast from the singlecopy expression vector. The genomic DNA of all recombinant strains was checked by Southern blotting to ensure singlecopy integration of the expression constructs (see Fig. 2-5). Complementation of *ccc2* mutant yeast with these constructs is shown in figures 3-2 and 3-3. Mutant proteins D756N, M769V, L776V, G943S and V995A appeared to fully complement *ccc2* mutants as did normal ATP7B. Mutations R778L and P992L weakly rescued *ccc2* mutant yeast, and R778Q partially rescued the mutant yeast. As expected, mutation of the CPC motif abrogated function of ATP7B. Interestingly, proposed normal variant T977M was the only WD mutation tested that resulted in a protein completely unable to complement *ccc2* mutant yeast.

These results are supported by the Fet3p oxidase assay data (Fig. 3-2 and 3-3). When the oxidase assay results were interpreted, the ratio of holo-Fet3p activity detected in BCS/ascorbate buffer, to total-Fet3p activity detected in copper buffer was

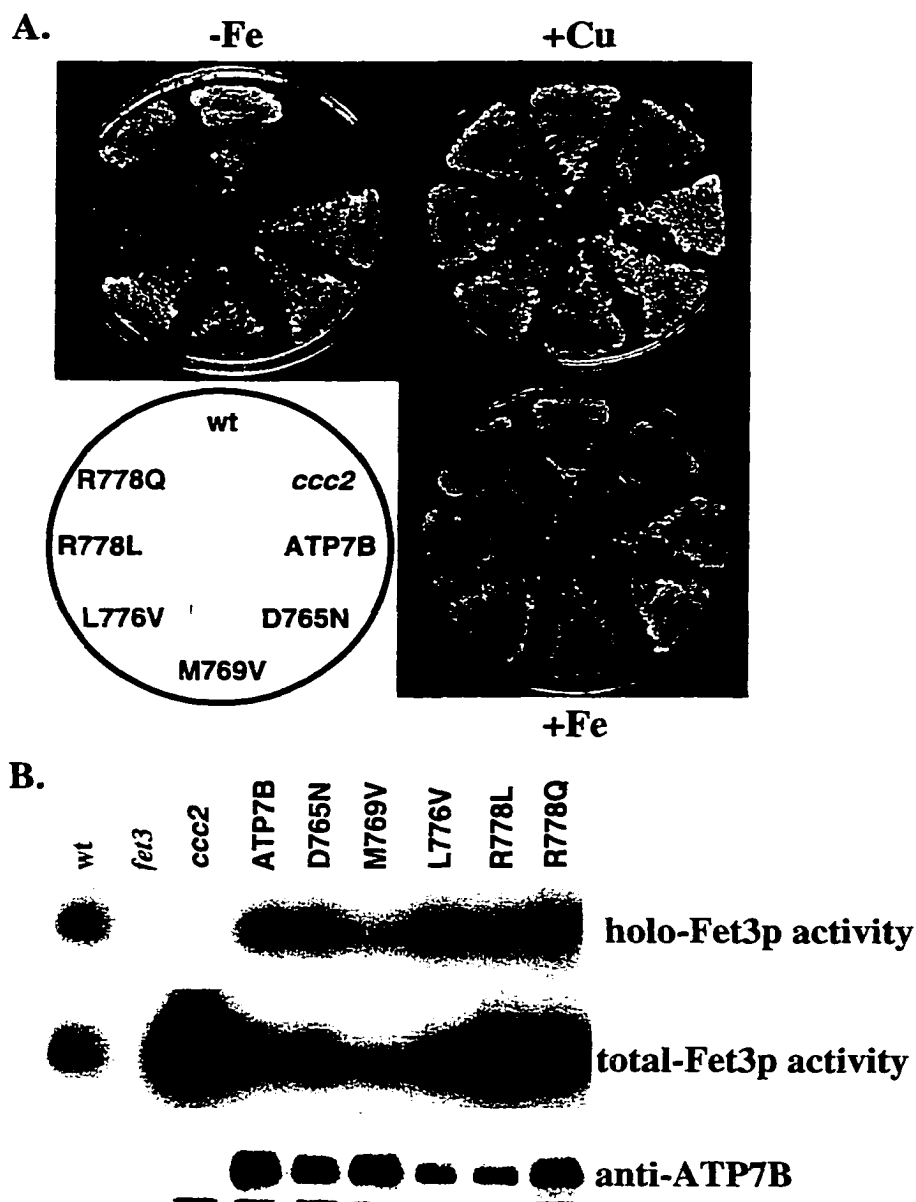


**Figure 3-2: Complementation of *ccc2* mutant yeast by WD mutants.**

Disease mutation constructs were expressed in the *ccc2* mutant background and are designated in the legend by mutation. Wild-type (wt) and *ccc2* mutant strains harbour empty expression vectors. **A**, Plating assays were performed as described in 2B-10. **B**, Fet3p oxidase assays were performed as described in 2B-11. Holo-Fet3p activity, Fet3p copper loaded *in vivo*, was detected by homogenising yeast in buffer containing the copper chelator BCS and reducing agent ascorbate to prevent adventitious copper loading of apo-Fet3p during processing. Total-Fet3p activity, holo-Fet3p plus apo-Fet3p activity, was detected by homogenising yeast in the presence of copper to reconstitute apo-Fet3p *in vitro*.

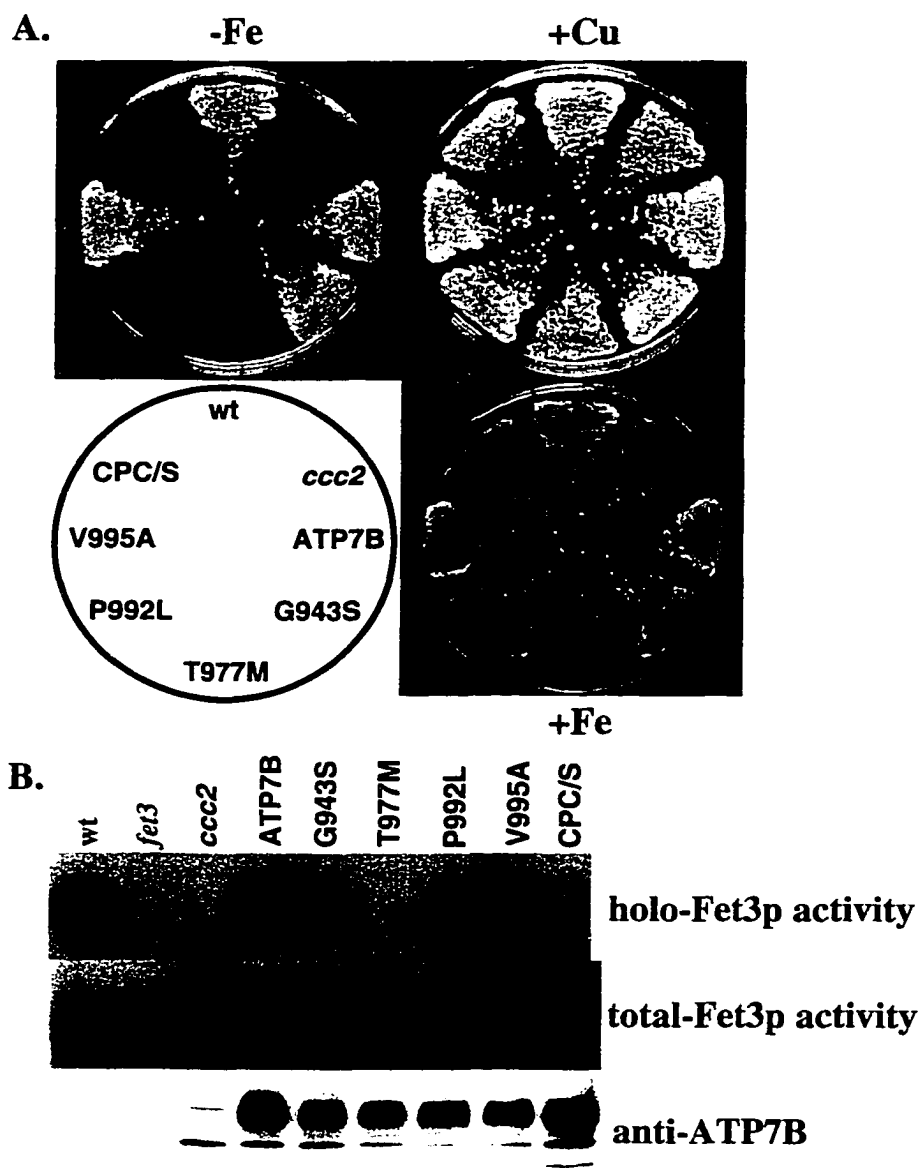


**Figure 3-3: Complementation of *ccc2* mutant yeast by WD mutants.**

Disease mutation constructs were expressed in the *ccc2* mutant background and are designated in the legend by mutation. Wild-type (wt) and *ccc2* mutant strains harbour empty expression vectors. **A**, Plating assays were performed as described in 2B-10. **B**, Fet3p oxidase assays were performed as described in 2B-11. Holo-Fet3p activity, Fet3p copper loaded *in vivo*, was detected by homogenising yeast in buffer containing the copper chelator BCS and reducing agent ascorbate to prevent adventitious copper loading of apo-Fet3p during processing. Total-Fet3p activity, holo-Fet3p plus apo-Fet3p activity, was detected by homogenising yeast in the presence of copper to reconstitute apo-Fet3p *in vitro*.

informative. In wild-type, and ATP7B complemented *ccc2* mutant yeast protein extracts, the amounts of holo-Fet3p, and total Fet3p activity, were similar indicating that there is little apo-Fet3p present. However, yeast expressing R778L, R778Q, and P992L mutant ATP7B proteins exhibit reduced holo-Fet3p activity but greatly increased total-Fet3p activity indicating the presence of large amounts of apo-Fet3p. This implies that ATP7B mutants with reduced function cannot deliver enough copper to Fet3p during its biosynthesis *in vivo* leading to an accumulation of the apo-enzyme form. Therefore the greater the amount of total-Fet3p activity in comparison to holo-Fet3p activity, the greater the defect in mutant ATP7B function. For example, R778L had a higher ratio of total-Fet3p to holo-Fet3p activity than did R778Q indicating that the R778L mutation affected ATP7B function more severely. These oxidase assay results were reproduced in several experiments.

Growth curves of yeast, grown in iron-limited medium, were employed to quantify the relative capability of WD mutant proteins, expressed from singlecopy constructs, to complement *ccc2* mutant yeast (Table 3-1, Fig. 3-4). The growth rate data agreed well with the Fet3p oxidase assay results indicating that growth was dependent on the ability of mutant ATP7B proteins to incorporate copper into Fet3p *in vivo*. Since all of the proposed WD mutations were able to at least partially complement *ccc2* mutant yeast in singlecopy, cells were subjected to further stress by heat shock at 37°C (Table 3-1). Mutations R778L, R778Q, and P992L that were already affected at 30°C showed a more severe phenotype when grown on iron-limited medium at 37°C. R778L and P992L were unable to complement *ccc2* mutant yeast, whereas R778Q did so very weakly. The only mutant profoundly affected by heat stress was M769V, which was unable to complement *ccc2* mutant yeast at 37°C. All other mutants tested were unaffected by heat stress.

When overexpressed from the multicopy vector, all mutations tested with the exception of T977M and CPC/S were able to fully complement *ccc2* mutant yeast at 30°C and 37°C (data not shown).

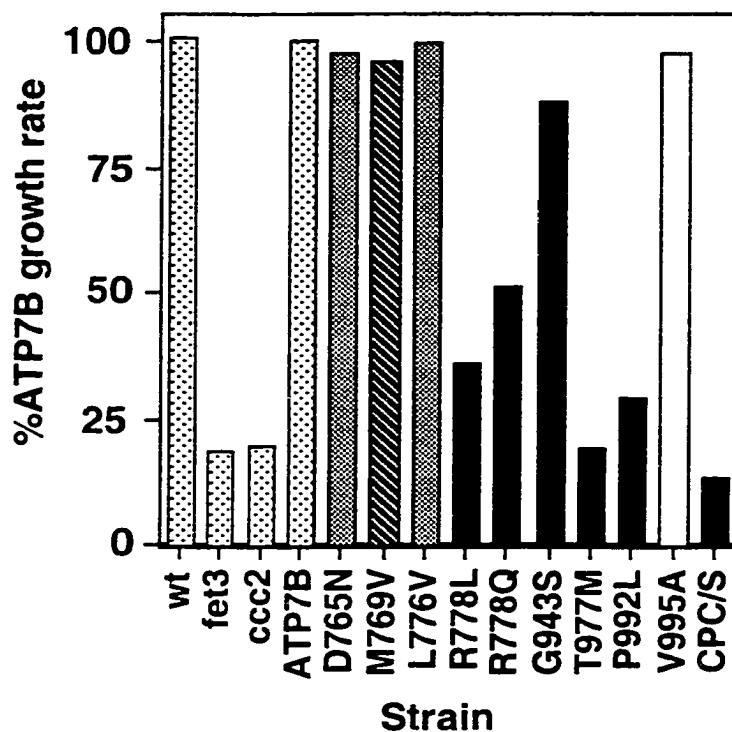


**Figure 3-4: Growth rates of yeast strains in iron-limited medium.**

Data are expressed as percent growth rate of yeast expressing normal ATP7B. Disease mutation constructs were expressed in the *ccc2* mutant background and are designated in the legend by mutation. Black bars designate ATP7B variants functionally designated as WD causing mutations. White bars indicate normal variants. Grey bars indicate possible normal variants or WD mutant proteins that are incorrectly localized in hepatocytes. The black slash bar indicates a ATP7B variant functionally designated as a mutation due to profound temperature sensitivity.

**Table 3-1: Growth rates of yeast strains expressing WD mutant ATP7B proteins.**

Growth curves were measured at 30°C in iron-limited medium as described in section 3B-4.

<sup>a</sup> statistically significant difference from ATP7B (t-test,  $p > 0.001$ )

<sup>b</sup> statistically significant difference from R778Q (t-test,  $p > 0.001$ )

Strain	Original Designation	Growth rate ( $\Delta A_{600}$ / hour)	Heat sensitive	Functional Designation
wild-type		$0.1146 \pm 0.0025$	no	
<i>fet3</i>		$0.0210 \pm 0.0014^a$	no	
<i>ccc2</i>		$0.0226 \pm 0.0020^a$	no	
ATP7B		$0.1140 \pm 0.0012$	no	
CPC/S		$0.0155 \pm 0.0008^a$	no	
D765N	mutation	$0.1110 \pm 0.0020$	no	normal variant or mislocalised
R778L	mutation	$0.0411 \pm 0.0016^{a,b}$	yes	mutation
R778Q	mutation	$0.0581 \pm 0.0017^a$	yes	mutation
G943S	mutation	$0.1001 \pm 0.0037^a$	no	mutation
P992L	mutation	$0.0330 \pm 0.0039^{a,b}$	yes	mutation
M769V	possible mutation	$0.1094 \pm 0.0011$	yes	mutation
L776V	possible mutation	$0.1131 \pm 0.0013$	no	normal variant or mislocalised
T977M	possible normal variant	$0.0220 \pm 0.0024^a$	no	mutation
V995A	possible normal variant	$0.1109 \pm 0.0037$	no	normal variant

### 3d) DISCUSSION.

ATP7B is able to provide the putative copper-transporting activity required for delivery of copper to Fet3p, restoring its activity, and correcting the high-affinity iron uptake deficiency phenotype of the yeast *ccc2* mutant strain. Using growth rates of yeast expressing ATP7B mutant proteins, differences in the ability of these mutant proteins to complement *ccc2* mutant yeast relative to normal ATP7B could be quantified. These data appear to agree well with the degree to which ATP7B mutant proteins are able to incorporate copper into Fet3p

The WD mutations analysed in this study are found within the putative transmembrane domain of ATP7B. The predicted transmembrane domain of ATP7B harbours a large proportion of WD-causing missense mutations, underscoring its importance for the structure and function of this protein. Based on extensive biochemical work done on the related sarcoplasmic reticulum calcium transporting P-type ATPase (Vilsen *et al.* 1989; Green *et al.* 1993; MacLennan *et al.* 1992; MacLennan *et al.* 1997; Clarke *et al.* 1989; Stokes *et al.* 1994), the transmembrane segments of ATP7B are likely involved in binding of copper, perhaps via the conserved CPC motif, prior to its translocation across the membrane bilayer (see section 1C-1, 1C-2). Besides providing the topological framework for proper protein folding, the transmembrane segments of P-type ATPase undergo conformational changes during cation transport that result in delivery of cations across membranes (Vilsen *et al.* 1989; MacLennan *et al.* 1997; Stokes *et al.* 1994). Mutations in the transmembrane segments that effect any of these potential functions would be deleterious to ATP7B function. For example, mutations may prevent or reduce copper binding to the predicted transmembrane domain of ATP7B prior to transport rendering the protein inactive. Transmembrane domain mutations may alter the structure of ATP7B such that the protein is unable to undergo conformational changes, or does so slowly, thereby affecting ATP7B function. The detailed biochemical mechanism by which WD mutations affect ATP7B function cannot be ascertained from yeast complementation data.

In this study, five variants classified as WD mutations were analysed: D765N, R778L, R778Q, G943S, and P992L. D765N, a rare mutation found in patients of Italian descent (Figus *et al.* 1995), fully complements the *ccc2* mutant yeast at both 30°C and 37°C indicating normal copper transport function in this assay. This mutation may be a rare normal variant not yet detected on normal chromosomes, or could result in a mutant protein that has normal copper transport activity but is incorrectly localised in mammalian cells.

The WD mutation R778L is the most common mutation in patients of Asian descent (Thomas *et al.* 1994; Chuang *et al.* 1996; Nanji *et al.* 1997) representing up to 27% of WD alleles found in this population. In homozygous form, this mutation is associated with early onset WD with hepatic presentation (Nanji *et al.* 1997; Cox *et al.* 1999). This correlates well with the functional data. R778L in singlecopy was able to complement *ccc2* mutant yeast at only 36.1% of that of yeast expressing normal ATP7B. It could not complement *ccc2* mutant yeast at 37°C. This mutation has severe effects on the function of ATP7B confirming its prediction as a disease causing mutation. Interestingly, the mutation R778Q found in Taiwanese patients (Chuang *et al.* 1996), had a less severe effect on ATP7B function than R778L, consistent with the fact that glutamine is more closely related to arginine than is leucine. R778Q was able to complement *ccc2* mutant yeast in singlecopy at 51% of ATP7B expressing yeast and at 37°C complements *ccc2* mutant yeast very weakly. Homozygous R778Q mutation might be predicted to result in a milder form of WD than seen for R778L. Other reported variants of this residue are R778G and R778W (Chuang *et al.* 1996) for which there are no functional data.

Mutation G943S was found in the Bangladeshi population and resulted in neurologic disease with onset in late childhood in a homozygous patient (Thomas *et al.* 1994). Complementation was slightly impaired (86%) when expressed in singlecopy compared with normal ATP7B consistent with a milder WD presentation. P992L was found in a Japanese family (Nanji *et al.* 1997). This change is found in a residue highly conserved in copper transporting P-type ATPases. P992L in singlecopy had a severely impaired ability to complement *ccc2* mutant yeast compared with normal (29.1 %) at 30°C and is completely impaired at 37°C supporting its identity as a WD causing mutation.

Two mutations tested in this study, M769V and L776V, were originally not classified with certainty as disease-causing mutations or normal variants (Thomas *et al.* 1994). These amino acid changes were found as the only mutation on a few WD chromosomes, and are relatively conservative changes. However, these mutations have not been found on normal chromosomes, and the mutated residues are conserved in ATP7A. When analysed by complementation, M769V expressed in singlecopy complemented *ccc2* mutant yeast to a level equivalent to normal ATP7B at 30°C, however it was a temperature sensitive mutation since it was unable to complement at 37°C. Since 37°C is the temperature at which ATP7B functions in the human cell, M769V should be considered a disease-causing mutation in patients. L776V was able to fully complement the *ccc2* mutant yeast strain expressed from a singlecopy and was not effected by heat stress. This mutation may be a rare normal variant not yet identified on

normal chromosomes, or a mutation that affects the intracellular localisation of ATP7B, thereby impairing cellular copper efflux.

In this study, two mutations originally classified as normal variants (Thomas *et al.* 1994) were tested for function by yeast complementation. T977M and V995A are relatively conservative amino acid changes. However Waldenstrom *et al.* (1996) reported that T977M was the only mutation found on seven WD chromosomes from patients of northern European descent, but no normal chromosomes were tested. By use of yeast complementation, T977M was found to be completely unable to complement *ccc2* even when overexpressed. These results demonstrate that this mutation results in a non-functional protein and should be considered a WD-causing mutation in patients. V995A had normal function in our assay consistent with its classification as a normal variant.

The CPC motif is evolutionarily conserved in heavy metal transporters (Bull *et al.* 1994; Solioz, 1998; Solioz *et al.* 1996) and is predicted to be involved in copper-binding within the predicted transmembrane domains of these proteins during transport. The first cysteine and proline of the motif are invariant in all heavy-metal transporting P-type ATPases leading to the proposed designation of CPx-type ATPase for this class of proteins (Solioz *et al.* 1996). The last cysteine residue of the motif is replaced in some CPx-type ATPases by serine or histidine. The functional significance of these changes is unknown but they presumably do not adversely affect the metal-transporting function of these proteins. Mutation of both cysteine residues, to serine, within the CPC motif, in the sixth transmembrane segment of ATP7B, resulted in a protein unable to complement *ccc2* mutant yeast when expressed in singlecopy or overexpressed from a multicopy vector. These results complement those published by Hung *et al.* (1997) who studied ATP7B, and Yoshimizu *et al.* (1998) who studied CUA-1, the *C. Elegans* orthologue of ATP7B. In those studies, the CPC motif was mutated to CAC or CPA respectively and in both cases resulted in a mutant protein unable to complement *ccc2* mutant yeast. Taken together, data available to date are consistent with an essential role for this motif in ATP7B function as well as related CPx-type ATPases. Mutations in this motif have not yet been reported in patients with WD.

Yeast complementation has been used by other groups to study the effect of WD mutations on ATP7B. Iida *et al.* (1998) report that mutations D1027A and T1029A, within the conserved DKTG motif, and the WD mutation N1270S are unable to complement *ccc2* mutant yeast. H1069Q, the most common WD mutation in northern European populations (Thomas *et al.* 1994), had a reduced ability to complement in their assay. This result is in contrast to reports that the H1069Q mutation and the equivalent mutation in ATP7A result in proteins unable to complement *ccc2* mutant yeast (Hung *et*

*al.*1997; Payne *et al.*1998a). However, yeast complementation is sensitive to the level of protein expressed, which may explain this discrepancy. H1069Q likely results in a severely impaired, but not inactive ATP7B protein.

Most of the putative WD mutant proteins tested by yeast complementation in this study exhibited partial or normal ability to complement *ccc2* mutant yeast compared with normal ATP7B protein. All mutants, with the exception of T977M and CPC/S, were able to fully complement *ccc2* mutant yeast when overexpressed from a multicopy vector, even under conditions of heat stress. These data indicate that these WD mutant ATP7B proteins retain at least partial ability to transport copper. However, cellular copper homeostasis, mediated by ATP7B, is likely dependent on both copper transport activity, and localisation to the correct intracellular compartment. ATP7B plays a dual functional role in the hepatocyte. One role is biosynthetic, delivering copper to apo-ceruloplasmin within the Golgi network (Murata *et al.*1995). The other role of ATP7B is to transport excess copper out of the cell (Schilsky *et al.*1994; Gross *et al.*1989). ATP7B, normally localised in the trans-Golgi network (TGN) of hepatocytes (Hung *et al.*1997), trafficks from the TGN to an endosomal vesicle compartment (J. Mercer, personal communication) when cells are exposed to elevated copper levels, and recycles back when copper is removed. The observed copper-dependent trafficking may represent a post-translationally inducible switch from a primarily biosynthetic role in the TGN to a primarily excretory role, involving membrane vesicles, under conditions of copper overload. WD missense mutations, such as those analysed in this study, may affect copper-dependent trafficking, resulting in a potentially active protein unable to exit the TGN in response to copper, thereby severely reducing biliary copper excretion. However, partially or fully active mutant ATP7B proteins trapped in the secretory pathway could transport sufficient copper to constitute apo-ceruloplasmin during its biosynthesis. This hypothesis may in part explain the phenotype of patients with hepatic copper accumulation but normal serum ceruloplasmin levels. The intracellular localisation of WD mutant ATP7B proteins expressed in mammalian cells must be analysed to obtain a clear picture of ATP7B function in normal and disease states. Results addressing this issue are presented in the next chapter.

**CHAPTER 4****SUBCELLULAR LOCALIZATION OF ATP7B MUTANT PROTEINS.**

#### 4A) INTRODUCTION.

Complementation of the yeast *ccc2* mutant has been used as an assay to study the functional effect of WD mutations found within the transmembrane domain of ATP7B (Chapter 3) as the first step to understand the role of ATP7B mutant proteins in WD pathogenesis. However, hepatic copper homeostasis mediated by ATP7B is dependent on both copper transport activity and localisation to the correct intracellular compartment. ATP7B plays a dual functional role in the hepatocyte. One role is biosynthetic, delivering copper to apo-ceruloplasmin within the Golgi network (Murata *et al.* 1995; Yamada *et al.* 1993a; Cox *et al.* 1998; Terada *et al.* 1998). The other role of ATP7B is to transport excess copper out of the cell via the bile (Schilsky *et al.* 1994; Cox *et al.* 1998; Terada *et al.* 1999; Schilsky *et al.* 1998). ATP7B is localised in the trans-Golgi network of hepatocytes under low copper conditions, and trafficks to cytoplasmic vesicles when cells are exposed to elevated copper levels, then recycles back to the Golgi when copper is removed (Hung *et al.* 1997; Schaefer *et al.* 1999a). The observed copper-dependent trafficking probably represents a post-translationally inducible switch from a primarily biosynthetic role in the trans-Golgi network, to a primarily excretory role involving membrane vesicles, under conditions of copper overload (Forbes *et al.* 1998; Schaefer *et al.* 1999a).

Localisation studies done on the common WD mutation, H1069Q, revealed that ATP7B protein with this mutation was mislocalised to the endoplasmic reticulum of mammalian cells (Payne *et al.* 1998b). H1069Q was rapidly degraded in this compartment, leading to reduced ATP7B protein levels, and reduced copper efflux compared to normal ATP7B protein (Payne *et al.* 1998b).

ATP7A undergoes a copper-dependent trafficking event similar to ATP7B except that ATP7A moves from the trans-Golgi network to the plasma membrane following copper stimulation (Petris *et al.* 1996). There have been reports published attempting to correlate the disease severity of Menkes disease mutations with the intracellular localisation of the corresponding ATP7A mutant proteins (La Fontaine *et al.* 1999; Ambrosini *et al.* 1999). The ATP7A mutation A1362V is associated with a mild form of Menkes disease in humans, as is the brindled allele of the Mottled mouse (*Mo<sup>Br</sup>*), which has an in frame deletion of A799 and L800. Analysis of homozygous fibroblasts from mice or patients, by immunofluorescence microscopy, revealed that A1362V and *Mo<sup>Br</sup>* were localised to the trans-Golgi network but could not move to the plasma membrane in response to copper. The mutant fibroblasts accumulated more copper than control fibroblasts. Since the mutant proteins are associated with a milder Menkes disease

phenotype, it was assumed that some copper transport activity was retained. From these data it appears that movement from the trans-Golgi network and localisation to the plasma membrane were essential for copper efflux by ATP7A/Atp7a (La Fontaine *et al.* 1999; Ambrosini *et al.* 1999). However, these ATP7A studies lacked functional data on the mutant proteins analysed. Therefore it could not be determined conclusively if the Menkes disease phenotype observed in cell-lines is caused by defective ATP7A localisation alone, or if the phenotype was caused by defects in ATP7A copper transport activity.

Analysis of WD mutant proteins described in Chapter 3 revealed that several were able to completely, or nearly completely, complement the defective high-affinity iron uptake phenotype of *ccc2* mutant yeast cells indicating that these mutant ATP7B proteins retained normal, or partially reduced, copper transport activity (Forbes *et al.* 1998). On the basis of these data, it was hypothesised that mutant proteins retaining all, or most, copper transport activity, may be rare normal variants not yet found on normal chromosomes, or mutant proteins with normal capability to transport copper that are mislocalised in hepatocytes. Secondly, it was hypothesised that mutant ATP7B proteins retaining at least some copper transport capability, that are unable to undergo copper-dependent trafficking from the trans-Golgi network to the vesicular compartment, or are mislocalised, would not mediate adequate biliary copper efflux leading to hepatic copper accumulation. However, mutant proteins such as these could still transport sufficient copper into the Golgi for incorporation into ceruloplasmin.

This chapter describes preliminary work done to study the copper-dependent localisation, and potential mislocalization, of WD mutant ATP7B proteins that have been previously assayed for function (Chapter 3) (Forbes *et al.* 1998). The goal of this work was to attempt to understand the interrelationship between ATP7B intracellular localisation, copper-dependent trafficking, and copper transport function, with respect to WD pathogenesis. To do so, the intracellular localisation of ATP7B mutant proteins has been analysed using transient transfection and immunofluorescence microscopy.

## **4B) MATERIALS AND METHODS.**

### **4B-1) Cell culture and antibodies.**

Cell lines used in this study were HepG2, HeLa, and Chinese Hamster ovary cells (CHO) originally obtained from the American Type Cell Culture (ATCC) resource. Cells were maintained in Dulbecco's modified eagle medium (DMEM) containing 10% fetal calf serum, and 100 U/mL each of penicillin and streptomycin. All cell culture reagents were obtained from Gibco/ Life Technologies. Cells were maintained at 37°C in a 5%

carbon dioxide atmosphere. The ATP7B specific antibodies were affinity purified anti-ATP7B.N60 described section 2B-7. Secondary antibodies were goat-anti-rabbit IgG monoclonal antibodies conjugated to FITC fluorophor (Jackson Laboratories). Endoplasmic reticulum was detected using concanavalin A (ConA), conjugated with AMCA-S fluorophor (Molecular Probes, U.S.A). Golgi-58K mouse monoclonal antibodies, and sheep anti-mouse IgG monoclonal antibodies conjugated to Cy3 fluorophor (Sigma) were used to detect the Golgi network. The Golgi network was detected in some experiments using wheat-germ agglutinin (WGA), conjugated with AMCA-S fluorophor (Molecular Probes, U.S.A).

#### **4B-2) Transient transfection.**

ATP7B cDNA and site-directed mutant variants were constructed as previously described (Forbes *et al.* 1998) (Chapter 3). For transient transfection into mammalian cells, ATP7B normal and mutant cDNAs were restriction enzyme digested with Bam HI and Sal I from pUC19 vector, gel purified, and cloned into the mammalian expression vector pCDNA1 (Invitrogen) using Bam HI and Xho I sites in the vector. Expression plasmids were isolated from 100 mL cultures of bacteria grown in LB medium containing 100 µg/mL carbenicillin using ion exchange chromatography (Qiagen Midi Prep kit, Qiagen) according to the manufacturer's protocol.

One day prior to transfection, cells were plated 40-50% confluent onto sterile glass coverslips (10 mm diameter, Fisher Scientific) contained in six-well tissue culture plates in 2 mL of medium. Cells grown overnight were transfected using 1.5 µg of plasmid DNA, and 15 µL of LipoFectin reagent (Gibco/Life Technologies) according to manufacturer's protocols. The cells were incubated with the transfection mixture for 6-8 hours followed by replacement with standard medium. Following overnight growth, medium was left unsupplemented, was supplemented with 250 µM copper chloride, or 50 µM BCS. The additives used in individual experiments are detailed in the appropriate figures. The cells were incubated for a further 2-3 hours prior to immunofluorescence experiments.

#### **4B-3) Indirect immunofluorescence microscopy.**

Cells attached to coverslips were transferred to a new 6-well plate and processed for immunofluorescence. Cells were rinsed twice with TBS then fixed for 20 min. at 4°C with 4% paraformaldehyde made in TBS. Fixed cells were rinsed twice with TBS then made permeable by incubation for 10 min. in 0.5% Triton X-100 (membrane grade, Boehringer Mannheim) made in TBS. Permeable cells were blocked for 30 min. with 2% milk powder in TBS. Affinity purified anti-ATP7B.N60 antibodies were used as primary

antibodies incubated for 2-3 hours at room temperature at a 1/100 dilution in blocking buffer. To detect the Golgi network, Golgi-58K antibodies were used in addition to anti-ATP7B.N60 at a 1/100 dilution. After primary incubation with the primary antibodies, cells were rinsed twice with TBS containing 0.5% Tween-20 (TBST) then washed 3x5 min. in the same. Secondary antibodies were incubated for 1 hr. at room temperature in blocking buffer using a 1/100 dilution of goat anti-rabbit IgG-FITC to detect anti-ATP7B.N60. Sheep anti-mouse IgG-Cy3 was used at a 1/1000 dilution to detect Golgi-58 K antibodies. To visualise the endoplasmic reticulum AMCA-S labelled ConA was added to the secondary antibodies mixture at a final concentration of 100  $\mu\text{g}/\text{mL}$ . To detect the Golgi network in HeLa cells, AMCA-S labelled WGA was added to the secondary antibodies mixture at a final concentration of 100  $\mu\text{g}/\text{mL}$ . After incubation with the secondary antibodies, cells were rinsed three times with TBST, then washed 4x5 min. with TBST. Coverslips were then mounted onto slides using mounting media (Vectashield, Vector Laboratories) and sealed with clear nail polish (Mabelline). Microscopy was performed on a Leica DMRE fluorescent microscope with filters for FITC, rhodamine, or Dapi using a 100x oil-immersion objective lens. Photographs were taken with 400 speed film (Kodak Gold) using 20 and 40 sec. exposures.

#### **4C) RESULTS.**

##### **4C-1) Specificity of antibodies.**

The antibodies used for immunofluorescence was affinity purified anti-ATP7B.N60, which recognises the copper-binding domain of ATP7B. These antibodies can detect ATP7B protein expressed in yeast on immunoblots, while the pre-immune serum cannot (section 2C-3). Anti-ATP7B.N60 antibodies were able to recognise endogenous ATP7B protein expressed in HepG2 cells (Fig. 4-1). Pre-incubation of the antibodies with 5 $\mu\text{g}$  of protein from yeast expressing ATP7B completely eliminated the signal, whereas the same amount of protein from control yeast extracts did not. Additionally, anti-ATP7B.N60 gave no specific signal in HeLa, or CHO cells, which express ATP7A but not ATP7B. These data demonstrate that anti-ATP7B.N60 antibodies were specific for ATP7B and did not cross react with ATP7A in this application. The ATP7B.C10 antibodies against the C-terminus of ATP7B did not work in immunofluorescence studies.

##### **4C-2) Copper-induced trafficking of ATP7B.**

HepG2 cells are liver hepatoblastoma cells expressing endogenous ATP7B and were initially chosen as a biologically relevant cell line for studying mutant ATP7B

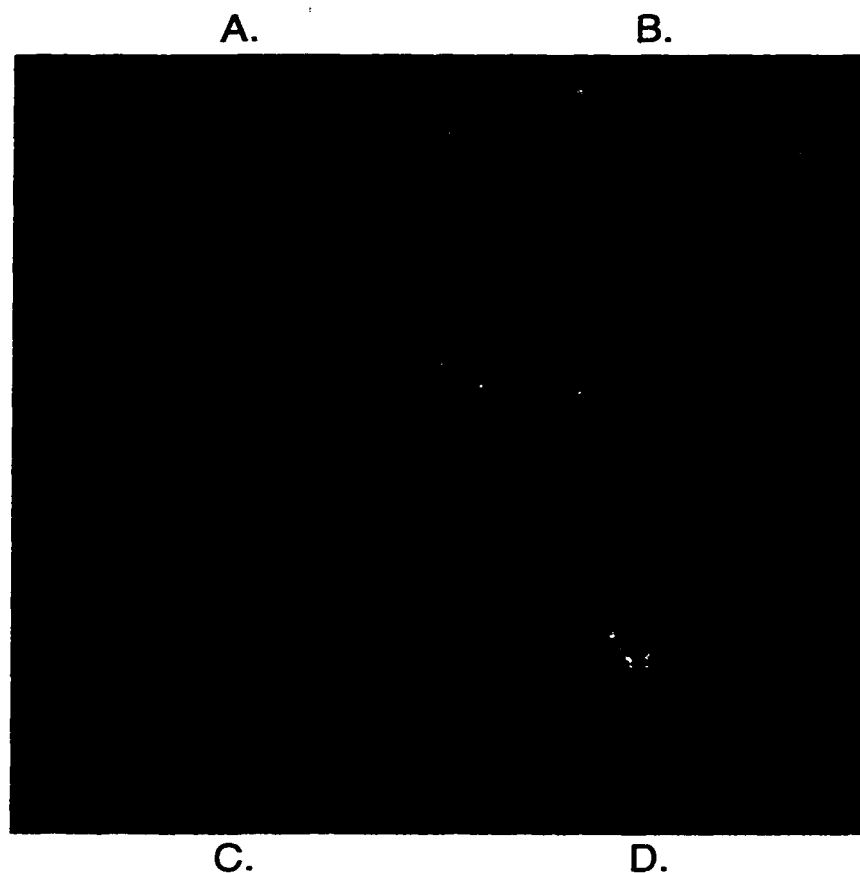


**Figure 4-1: Specificity of Antibodies.**

Endogenous ATP7B in HepG2 cells was detected by immunofluorescence microscopy, as described in 4B-3, using Anti-ATP7B.N60 antibodies as follows: **A.**, no primary antibodies. **B.**, Anti-ATP7B.N60 antibodies were used as the primary antibody at a 1/100 dilution. **C.**, Anti-ATP7B.N60 antibodies, used at a 1/100 dilution, were pre-incubated with 5 $\mu$ g of protein extract from yeast expressing ATP7B prior to their use as the primary antibody. **D.**, Anti-ATP7B.N60 antibodies, at a 1/100 dilution, were pre-incubated with 5 $\mu$ g of protein extract from control yeast not expressing ATP7B, prior to their use as the primary antibody. Microscopy was performed with a 20x lens.

localisation and copper-induced trafficking. Endogenous ATP7B detected by immunofluorescence with anti-ATP7B.N60 antibodies gave distinct Golgi localisation in standard medium, and redistributed almost entirely to cytoplasmic vesicles (little residual Golgi staining) upon addition of 500  $\mu$ M copper sulphate to the growth media as was originally described by Hung *et al.* (1997). A single haemagglutinin (HA) epitope tag was added to the C-terminus of ATP7B by incorporation into a PCR primer in order to differentiate transiently transfected ATP7B proteins, from endogenous ATP7B protein. The tagged protein was poorly recognised by the anti-HA monoclonal antibodies in immunofluorescence experiments under all conditions attempted, and HepG2 proved difficult to transfect efficiently. This approach was terminated in favour of transient transfection of ATP7B into HeLa cells, which do not express ATP7B, followed by indirect detection of the transfected protein using ATP7B specific antibodies. This was successful in that ATP7B was distinctly visible in the Golgi network of transfected HeLa cells, with no background staining visible in non-transfected cells. However, ATP7B did not visibly relocate to cytoplasmic vesicles in response to copper when expressed in HeLa cells (Fig. 4-2). It remained localised to Golgi membranes at all copper concentrations attempted. HeLa cells were therefore judged to be unsuitable for further studies on copper-dependent trafficking.

The final cell-type used was CHO cells, which have been used extensively for work on ATP7A (Petris *et al.* 1998; Petris *et al.* 1996; Strausak *et al.* 1999). Transfection of ATP7B into CHO cells, followed by immunofluorescence with anti-ATP7B.N60, antibodies revealed strong expression of ATP7B, and perinuclear staining, co-localising with Golgi-58K marker antibodies under low copper conditions (Fig. 4-3). The addition of copper chelator BCS to the medium gave slightly more distinct localisation to the Golgi network than that seen in standard medium and was used in all experiments. Negligible background staining was observed in untransfected cells. Addition of copper to the growth medium caused a distinct redistribution of ATP7B from the Golgi network to a cytoplasmic vesicular localisation in transiently transfected CHO cells (Fig. 4-3). Residual Golgi network localised ATP7B protein was evident in most cells, however, in cells expressing low amounts of ATP7B, redistribution appeared complete suggesting that some degree of residual Golgi localisation was due to ATP7B overexpression.

Normal ATP7B protein was mislocalised to the endoplasmic reticulum in approximately 10-20% of transfected cells. Mislocalization was observed mostly in cells staining very brightly with antibodies, and was likely the result of ATP7B overexpression overloading the cell's secretory pathway. CHO cells appeared to be more sensitive to endoplasmic reticulum mislocalization of normal ATP7B protein than HeLa cells. In

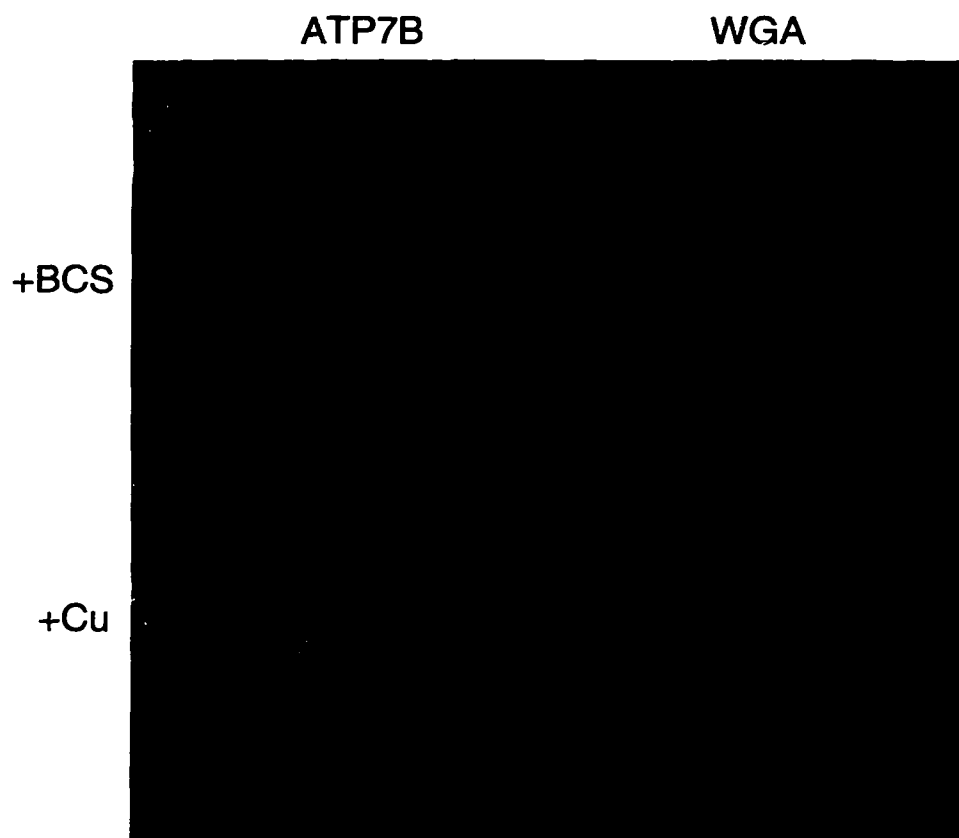


**Figure 4-2: Copper-dependent subcellular localization of ATP7B transiently expressed in HeLa cells.**

Composite image showing the subcellular localization of ATP7B transiently expressed in HeLa cells. Two-three hours prior to processing for immunofluorescence, cells were treated with either the copper chelator BCS (50  $\mu\text{M}$ ), or copper chloride (250  $\mu\text{M}$ ). ATP7B protein was detected with affinity-purified rabbit polyclonal antibodies against its copper-binding domain. The Golgi network was detected with WGA. All proteins and markers were detected simultaneously. Each row represents the same cell. Microscopy was performed using a 100x oil immersion lens.

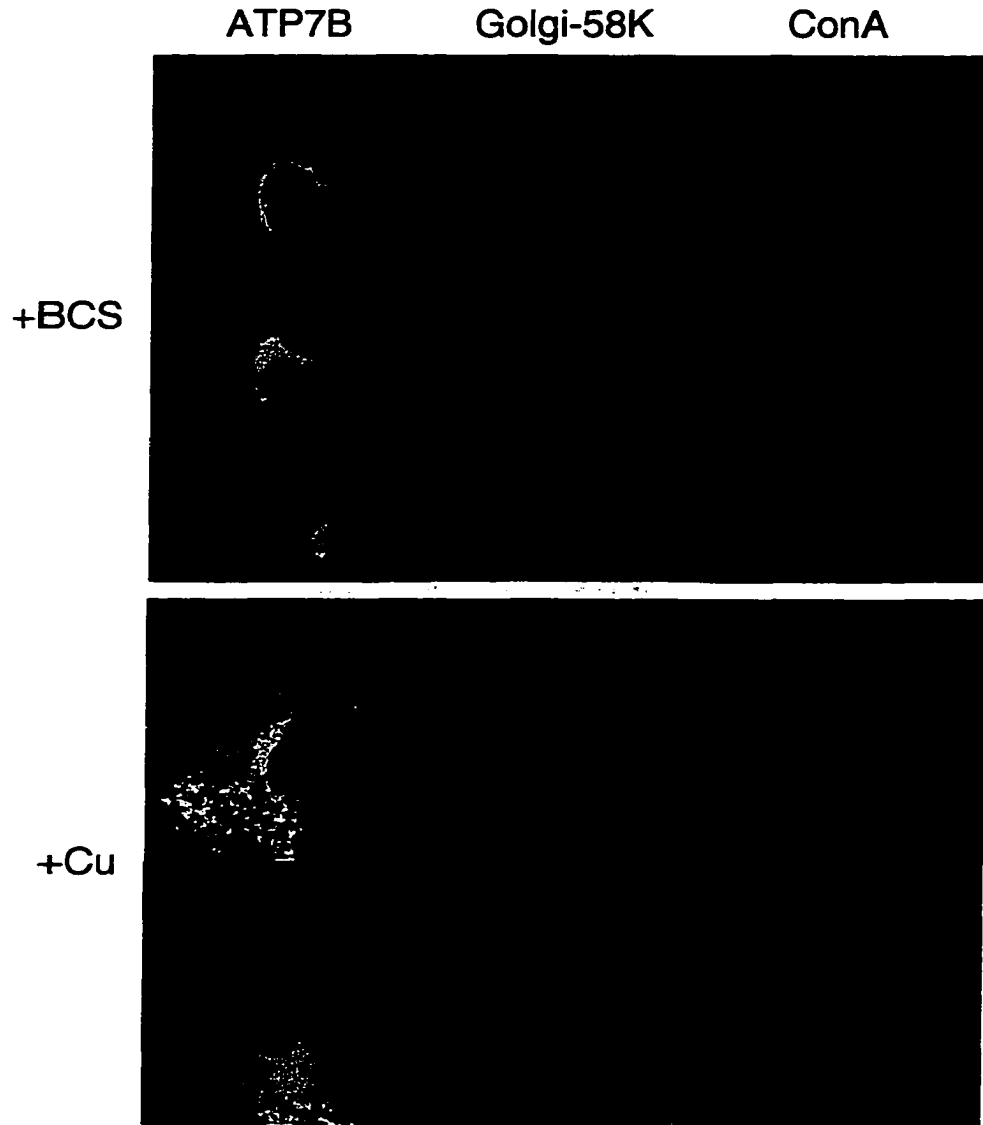


**Figure 4-3: Copper induced redistribution of ATP7B transiently expressed in CHO cells.**

Composite image showing the copper-dependent subcellular localization of ATP7B. CHO cells were transiently transfected with an *ATP7B* expression construct. Two-three hours prior to processing for immunofluorescence, cells were treated with either the copper chelator BCS (50  $\mu\text{M}$ ), or copper chloride (250  $\mu\text{M}$ ). ATP7B protein was detected with affinity-purified rabbit polyclonal antibodies against its copper-binding domain. The Golgi network was detected with mouse monoclonal Golgi-58K antibodies. The endoplasmic reticulum was detected with fluorescent ConA. All proteins and markers were detected simultaneously. Each row represents the same cell. Microscopy was performed using a 100x oil immersion lens.

HeLa cells, transiently transfected normal ATP7B protein exhibited distinct Golgi network localisation in nearly all transfected cells, even in those highly overexpressing the protein (Fig4-2). Very little diffuse, reticular, cytoplasmic staining of ATP7B characteristic of localisation to the endoplasmic reticulum was observed.

#### 4C-3) Localisation of ATP7B WD mutant proteins.

The ATP7B WD mutant proteins analysed in this study were D765N, L776V, and G943S, which had normal, or nearly normal, capability to complement *ccc2* mutant yeast indicating normal copper transport activity (Forbes *et al.*1998). R778L was chosen as a representative of a severely defective, but not inactive, WD mutant ATP7B protein (Forbes *et al.*1998). A protein with the CPC motif mutated (CPC/S) was chosen as an example of a mutant protein completely unable to transport copper in our complementation assay (Forbes *et al.*1998). M769V had temperature-dependent activity in our yeast complementation assay (no complementation at 37°C) (Forbes *et al.*1998). These mutations are all found in the predicted transmembrane domain of ATP7B (Fig. 3-1). D765N, M769V, L776V, and R778L are found in the fourth membrane-spanning segment. G943S and CPC/C are found in the putative fifth and sixth transmembrane segments respectively.

Immunofluorescent detection of ATP7B mutant proteins was carried out in transiently transfected CHO cells to assess copper-dependent localisation and potential mislocalization. Since HeLa cells rarely exhibit mislocalised ATP7B protein, ATP7B mutants mislocalised in a large proportion of transfected HeLa cells, as well as CHO cells, supports a true mislocalization phenotype rather than an overexpression artifact. Transiently transfected HeLa cells were therefore used as a control for overexpression-induced ATP7B mislocalization.

The putative WD mutants D765N and L776V were partially localised to the Golgi of transfected CHO cells in copper limited medium (Table 4-1; Fig. 4-4; Fig. 4-5). The majority of mutant protein was localised to the endoplasmic reticulum. Addition of copper to the growth medium resulted in redistribution of both D765N and L776V Golgi localised protein to cytoplasmic vesicles. However endoplasmic reticulum staining remained prominent. D765N and L776V were mislocalised in HeLa cells showing a

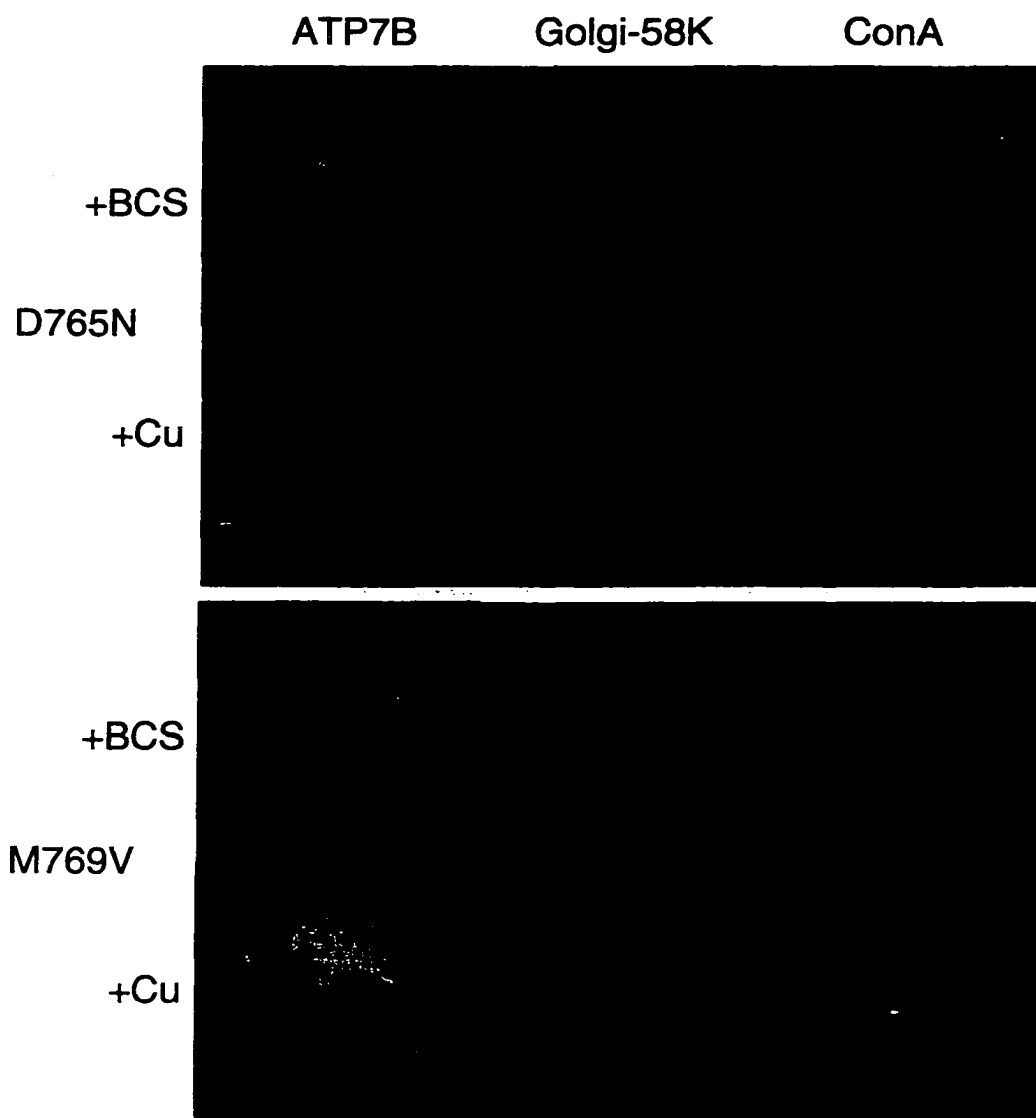


**Figure 4-4: Copper-induced redistribution of ATP7B Wilson disease mutant proteins transiently expressed in CHO cells.**

Composite image showing the copper-dependent subcellular localization of ATP7B. CHO cells were transiently transfected with an *ATP7B* expression construct. Two-three hours prior to processing for immunofluorescence, cells were treated with either the copper chelator BCS (50  $\mu\text{M}$ ), or copper chloride (250  $\mu\text{M}$ ). ATP7B protein was detected with affinity-purified rabbit polyclonal antibodies against its copper-binding domain. The Golgi network was detected with mouse monoclonal Golgi-58K antibodies. The endoplasmic reticulum was detected with fluorescent ConA. All proteins and markers were detected simultaneously. Each row represents the same cell. Microscopy was performed using a 100x oil immersion lens.

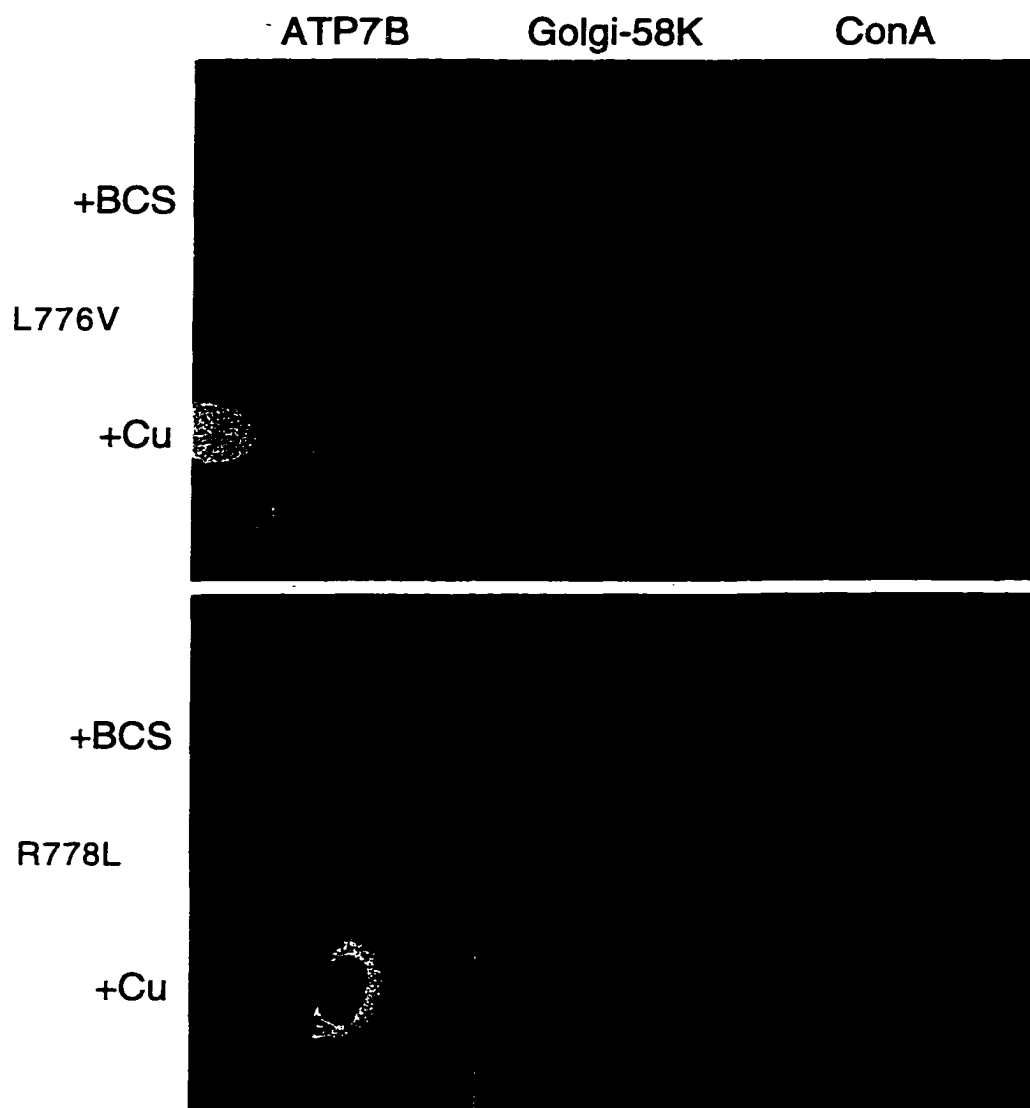


**Figure 4-5: Copper-induced redistribution of ATP7B Wilson disease mutant proteins transiently expressed in CHO cells.**

Composite image showing the copper-dependent subcellular localization of ATP7B. CHO cells were transiently transfected with *ATP7B* expression constructs. Two-three hours prior to processing for immunofluorescence, cells were treated with either the copper chelator BCS (50  $\mu$ M), or copper chloride (250  $\mu$ M). ATP7B protein was detected with affinity-purified rabbit polyclonal antibodies against its copper-binding domain. The Golgi network was detected with mouse monoclonal Golgi-58K antibodies. The endoplasmic reticulum was detected with fluorescent ConA. All proteins and markers were detected simultaneously. Each row represents the same cell. Microscopy was performed using a 100x oil immersion lens.

diffuse staining pattern characteristic of the endoplasmic reticulum instead of tight Golgi network staining as marked by WGA (Fig. 4-7). Therefore the D765N and L776V WD mutations result in mislocalization of the mutant proteins, but any Golgi network localised mutant protein appears to retain the ability to redistribute to cytoplasmic vesicles when stimulated by copper.

**Table 4-1. Summary of localisation and functional data for ATP7B Wilson disease mutant proteins.**

<b>ATP7B Mutant Protein</b>	<b>Golgi Network Localisation</b>	<b>Endoplasmic Reticulum Mislocalization</b>	<b>Copper-dependent Redistribution</b>
-----------------------------	-----------------------------------	--	--

**Normal or near normal function in yeast (Forbes *et al.* 1998)**

<b>D765N</b>	partial	extensive	normal
<b>L776V</b>	partial	extensive	normal
<b>G943S</b>	normal	partial	negligible

**Impaired function in yeast (Forbes *et al.* 1998)**

<b>R778L</b>	not determined	very extensive	not determined
<b>M769V</b>	normal	none	normal
<b>CPC/S</b>	normal	partial	negligible

The M769V mutant protein was localised to the Golgi network under copper-limited conditions, and redistributed to cytoplasmic vesicles in response to copper in a manner indistinguishable from normal ATP7B when transfected into CHO cells (Table 4-1; Fig. 4-4). There was no excessive endoplasmic reticulum M769V staining compared to normal ATP7B seen in transfected CHO cells. M769V was localised to the Golgi network in transfected HeLa cells (Fig. 4-4; Fig. 4-7). These data indicate that the M769V mutation had no effect on ATP7B localisation or copper-induced trafficking.

R778L mutant protein was predominantly and very extensively localised to the endoplasmic reticulum when expressed in CHO cells and exhibited very diffuse reticular staining in HeLa cells (Table 4-1; Fig. 4-5, Fig. 4-7). This phenotype was observed in virtually all transfected cells in both cell types. The endoplasmic reticulum staining was so strong it could not be determined if copper addition had any effect on the mutant proteins localisation. The R778L mutation clearly disrupts normal localisation of ATP7B protein.

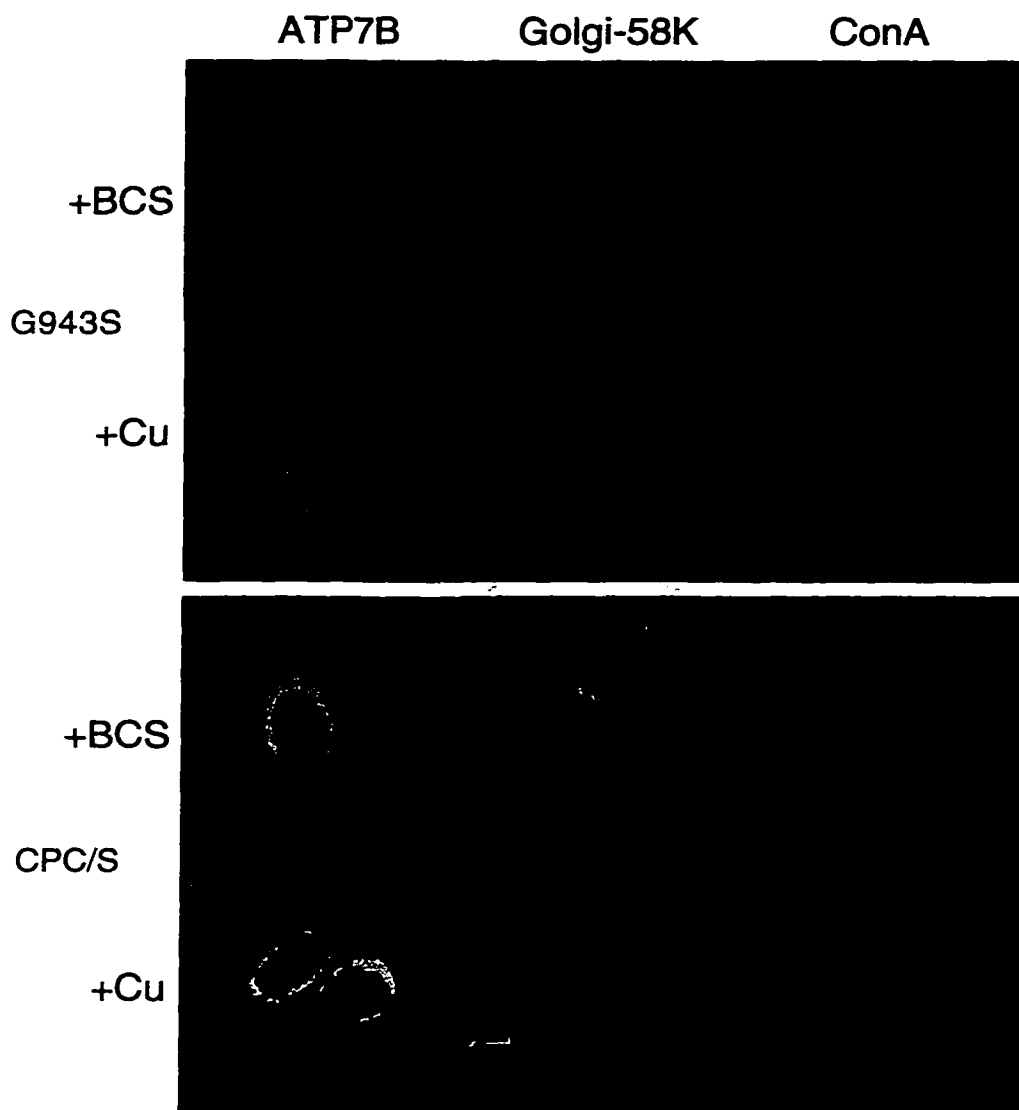


**Figure 4-6: Copper-induced redistribution of ATP7B Wilson disease mutant proteins transiently expressed in CHO cells.**

Composite image showing the copper-dependent subcellular localization of ATP7B. CHO cells were transiently transfected with *ATP7B* expression constructs. Two-three hours prior to processing for immunofluorescence, cells were treated with either the copper chelator BCS (50  $\mu$ M), or copper chloride (250  $\mu$ M). ATP7B protein was detected with affinity-purified rabbit polyclonal antibodies against its copper-binding domain. The Golgi network was detected with mouse monoclonal Golgi-58K antibodies. The endoplasmic reticulum was detected with fluorescent ConA. All proteins and markers were detected simultaneously. Each row represents the same cell. Microscopy was performed using a 100x oil immersion lens.

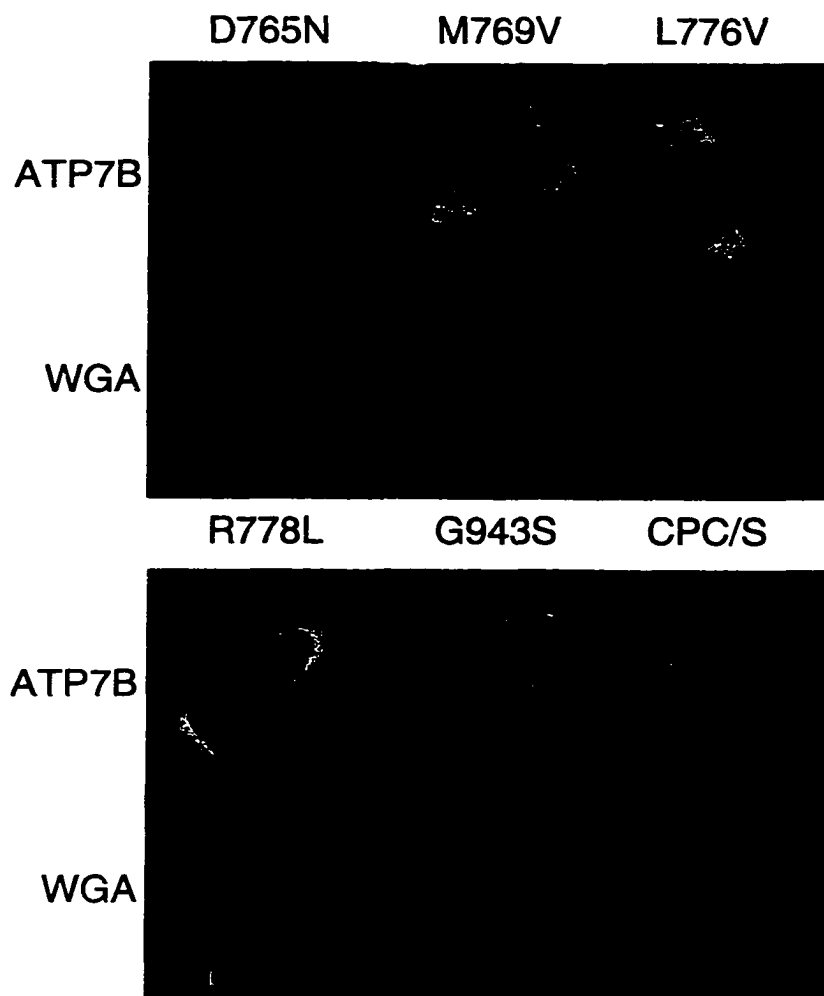


**Figure 4-7: Localisation of ATP7B Wilson disease mutant proteins transiently expressed in HeLa cells.**

Composite image showing the subcellular localization of ATP7B mutant proteins transiently expressed in HeLa cells. ATP7B protein was detected with affinity-purified rabbit polyclonal antibodies against its copper-binding domain. The Golgi network was detected with WGA. All proteins and markers were detected simultaneously. Each column represents the same cell. Microscopy was performed using a 100x oil immersion lens. No copper or BCS were added to the cells prior to immunofluorescence.

G943S and CPC/S mutant ATP7B proteins were predominantly localised to the Golgi network under copper-limited conditions when expressed in CHO cells (Table 4-1; Fig4-6; Fig. 4-7). Addition of copper to the growth medium resulted in very little or no visible redistribution of either mutant protein to cytoplasmic vesicles. G943S was also partly localised to the endoplasmic reticulum under copper-limited, or copper-supplemented condition in CHO cells. The proportion of cells exhibiting endoplasmic reticulum G943S stain, and the extent of endoplasmic reticulum staining, appeared to be slightly greater than normal ATP7B but less than seen for D765N, L776V, or especially R778L under copper-limited conditions. In copper-treated CHO cells, the extent of G943S endoplasmic reticulum staining appeared to slightly increase. CPC/S exhibited slightly more endoplasmic reticulum staining compared with normal ATP7B expressed in CHO cells. These data indicate that the G943S and CPC/S mutations result in mutant proteins whose localisation was insensitive to copper, and in the case of G943S appeared to be somewhat mislocalised to the endoplasmic reticulum.

#### 4D) DISCUSSION.

The effect of WD mutations on the intracellular localisation and copper-induced trafficking of ATP7B has been investigated. ATP7B was localised to the Golgi network in HepG2 cells, and transiently transfected HeLa and CHO cells, under copper-limited conditions. Addition of copper to growth medium resulted in the redistribution of ATP7B to cytoplasmic vesicles in CHO and HepG2 cells. These results confirm those previously reported (Hung *et al.* 1997; Schaefer *et al.* 1999a; La Fontaine *et al.* 1998). Interestingly, copper had no effect on the localisation of ATP7B in HeLa cells. The protein remained tightly associated with the Golgi network. A similar result was reported when ATP7B was stably expressed in Menkes disease patient fibroblasts (La Fontaine *et al.* 1998). ATP7B was able to rescue the copper sensitivity of the fibroblasts and mediate copper efflux as well as ATP7A did. However, ATP7B did not observably change its localisation in response to copper as did ATP7A. An interpretation of these data, combined with my HeLa cell data, suggests that ATP7B may require additional factors, not found in every cell type, and not required for ATP7A trafficking, in order to redistribute when stimulated by copper. This putative factor may be a protein generally involved in protein sorting within the secretory pathway, that ATP7B docks with when stimulated by copper, in order to change its localisation. The putative factor may be a second subunit of ATP7B analogous to the  $\beta$ -subunit of the  $\text{Na}^+/\text{K}^+$ -ATPase (Skou *et al.* 1992) that could be required for protein trafficking when stimulated by copper. This putative trafficking factor is not likely required for transport function, since ATP7B was

still able to mediate copper efflux (La Fontaine *et al.*1998). Immunoprecipitation of ATP7B from HepG2 cell extracts did not reveal any proteins, besides the cuprochaperone protein ATOX1 that interacted with ATP7B (Hamza *et al.*1999; Hung *et al.*1997). However, co-immunoprecipitation may not reveal all proteins that interact weakly, or transiently, with ATP7B, especially if the proteins are not abundant in the cell. Further studies are required to pursue this hypothesis.

The WD mutation D765N is a rare mutation found in patients of Italian descent (Figus *et al.*1995), and L776V was originally not classified with certainty as a mutation or normal variant due to the conservative nature of the amino acid substitution (Thomas *et al.*1994). Both D765N and L776V mutant proteins were analysed for function by yeast complementation and were found to complement *ccc2* mutant yeast in a manner indistinguishable from normal ATP7B (Chapter 3) (Forbes *et al.*1998). On the basis of these functional data, it was hypothesised that these mutations were rare normal variants not yet found in the normal population, or resulted in ATP7B proteins with normal function that were mislocalised in hepatocytes thereby causing WD. Immunofluorescent detection of these mutant proteins transiently transfected into CHO cells revealed that both proteins were localised in part to the Golgi network and were capable of redistribution to cytoplasmic vesicles when stimulated by copper. However, D765N and L776V proteins also exhibited extensive localisation to the endoplasmic reticulum of CHO cells suggesting that the proteins were mislocalised. These mutations likely cause ATP7B protein to misfold and be retained in the endoplasmic reticulum. Based on data to date, it can be hypothesised that D765N and L776V proteins could result in a milder WD presentation. These mutant proteins have apparently normal activity in the yeast assay (Forbes *et al.*1998) and at least some proportion of the mutant proteins is normally localised to the Golgi and able to redistribute to cytoplasmic vesicles in response to copper. Therefore homozygous or compound heterozygous patients carrying these mutations may have ceruloplasmin activity levels within the normal range, and liver copper levels may be elevated, but perhaps less so than in patients with more severe mutations such as frameshifts. Due to the rarity of the mutations, there is insufficient phenotypic data available for WD patients homozygous for either D765N or L776V to confirm this hypothesis.

The WD mutation R778L is a common mutation found in patients of Asian descent, and in homozygous form, is associated with an early onset of WD with hepatic presentation (Nanji *et al.*1997; Cox *et al.*1999). Functional analysis of this mutant protein by yeast assay revealed a severe defect in the ability of R778L mutant protein to complement *ccc2* mutant yeast, indicative of impaired copper transport function (Forbes

*et al.*1998). Localisation data presented in this chapter has revealed extensive mislocalization of the mutant protein to the endoplasmic reticulum of CHO cells. R778L mutation likely causes the mutant ATP7B protein to misfold and be retained in the endoplasmic reticulum, in addition to reducing its copper transport ability (Forbes *et al.*1998). These data, are consistent with the severe WD phenotype observed in R778L homozygous patients.

The mutation M769V was originally not definitively classified as a WD mutation, or rare normal variant (Thomas *et al.*1994). The mutation was not found in normal individuals, and the methionine residue is conserved in ATP7A, however the mutant amino acid substitution was considered to be relatively conservative. Since the original publication, M769V has been found in many more WD patients, but not in normal individuals, supporting its designation as a disease associated mutation (D.W.C., unpublished data). Functional data obtained by yeast complementation analysis revealed that the mutant protein was able to fully complement *ccc2* mutant yeast at 30°C, but was profoundly temperature sensitive, unable to complement in singlecopy at 37°C (Chapter 3) (Forbes *et al.*1998). Based on these data it was concluded that M769V was indeed a disease causing mutation in patients. However, M769V protein was not completely non-functional, as overexpression of M769V from a multicopy vector was able to fully complement *ccc2* mutant yeast at 37°C (Forbes *et al.*1998). Immunofluorescence data presented in this chapter has revealed that M769V protein is localised to the Golgi of CHO cells and redistributes to cytoplasmic vesicles when incubated with copper in a manner indistinguishable from normal ATP7B protein. These localisation data were obtained from cells grown at 37°C suggesting that the temperature-sensitive phenotype of the protein in yeast was due to reduced activity and not to temperature-induced mislocalization. Little endoplasmic reticulum localisation was detected (no more than normal ATP7B) for M769V in CHO cells suggesting that the mutant protein was not severely misfolded. Since M769V retains at least some capability to transport copper at 37°C, and is able to undergo normal copper-induced redistribution into vesicles, WD patients carrying homozygous M769V may have residual ATP7B dependent copper excretion, and holo-ceruloplasmin levels at the upper end of the WD range. There is insufficient phenotypic data yet available for M769V homozygotes to confirm or deny this hypothesis.

WD mutation G943S appears to be localised normally to the Golgi of CHO and HeLa cells, but in CHO cells appears to be non-responsive to copper, exhibiting no obvious copper-induced redistribution. G943S also appears to be partially mislocalised to the endoplasmic reticulum under low copper conditions in CHO cells. These data

suggest that the G943S protein was somewhat misfolded resulting in endoplasmic reticulum retention. Addition of copper to the growth medium appears to exacerbate the observed mislocalization of G943S in CHO cells, although Golgi network localisation was still apparent. Copper binding to this mutant protein may induce further conformational changes that enhance endoplasmic reticulum retention, but are not able to trigger movement to cytoplasmic vesicles. G943S is found within the fifth transmembrane segment, and the Ser substitution may prevent putative transmembrane domain conformational changes required to initiate trafficking out the Golgi in response to copper. G943S is a mutation found in the Bangladeshi population and was associated with mild WD in a homozygous patient (Thomas *et al.* 1994). Functional data revealed that the G943S protein had a slight but statistically significant reduction in its ability to complement *ccc2* mutant yeast indicative of slightly reduced copper transport ability consistent with the milder disease presentation (Forbes *et al.* 1998; Thomas *et al.* 1994). Under copper-limited conditions, G943S protein in the Golgi network should have sufficient activity for normal copper incorporation into ceruloplasmin. However, since the protein could not redistribute in response to copper, or did so poorly, biliary copper efflux is predicted to be impaired. There are insufficient numbers of WD patients carrying G943S to confirm this hypothesis.

The final mutant ATP7B protein analysed in this study was CPC/S. CPC/S is not a mutation found in WD patients, but is a mutant protein variant with mutations (Cys-Ser) in the CPC motif conserved in CPx-type ATPases. Due to its conservation, and functional analogy to ion binding sites in P-type ATPases, this motif is considered to be critical for ATP7B function perhaps acting as a copper-binding site within the transmembrane domain (Solioz, 1998; Bull *et al.* 1994). Indeed, mutation of the CPC motif resulted in a non-functional ATP7B protein completely unable to complement *ccc2* mutant yeast (Forbes *et al.* 1998; Yoshimizu *et al.* 1998; Hung *et al.* 1997) even when expressed from a multicopy vector (Forbes *et al.* 1998). CPC/S was the only non-functioning ATP7B mutant protein analysed by immunofluorescence in this study, and its localisation, normal in the Golgi network, appeared to be non-responsive to copper. This result supports the hypothesis that copper-dependent trafficking depends in part on copper transport function (Ambrosini *et al.* 1999). Perhaps mutations in this motif prevent copper binding to the putative transmembrane domain of ATP7B required for copper transport, and also required as a trafficking initiation signal. The CPC/S mutation may prevent putative transmembrane domain conformational changes that may be required to allow copper-induced redistribution. Alternatively, the CPC/S mutant ATP7B protein may be partially misfolded and therefore unable to traffick or transport copper.

From the data presented in Chapter 3, which addressed the functional significance of the WD mutations in the copper transport function of ATP7B, two hypotheses were made. It was predicted that mutant ATP7B proteins with normal or near normal function could be either rare normal variants or mutant proteins that are mislocalised in hepatocytes thereby causing WD. Immunofluorescence and functional data for the WD mutations D765N, L776V, R778L, and G943S presented in this thesis together with studies done in other laboratories on ATP7A (La Fontaine *et al.* 1999; Ambrosini *et al.* 1999) and on the H1069Q WD mutation (Payne *et al.* 1998b) support this hypothesis. Secondly it was hypothesised that mutant proteins with normal or near normal activity trapped in the Golgi network and unable to redistribute to endosomal vesicles in response to copper could result in normal holo-ceruloplasmin biosynthesis, but reduced biliary copper efflux leading to a milder form of WD. Data presented in this chapter support this hypothesis as well. These hypotheses may in part explain the clinical variability seen in patients with WD. The relevance of the localisation data obtained during this study, combined with functional data from Chapter 3, to normal copper excretion and WD pathogenesis is discussed in more detail in Chapter 6.

**CHAPTER 5****ANALYSIS OF THE ATP7B COPPER-BINDING DOMAIN.**

Data presented in this chapter have been published in:

Forbes, J.R., Hsi, G. and Cox, D.W. (1999) Role of the copper-binding domain in the copper transport function of ATP7B, the P-type ATPase defective in Wilson disease. *J.Biol.Chem.*, **274**:12408-12413.

Gloria Hsi contributed to sequencing and assembly of the mutant *ATP7B* constructs described in this chapter.

## 5A) INTRODUCTION.

Heavy-metal transporting P-type ATPases (designated CPx-type ATPases) are distinguished from other P-type ATPases, in part by the presence of a large N-terminal metal-binding domain (Solioz, 1998). There have been several hypotheses presented regarding the role of copper binding to the copper-binding domain in the overall function of CPx-type ATPases. The copper-binding domain has been proposed to remove copper from cytosolic ligands and to transiently bind copper prior to transport (Vulpe *et al.* 1993; Bull *et al.* 1994). A recent study has substantiated this hypothesis (Pufahl *et al.* 1997). Atx1p is a yeast copper chaperone protein required upstream of Ccc2p for iron and copper homeostasis in yeast (Lin *et al.* 1997). Biophysical analysis of Atx1p determined that Cu(I) was bound by sulphur atoms in either a two, or three, co-ordinate geometry (Pufahl *et al.* 1997). Yeast two-hybrid analysis demonstrated that Atx1p, which contains one copper-binding motif, was able to interact directly with the putative copper-binding domain of Ccc2p, but no other predicted domain of Ccc2p (Pufahl *et al.* 1997). This interaction was dependent on copper ions and suggested that Atx1p could donate copper to Ccc2p by direct interaction and facile copper exchange between homologous GMxCxxCxxxIE motifs (Pufahl *et al.* 1997). Atx1p was later shown to be able to transfer bound mercury to the copper-binding domain of Ccc2p supporting the metal exchange hypothesis (Rosenzweig *et al.* 1999). The basic, lysine rich, face of Atx1p was required for yeast two-hybrid interaction between Atx1p, and the copper-binding domain of Ccc2p, which appears to be somewhat acidic, suggesting that charge interactions may be required for docking and copper transfer between the two proteins (Portnoy *et al.* 1999). A human functional orthologue of Atx1p exists (ATOX1: originally designated HAH1) and is able to functionally replace Atx1p in yeast (Klomp *et al.* 1997). ATOX1 has been shown to interact with the copper-binding domains of both ATP7B and ATP7B using yeast two-hybrid and co-immunoprecipitation strategies (Larin *et al.* 1999; Hamza *et al.* 1999). Taken together, these data support the hypothesis that copper removed from a cytosolic chaperone protein and transiently bound to the ATP7B copper-binding domain is the source of copper for subsequent transport.

Pufahl *et al.* (1997) have suggested the following mechanism for copper transfer from Atx1p to Ccc2p: 1) Atx1p, with copper bound in a linear arrangement between the cysteines within its copper-binding motif, docks with a copper-binding subdomain of Ccc2p. 2) A cysteine residue from the Ccc2p copper-binding motif binds to the chaperone-bound copper atom, forming a three co-ordinate binding intermediate. 3)

Rapid ligand switching occurs, resulting in transfer of copper to the copper-binding motif of Ccc2p, and release of apo-Atx1p.

Another proposed role for the copper-binding domain is that of a copper sensor (Vulpe *et al.* 1993; DiDonato *et al.* 1997; Petris *et al.* 1996). When mammalian cells were exposed to high concentrations of copper, ATP7A and ATP7B underwent a reversible copper-regulated trafficking event, from the trans-Golgi network to the plasma membrane or a post-Golgi vesicular compartment respectively (Hung *et al.* 1997; Petris *et al.* 1996). This trafficking may represent a change in physiologic function of ATP7B from cupro-enzyme biosynthesis in the Golgi network, to a copper efflux function in the plasma membrane or secretory vesicles. The observed trafficking event may be triggered by conformational changes induced by cooperative copper binding to the N-terminal domains of these proteins (DiDonato *et al.* 1997; Jensen *et al.* 1999a).

The metal binding properties of the ATP7B copper-binding domain are beginning to be understood (see section 1C-3). However the functional significance of copper binding to the copper-binding domain of ATP7B is not yet well characterised. Described in this chapter are the functional consequences of mutations and deletions in the copper-binding domain of ATP7B, assayed by yeast complementation, in order to better understand the role of this domain in the overall copper transport function of ATP7B.

## **5B) MATERIALS AND METHODS.**

### **5B-1) Yeast strains.**

Yeast strains and transformation procedures were performed as described in section 2B-8.

### **5B-2) Expression constructs.**

The full-length 4.5 kilobase *ATP7B* cDNA was constructed as described in section 2B-2. Site directed mutagenesis (QuickChange, Stratagene) of the *ATP7B* cDNA was carried out using synthesised oligonucleotides which carried the desired codon changes as described in section 3B-2. Mutagenic primers are listed in the Appendix (Table A-4). Both of the cysteines (C) within each of the six GMxCxxCxxxIE heavy metal binding motifs were mutated on separate cDNAs to serine (S). Mutant cDNA fragments were restriction enzyme digested using natural restriction sites found in the *ATP7B* coding region, gel purified, then re-ligated, in different combinations to create the full-length *ATP7B* mutant constructs. The copper-binding domain deletion (designated Cudel) was created by PCR amplification of two fragments. A 5' fragment containing nucleotides 1-189 and a 3' fragment containing nucleotides 1797 - 2847 were ligated at

an artificial Xho I site, deleting nucleotides 190 - 1796 which encode the six metal binding motifs. Construct Cu1-5del was made by ligating the 5' 189 bp fragment to the natural Xho I site (nucleotide position 1621) of *ATP7B* deleting copper motifs 1-5. The constructs Cu3-6del and Cu4-6Del were made by PCR amplifying nucleotides 1-555 and 1-888 respectively, incorporating an Xho I site at the 3' end of each fragment. These were ligated onto the artificial Xho I site of Cudel to create the final constructs. The primers used for these deletion constructs are listed in the Appendix (Table A-5). Cu3-5del was constructed by ligating the 555 bp fragment to the natural Xho I site of *ATP7B*. All DNA manipulations were carried out as described in section 2B-1. All mutated or deleted constructs were sequenced to confirm that there were no secondary mutations (Thermosequenase, Amersham). For expression of *ATP7B* in yeast, cDNAs were cloned into the expression vectors pG3 and pG4 as described in section 2B-9. Genomic DNA from yeast strains harbouring was analysed by southern blotting, as described in section 2B-9, to ensure singlecopy construct integration. Construction of mutant *ATP7B* constructs was aided by technical assistance from Gloria Hsi who performed some sequencing, mutant construct assembly, and screening for singlecopy integrations.

### **5B-3) Complementation assay and oxidase assay.**

The complementation assay, growth curves, and oxidase assay, were performed as described in sections 2B-10, 3B-4, and 2B-11. Growth curves in iron-limited medium were generated over 24 hr. period. Optical density (absorbance at 600 nm) of triplicate cultures, was taken at times 0, 3, 6, 12, and 24 hr. Growth rates were calculated from the linear exponential growth phase of the cultures using the 3, 6, and 12 hr. time points.

### **5B-4) Polyclonal antibodies against ATP7B.**

A rabbit polyclonal antiserum against the C-terminal 10 kDa fragment of *ATP7B* was prepared as described in section 2B-6. Purification of specific antibodies from the antiserum was performed by affinity chromatography described in section 2B-7.

### **5B-5) Protein preparations and immunoblotting.**

Soluble yeast membrane proteins (10 µg) prepared for the Fet3p oxidase assay, as described in section 2B-11, were used for immunoblotting as described in section 2B-4. Immunoblotting was performed using column affinity purified anti-*ATP7B*.C10 as the primary antibody, at a 1/7,500 dilution. Secondary antibodies were horseradish peroxidase conjugated goat anti-rabbit antibodies at a dilution of 1/10,000 (Pierce Chemical). Bound antibodies were detected by ECL, using Supersignal substrate (Pierce Chemical).

## 5C) RESULTS.

The copper-binding domains of the mutant ATP7B expression constructs analysed for function in this study are shown in Fig. 5-1. All constructs were expressed in *ccc2* mutant yeast from the singlecopy integrating vector unless otherwise noted.

Series 1 constructs were those in which the cysteine residues of the copper-binding motifs were mutated to serine sequentially from the N-terminal to C-terminal end of the copper-binding domain (Fig. 5-1). These were analysed for function based on their ability to complement the high-affinity iron uptake deficiency phenotype of *ccc2* mutant yeast. When expressed in yeast, all proteins but Cu1-6C/S were able to complement the *ccc2* yeast mutant allowing the cells to grow on iron-limited medium (Fig. 5-2). Mutant proteins unable to fully complement *ccc2* mutant yeast at singlecopy expression levels, could often complement when overexpressed from a multicopy vector (Chapter 3) (Forbes *et al.* 1998). Overexpression from the multicopy vector produced approximately 30-fold more ATP7B protein than from the singlecopy vector, and saturated the yeast cell membranes with ATP7B protein (Chapter 2). If a mutant protein failed to complement when expressed in multicopy it was considered completely non-functional. Cu1-6C/S also failed to complement when expressed from the multicopy vector indicating that the mutant protein was non-functional (data not shown).

Fet3p oxidase assays were also used to measure the function of series 1 ATP7B copper-binding domain mutants. Fet3p receives its copper from Ccc2p within a vesicular compartment and therefore serves as a marker protein for copper transport across the vesicular membrane (Yuan *et al.* 1997). In wild-type yeast and those expressing normal ATP7B, there is little difference between holo- and total-Fet3p activity indicating little or no excess apo-Fet3p production. If high-affinity iron uptake is reduced or absent, Fet3p expression is induced in an attempt to compensate (Askwith *et al.* 1994). Therefore a high ratio of total-Fet3p to holo-Fet3p activity indicates an ATP7B mutant protein with absent or reduced function (Forbes *et al.* 1998). The Fet3p assay results for the first series of ATP7B mutant proteins showed, with the exception of Cu1-6C/S, little or no difference between holo- and total-Fet3p activity indicating that the first series of copper-binding domain mutant ATP7B proteins analysed have activity comparable to normal ATP7B (Fig. 5-2). The sixth subdomain alone was sufficient for ATP7B function. Cu1-6C/S protein was non-functional judged by its inability to generate detectable holo-Fet3p activity, and the high level of total-Fet3p activity.

As described in Chapter 3, growth curve analysis demonstrated that *ccc2* mutant yeast expressing ATP7B grows at a rate equal to the wild-type strain in iron-limited medium (Forbes *et al.* 1998). Differences in the ability of mutant ATP7B proteins to

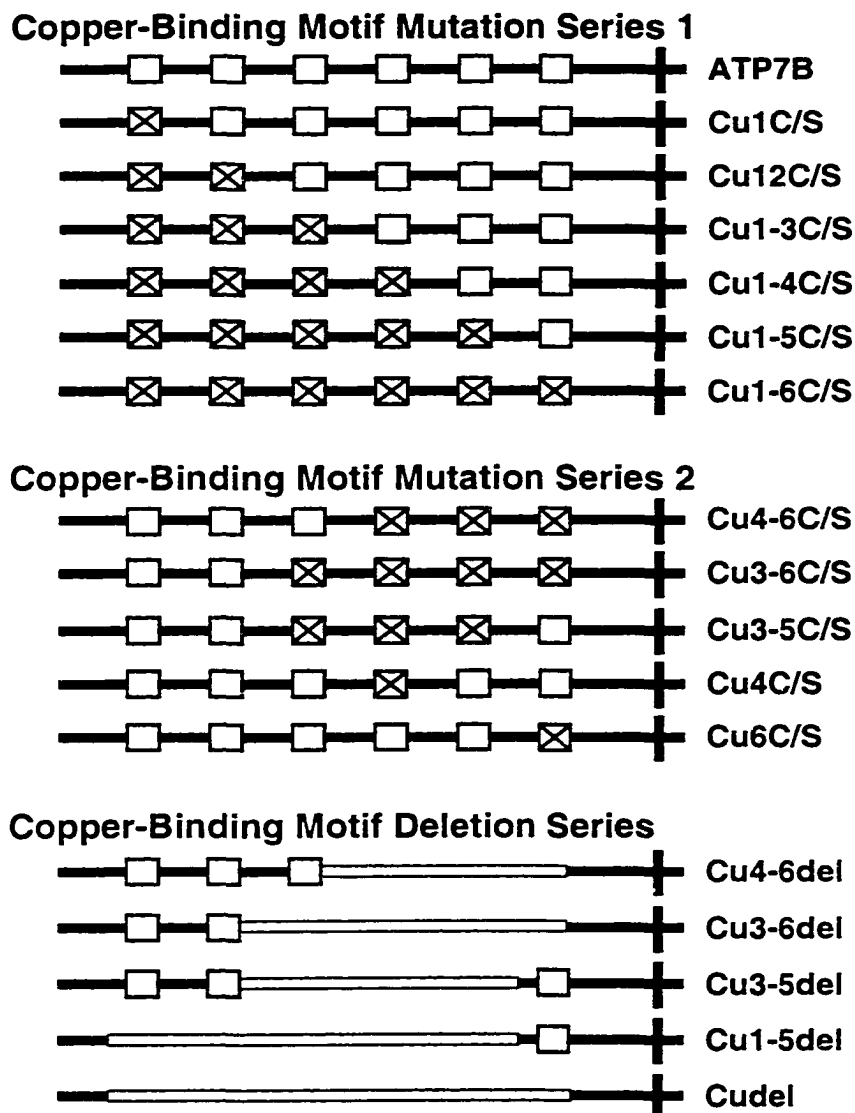


**Figure 5-1: ATP7B expression constructs.**

Normal copper-binding motifs (CxxC) are indicated by open squares. Crossed squares denote copper-binding motifs in which the cysteine residues were mutated to serine (SxxS). Deleted regions of ATP7B are indicated by open bars. The upright black bar represents the first transmembrane segment. The schematics are oriented N- to C-terminal (L-R) and are not to scale. Only the copper-binding domains of the full-length constructs are shown.

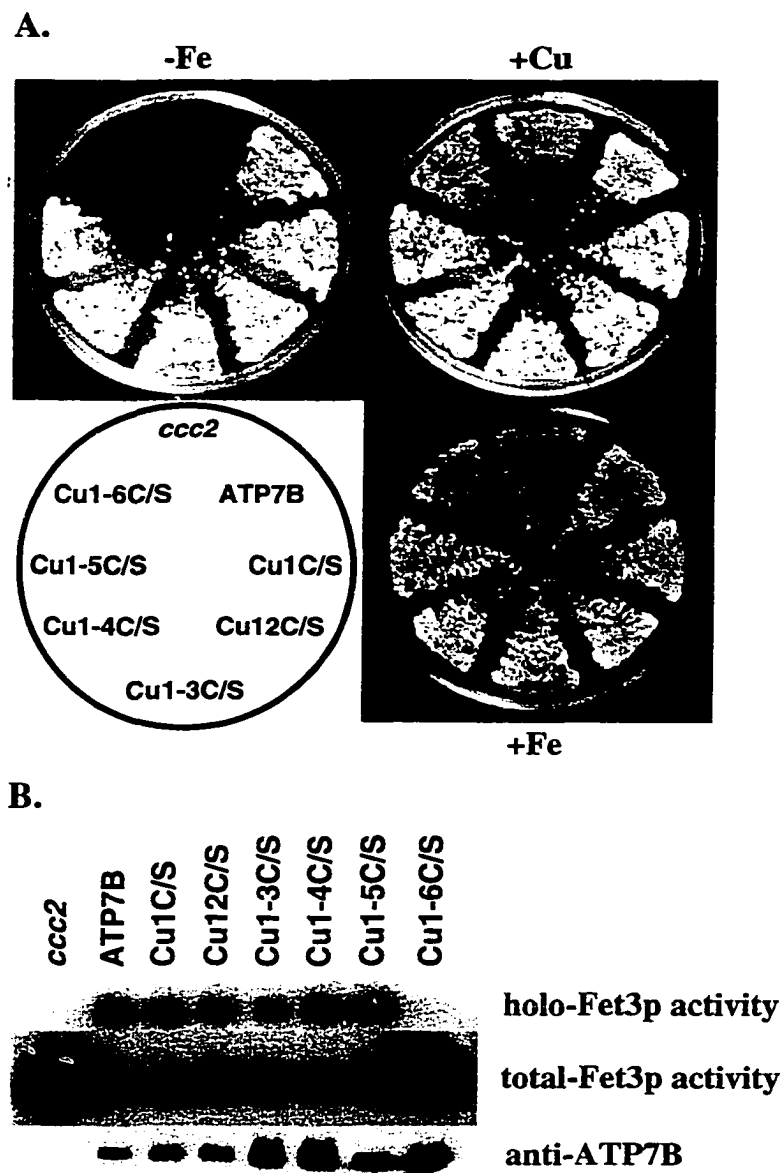


**Figure 5-2: Complementation of *ccc2* mutant yeast by ATP7B copper-binding domain mutation series 1 constructs.**

A, Plating assays were performed as described in 2B-10. B, Fet3p oxidase assays were performed as described in 2B-11. Holo-Fet3p activity, Fet3p copper loaded *in vivo*, was detected by homogenising yeast in buffer containing the copper chelator BCS and reducing agent ascorbate to prevent adventitious copper loading of apo-Fet3p during processing. Total-Fet3p activity, holo-Fet3p plus apo-Fet3p activity, was detected by homogenising yeast in the presence of copper to reconstitute apo-Fet3p *in vitro*. Immunoblots were performed, using anti-ATP7B.C10 antibodies, on 10 $\mu$ g of solubilised membrane protein prepared for the oxidase assay.

complement *ccc2* mutant yeast were quantified, which was useful as a relative measure of ATP7B function. Growth rates, in iron-limited medium, of yeast in expressing ATP7B and Cu1-5C/S were calculated from the linear exponential phase of growth curves done in triplicate (Table 5-1). The *ccc2* yeast strain expressing the Cu1-5C/S grew at a rate identical to normal ATP7B. These results confirm that the sixth copper-binding subdomain alone was sufficient for normal transport activity of ATP7B.

**Table 5-1: Growth rates of yeast expressing ATP7B copper-binding domain proteins.**

Strain	Growth Rate	% ATP7B
<i>ccc2</i>	0.017±0.004	13.5
ATP7B	0.126±0.000	100
Cu1-5C/S	0.128±0.001	101.5
Cu1-5Del	0.120±0.001	95.2

To determine if copper-binding subdomains at the N-terminal end of the copper-binding domain were involved in copper transport, Series 2 copper-binding domain mutants were made (Fig. 5-1). Cu4-6C/S and Cu3-6C/S were made in which the cysteines of copper-binding motifs four to six and three to six were mutated to serine respectively. These proteins did not restore the ability of *ccc2* mutant yeast to grow on iron-limited medium, and generated no detectable holo-Fet3p activity, but had a high total-Fet3p activity indicating they were non-functional (Fig. 5-3). Additionally, expression of these constructs from the multicopy vector failed to complement *ccc2* mutant yeast (Data not shown). However, Cu3-5C/S was able to complement *ccc2* mutant yeast and deliver copper to Fet3p as well as normal ATP7B as indicated by similar levels of holo-, and total-Fet3p oxidase activity (Fig. 5-3). These data demonstrate that two or three N-terminal subdomains alone are not sufficient for ATP7B function, and reinforce the functional importance of the sixth copper-binding subdomain.

To determine if the sixth copper-binding subdomain was essential for ATP7B function, a construct was made (Cu6C/S) in which the cysteine residues within the sixth motif only were mutated to serine. This protein when expressed in yeast was able to deliver copper to Fet3p and complement *ccc2* mutant yeast as well as normal ATP7B judged by the similar levels of holo- and total-Fet3p oxidase activity (Fig. 5-3). These results indicate that while the sixth copper-binding subdomain is sufficient for ATP7B function when present in isolation, it is not essential for function when other nearby copper-binding subdomains are intact.

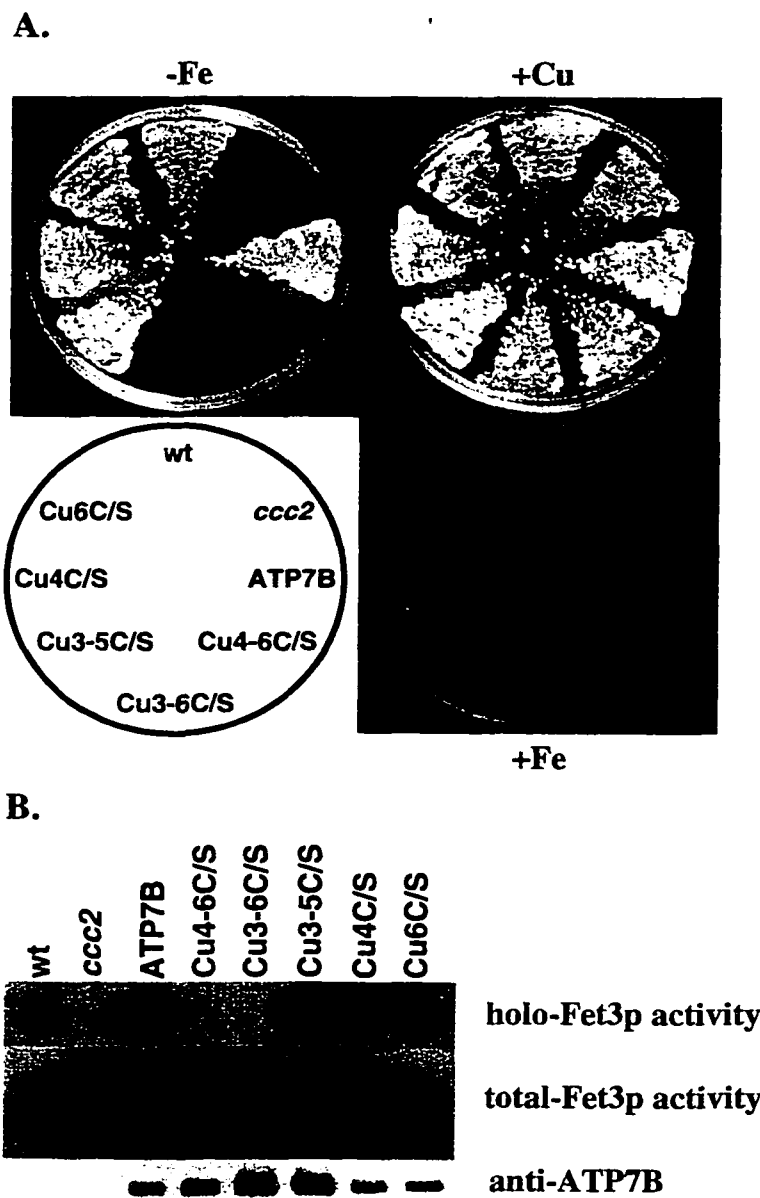


**Figure 5-3: Complementation of *ccc2* mutant yeast by ATP7B copper-binding domain mutation series 2 constructs.**

**A.** Plating assays were performed as described in 2B-10.

**B.** Fet3p oxidase assays were performed as described in 2B-11. Holo-Fet3p activity, Fet3p copper loaded *in vivo*, was detected by homogenising yeast in buffer containing the copper chelator BCS and reducing agent ascorbate to prevent adventitious copper loading of apo-Fet3p during processing. Total-Fet3p activity, holo-Fet3p plus apo-Fet3p activity, was detected by homogenising yeast in the presence of copper to reconstitute apo-Fet3p *in vitro*. Immunoblots were performed, using anti-ATP7B.C10 antibodies, on 10  $\mu$ g of solubilised membrane protein prepared for the oxidase assay.

The rodent homologues of ATP7B all are lacking the 4th copper-binding motif (Wu *et al.* 1994; Theophilos *et al.* 1996). However the spacing, and sequence properties between the third and fifth motif are conserved, leading to the conclusion that the fourth motif is not essential for function. As expected, Cu4C/S complemented *ccc2* mutant yeast cells allowing normal growth on iron-limited medium, and delivered copper to Fet3p as well as normal ATP7B (ratio of holo- and total-Fet3p oxidase activity similar to ATP7B: Fig. 5-3).

A series of copper-binding domain deletion constructs were analysed for function. Cu4-6del and Cu3-6del were made so that the third or second copper-binding motifs respectively were in a similar position relative to the beginning of the first membrane spanning segment as was the sixth copper-binding motif. Neither of these constructs could restore the ability of *ccc2* mutant yeast to grow on iron-limited medium (Fig. 5-4). Expression of Cu4-6del or Cu3-6del proteins resulted in no detectable holo-Fet3p activity, but had a high level of total-Fet3p activity indicating they were non-functional (Fig. 5-4). These data indicate that the N-terminal subdomains of the copper-binding domain are not equivalent to, and cannot replace the C-terminal subdomains. Deletion of the third to fifth copper-binding motifs (Cu3-5del) resulted in a protein unable to complement *ccc2* mutant yeast (Fig. 5-4). Cu3-5del protein was also shown to be non-functional, generating no detectable holo-Fet3p activity, and having a high level of total-Fet3p activity (Fig. 5-4). None of these deletion constructs could complement *ccc2* mutant yeast when overexpressed from the multicopy vector further supporting that they were non-functional (data not shown).

Cu1-5del was able to complement *ccc2* mutant yeast (Fig. 5-4). The mutant protein delivered copper to Fet3p, and restored the ability of the mutant yeast strain to grow on iron-limited medium. Growth curve analysis revealed that Cu1-5del protein allowed *ccc2* mutant yeast to grow at a rate 95% of normal ATP7B expressing *ccc2* mutant yeast (Table. 5-1). Deletion of the entire copper-binding domain (Cudel) resulted in a protein unable to complement *ccc2* mutant yeast (Fig. 5-4) even when overexpressed from a multicopy vector (data not shown). Expression of Cudel resulted in no detectable holo-Fet3p activity, but had a high level of total-Fet3p activity indicating the protein was non-functional.

Judged by immunoblot analysis, several mutant proteins appear to have a higher steady-state protein level with respect to normal ATP7B. This result was reproduced in multiple protein preparations (membrane and total cell extracts) and immunoblotting experiments. All of these mutant constructs have been confirmed to be correctly integrated in singlecopy by southern blots of genomic DNA isolated from these strains

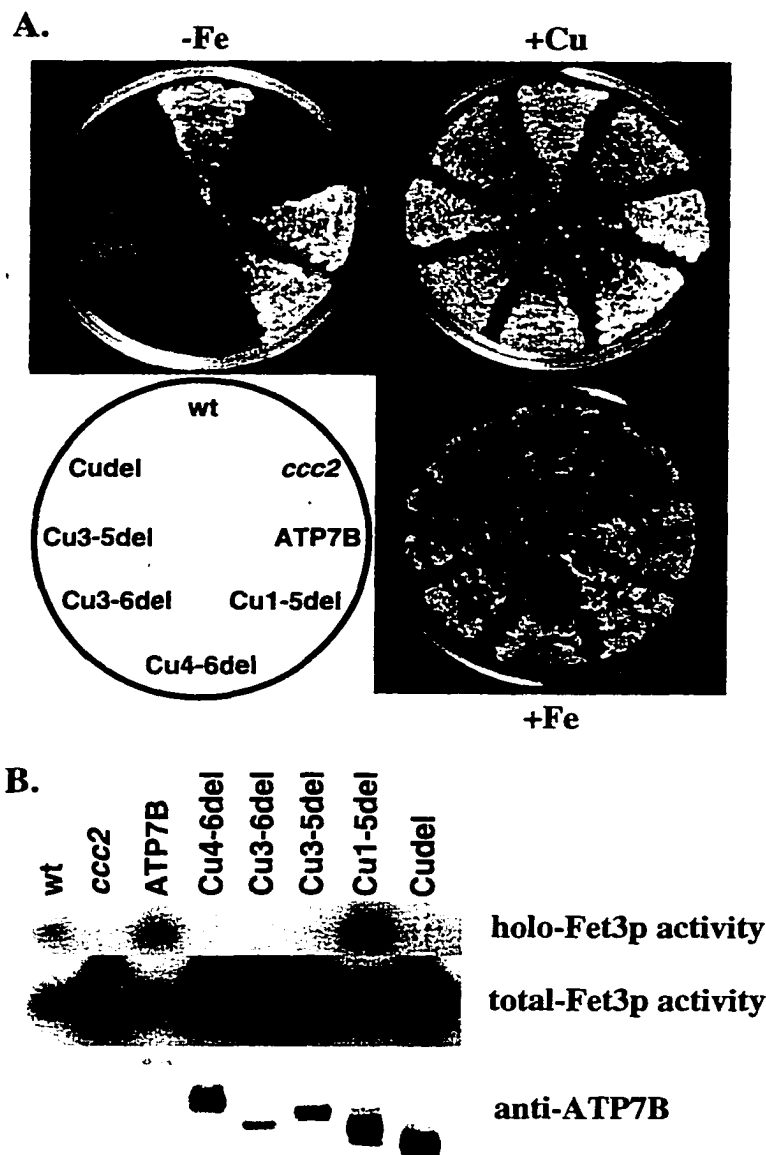


**Figure 5-4 Complementation of *ccc2* mutant yeast by ATP7B copper-binding domain deletion series constructs.**

**A,** Plating assays were performed as described in 2B-10. **B,** Fet3p oxidase assays were performed as described in 2B-11. Holo-Fet3p activity, Fet3p copper loaded *in vivo*, was detected by homogenising yeast in buffer containing the copper chelator BCS and reducing agent ascorbate to prevent adventitious copper loading of apo-Fet3p during processing. Total-Fet3p activity, holo-Fet3p plus apo-Fet3p activity, was detected by homogenising yeast in the presence of copper to reconstitute apo-Fet3p *in vitro*. Immunoblots were performed, using anti-ATP7B.C10 antibody, on 10 µg of solubilised membrane protein prepared for the oxidase assay.

probed with ATP7B cDNA (Data not shown). In most cases, the mutants exhibiting higher protein levels do not complement *ccc2* mutant yeast. Constructs Cu1-3C/S, Cu1-4C/S, and Cu3-5C/S do fully complement *ccc2* mutant yeast and the proteins appear to be more abundant relative to normal ATP7B. However, since Cu1-5C/S was detected at a level equal to normal ATP7B and is able to fully complement *ccc2* mutant yeast, it is unlikely that the relatively high steady-state level of Cu1-3C/S, Cu1-4C/S, and Cu3-5C/S proteins affect these conclusions.

## 5D) DISCUSSION.

The yeast complementation assay described in Chapter 2 of this thesis was used to study the functional consequences of mutation and deletions in the copper-binding domain of ATP7B. The copper-binding domain of ATP7B is absolutely required for its copper transport function when expressed in yeast. Mutation or deletion of all six copper-binding subdomains resulted in a protein unable to complement *ccc2* mutant yeast or deliver copper to Fet3p. These data indicate that binding of copper to this domain, is a requirement for transport of copper across membranes by ATP7B.

The data presented in this chapter indicate that the copper-binding subdomains, of the copper-binding domain, nearer in primary sequence to the predicted transmembrane domain of ATP7B were important for the copper-transporting activity of ATP7B. Mutation or deletion of the first five subdomains resulted in a protein with normal function. However, the presence of the first two or three N-terminal subdomains alone was not sufficient for function. The sixth subdomain was sufficient, but not essential for normal function of ATP7B, since mutation of only the sixth copper-binding motif had no apparent functional effect on the ability of the Cu6C/S to complement *ccc2* mutant yeast. This result is consistent with the fact that most prokaryotic and lower eukaryotic CPx-type ATPases have only one to three heavy-metal binding subdomains, suggesting that subdomains close to the transmembrane domain are required for copper delivery to the channel prior to transport through the membrane (Solioz, 1998). However, the results presented in this chapter are considerably different from results reported for ATP7A (Payne *et al.* 1998a). That study presented a series of copper-binding motif mutations in ATP7A, which corresponded to our mutation Series 1 constructs, analysed by complementation of *ccc2* mutant yeast. The authors found that mutation (cysteine to serine) of any more than the first two copper-binding motifs of ATP7A resulted complete loss of ATP7A function. These results suggested that the N-terminal subdomains of the ATP7A copper-binding domain are more critical for function than the C-terminal subdomains, which compared with our results, suggest a structural or functional

difference between the copper-binding domains of ATP7A and ATP7B. Sequence alignments between the copper-binding domains of ATP7A and ATP7B reveal that while the copper-binding motifs are highly conserved at the sequence level, the spacing between them is not (Bull *et al.* 1993). There are several, multiple amino acid insertions and deletions in the ATP7A domain compared to ATP7B. Most notably there is a large 78 amino acid insertion between copper-binding motifs one and two, and an 18 amino acid deletion between copper-binding motifs four and five. Overall, motifs 2-6 of ATP7A are more closely spaced than in ATP7B, with the first motif of ATP7A being further N-terminal in primary structure. Additionally, the sixth copper-binding motif of ATP7B is closer in primary structure relative to its first predicted transmembrane segment, in comparison with the sixth motif of ATP7A relative to its first predicted transmembrane segment (Vulpe *et al.* 1993; Bull *et al.* 1993). On the basis of sequence alignments between ATP7A and ATP7B together with the NMR structure of ATP7A.Cu<sub>4</sub> (Gitschier *et al.* 1998), these insertions/deletions would occur between individual subdomains and should therefore not affect their individual folding, only the spacing between subdomains. This difference in motif spacing between ATP7A and ATP7B may represent a different domain structure between the two proteins. As a result the N-terminal subdomains of the ATP7A copper-binding domain may play a more critical role in copper transport than in ATP7B.

Lutsenko *et al.* (1997) reported that during purification of a fusion protein between the maltose-binding protein and the N-terminal copper-binding domain of ATP7B, a major proteolytic fragment was co-purified. This fragment was recognised by antibodies against the copper-binding domain, and was able to bind to metal-chelate chromatography resin charged with copper. Based on these observations and molecular weight estimates, the degradation product was judged to contain two or three copper-binding subdomains and was proposed to represent a large proteolytically sensitive subdomain of the copper-binding domain (Lutsenko *et al.* 1997). We also observed consistent degradation of full-length ATP7B protein when isolating 100,000g membrane pellets from yeast (data not shown). On the basis of molecular weight estimates, this degradation fragment would contain two or three copper-binding subdomains. To test the hypothesis that the copper-binding domain may be divided into two large subdomains (2-4 individual subdomains each), and to determine if these domains were functionally interchangeable, ATP7B deletion constructs were used (Fig. 5-1.). Constructs in which either the second or third copper-binding motifs were placed in a similar position as the sixth (Cu3-6del and Cu4-6del respectively), were unable to complement *ccc2* mutant yeast or deliver copper to Fet3p indicating that they were non-functional. These data

suggest that the N-terminal copper-binding subdomains of the ATP7B copper-binding domain are not functionally identical to, and cannot replace, the C-terminal subdomains even when placed in a similar sequence position. The copper-binding subdomains from the N-terminal end of the copper-binding domain may fold, with respect to each other, such that the orientation of the copper-binding cysteine residues was not correct to deliver copper to the transmembrane domain of ATP7B for transport. This hypothesis is supported by the result from Cu3-5del. This ATP7B deletion mutant was unable to complement *ccc2* mutant yeast even when overexpressed from a multicopy vector suggesting that it was unable to transport copper. Since Cu1-5del, with the sixth subdomain alone, was able to complement *ccc2* mutant yeast, addition of copper-binding subdomains one and two to the sixth subdomain may change the overall fold of the mutant copper-binding domain so that even the sixth subdomain is no longer in the correct position to deliver copper to the transmembrane channel. These results support, but do not prove, the hypothesis that the N-terminal two or three copper-binding subdomains may represent an independently, differently, folded second large subdomain of the ATP7B copper-binding domain. These data also suggest that while the folded structure of individual copper-binding subdomains is likely conserved (Gitschier *et al.* 1998), it is the fold of multiple subdomains with respect to each other and the transmembrane channel that is essential for the overall function of the copper-binding domain.

Since the crystal structure of Atx1p and the NMR structure of ATP7A.Cu4 have been solved and found to be very similar overall (Gitschier *et al.* 1998; Rosenzweig *et al.* 1999), individual ATP7B copper-binding subdomains are likely homologous to these structures. The primers used to create the deletion constructs Cu4-6del, Cu3-6del, and Cu3-5del were based on sequence data alone before unambiguous structural information was available. Consequently, these primers result in a duplication/insertion of several amino acids, including two from the engineered Xho I site used to create the deletions, that occur within ATP7B sequences corresponding to the third loop and third  $\beta$ -sheet of Atx1p and ATP7A.Cu4. These amino acid changes, rather than the postulated non-equivalence between subdomains, are likely responsible for the loss of ATP7B activity due to misfolding of the engineered copper-binding subdomain replacing subdomain six nearest to the channel in the mutant proteins. However, the other copper-binding subdomains present in the constructs should remain intact. If correctly folded, positioned, and spaced, these subdomains should be capable of delivering copper to the transmembrane channel. However, deletion construct data presented in this chapter indicate that this is not the case. The deletion series 1 constructs support the hypothesis

that intact copper-binding subdomains nearest the channel are essential for function and that it may be the spacing and orientation of these subdomains with respect to the channel that is critical for function. Therefore it is predicted that any intact copper-binding domain when correctly positioned with respect to the transmembrane channel should support ATP7B function.

Iida *et al.* (1998) used deletion analysis, and a yeast complementation assay similar to ours, to study the copper-binding domain of ATP7B. The authors sequentially deleted copper-binding motifs from the C- to N-terminus of the copper-binding domain. They found that none of these constructs, including one in which the sixth motif alone was deleted, were able to complement *ccc2* mutant yeast. A construct containing only the sixth subdomain (1-5 deleted) was functional. From this data they concluded that the sixth subdomain was essential for ATP7B copper-transport function. This conclusion does not agree with data presented here which shows that mutation of the sixth motif only does not affect ATP7B function indicating that the subdomain is important but not essential. Since Iida *et al.* analysed only deletion constructs, the spacing and folding orientation, of the entire copper-binding domain with respect to the transmembrane channel provided by the sixth subdomain is likely essential for ATP7B function, rather than its copper binding capacity.

Yeast complementation data presented in this chapter has revealed that mutant ATP7B protein with only one copper-binding subdomain is capable of fully complementing the iron-uptake deficiency of the *ccc2* mutant yeast. Biochemical evidence suggests that copper binding to the copper-binding domain of ATP7B may be cooperative (DiDonato *et al.* 1997). If the observed cooperative binding was required for copper-transport, one or a few subdomains alone would not be predicted to be sufficient for normal function. Therefore, cooperative copper binding is not likely critical for copper-transport function of ATP7B. Instead, cooperative copper binding to the N-terminal domain may induce conformation changes in the protein, which acts as a signal to initiate copper-induced trafficking from the trans-Golgi network to the membrane vesicles or plasma membrane. Preliminary results support this hypothesis. DiDonato *et al.* (M. DiDonato and B. Sarkar, personal communication) have observed, using circular dichroism spectroscopy, that the apo-form of purified ATP7B copper-binding domain protein has secondary structure that consisted of mostly beta-type structures ( $\beta$ -sheets,  $\beta$ -turns, etc.). Upon addition of a two fold molar excess of copper to the apo-protein, secondary structure switched to predominantly  $\alpha$ -helix. Further addition of copper had little effect on secondary structure, however, the tertiary structure changed. These data were supported by the observed quenching of tryptophan fluorescence upon addition of

copper to the apo-protein. Therefore, conformation changes in the copper-binding domain may act cooperatively as a copper sensor, to trigger movement of ATP7B out of the trans-Golgi network in response to excess cellular copper.

Yeast complementation data presented in this chapter may also explain in part why ATP7B has six copper-binding subdomains while most other CPx-type ATPase have only one to three. For example, Ccc2p has only two copper-binding subdomains and does not alter its subcellular localisation in response to copper (Yuan *et al.* 1997). On the basis of these data, it is proposed that the copper-binding subdomains closest to the transmembrane channel of ATP7B are directly involved in copper transport, transferring copper to residues within the channel, for subsequent translocation across the membrane. The remaining N-terminal subdomains may not be directly involved in copper transport. Instead they may act cooperatively to induce conformational changes in the domain, sensing cytosolic copper concentrations, thereby inducing redistribution of ATP7B within the cell. These hypotheses are discussed in more detail in section 6B.

**CHAPTER 6****CONCLUSIONS AND FUTURE DIRECTIONS.**

When this thesis was initiated, very little was known about the molecular basis of copper homeostasis in eukaryotes. The genes for Wilson disease (WD) and Menkes disease (MD) had just been cloned, and initial studies on copper pathways in yeast were appearing. Since that time much has been learned about the biology of eukaryotic copper homeostasis particularly through the study of yeast and application of those data to mammalian systems. More specifically the molecular pathology of disorders of copper transport such as WD and MD, have begun to be elucidated beginning with gene cloning, and in the process has increased our understanding of pathways in mammalian copper (and iron) homeostasis.

The general goal of this thesis was to perform a structure/function analysis on ATP7B in order gain understanding of the biochemical and physiological function of this protein. In the course of doing so a large number of resources have been created such as antibodies, cDNA constructs, and functional assays that are being used in our laboratory and in the laboratories of collaborative researchers throughout the world to further understand the role of ATP7B in normal and disease states. These studies include further work in our laboratory characterising the functional effect of WD mutations on ATP7B function (Matthew Chen). Identification of molecular determinants of ATP7B copper induced trafficking (Gloria Hsi) and studies on the tissue distribution of ATP7B and metallochaperones by immunohistochemistry (Steven Moore). All of these studies are dependent on materials and/or methods created toward the completion of this thesis. Studies done in collaborative laboratories include those that have been published examining the biochemical properties of copper binding by the ATP7B copper-binding domain (DiDonato *et al.* 1997), which was aided by cDNA constructs, and antibodies, generated towards completion of this thesis. This work is currently being carried forward to structural studies by x-ray crystallography (Dr. B. Sarkar, Hospital for Sick Children; Dr. Michael James, University of Alberta, Canada). The ATP7B cDNA created in our laboratory is currently being used in gene therapy trials as a potential treatment for WD (HepaVac, Germany). Other collaborative research include kinetic studies on the mechanism of copper transport by ATP7B and the ATP7B mutants (Dr. Stewart Daly, Montreal General Hospital Research Institute, Canada) using cDNA constructs and

antibodies generated in our laboratory. Also being investigated is the cell-biology of biliary copper transport and copper dependent trafficking of ATP7B being done in collaboration with Dr. Roel Vonk (University of Groningen, The Netherlands), and Dr. Julian Mercer (Deakin University, Australia) to whom contributed cDNA constructs and antibodies have been contributed. The functional effect of *ATP7B* mutations is being studied by Dr. Mark Solioz (Switzerland) using our complementation assay.

## **6A) ATP7B AND WILSON DISEASE.**

The effect of WD mutations on the function of ATP7B was investigated with two goals. First, understanding the effect of disease mutations on the function and intracellular localisation of ATP7B, in order to shed light on the biological role of this protein in health and disease. Secondly, as a practical benefit, the yeast complementation functional assay and immunofluorescence microscopy was used as a means to help distinguish true WD missense mutations from rare normal variants.

### **6A-1) Effect of WD mutations on ATP7B: mutation or normal variant?**

Molecular diagnosis of disease, done by assay for disease-associated mutations in patients, is increasingly relied upon in modern medicine. For diagnostic purposes, it is crucial to be sure whether or not a mutation is indeed disease causing. In the case of WD, early diagnosis and treatment is required to prevent irreversible liver damage. Conversely, many of the chelators used for treatment have adverse side effects therefore misdiagnosis could be harmful. (Danks, 1995; Cox *et al.* 1998). Functional analysis of missense mutations is therefore an important adjunct to mutation screening in patients to confirm whether or not a mutation is likely to be responsible for disease. The yeast complementation assay for ATP7B function developed as described in Chapter 2 provides an ideal method to test putative mutations. It is relatively easy to perform, is sensitive, and can be used to assay a large number of mutant proteins in a short time.

The set of disease mutations analysed in this thesis were those found within the predicted transmembrane domain of ATP7B. The transmembrane domain in particular was targeted because initial genetic studies found many missense mutations clustered in this region, particularly the fourth membrane spanning segment, suggesting a mutation hotspot, or perhaps indicative of a critical role for predicted transmembrane segment four in ATP7B function (Thomas *et al.* 1994; Shah *et al.* 1997). New mutations have subsequently been identified in the predicted transmembrane domain of the ATP7B (for reference see the Human Genome Organisation Wilson disease database

<http://www.medgen.med.ualberta.ca/database.html>). To date, 36% of missense mutations (22% of all mutations) are found in the predicted transmembrane domain of ATP7B although the observed clustering is somewhat biased due to selective mutation detection strategies that target apparently frequently mutated regions of the gene in suspected WD patients.

Using the yeast complementation assay described in Chapter 2 disease mutations could be distinguished from normal variants (Chapter 3) (Forbes *et al.* 1998). Mutations such as P992L, R778L, R778Q were originally classified with confidence by genetic means to be disease causing, due to the non-conservative nature of the amino acid substitution, because the original amino acid was conserved in ATP7A, and the mutations were not found on normal chromosomes (Thomas *et al.* 1994). Consistent with this disease mutation classification, P992L, R778L, and R778Q mutations resulted in ATP7B proteins with reduced function.

One result was somewhat surprising. Included in this study were two ATP7B mutations (V995A, T977M) originally classified as possible normal variants (Thomas *et al.* 1994). Results from functional analysis of V995A, which revealed apparently normal activity, was consistent with classification as a normal variant. However, T977M was found to be an apparent null mutation with no function in our assay. This mutation originally classified as a normal variant, had the most severe effect on ATP7B function of all patient derived mutants that were analysed and therefore should be considered disease causing.

The mutations M769V and T977M highlight the importance of including functional data in mutation screening protocols. Since its original discovery, M769V has been found in additional patients, and diagnosis of WD based on this finding could not be made with complete confidence, since M769V was not originally classified as a disease causing mutation with certainty (Thomas *et al.* 1994). T977M in particular, may have been identified in patients and dismissed as a normal variant leading to misdiagnosis of the patient, or continued effort to find another mutation. Both of these mutations have now been classified as disease causing by functional means, and WD diagnosis based on the presence of these mutations in patients can be made with certainty.

Functional analysis of ATP7B mutant proteins, while very useful to distinguish disease-causing mutations from normal variants, it is not always definitive. For example, functional analysis of ATP7B mutant proteins identified in WD patients revealed that mutant proteins D765N, L776W, G943S were able to completely, or nearly completely, complement the defective high-affinity iron uptake phenotype of *ccc2* mutant yeast cells (Forbes *et al.* 1998) (Chapter 3). These results indicate that these mutant ATP7B proteins

retained normal or partial copper transport activity. However in order for ATP7B to perform its normal biological function, it must localise to the proper cellular compartment. Therefore it was hypothesised that mutant proteins retaining all or most copper transport activity in yeast may be rare normal variants not yet found on normal chromosomes, or mutant proteins with normal capability to transport copper that are mislocalised in hepatocytes.

Immunofluorescent microscopy studies were employed to distinguish these possibilities (Chapter 4). Immunolocalisation of D765N and L776V revealed that these proteins were mislocalised to the endoplasmic reticulum. G943S was somewhat mislocalised to the endoplasmic reticulum but was also insensitive to copper, such that it was unable to redistribute from the Golgi network to vesicles. Based on these data showing aberrant cellular localisation or trafficking, it can be concluded that these mutations are disease causing. The physiologic aspects of these data will be discussed in the next section (6A-2).

As a method to functionally classify ATP7B missense mutations as disease causing or normal variants, yeast complementation combined with immunofluorescence microscopy is a powerful tool. Studies in the Cox laboratory continue to analyse missense mutations, identified in WD patients, for function and localisation. Mutations of particular interest, are those that appear to be relatively conservative amino acid substitutions, and those not part of a sequence motif related to a particular function (such as the ATP binding domain), that are more difficult to classify based on sequence information alone.

#### **6A-2) Allelic variation in ATP7B relating to WD biochemical phenotype: insight into normal copper homeostasis.**

The main biochemical phenotype of WD is hepatic copper accumulation due to impaired biliary copper efflux (Danks, 1995; Cox *et al.* 1998). Normal adults typically have 20-50 µg copper per gram dry liver whereas WD patients have greater than 250 µg/g which can approach 2000 µg/g (Danks, 1995; Cox *et al.* 1998). Hepatic copper levels vary among normal individuals and WD patients depending on dietary copper intake and bioavailability, as well as genetic factors (reviewed in Danks, 1995; Bremner, 1998; Wapnir, 1998; Uauy, 1998; Linder *et al.* 1998). Since diseases such as cholestasis and primary biliary cirrhosis can also lead to highly elevated hepatic copper levels, serum ceruloplasmin levels, currently measured immunologically or less commonly by oxidase activity, are used as a further diagnostic biochemical marker of WD (Cox *et al.* 1998; Danks, 1995; Bremner, 1998). Apo-ceruloplasmin biosynthesis is normal in WD patients,

but copper incorporation into the protein during biosynthesis is impaired such that patients have reduced circulating holo-ceruloplasmin levels (Murata *et al.* 1995; Yamada *et al.* 1993a; Danks, 1995; Sato *et al.* 1991). Total ceruloplasmin (holo- plus apo-ceruloplasmin combined) levels vary considerably in normal individuals (see Section 1B). This is due to factors such as pregnancy, acute inflammation, infection, and oral contraception (Danks, 1995). Genetic variation of the ceruloplasmin gene may also influence circulating ceruloplasmin levels. Although total ceruloplasmin levels vary, there is usually little apo-ceruloplasmin found in the plasma of normal individuals (Danks, 1995; Cox *et al.* 1998). WD patients usually have low plasma holo-ceruloplasmin levels, and elevated levels of circulating apo-ceruloplasmin, but this is not always the case. Some WD patients have circulating holo-ceruloplasmin levels within the normal range.

There have been hypotheses made to explain normal holo-ceruloplasmin levels seen in some WD patients in the absence of normal ATP7B function. One hypothesis is that copper may be incorporated into ceruloplasmin by diffusion when hepatic cytosolic copper levels reach saturation. Ceruloplasmin is copper loaded by ATP7B within the membrane enclosed lumen of the trans-Golgi network (Sato *et al.* 1991; Murata *et al.* 1995). Ionic copper entering this compartment by diffusion would have to pass through the membrane, a feat that is very thermodynamically unfavourable for a charged, hydrophilic cation, and which would require a large concentration gradient (Guyton, 1991; Ballatori, 1991). Since most of the cytosolic copper in WD or experimentally copper loaded hepatocytes, is bound by metallothioneins and metallochaperones (Weiner *et al.* 1980; Bingle *et al.* 1992; Nartey *et al.* 1987; Freedman *et al.* 1989; Baerga *et al.* 1992), there would not likely be a large enough concentration of ionic copper to drive diffusional passage through the trans-Golgi membrane. Therefore copper incorporation into ceruloplasmin by this mechanism is unlikely. This is supported by studies on the LEC rat, which show that in the absence of functional ATP7B, there is no significant copper incorporation into ceruloplasmin even in the presence of highly elevated hepatic copper levels (Suzuki *et al.* 1995; Suzuki *et al.* 1999; Rui *et al.* 1997). During those LEC rat studies, holo-ceruloplasmin levels were observed to increase in the rat serum immediately preceding onset of liver failure. Since the reappearance of plasma holo-ceruloplasmin was accompanied by plasma markers of liver failure and breakdown, the likely cause of ceruloplasmin copper loading in the LEC rat was the disruption of intracellular membranes. This may also occur in some WD patients at the onset of liver failure.

Another hypothesis is that copper may be transported into the trans-Golgi network in a facilitated manner, but non-specifically, by another ion transporter when copper levels in the liver become elevated. Although this explanation is plausible, there is no supporting evidence at this time. The presence of a second transporter capable of delivering copper to ceruloplasmin seems unlikely, because if it were true, ceruloplasmin levels would be expected to be normal in all WD patients, since all have elevated hepatic copper levels (Danks, 1995; Cox *et al.* 1998).

Changes in *ATP7B* function and localisation due to allelic variation of the *ATP7B* gene can explain in part the variation of diagnostic biochemical parameters in patients with WD, in particular, normal holo-ceruloplasmin levels. As described in the chapter 3, several of the WD mutants that were analysed for function (G943S, D765N, L776V) had normal or nearly normal function assessed by complementation assay (Forbes *et al.* 1998). Based on this data it was hypothesised that mutant *ATP7B* proteins retaining at least some copper transport activity, that are unable to undergo copper-dependent trafficking from the trans-Golgi network to the vesicular compartment (endosomes) or are mislocalised, would not mediate adequate biliary copper efflux leading to hepatic copper accumulation. However, mutant proteins such as these may transport sufficient copper into the Golgi network for incorporation into ceruloplasmin giving apparently normal circulating holo-ceruloplasmin measurements in individuals carrying these mutations.

This hypothesis has been substantiated by immunofluorescence data presented in Chapter 4 and has direct impact on the diagnosis of WD. Mutations such as G943S, that result in *ATP7B* proteins with transport activity that are restricted to the Golgi network, would be predicted to incorporate copper into ceruloplasmin but not effectively mediate copper efflux. Similarly, mutations such as D765N and L776V that apparently have full activity, and are substantially, but not completely, mislocalised, may result in enough normally localised protein to incorporate copper into ceruloplasmin, while ineffectively mediating copper efflux. Therefore WD patients carrying these mutations, even in compound heterozygous form, may have normal or borderline holo-ceruloplasmin levels, and their diagnosis may be missed if emphasis is placed on ceruloplasmin for initial screening. These data are of particular importance for the diagnosis of presymptomatic siblings of an affected individual if all have normal or borderline ceruloplasmin levels. Presymptomatic siblings may be misdiagnosed as heterozygous carriers.

Allelic variation of *ATP7B* may also contribute to differences in hepatic copper levels seen in WD patients. Mutations such as D765N and L776V, apparently have normal copper transport activity in our assay, are mislocalised to the endoplasmic reticulum, but still exhibit some proportion of normally localised protein that is capable

of undergoing copper dependent redistribution. M769V has normal intracellular localisation and trafficking, and has greatly reduced, but not absent apparent transport activity. Although variation in hepatic copper levels depends largely on dietary copper intake, mutant proteins such as these may mediate enough biliary copper efflux to maintain hepatic copper levels at the middle or lower end of the range seen in patients with WD, perhaps leading to a less severe clinical phenotype. This prediction is supported by preliminary clinical data. Generally, WD patients who are compound heterozygotes for mutations such as frameshifts, and nonsense mutations predicted to destroy the protein have an early age of WD disease onset (average 7.2 years) (Cox *et al.* 1999). Compound heterozygote patients for missense mutations predicted to be less damaging to ATP7B function, typically have a later age of WD onset (average 16.8 years) (Cox *et al.* 1999).

Chelation therapy for WD using penicillamine or trientine does not remove hepatic copper from Wilson disease patients (Danks, 1995; Cox *et al.* 1998; McQuaid *et al.* 1992; McArdle *et al.* 1989). Instead, it appears to reduce further hepatic copper accumulation by increasing urinary copper excretion and protects hepatocytes against further damage by inducing metallothioneins (Danks, 1995; Cox *et al.* 1998). Using data presented in this thesis, it can be suggested that patients with ATP7B variants retaining partial function, and at least partial normal localisation, that are therefore potentially capable of limited copper efflux, could respond better to chelation therapy, or dietary control of ingested copper, than those patients with no functional or correctly localised ATP7B protein. Consistent with this proposal, penicillamine treatment of patients with primary biliary cirrhosis, who had elevated hepatic copper levels, led to reduced hepatic copper (Deering *et al.* 1977). Since penicillamine itself does not remove copper, hepatic copper reduction was likely due to ATP7B dependent efflux. However the suggested correlation has the caveat that dietary copper intake fluctuation during treatment may also have contributed to the observed copper reduction in patients.

In future studies, the ideal physiologic method to test these hypotheses would be to use the LEC rat model of WD. Infusion of recombinant adenovirus expressing ATP7B into the LEC rat has been shown restore holo-ceruloplasmin synthesis and biliary copper efflux (Terada *et al.* 1999; Terada *et al.* 1998). Similar experiments could be performed using mutant ATP7B variants. The effect of ATP7B mutant proteins on holo-ceruloplasmin synthesis, and hepatic copper accumulation, could be determined *in vivo* as described (Terada *et al.* 1999; Terada *et al.* 1998), and be related to the mutant proteins activity and intracellular localisation.

A simpler, and perhaps more controllable method, would be to use transformed LEC rat hepatocytes stably transfected with mutant *ATP7B* cDNAs. These cell lines could be used to determine the effect of *ATP7B* mutations on intracellular localisation, and trafficking using methods similar to those described in Chapter 4 of this thesis. Simultaneously, the amount of total ceruloplasmin protein secreted into the medium, and the oxidase activity of the secreted protein, could be measured directly as has been described (Nakamura *et al.* 1995) to determine the relative amount of holo-ceruloplasmin produced by different *ATP7B* mutant proteins. *ATP7B* dependent copper efflux from the cultured hepatocytes could be measured indirectly, by measuring cellular copper accumulation, as has been described (Nakamura *et al.* 1995; La Fontaine *et al.* 1999; Ambrosini *et al.* 1999). In this way the effect of a WD mutation on localisation and function could be related to physiologic biochemical parameters.

A recent publication has shown that *ATP7B* expression was able to rescue the copper accumulation defect of MD patient fibroblasts (La Fontaine *et al.* 1998). However, they noted that *ATP7B* did not apparently redistribute out of the Golgi network to cytoplasmic vesicles in response to extracellular copper. Since *ATP7B* was able to mediate copper efflux without apparent copper induced redistribution, the physiologic relevance of redistribution in normal copper homeostasis may be questioned. The data presented in this thesis does support a physiological role for *ATP7B* redistribution. G943S retains nearly normal apparent copper transport activity, but its localisation is restricted to the Golgi network and endoplasmic reticulum. Since homozygous G943S is associated with WD (Thomas *et al.* 1994), G943S likely causes WD not by defective copper transport activity, but by an inability to relocate to vesicles, in order to mediate biliary copper efflux. The experiments listed in the preceding paragraph would help confirm the biological significance of copper-dependent redistribution to copper efflux. For example, if a mutant protein like G943S mediates cellular copper efflux from LEC rat hepatocytes, while being restricted to the Golgi, then the biological significance of redistribution is questionable.

While functional and localisation data can provide a likely mechanism to explain variation in the biochemical features of WD, the overall phenotype of the disease in patients cannot be readily explained and is beyond the scope of this thesis. For example, patients with the neurological form of WD have hepatic copper accumulation and reduced serum ceruloplasmin, but may not show clinical evidence of liver disease (Cox *et al.* 1998). This cannot be reconciled by allelic variation of *ATP7B* alone. Diet may play a role (Wapnir, 1998). Some individuals may accumulate different amounts of hepatic copper at different rates, dependent on the amount, and bioavailability of copper ingested,

which may effect WD progression. For example, copper is poorly absorbed from high fibre diets compared with high protein diets (Wapnir, 1998). Genetic factors likely play a role as well. For example proteins such as cMOAT (see section 1D-4) may reduce copper accumulation in the absence of normal ATP7B function. Allelic variation, of the gene encoding cMOAT may effect hepatic copper levels in some individuals. There may be allelic variation in metallothionein genes, or regulatory proteins that control them, that increases or decreases the protective effect of metallothioneins against hepatic copper in the absence of normal ATP7B in different individuals (Kelly *et al.* 1996). Since bile is the main route of copper excretion, cholestatic diseases such as primary biliary cirrhosis, or extrahepatic biliary atresia can lead to hepatic copper accumulation (Beshgetoor *et al.* 1998). Two genes involved in hereditary cholestasis, *FIC1* and *PFIC2*, encoding P-type and ABC-cassette ATPase transport proteins respectively, have been identified and appear to be involved in hepatic bile acid transport (Strautnieks *et al.* 1998; Bull *et al.* 1998). WD patients heterozygous for a mutant copy of one of these genes may accumulate more copper and be more susceptible to liver damage than other individuals. These are only a few examples of potential genetic loci that might modify overall the WD phenotype.

## **6B) ROLE OF THE ATP7B COPPER-BINDING DOMAIN.**

There have been two major hypotheses presented regarding the biochemical outcome of copper binding to the copper-binding domain in the overall function of CPx-type ATPases. The copper-binding domain has been proposed to remove copper from cytosolic ligands and transiently bind copper prior to transport (Vulpe *et al.* 1993; Bull *et al.* 1994). Another proposed role for the copper-binding domain is that of a copper sensor (Vulpe *et al.* 1993; DiDonato *et al.* 1997; Petris *et al.* 1996), perhaps acting in response to cytosolic copper concentrations to trigger copper-dependent changes in intracellular localisation. These hypothesis are not mutually exclusive. The goal of the work presented in this thesis on the copper-binding domain was to contribute to the understanding of the role of this domain in the overall biological function of ATP7B. The specific hypothesis was that the copper-binding domain of ATP7B is essential for its function as a copper transporter.

### **6B-1) Requirement for the copper-binding domain of ATP7B for copper transport.**

Through studies in yeast, data have been generated that support a direct requirement for the copper-binding domain of ATP7B, and more generally CPx-type ATPases including ATP7A, for their ability to transport copper (Iida *et al.* 1998; Payne *et al.* 1998b; Forbes *et al.* 1999). Due to the extensive conservation of proteins in eukaryotic

intracellular copper transport pathways, yeast complementation provides an experimental system that is representative of the physiologic conditions under which ATP7B normally functions *in vivo* (Amaravadi *et al.* 1997; Lin *et al.* 1997; Klomp *et al.* 1997; Glerum *et al.* 1996; Culotta *et al.* 1997; Zhou *et al.* 1997; Dancis *et al.* 1994b; Yuan *et al.* 1995). As shown in Chapter 5, at least one copper-binding subdomain close to the channel is required for ATP7B to complement *ccc2* mutant yeast, suggestive of a requirement for copper binding to the copper-binding domain as a prerequisite for copper transport *in vivo*. Consistent with this hypothesis, all known CPx-type ATPase from prokaryotes and eukaryotes have at least one copper-binding subdomain in close proximity to the predicted transmembrane channel (Bull *et al.* 1994; Solioz, 1998).

Since there is essentially no free copper in eukaryotic cells (Rae *et al.* 1999), copper transiently bound to the ATP7B copper-binding domain, removed from ATOX1, is likely the major source of copper transferred to the predicted transmembrane domain for subsequent transport under normal physiologic conditions. This hypothesis is supported by recent studies using yeast and mammalian two-hybrid analysis, together with column interaction/retention assays, and co-immunoprecipitation assays, which determined that ATOX1 could interact with the copper-binding domain of ATP7B *in vivo* and *in vitro* (Larin *et al.* 1999; Hamza *et al.* 1999). The interaction was dependent on the presence of copper. Mutation of the cysteine residues within either the ATOX1, or ATP7B (all six), copper-binding motifs abolish interaction. These data agree with those already published for yeast two-hybrid interactions between Atx1p and the copper-binding domain of Ccc2p (Pufahl *et al.* 1997) (Chapter 5). The interaction between Atx1p and Ccc2p was shown to result in quantitative, and unidirectional metal transfer from the chaperone to its target protein, at equilibrium concentrations (Rosenzweig *et al.* 1999). A transient interaction between cuprochaperone and target protein as has been proposed (Pufahl *et al.* 1997; Portnoy *et al.* 1999). Consistent with this proposal, Larin *et al.* (1999) report that the yeast and mammalian two-hybrid interaction between ATP7B and ATOX1 appeared weak. Similarly, Hamza *et al.* (1999) report that only 3-5% of cellular ATOX1 co-immunoprecipitates with ATP7B, and there is no concentration of ATOX1 near ATP7B containing membranes in HepG2 cells, even in the presence of excess copper, based on confocal immunofluorescence microscopy. Furthermore, Hamza *et al.* (1999) analysed the ability of three transiently expressed WD mutant variants of ATP7B, with missense mutations in the copper-binding domain, to co-immunoprecipitate ATOX1 from mammalian COS cell protein extracts. These mutations, G85V, L492S, and G591D all resulted in significantly reduced ability of the mutant ATP7B proteins to co-immunoprecipitate ATOX1. The mutant proteins were properly localised within the cells

suggesting no gross misfolding. Since the ATP7B mutants analysed result in WD (Loudianos *et al.* 1998), it was concluded that interaction between the copper-binding domain of ATP7B and ATOX1 is essential for normal mammalian copper homeostasis (Hamza *et al.* 1999). Similarly, a copper-binding domain missense mutation in the *Arabidopsis thaliana* ATP7B orthologue RAN-1, resulted in severely impaired copper delivery to essential cuproenzymes involved in ethylene production in plants (Hirayama *et al.* 1999). Impaired interaction of RAN-1 with the plant ATOX1 orthologue may be biochemical basis of this defect (Hamza *et al.* 1999). Taken all together, these studies support the idea that transient, copper dependent interaction, followed by copper exchange between the ATOX1 and the copper-binding of ATP7B, are essential for ATP7B function *in vivo*. These data, combined with yeast complementation data presented in Chapter 5, support the model that copper transiently bound by the ATP7B copper-binding subdomains nearest the channel, is then delivered for the predicted transmembrane domain for subsequent transport.

Missense mutations within the copper-binding domain are not often considered to be disease causing due to postulated functional redundancy of the six copper-binding subdomains (Tumer *et al.* 1999; Cox *et al.* 1999), together with the view that the six subdomains may act as independent structures. An interesting aspect of the results reported by Hamza *et al.* (1999) is that single missense mutations within individual copper-binding subdomains, appear to affect the whole copper-binding domain. WD mutation G85V is found in the first subdomain, L492S in the fifth subdomain, and G591D in the sixth subdomain (Hamza *et al.* 1999; Loudianos *et al.* 1998). G85 and G591 are equivalent amino acids in their respective subdomains. The normal residues in these positions are evolutionarily conserved, are structurally important based on available structural information, and therefore the mutations are predicted to affect the individual subdomain structure (Gitschier *et al.* 1998; Rosenzweig *et al.* 1999; Hamza *et al.* 1999). Since the mutations analysed prevented any substantial interaction between ATOX1 and ATP7B (Hamza *et al.* 1999), these data suggest that the entire copper-binding domain may be misfolded and non-functional, due to individual subdomain misfolding. These data support the hypothesis of Forbes *et al.* (1999) (Chapter 5), which states that normal function of the copper-binding subdomain, is likely dependent on proper folding of individual copper-binding subdomains, as well as proper overall folding and orientation of the six individual subdomains with respect to each other, and to the predicted transmembrane channel (Forbes *et al.* 1999). Another implication of the Hamza *et al.* (1999) data, is that mutations found in WD patients within the copper-binding domain of

ATP7B, must be considered to be potentially disease causing, since even a missense mutation within an individual subdomain may have severe functional effects on ATP7B.

While the copper-binding domain of ATP7B is likely required for copper transport *in vivo*, a recent report presented data suggesting that the copper-binding domain of ATP7A is not required for copper transport under defined conditions *in vitro*. Voskoboinik *et al.* (1999) have shown *in vitro*, by measuring ATP-dependent copper uptake into plasma membrane vesicles, that ATP7A mutant protein with all six copper-binding motifs mutated from Cys to Ser is capable of 55-70% of normal ATP7A copper transport activity. As previously described (Voskoboinik *et al.* 1998), mutant and normal ATP7A copper transport activity was entirely dependent on the presence of DTT, a copper chelator and reducing agent, and high concentrations of histidine, a physiologic plasma copper ligand that is present in trace amounts *in vivo* (Linder *et al.* 1998; Voskoboinik *et al.* 1998; Voskoboinik *et al.* 1999; Pufahl *et al.* 1997). Both histidine and DTT may potentiate the bypassing of the copper-binding domain *in vitro*, perhaps by directly delivering copper to the predicted transmembrane channel (Voskoboinik *et al.* 1999; Voskoboinik *et al.* 1998). These data suggest the possibility that the copper-binding domain of ATP7A (or ATP7B) may not be required for copper transport *in vivo* under conditions of copper overload if sufficient cytoplasmic copper is readily available for transport. Under these conditions glutathione may act as a copper donor to ATP7B (Freedman *et al.* 1989).

Further study is required to precisely determine the preferred form of copper used for transport by ATP7B and the role of the copper-binding domain in transport. Vesicular copper uptake assays performed *in vitro*, using normal, and mutant ATP7A and ATP7B proteins, and purified copper-loaded ATOX1 as a copper donor, should confirm the hypothesis that ATOX1 is the preferred copper donor for ATP7B. Copper bound to ATOX1 is predicted to be the preferred substrate for ATP7B dependent copper transport under conditions of chelator limited ionic copper in a manner analogous to that seen for the copper delivery from chaperone Ccs1p to its target Sod1p (Rae *et al.* 1999) (See 1C-3). Furthermore it can be predicted from data presented in Chapter 5 that at least one copper-binding subdomain close to the putative transmembrane channel would be required for copper transport *in vitro* by ATP7B using ATOX1 as the copper donor.

### **6B-2) Requirement of the copper-binding domain of ATP7B for copper dependent trafficking.**

One of the earliest proposed roles for the copper-binding domain of CPx-type ATPase, was that of a copper sensor (Vulpe *et al.* 1993; DiDonato *et al.* 1997; Petris *et*

*al.* 1996), perhaps acting in response to cytosolic copper concentrations to trigger copper-dependent changes in intracellular localisation (see section 1E-5). This hypothesis was initially supported by work suggesting that copper binding to the copper-binding domain of ATP7B was cooperative, and induces conformational changes in the copper-binding domain (DiDonato *et al.* 1997; Forbes *et al.* 1999). Two recent reports further substantiate the hypothesis (Strausak *et al.* 1999; Goodyer *et al.* 1999). They report that mutation of all six metal binding motifs of ATP7A resulted in complete loss of copper dependent redistribution, such that all mutant protein was restricted to the Golgi network, unable to move to the plasma membrane in response to copper. These data suggest that binding of copper to the copper-binding domain of ATP7A is a requirement for redistribution between intracellular compartments. Studies to determine the effect of mutations in the copper-binding domain of ATP7B are currently being done in collaboration with Dr. Julian Mercer using the constructs described in Chapter 5. Likely, the copper-binding domain of ATP7B will be required for copper dependent localisation as seen for ATP7A.

Data described in Chapter 5 suggest a functional difference between the copper binding domains of ATP7A and ATP7B, and combined with recent data, suggests that the copper-binding domains of both proteins may be functionally divided. Yeast complementation analysis of ATP7A mutant proteins suggested that the N-terminal three copper-binding subdomains are critical for copper transport (Payne *et al.* 1998a). Intracellular trafficking data from Strausak *et al.* (1999) suggests that the copper-binding subdomains nearest the channel of ATP7A, subdomains five and six, are required for redistribution from the Golgi network to the plasma membrane. Together these data suggest that the copper-binding domain of ATP7A is functionally divided, and each part plays a different but complementary role in overall ATP7A biological function. In contrast to ATP7A, the C-terminal most copper-binding subdomains of ATP7B were most important for function in yeast complementation assays and by inference copper transport (Chapter 5)(Iida *et al.* 1998; Forbes *et al.* 1999). There may be structural differences between the copper-binding domains of ATP7A and ATP7B, due to the presence of large amino acid deletions/insertions between several of the individual subdomains, that may lead to a different arrangement, and orientation of individual subdomains within the larger copper-binding domain (see section 5D). Taken together, these data suggest that the copper-binding domains of ATP7A and ATP7B may fold differently from each other such that different copper-binding subdomains are involved in copper transport or copper-dependent intracellular redistribution by each protein. By analogy with ATP7A, it can be predicted that the copper-binding domain of ATP7B is functionally divided such that the C-terminal most copper-binding subdomains are

involved in copper transport and the N-terminal most subdomains are involved in redistribution. This hypothesis will be confirmed or denied through collaborative research with Dr. Mercers group.

### **6B-3) Proposed mechanisms of ATP7B copper-binding domain function.**

The copper-binding domain of ATP7B is required for copper transport activity and likely copper-dependent redistribution. A possible biochemical mechanism to incorporate these data and hypotheses into a working model can be proposed (Fig. 6-1):

- 1) Copper is delivered to the copper-binding domain of ATP7B by direct interaction and transfer from ATOX1.
- 2) Copper is transferred from the C-terminal most copper-binding subdomains to the putative transmembrane channel (CPC motif) for subsequent translocation through the membrane.
- 3) As proposed by Pufahl *et al.* (1997), copper transfer from chaperone, to ATPase subdomains, to the channel is thermodynamically driven by local copper concentration and a gradient of increasing affinity copper-binding sites. The gradient is maintained by translocation of copper through the membrane. The transfer from metallochaperone to target protein appear to be specific, rapid, and unidirectional (Rae *et al.* 1999; Rosenzweig *et al.* 1999).
- 4) As the occupancy of the copper-binding domain by copper increases, particularly in the N-terminal 1-4 subdomains, cooperative conformational changes occur over the whole domain. These putative changes may induce conformational changes (see section 5D) in the rest of the protein, allowing it to move out of the Golgi and into endosomal vesicles, perhaps by shifting the orientation of helices in the predicted transmembrane domain. Copper induced conformational changes may allow protein-protein interactions between ATP7B and other proteins needed to mediate the trafficking event by creating or unmasking molecular recognition motifs. Potential targeting motifs in ATP7B include a C-terminal di-leucine motif, and motifs within the predicted transmembrane domain such as have been identified in ATP7A (Francis *et al.* 1998; Petris *et al.* 1998; Francis *et al.* 1999) (see section 1D-5). Future studies will reveal if these motifs exist and are important for ATP7B function. After redistribution, copper transport into endosomal vesicles continues to occur, using copper-binding subdomains five and six close to the predicted transmembrane channel.
- 5) As cytoplasmic copper levels decrease, copper is removed from the copper-binding domain allowing recycling back to the Golgi network. Copper removal occurs either by copper transport by ATP7B, perhaps involving intra-subdomain exchange of the copper to subdomains near to the channel prior to transport, or by exchange back to chaperone proteins. The biological outcome of this mechanism is to incorporate copper into ceruloplasmin (and other enzymes) in the trans-Golgi network,

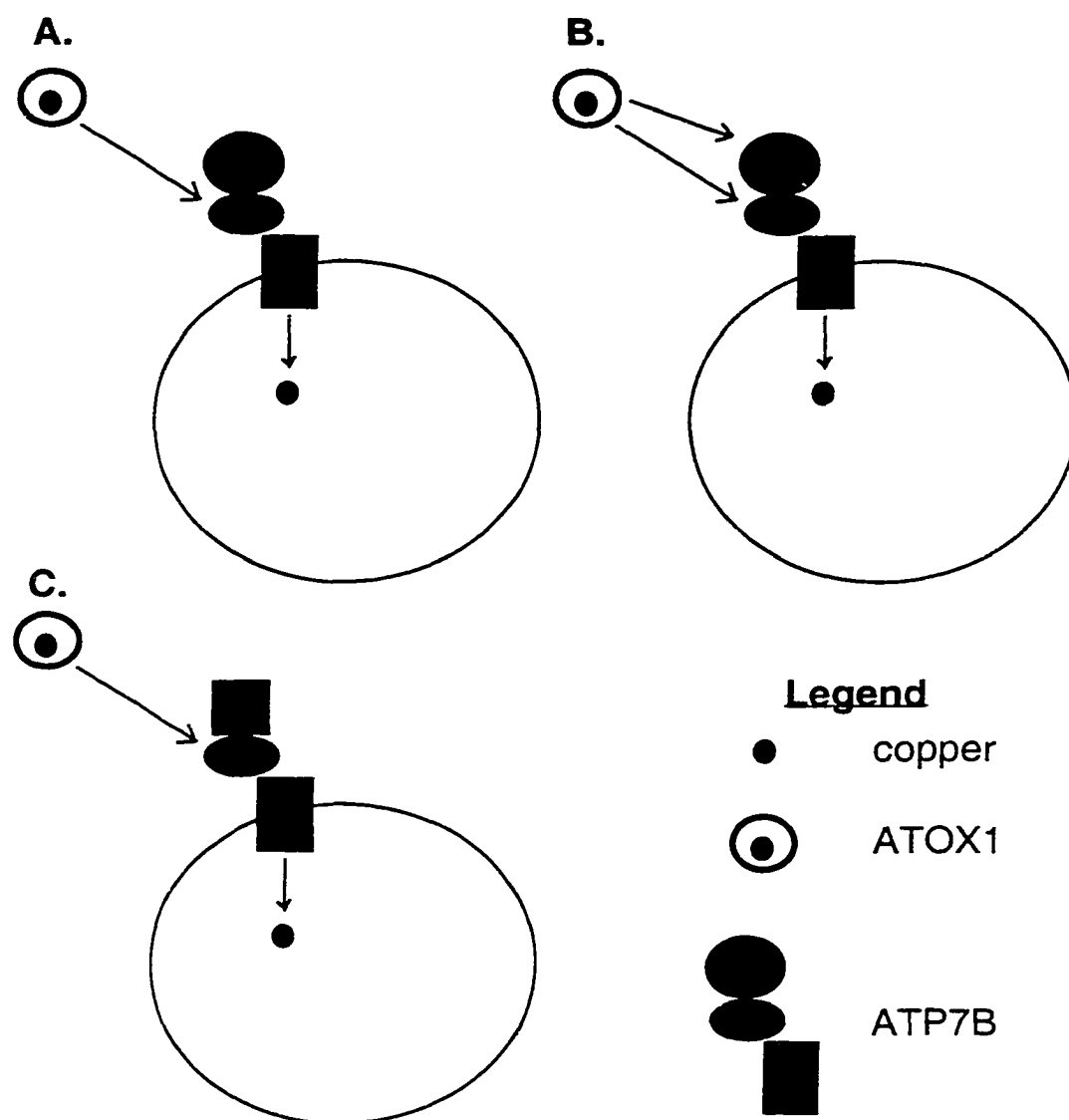


**Figure 6-1: Role of the copper-binding domain in copper transport by ATP7B.**

**A.**, Under low cytosolic copper conditions, copper is delivered to copper-binding subdomains five and six of ATP7B by ATOX1. Copper bound to these subdomains is delivered to the transmembrane domain for transport into the Golgi network lumen. **B.**, Under conditions of elevated cytosolic copper, copper is bound by copper-binding subdomains one to four in addition to subdomains five and six. **C.**, As copper occupancy of the copper-binding domain increases, conformation changes occur, which trigger ATP7B redistribution into cytoplasmic vesicles. Under these conditions copper transport occurs as in A., resulting in copper transport into cytoplasmic vesicles for efflux into the bile (See Fig.1-3).

while limiting cellular copper efflux when cytosolic copper levels are low. As cytoplasmic copper levels rise, ATP7B moves mostly to the vesicular/endosomal compartment to mediate biliary copper efflux (refer to section 1D-4 and 1D-5 for more detail about copper efflux).

This mechanism suggests that copper is delivered from the copper-binding domain to the transmembrane channel for transport and based on available evidence is the most likely hypothesis. Yeast complementation data do support a requirement for the copper-binding domain for ATP7B copper-transport function *in vivo* but not necessarily a role limited to copper delivery to the channel for transport. A possible modification of the former mechanism is that the copper-binding domain plays an additional regulatory role. The apo-copper-binding domain may fold such that the predicted transmembrane channel or ATP-binding site is partially occluded (Dameron *et al.* 1998), or interact with other ATP7B domains slowing transitions between phosphorylated enzyme intermediates thereby reducing copper-transport activity. Copper binding to the copper-binding domain may result in conformational changes that relieve this inhibition and increase copper transport activity in response to cytosolic copper levels. Alternatively, copper binding to the copper-binding domain of ATP7B may induce conformation changes that up-regulate copper transport activity in response to copper. Voskoboinik *et al.* (1999) showed a reduction of copper transport of between 30-45% when the copper-binding domain of ATP7A was mutated which may be indicative of down-regulated transport activity due to the mutant N-terminal domain being unable to sense and respond to copper. Furthermore, kinetic analysis of the ATP7A mutant protein revealed that the copper-binding domain mutations reduced the  $V_{max}$  but did not effect the  $K_m$  suggesting that enzyme turnover was reduced (Voskoboinik *et al.* 1999). Yeast complementation data presented in Chapter 5 did not reveal any substantial decrease in ATP7B function when the first five copper binding domains were mutated or deleted. However, the change in activity could have been too small to detect. If the occlusion/inhibition mechanism is correct, one would assume that ATP7B should be more active when the copper-binding domain is completely deleted, compared with all-six motifs being mutated, which can be directly tested by vesicular copper uptake assays. Using yeast complementation assays, ATP7B mutant protein with the copper-binding domain deleted was completely unable to complement *ccc2* mutant yeast, as was the protein in which all six copper-binding motifs were mutated (Chapter 5). Based on these data, the occlusion/inhibition mechanism is unlikely. The copper-binding domain may act to positively regulate copper-transport in response to copper in addition to its role in intracellular trafficking and copper-delivery to the ATP7B channel for transport.

## 6C) CONCLUSIONS.

Upon completion of this thesis, the proposed goals have been achieved. To reiterate, the general aim of this thesis was to use structure/function analysis of ATP7B, to aid in elucidating its biochemical and physiologic function. I have created the methods and resources needed to perform a structure/function analysis of ATP7B.

The specific goals of this thesis were as follows: 1) To study the effect of selected, genetically identified WD mutations on ATP7B function and intracellular localisation, in order to gain insight into the normal function of ATP7B, the molecular pathogenesis of WD, and as an aid to discriminate true WD missense mutations from rare normal variants by functional analysis. Hypothesis: Changes in the function and intracellular localisation of ATP7B, due to allelic variation, can explain in part the variable biochemical features observed in WD patients. I have been able to determine by functional means, whether or not a ATP7B mutation is likely to be disease causing or a rare normal variant. Through functional and cellular analysis of ATP7B WD mutant proteins, I have obtained data, and provided a likely biochemical mechanism, that can explain in part the biochemical variability observed in WD patients. I have provided evidence supporting the requirement of ATP7B copper-induced redistribution for normal copper efflux. 2) To study the role of the ATP7B copper-binding domain with respect to the putative copper transport function of ATP7B. Hypothesis: The copper-binding domain of ATP7B is essential for the proteins function as a copper transporter. I have provided evidence that the copper-binding domain is required for ATP7B copper transport activity, and have provided a putative mechanism explaining that requirement.

**BIBLIOGRAPHY.**

Alexander, J. and Aeseth, J. (1980) Biliary excretion of copper and zinc in the rat as influenced by diethylmaleate, selenite, and diethyldithiocarbamate. *Biochem.Pharmacol.*, **29**:2129-2133.

Amaravadi, R., Glerum, D.M. and Tzagaloff, A. (1997) Isolation of a cDNA encoding the human homolog of *COX17*, a yeast gene essential for mitochondrial copper recruitment. *Hum.Mol.Genet.*, **99**:329-333.

Ambrosini, L. and Mercer, J.F.B. (1999) Defective copper-induced trafficking and localization of the Menkes protein in patients with mild and copper-treated classical Menkes disease. *Hum.Mol.Genet.*, **8**:1547-1555.

Askwith, C., Eide, D., Van Ho, A., Bernard, P.S., Li, L., Davis-Kaplan, S., Sipe, D.M., *et al.* (1994) The *FET3* gene of *S. cerevisiae* encodes a multicopper oxidase required for ferrous iron uptake. *Cell*, **76**:403-410.

Askwith, C.C. and Kaplan, J. (1998) Site-directed mutagenesis of the yeast multicopper oxidase Fet3p. *J.Biol.Chem.*, **273**:22415-22419.

Ausubel, F.M., Brent, R., Kingston, R.E., Moore, D.D., Seidman, J.G., Smith, J.A. and Struhl, K. (1998) *Current Protocols in Molecular Biology*. John Wiley and Sons, Inc., New York. pp. 1.0.1-A.5.45.

Babcock, M., de Silva, D., Oaks, R., Davis-Kaplan, S., Jiralerspong, S., Montermini, L., Pandolfo, M., *et al.* (1997) Regulation of mitochondrial iron accumulation by Yfh1p, a putative homolog of frataxin. *Science*, **276**:1709-1712.

Baerga, I.D., Maickel, R.P. and Green, M.A. (1992) Subcellular distribution of tissue radiocopper following intravenous administration of <sup>67</sup>Cu-labelled Cu-PTSM. *Int.J.Appl.Instrum.*, **19**:697-701.

Ballatori, N. (1991) Mechanism of metal transport across liver cell plasma membranes. *Drug Metab.Rev.*, **23**:83-132.

Beers, J., Glerum, D.M. and Tzagoloff, A. (1997) Purification, characterisation, and localization of yeast Cox17p, a mitochondrial copper shuttle. *J.Biol.Chem.*, **272**:33191-33196.

Beshgetoor, D. and Hambridge, M. (1998) Clinical conditions altering copper metabolism in humans. *Am.J.Clin.Nutr.*, **67**:1017S-1021S.

Bingham, M.J. and McArdle, H.J. (1994) A comparison of copper uptake by liver plasma membrane vesicles and uptake by isolated cultured rat hepatocytes. *Hepatology*, **20**:1024-1031.

Bingham, M.J., Ong, T.J., Ingledew, W.J. and McArdle, H.J. (1996) ATP-dependent copper transporter, in the Golgi apparatus of rat hepatocytes, transports Cu(II) not Cu(I). *Am.J.Physiol.*, **271**(5):G741-G746.

Bingle, C.D., Srani, S.K.S. and Epstein, O. (1992) Copper metabolism in hypercupremic human livers. *J.Hepatology*, **15**:94-101.

Bofill, R., Palacios, O., Capdevila, M., Gonzalez-Duarte, R., Atrian, S. and Gonzalez-Duarte, P. (1999) A new insight into the Ag<sup>+</sup> and Cu<sup>+</sup> binding sites in the metallothionein beta domain. *J.Inorg.Biochem.*, **73**:57-64.

Bradley, M.K. (1990) Overexpression of proteins in eukaryotes. *Methods Enzymol.*, **182**:112-132.

Bremner, I. (1998) Manifestations of copper excess. *Am.J.Clin.Nutr.*, **67**:1069S-1073S.

Buiakova, O.I., Xu, J., Lutsenko, S., Zeitlin, S., Das, K., Das, S., Ross, B.M., *et al.* (1999) Null mutation of the murine *Atp7b* (Wilson disease) gene results in intracellular copper accumulation and late-onset hepatic nodular transformation. *Hum.Mol.Genet.*, **8**:1665-1671.

Bull, L.N., van Eijk, M.J., Pawlikowska, L., DeYoung, J.A., Juijn, J.A., Liao, M., Klomp, L.W., *et al.* (1998) A gene encoding a P-type ATPase mutated in two forms of hereditary cholestasis. *Nat.Genet.*, **18**:19-24.

Bull, P.C. and Cox, D.W. (1994) Wilson disease and Menkes disease: new handles on heavy-metal transport. *Trends Genet.*, **10**:246-252.

Bull, P.C., Thomas, G.R., Rommens, J.M., Forbes, J.R. and Cox, D.W. (1993) The Wilson disease gene is a putative copper transporting P-type ATPase similar to the Menkes gene. *Nat.Genet.*, **5**:327-337.

Butt, T.R., Sternberg, E.J., Gorman, J.A., Hamer, D., Rosenberg, M. and Crooke, S.T. (1984) Copper metallothionein of yeast, structure of the gene, and regulation of expression. *Proc.Natl.Acad.Sci.USA*, **81**:3332-3336.

Calvo, P.A., Frank, D.W., Bieler, B.M., Berson, J.F. and Marks, M.S. (1999) A cytoplasmic sequence in human tyrosinase defines a second class of di-leucine-based sorting signals for late endosomal and lysosomal delivery. *J.Biol.Chem.*, **274**:12780-12789.

- Carri, M.T., Galiazzo, F., Ciriolo, M.R. and Rotilio, G. (1991) Evidence for co-regulation of Cu,Zn superoxide dismutase and metallothionein gene expression in yeast through transcriptional control by copper via the *ACE1* factor. *FEBS Lett.*, **278**:263-266.
- Casareno, R.L.B., Waggoner, D. and Gitlin, J.D. (1998) The copper chaperone CCS directly interacts with copper/zinc superoxide dismutase. *J.Biol.Chem.*, **273**:23625-23628.
- Chelly, J., Turner, Z., Tonnesen, T., Petterson, A., Ishikawa-Brush, Y., Tommerup, N., Horn, N., *et al.* (1993) Isolation of a candidate gene for Menkes disease that encodes a potential heavy metal binding protein. *Nat.Genet.*, **3**:14-19.
- Chuang, L-M., Wu, H-P., Jang, M-H., Wang, T-R., Sue, W-C., Lin, B.J., Cox, D.W., *et al.* (1996) High frequency of two mutations in codon 778 in exon 8 of the *ATP7B* gene in Taiwanese families with Wilson disease. *J.Med.Genet.*, **33**:521-523.
- Clarke, D.M., Loo, T.W., Inesi, G. and MacLennan, D.H (1989) Location of high affinity  $Ca^{2+}$ -binding sites within the predicted transmembrane domain of the sarcoplasmic reticulum  $Ca^{2+}$ -ATPase. *Nature*, **339**:476-478.
- Cobine, P., Wickramasinghe, W.A., Harrison, M.D., Weber, T., Solioz, M. and Dameron, C.T. (1999) The *Enterococcus hirae* copper chaperone CopZ delivers copper(I) to the CopY repressor. *FEBS Lett.*, **445**:27-30.
- Cotton, F.A. and Wilkinson, G. (1988) *Advanced inorganic chemistry*. Ed. 5. John Wiley and Sons, New York. pp. 1-1455.
- Cox, D.W., Forbes, J.R. and Nanji, M.S. (1999) The copper transporting ATPase defective in Wilson disease. In Sarkar, B. (ed.), *Metals and Genetics*. Plenum Publishers, New York. p. 255-264.
- Cox, D.W. and Roberts, E.A. (1998) Wilson disease. In Feldman, M., Schlarschmidt, B.F. and Sleisenger, M.H. (eds.), *Sleisenger and Fordtran's Gastrointestinal and Liver Disease*. Ed. 6. W.B. Saunders, Philadelphia. p. 1104-1111.
- Culotta, V.C., Howard, W.R. and Liu, X.F. (1994) *CRS5* encodes a metallothionein-like protein in *Saccharomyces cerevisiae*. *J.Biol.Chem.*, **269**:25295-25302.
- Culotta, V.C., Joh, H-D., Lin, S-J., Slekar, K.H. and Strain, J. (1995) A physiological role for *Saccharomyces cerevisiae* copper/zinc dismutase in copper buffering. *J.Biol.Chem.*, **270**:29991-29997.
- Culotta, V.C., Klomp, L.W.J., Strain, J., Casareno, R.L.B., Krems, B. and Gitlin, J.D. (1997) The copper chaperone for superoxide dismutase. *J.Biol.Chem.*, **272**:23469-23472.

- Daganais, S.L., Guevara-Fujita, M., Loechel, R., Burgess, A.C., Miller, D.E., Yuzbasiyan-Gurkan, V., Brewer, G.J., *et al.* (1999) The canine copper toxicosis locus is not syntenic with *ATP7B* or *ATX1* and maps to a region showing homology to human 2p21. *Mamm.Genome*, **10**:753-756.
- Dameron, C.T. and Harrison, M.D. (1998) Mechanisms for protection against copper toxicity. *Am.J.Clin.Nutr.*, **67**:1091S-1097S.
- Dancis, A., Haile, D., Yuan, D.S. and Klausner, R.D. (1994a) The *Saccharomyces cerevisiae* copper transport protein (Ctr1p). *J.Biol.Chem.*, **269**:25660-25667.
- Dancis, A., Yuan, D.S., Haile, D., Askwith, C., Eide, D., Moehle, C., Kaplan, J., *et al.* (1994b) Molecular characterisation of a copper transport protein in *S. cerevisiae*: an unexpected role for copper in iron transport. *Cell*, **76**:393-402.
- Danks, D.M. (1995) Disorders of copper transport. In Scriver, C.R., Beaudet, A.L., Sly, W.S. and Valle, D. (eds.), *The Metabolic and Molecular Basis of Inherited Disease*. Ed. 7. McGraw-Hill, New York. p. 2211-2235.
- Darwish, H.M., Cheney, J.C., Schmitt, R.C. and Ettinger, M.J. (1984) Mobilization of copper(II) from plasma components and mechanism of hepatic copper transport. *Am.J.Physiol.*, **246**:G48-G55.
- Darwish, H.M., Hoke, J.E. and Ettinger, M.J. (1983) Kinetics of Cu(II) transport and accumulation by hepatocytes from copper-deficient mice and the brindled mouse model of Menkes disease. *J.Biol.Chem.*, **258**:13621-13626.
- Darwish, H.M., Schmitt, R.C., Cheney, J.C. and Ettinger, M.J. (1984) Copper efflux kinetics from rat hepatocytes. *Am.J.Physiol.*, **246**:G48-G55.
- Davis-Kaplan, S.R., Askwith, C.C., Bengtzen, A.C., Radisky, D. and Kaplan, J. (1998) Chloride is an allosteric effector of copper assembly for the yeast multicopper oxidase Fet3p: An unexpected role for intracellular chloride channels. *Proc.Natl.Acad.Sci.USA*, **95**:13641-13645.
- de Silva, D., Davis-Kaplan, S., Fergestad, J. and Kaplan, J. (1997) Purification and characterization of Fet3 protein, a yeast homologue of ceruloplasmin. *J.Biol.Chem.*, **272**:14208-14213.
- Deering, T.B., Dickson, E.R., Fleming, C.R., Geall, M.G., McCall, J.T. and Baggenstoss, A.H. (1977) Effect of D-penicillamine on copper retention in patients with primary biliary cirrhosis. *Gastroenterology*, **72**:1208-1212.

DiDonato, M., Narindrasorasak, S., Forbes, J.R., Cox, D.W. and Sarkar, B. (1997) Expression, purification and metal binding properties of the N-terminal domain from the Wilson Disease putative Cu-transporting ATPase (ATP7B). *J.Biol.Chem.*, **272(52)**:32279.

Dijkstra, M., Havinga, R., Vonk, R.J. and Kuipers, F. (1996) Bile secretion of cadmium, silver, zinc, and copper in the rat. Involvement of various transport systems. *Life Sci.*, **59**:1237-1246.

Dijkstra, M., In 't Veld, G., van den Berg, G.J., Muller, M., Kuipers, F. and Vonk, R.J. (1995) Adenosine triphosphate-dependent copper transport in isolated rat liver plasma membranes. *J.Clin.Invest.*, **95**:412-416.

Dijkstra, M., Kuipers, F., van den Berg, G.J., Havinga, R. and Vonk, R.J. (1997) Differences in hepatic processing of dietary and intravenously administered copper in rats. *Hepatology*, **26**:962-966.

Dijkstra, M., van den Berg, G.S., Wolters, H., In't Veld, G., Sloof, M.J., Heymans, H.S., Kuipers, F., *et al.* (1996) Adenosine triphosphate-dependent copper transport in human liver. *J.Hepatology*, **25(1)**:37-42.

Elble, R. (1992) A simple and efficient procedure for transformation of yeasts. *Biotechniques*, **13**:18-20.

Farrell, R.A., McArdle, H.J. and Camakaris, J. (1993) Effects of metallothioneins on the observed copper distribution in cell extracts. *J.Inorg.Biochem.*, **49**:9-22.

Figus, A., Angius, A., Loudianos, G., Bertini, C., Dessi, V., Loi, A., Deiana, M., *et al.* (1995) Molecular pathology and haplotype analysis of Wilson disease in Mediterranean populations. *Am.J.Hum.Genet.*, **57**:1318-1324.

Fogel, S. and Welch, J.W. (1982) Tandem gene amplification mediates copper resistance in yeast. *Proc.Natl.Acad.Sci.USA*, **79**:3542-3546.

Fontaine, S.L., Firth, S.D., Lockhart, P.J., Paynter, J.A. and Mercer, J.F (1998) Eukaryotic expression vectors that replicate to low copy number in bacteria: transient expression of the Menkes protein. *Plasmid*, **39**:245-251.

Forbes, J.R. and Cox, D.W. (1998) Functional characterization of missense mutations in ATP7B: Wilson disease mutation or normal variant? *Am.J.Hum.Genet.*, **63**:1663-1674.

Forbes, J.R., Hsi, G. and Cox, D.W. (1999) Role of the copper-binding domain in the copper transport function of ATP7B, the P-type ATPase defective in Wilson disease. *J.Biol.Chem.*, **274**:12408-12413.

- Francis, M.J., Jones, E.E., Levy, E.R., Ponnambalam, S., Chelly, J. and Monaco, A.P. (1998) A Golgi localization signal identified in the Menkes recombinant protein. *Hum.Mol.Genet.*, **7**:1245-1252.
- Francis, M.J., Jones, E.M., Levy, E.R., Martin, R.L., Ponnambalam, S. and Monaco, A.P. (1999) Identification of a di-leucine motif within the C-terminus domain of the Menkes disease protein that mediates endocytosis from the plasma membrane. *J.Cell Sci.*, **112**:1721-1732.
- Freedman, J.H. and Peisach, J. (1989) Intracellular copper transport in cultured hepatoma cells. *Biochem.Biophys.Res.Comm.*, **164**:134-140.
- Frieden, E. and Hsieh, H.S. (1976) Ceruloplasmin: The copper transport protein with essential oxidase activity. *Adv.Enzymol.*, **44**:187-236.
- Fuentealba, I., Haywood, S. and Foster, J. (1989a) Cellular mechanisms of toxicity and tolerance in the copper-loaded rat. II. Pathogenesis of copper toxicity in the liver. *Exp.Mol.Pathol.*, **50**:26-37.
- Fuentealba, I., Haywood, S. and Trafford, J. (1989b) Variations in the intralobular distribution of copper in the livers of copper-loaded rats in relation to the pathogenesis of copper storage diseases. *J.Comp.Path.*, **100**:1-11.
- Furst, P., Hu, S., Hackett, R. and Hamer, D. (1988) Copper activates metallothionein gene transcription by altering the conformation of a specific DNA binding protein. *Cell*, **55**:705-717.
- Gamonet, F. and Lauquin, G.J. (1998) The *Saccharomyces cerevisiae* *LYS7* gene is involved in oxidative stress protection. *Eur.J.Biochem.*, **251**:716-723.
- Georgatsou, E., Mavrogiannis, L.A., Fragiadakis, G.S. and Alexandraki, D. (1997) The yeast Fre1p/Fre2p cupric reductases facilitate copper uptake and are regulated by the copper-modulated Mac1p activator. *J.Biol.Chem.*, **272**:13786-13792.
- Gitschier, J., Moffat, B., Reilly, D., Wood, W.I. and Fairbrother, W.J. (1998) Solution structure of the fourth metal-binding domain from the Menkes copper-transporting ATPase. *Nat.Struct.Biol.*, **5**:47-54.
- Glerum, D.M., Shtanko, A. and Tzagaloff, A. (1996) Characterization of *COX17*, a yeast gene involved in copper metabolism and assembly of cytochrome oxidase. *J.Biol.Chem.*, **271**:14504-14509.
- Goodyer, I.D., Jones, E.E., Monaco, A.P. and Francis, M.J. (1999) Characterization of the Menkes protein copper-binding domains and their role in copper-induced relocalization. *Hum.Mol.Genet.*, **8**:1473-1478.

- Gralla, E.B., Thiele, D.J., Silar, P. and Valentine, J.S. (1991) ACE1, a copper specific transcription factor, activates expression of the yeast copper, zinc superoxide dismutase gene. *Proc.Natl.Acad.Sci.USA*, **88**:8558-8562.
- Green, N.M. and Stokes, D.L. (1993) Structural modelling of P-type ion pumps. *Acta.Physiol.Scand.*, **146**:59-68.
- Gross, J.B., Myers, B.M., Kost, L.J., Kuntz, S.M. and LaRusso, N.F. (1989) Biliary copper excretion by hepatocyte lysosomes in the rat. *J.Clin.Invest.*, **83**:30-39.
- Gruenberg, J. and Maxfield, F.R. (1995) Membrane transport in the endocytic pathway. *Curr.Opin.Cell Biol.*, **7**:552-563.
- Gunes, C., Heuchel, R., Georgiev, O., Muller, K.H., Lichtlen, P., Bluthmann, H., Marino, S., *et al.* (1998) Embryonic lethality and liver degeneration in mice lacking the metal-responsive transcriptional activator MTF-1. *EMBO J.*, **17**:2846-2856.
- Guyton, A.C. (1991) *Textbook of Medical Physiology*. Ed. 8. W.B. Saunders Company, Philadelphia. pp. 1-1014.
- Hamza, I., Schaefer, M., Klomp, L.W. and Gitlin, J.D. (1999) Interaction of the copper chaperone HAH1 with the Wilson disease protein is essential for copper homeostasis. *Proc.Natl.Acad.Sci.USA*, **96**:13363-13368.
- Harada, M., Sakisaka, S., Yoshitake, M., Shakadoh, S., Gondoh, K., Sata, M. and Tanikawa, K. (1993) Biliary copper excretion in acutely and chronically copper-loaded rats. *Hepatology*, **17**:111-117.
- Harlow, E. and Lane, D. (1988) *Antibodies: A laboratory manual*. Cold Spring Harbor Laboratory, Cold Spring Harbor, New York. pp. 1-726.
- Harris, L.Z., Klomp, L.W.J. and Gitlin, J.D. (1998) Aceruloplasminemia: an inherited neurodegenerative disease with impairment of iron homeostasis. *Am.J.Clin.Nutr.*, **67**:972S-977S.
- Harris, Z.L., Durley, A.P., Man, T.K. and Gitlin, J.D. (1999) Targeted gene disruption reveals an essential role for ceruloplasmin in cellular iron efflux. *Proc.Natl.Acad.Sci.USA*, **96**:10812-10817.
- Harris, Z.L., Takahashi, Y., Miyajima, H., Serizawa, M., MacGillivray, R.T.A. and Gitlin, J.D. (1995) Aceruloplasminemia: Molecular characterization of this disorder of iron metabolism. *Proc.Natl.Acad.Sci.USA*, **92**:2539-2543.
- Hassett, R. and Kosman, D.J. (1995) Evidence for Cu(II) reduction as a component of copper uptake by *Saccharomyces cerevisiae*. *J.Biol.Chem.*, **270**:128-134.

- Haywood, S., Loughran, M. and Batt, R.M. (1985) Copper toxicosis and tolerance in the rat. III. Intracellular localization of copper in the liver and kidney. *Exp.Mol.Pathol.*, **43**:209-219.
- Heuchel, R., Radtke, F., Georgiev, O., Stark, G. and Schaffner, W. (1994) The transcription factor MTF-1 is essential for basal and heavy metal-induced metallothionein gene expression. *EMBO J.*, **13**:2870-2875.
- Hirayama, T., Kieber, J.J., Hirayama, N., Kogan, M., Guzman, P., Nourizadeh, S., Alonso, J.M., *et al.* (1999) Responsive-To-Antagonist1, a Menkes/Wilson disease-related copper transporter, is required for ethylene signaling in *Arabidopsis*. *Cell*, **97**:383-393.
- Hopp, T.P. and Woods, K.R. (1981) Prediction of protein antigenic sites from amino acid sequences. *Proc.Natl.Acad.Sci.USA*, **78**:3834.
- Houwen, R., Dijkstra, M., Kuipers, F., Smit, E.P., Havinga, R. and Vonk, R.J. (1990) Two pathways for biliary copper excretion in the rat: The role of glutathione. *Biochem.Pharmacol.*, **39**:1039-1044.
- Hultgren, B.D., Stevens, J.B. and Hardy, R.M. (1986) Inherited, chronic, progressive hepatic degeneration in Bedlington Terriers with increased liver copper concentrations: Clinical and pathologic observations and comparison with other copper-associated liver diseases. *Am.J.Vet.Res.*, **47**:365-377.
- Hung, I.H., Suzuki, M., Yamaguchi, Y., Yuan, D.S., Klausner, R.D. and Gitlin, J.D. (1997) Biochemical characterization of the Wilson Disease protein and functional expression in the yeast *Saccharomyces cerevisiae*. *J.Biol.Chem.*, **272**:21461-21466.
- Iida, M., Terada, K., Sambongi, Y., Wakabayashi, T., Miuna, M., Koyama, K., Futai, M., *et al.* (1998) Analysis of functional domains of Wilson disease protein (ATP7B) in *Saccharomyces cerevisiae*. *FEBS Lett.*, **428**:281-285.
- Jensen, L.T., Howard, W.R., Strain, J.J., Winge, D.R. and Culotta, V.C. (1996) Enhanced effectiveness of copper ion buffering by *CUP1* metallothionein compared to *CRS5* metallothionein in *Saccharomyces cerevisiae*. *J.Biol.Chem.*, **271**:18514-18519.
- Jensen, P.Y, Bonander, N., Moller, L.B. and Farver, O. (1999a) Cooperative binding of copper(I) to the metal binding domains in Menkes disease protein. *Biochim.Biophys.Acta*, **1434**:103-113.
- Jensen, P.Y., Bonander, N., Horn, N., Tumer, Z. and Farver, O. (1999b) Expression, purification, and copper-binding studies of the first metal-binding domain of Menkes protein. *Eur.J.Biochem.*, **264**:890-896.

Kaiser, C., Michaelis, S. and Mitchell, A. (1994) *Methods in yeast genetics: A Cold Spring Harbor Laboratory course manual*. Cold Spring Harbor Laboratory Press, Cold Spring Harbor, New York. pp. 1-234.

Karin, M., Najarian, R., Haslinger, A., Valenzuela, P., Welch, J. and Fogel, S. (1984) Primary structure and transcription of an amplified genetic locus: the *CUP1* locus of yeast. *Proc.Natl.Acad.Sci.USA*, **81**:337-341.

Kelly, E.J. and Palmiter, R.D. (1996) A murine model of Menkes disease reveals a physiologic function of metallothionein. *Nat.Genet.*, **13**:219-222.

Klein, D., Lichmannegger, J., Heinzmann, U., Muller-Hocker, J., Michealson, S. and Summer, K.H. (1998) Association of copper to metallothionein in hepatic lysosomes of Long-Evans cinnamon (LEC) rats during the development of hepatitis. *Eur.J.Clin.Invest.*, **28**:302-310.

Klomp, L.W.J, Lin, S., Yuan, D.S., Klausner, R.D., Culotta, V.C. and Gitlin, J.D. (1997) Identification and functional expression of HAH1, a novel human gene involved in copper homeostasis. *J.Biol.Chem.*, **272**:9221-9226.

Knight, S.A.B., Labbe, S., Kwon, L.F., Kosman, D.J. and Thiele, D.J. (1996) A widespread transposable element masks expression of a yeast copper transport gene. *Genes Dev.*, **10**:1917-1929.

Kornfield, S. (1992) Structure and function of the mannose-6-phosphate/insulin-like growth factor II receptors. *Ann.Rev.Biochem.*, **61**:307-330.

La Fontaine, S., Firth, S.D., Camakaris, J., Englezou, A., Theophilos, M.B., Petris, M.J., Howie, M., *et al.* (1998) Correction of the copper transport defect of Menkes patient fibroblasts by expression of the Menkes and Wilson ATPase. *J.Biol.Chem.*, **273**:31375-31380.

La Fontaine, S., Firth, S.D., Lockhart, P.L., Brooks, H., Camakaris, J. and Mercer, J.F.B. (1999) Intracellular localization and loss of copper responsiveness of Mnk, the murine homologue of the Menkes protein, in cells from blotchy (*Mo<sup>blo</sup>*) and brindled (*Mo<sup>Br</sup>*) mouse mutants. *Hum.Mol.Genet.*, **8**:1069-1075.

Labbe, S., Zhu, Z. and Thiele, D.J. (1999) Copper-specific transcriptional repression of yeast genes encoding critical components in the copper transport pathway. *J.Biol.Chem.*, **272**:15951-15958.

Laemmli, U.K. (1970) Cleavage of structural proteins during the assembly of the head of bacteriophage T4. *Nature*, **227**:680-685.

- Larin, D., Mekios, C., Das, K., Ross, B., Yang, A.S. and Gilliam, T.C. (1999) Characterization of the interaction between the Wilson and Menkes disease proteins and the cytoplasmic copper chaperone, HAH1p. *J.Biol.Chem.*, **274**:28497-28504.
- Lin, S., Pufahl, R.A., Dancis, A., O'Halloran, T.V. and Culotta, V.C. (1997) A role for the *Saccharomyces cerevisiae* *ATX1* gene in copper trafficking and iron transport. *J.Biol.Chem.*, **272**:9215-9220.
- Linder, M.C., Wooten, L., Cerveza, P., Cotton, S., Shulze, R. and Lomeli, N. (1998) Copper transport. *Am.J.Clin.Nutr.*, **67**:965S-971S.
- Loudianos, G., Dessi, V., Lovicu, M., Angius, A., Nurchi, A., Sturniolo, G.C., Marcellini, M., *et al.* (1998) Further delineation of the molecular pathology of Wilson disease in the Mediterranean population. *Hum.Mutat.*, **12**:89-94.
- Lutsenko, S., Petrukhin, K., Cooper, M.J., Gilliam, C.T. and Kaplan, J.H. (1997) N-terminal domains of human copper-transporting adenosine triphosphatases (the Wilson and Menkes Disease proteins) bind copper selectively *in vivo* and *in vitro* with stoichiometry of one copper per metal-binding repeat. *J.Biol.Chem.*, **272**:18939-18944.
- Lutsenko, S. and Cooper, M.J. (1998) Localization of the Wilson disease protein product to the mitochondria. *Proc.Natl.Acad.Sci.U.S.A.*, **95**: 6004-6009.
- MacLennan, D.H., Clarke, D.M., Loo, T.W. and Skerjanc, I.S. (1992) Site-directed mutagenesis of the Ca<sup>2+</sup>-ATPase of sarcoplasmic reticulum. *Acta.Physiol.Scand.*, **146**:141-150.
- MacLennan, D.H., Rice, W.J. and Green, N.M. (1997) The mechanism of Ca<sup>2+</sup> transport by Sarco(Endo)plasmic reticulum Ca<sup>2+</sup>-ATPases. *J.Biol.Chem.*, **272**:28815-28818.
- Mallet, W.G. and Maxfield, F.R. (1999) Chimeric forms of Furin and TGN38 are transported from the plasma membrane to the trans-Golgi network via distinct endosomal pathways. *J.Cell Biol.*, **146**:345-359.
- Martins, L.J., Jensen, L.T., Simons, J.R., Keller, G.L. and Winge, D.R. (1998) Metalloregulation of *FRE1* and *FRE2* homolog in *Saccharomyces cerevisiae*. *J.Biol.Chem.*, **273**:23716-23721.
- McArdle, H.J., Gross, S.M., Creaser, I., Sargeson, A.M. and Danks, D.M. (1989) Effect of chelators on copper metabolism and copper pools in mouse hepatocytes. *Am.J.Physiol.*, **256**:G667-G672.
- McArdle, H.J., Gross, S.M. and Danks, D.M. (1988) Uptake of copper by mouse hepatocytes. *J.Cell.Physiol.*, **136**:373-378.

McArdle, H.J., Mercer, J.F.B., Sargeson, A.M. and Danks, D.M. (1990) Effects of cellular copper content on copper uptake and mouse metallothionein and ceruloplasmin mRNA levels in mouse hepatocytes. *J.Nutr.*, **120**:1370-1375.

McQuaid, A., Lamand, M. and Mason, J. (1992) The interaction of penicillamine with copper *in vivo* and the effect of hepatic metallothionein levels and copper/zinc distribution: the implications for Wilsons disease and arthritis therapy. *J.Lab.Clin.Med.*, **119**:744-750.

Mercer, J.F.B. (1998) Menkes syndrome and animal models. *Am.J.Clin.Nutr.*, **67**:1022S-1028S.

Mercer, J.F.B., Livingstone, J., Hall, B., Paynter, J.A., Begy, C., Chandrasekharappa, S., Lockhart, P., *et al.* (1993) Isolation of a partial candidate gene for Menkes disease by positional cloning. *Nat.Genet.*, **3**:20-25.

Mullock, B.M., Bright, N.A., Fearon, C.W., Gray, S.R. and Luzio, J.P. (1998) Fusion of the lysosomes with late endosomes produces a hybrid organelle of intermediate density and is NSF dependent. *J.Cell Biol.*, **140**:591-601.

Murata, Y., Yamakawa, E., Iisuka, T., Kodama, H., Abe, T., Seki, Y. and Kodama, M. (1995) Failure of copper incorporation into ceruloplasmin in the Golgi apparatus of LEC rat hepatocytes. *Biochem.Biophys.Res.Commun.*, **209**:349-355.

Nakamura, K., Endo, F., Ueno, T., Awata, H., Tanoue, A. and Matsuda, I. (1995) Excess copper and ceruloplasmin biosynthesis in long-term cultured hepatocytes from Long-Evans cinnamon (LEC) rats, a model of Wilson disease. *J.Biol.Chem.*, **270**:7656-7660.

Nanji, M.S., Nguyen, V.T.T., Kawasoe, J.H., Inui, K., Endo, F., Nakjima, T., Anezaki, T., *et al.* (1997) Haplotype and mutation analysis in Japanese patients with Wilson disease. *Am.J.Hum.Genet.*, **60**:1423-1429.

Nartey, N.O., Frei, J.V. and Cherian, M.G. (1987) Hepatic copper and metallothionein distribution in Wilson disease (hepatolenticular degeneration). *Lab.Invest.*, **57**:397-401.

Ooi, C.H., Rabinovich, E., Dancis, A., Bonifacino, J.S. and Klausner, R.D. (1996) Copper-dependent degradation of the *Saccharomyces cerevisiae* plasma membrane copper transporter Ctr1p in the apparent absence of endocytosis. *EMBO J.*, **15**:3515-3523.

Owen, C.A. and Ludwig, J. (1982) Inherited copper toxicosis in bedlington terriers. *Am.J.Pathol.*, **106**:432-434.

Palmiter, R.D. (1998) The elusive function of metallothioneins. *Proc.Natl.Acad.Sci.USA*, **95**:8428-8430.

Payne, A.S. and Gitlin, J.D. (1998a) Functional expression of the Menkes disease protein reveals common biochemical mechanisms among the copper-transporting P-type ATPases. *J.Biol.Chem.*, **273**:3765-3770.

Payne, A.S., Kelly, E.J. and Gitlin, J.D. (1998b) Functional expression of the Wilson disease protein reveals mislocalization and impaired copper-dependent trafficking of the common H1069Q mutation. *Proc.Natl.Acad.Sci.USA*, **95**:10854-10859.

Pena, M.M.O., Koch, K.A. and Thiele, D.J. (1998) Dynamic regulation of copper uptake and detoxification genes in *Saccharomyces cerevisiae*. *Mol.Cell.Biol.*, **18**:2514-2523.

Percival, S.S. and Harris, E.D. (1990) Copper transport from ceruloplasmin: characterization of the cellular uptake mechanism. *Am.J.Physiol.*, **258**:C140-C146.

Petris, M.J., Camakaris, J., Greenough, M., LaFontaine, S. and Mercer, J.F.B. (1998) A C-terminal di-leucine is required for localization of the Menkes protein in the trans-Golgi network. *Hum.Mol.Genet.*, **7**:2063-2071.

Petris, M.J., Mercer, J.F.B., Culvenor, J.G., Lockhart, P., Gleeson, P.A. and Camakaris, J. (1996) Ligand-regulated transport of the Menkes copper P-type ATPase efflux pump from the Golgi apparatus to the plasma membrane: a novel mechanism of regulated trafficking. *EMBO J.*, **15**:6084-6095.

Petrukhin, K.E., Lutsenko, S., Chernov, I., Ross, B.M., Kaplan, J.H. and Gilliam, T.C. (1994) Characterization of the Wilson disease gene encoding a P-type copper transporting ATPase: genomic organisation, alternative splicing, and structure/function predictions. *Hum.Mol.Genet.*, **3**:1647-1656.

Pinner, E., Gruenheid, S., Raymond, M. and Gros, P. (1997) Functional complementation of the yeast divalent cation transporter family SMF by NRAMP2, a member of the mammalian natural resistance-associated macrophage protein family. *J.Biol.Chem.*, **272**:28933-28988.

Portnoy, M.E., Rosenzweig, A.C., Rae, T., Huffman, D.L., O'Halloran, T.V. and Culotta, V.C. (1999) Structure-function analysis of the ATX1 metallochaperone. *J.Biol.Chem.*, **274**:15041-15045.

Pufahl, R.A., Singer, C.P., Peariso, K.L., Lin, S.J, Schmidt, P.J., Fahmi, C.J., Culotta, V.C., *et al.* (1997) Metal ion chaperone function of the soluble Cu(I) receptor Atx1. *Science*, **278**:853-856.

Radisky, D.C., Babcock, M.C. and Kaplan, J. (1999) The yeast frataxin homologue mediates mitochondrial iron efflux. Evidence for a mitochondrial iron cycle. *J.Biol.Chem.*, **274**:4497-4499.

- Radtke, F., Heuchel, R., Georgiev, O., Hergersberg, M., Gariglio, M., Dembic, C. and Schaffner, W. (1993) Cloned transcription factor MTF-1 activates the mouse metallothionein I promoter. *EMBO J.*, **12**:1355-1362.
- Rae, T.D., Schmidt, P.J., Pufahl, R.A., Culotta, V.C. and O'Halloran, T.V. (1999) Undetectable intracellular free copper: the requirement of a copper chaperone for superoxide dismutase. *Science*, **284**:805-808.
- Rosenzweig, A.C., Huffman, D.L., Hou, M.Y., Wernimont, A.K., Pufahl, R.A. and O'Halloran, T.V. (1999) Crystal structure of the Atx1 metallochaperone protein at 1.02 Å resolution. *Structure Fold.Des.*, **7**:605-617.
- Rui, M. and Suzuki, K.T. (1997) Copper in plasma reflects its status and subsequent toxicity in the liver of LEC rats. *Res. Commun.Chem.Pathol.Pharmacol.*, **98**:335-346.
- Sato, M. and Gitlin, J.D. (1991) Mechanisms of copper incorporation during the biosynthesis of human ceruloplasmin. *J.Biol.Chem.*, **266**:5128-5134.
- Schaefer, M., Hopkins, R.G., Failla, M.L. and Gitlin, J.D. (1999a) Hepatocyte-specific localization and copper-dependent trafficking of the Wilson disease protein in the liver. *Am.J.Physiol.*, **276**:G639-G646.
- Schaefer, M., Roelofsen, H., Wolters, H., Hofmann, W.J., Muller, M., Kuipers, F., Stremmel, W., *et al.* (1999b) Localization of the Wilson Disease Protein in Human Liver. *Gastroenterology*, **117**:1380-1385.
- Schena, M., Picard, D. and Yamamoto, K.R. (1991) Vectors for constitutive and inducible gene expression in yeast. *Methods Enzymol.*, **194**:389-398.
- Schilsky, M.L., Stockert, R.J., Kesner, A., Gorla, G.R., Gagliardi, G.S., Terada, K., Miura, N., *et al.* (1998) Copper resistant human hepatoblastoma mutant cell lines without metallothionein induction overexpress ATP7B. *Hepatology*, **28**:1347-1356.
- Schilsky, M.L., Stockert, R.J. and Sternlieb, I. (1994) Pleiotropic effect of LEC mutation: a rodent model of Wilson's disease. *Am.J.Physiol.*, **266**:G907-G913.
- Schmitt, R.C., Darwish, H.M., Cheney, J.C. and Ettinger, M.J. (1983) Copper transport kinetics by isolated rat hepatocytes. *Am.J.Physiol.*, **244**:G183-G191.
- Shah, A.B., Chernov, I., Zhang, H.T., Ross, B.M., Das, K., Lutsenko, S., Parano, E., *et al.* (1997) Identification and analysis of mutations in the Wilson disease gene (ATP7B): population frequencies, genotype-phenotype correlation, and functional analyses. *Am.J.Hum.Genet.*, **61**:317-328.

- Skou, J.C. and Esmann, M. (1992) The Na/K-ATPase. *J.Bioenerg.Biomembr.*, **24**:249-261.
- Solioz, M. (1998) Copper homeostasis by CPx-type ATPases: The new subclass of heavy metal P-type ATPases. In Bittar, E.E. and Anderson, J.P. (eds.), *Advances in Molecular and Cell Biology*. JAI Press, London. p. 167-203.
- Solioz, M. and Camakaris, J. (1997) Acylphosphate formation by the Menkes copper ATPase. *FEBS Lett.*, **412**:165-168.
- Solioz, M. and Odermatt, A. (1995) Copper and silver transport by CopB-ATPase in membrane vesicles of *Enterococcus hirae*. *J.Biol.Chem.*, **270**:1-5.
- Solioz, M. and Vulpe, C. (1996) CPx-type ATPases: a class of P-type ATPases that pump heavy metals. *Trends Biochem.Sci.*, **21**:237-241.
- Stearman, R., Yuan, D.S., Yamaguchi-Iwai, Y., Klausner, R.D. and Dancis, A. (1996) A permease-oxidase complex involved in high affinity iron uptake in yeast. *Science*, **271**:1552-1557.
- Stockert, R.J., Grushoff, P.S., Morell, A.G., Bentley, G.E., O'Brien, H.A., Scheinberg, I.H. and Sternleib, I. (1986) Transport and intracellular distribution of copper in the human hepatoblastoma cell line, HepG2. *Hepatology*, **6**:60-64.
- Stokes, D.L, Taylor, W.R. and Green, N.M. (1994) Structure, membrane topology, and helix packing of P-type ion pumps. *FEBS Lett.*, **346**:32-38.
- Strausak, D., La Fontaine, S., Hill, J., Firth, S.D., Lockhart, P.J. and Mercer, J.F. (1999) The role of GMXCXXC metal binding sites in the copper-induced redistribution of the Menkes protein. *J.Biol.Chem.*, **274**:11170-11177.
- Strautnieks, S.S., Bull, L.N., Knisely, A.S., Kocoshis, S.A., Dahl, N., Arnell, H., Sokal, E., *et al.* (1998) A gene encoding a liver-specific ABC transporter is mutated in progressive familial intrahepatic cholestasis. *Nat.Genet.*, **20**:233-238.
- Sugawara, N., Lai, Y., Yuasa, M., Dhar, S.K. and Arizono, K. (1999) Biliary excretion of copper, manganese, and horseradish peroxidase in Eisai hyperbilirubinemic mutant rats (EHBRs) with defective biliary excretion of glutathione. *Biol.Trace Elem.Res.*, **55**:181-189.
- Sugawara, N., Lai, Y.R., Arizono, K. and Ariyoshi, T. (1996) Biliary excretion of exogenous cadmium, and endogenous copper and zinc in the Eisai hyperbilirubinemic (EHB) rat with a near absence of biliary glutathione. *Toxicology*, **112**:87-94.

- Suzuki, K.T., Kanno, S., Misawa, S. and Aoki, Y. (1995) Copper metabolism leading to and following acute hepatitis in LEC rats. *Toxicology*, **97**:81-92.
- Suzuki, K.T., Shiobara, Y., Tachibana, A., Ogra, Y. and Matsumoto, K. (1999) Copper increases in both plasma and red blood cells at the onset of acute hepatitis in LEC rats. *Res. Commun. Chem. Pathol. Pharmacol.*, **103**:189-194.
- Tamai, K.T., Gralla, E.B., Ellerby, L.M., Valentine, J.S. and Thiele, D.J. (1993) Yeast and mammalian metallothioneins functionally substitute for yeast copper-zinc superoxide dismutase. *Proc. Natl. Acad. Sci. USA*, **90**:8013-8017.
- Tanzi, R.E., Petrukhin, K.E., Chernov, I., Pellequer, J.L., Wasco, W., Ross, B., Romano, D.M., *et al.* (1993) The Wilson disease gene is a copper transporting ATPase with homology to the Menkes disease gene. *Nat. Genet.*, **5**:344-350.
- Teem, J.L., Berger, H.A., Ostedgaard, L.S., Rich, D.P., Tsui, L.C. and Welsh, M.J. (1993) Identification of revertants for the cystic fibrosis  $\Delta F508$  mutation using STE6-CFTR chimeras in yeast. *Cell*, **73**:335-346.
- Terada, K., Aiba, N., Yang, X.L., Iida, M., Nakai, M., Miura, N. and Sugiyama, T. (1999) Biliary excretion of copper in LEC rat after introduction of copper transporting P-type ATPase, ATP7B. *FEBS Lett.*, **448**:53-56.
- Terada, K., Nakako, T., Yang, X.L., Iida, M., Aiba, N., Minamiya, Y., Nakai, M., *et al.* (1998) Restoration of holoceruloplasmin synthesis in LEC rat after infusion of recombinant adenovirus bearing WND cDNA. *J. Biol. Chem.*, **273**:1815-1820.
- Theophilos, M.B., Cox, D.W. and Mercer, J.F. (1996) The toxic milk mouse is a murine model of Wilson Disease. *Am. J. Hum. Genet.*, **5**:1619-1624.
- Thiele, D.J. (1988) *ACE1* regulates expression of the *Saccharomyces cerevisiae* metallothionein gene. *Mol. Cell. Biol.*, **8**:2745-2752.
- Thomas, G.R., Forbes, J.R., Roberts, E.A., Walshe, J.M. and Cox, D.W. (1994) The Wilson disease gene: the spectrum of mutations and their consequences. *Nat. Genet.*, **9**:210-217.
- Towbin, H., Staehelin, T. and Gordon, J. (1979) Electrophoretic transfer of proteins from polyacrylamide gels to nitrocellulose sheets, procedures and some applications. *Proc. Natl. Acad. Sci. USA*, **76**:4350-4354.
- Tumer, Z. and Horn, N. (1999) Molecular Genetics of Menkes disease. In Sarkar, B. (ed.), *Metals and Genetics*. Plenum Publishers, New York. p. 279-290.

Uauy, R., Olivares, M. and Gonzalez, M. (1998) Essentiality of copper in humans. *Am.J.Clin.Nutr.*, **67**:952S-959S.

van de Sluis, B.J., Breen, M., Nanji, M., van Wolferen, M., de Jong, P., Binns, M.M., Pearson, P.L., *et al.* (1999) Genetic mapping of the copper toxicosis locus in Bedlington terriers to dog chromosome 10, in a region syntenic to human chromosome region 2p13-p16. *Hum.Mol.Genet.*, **8**:501-507.

Vargas, E.J., Shoho, A.R. and Linder, M.C. (1994) Copper transport in the Nagase analbuminemic rat. *Am.J.Physiol.*, **267**:G259-G256.

Vaux, D.J., Watt, F., Grime, G.W. and Takacs, J. (1985) Hepatic copper distribution in primary biliary cirrhosis shown by the scanning proton microprobe. *J.Clin.Pathol.*, **38**:653-658.

Vilsen, B., Andersen, J.P., Clarke, D.M. and MacLennan, D.H. (1989) Functional consequences of proline mutations in the cytoplasmic and transmembrane sectors of Ca<sup>2+</sup>-ATPase of sarcoplasmic reticulum. *J.Biol.Chem.*, **264**:21024-21030.

Voskoboinik, I., Brooks, H., Smith, S., Shen, P. and Camakaris, J. (1998) ATP-dependent copper transport by the Menkes protein in membrane vesicles from cultured Chinese hamster ovary cells. *FEBS Lett.*, **435**:178-182.

Voskoboinik, I., Strausak, D., Greenough, M., Brooks, H., Petris, M., Suzanne, Smith., Mercer, J.F.B, *et al.* (1999) Functional analysis of the N-terminal CXXC metal-binding motifs in the human Menkes copper-transporting P-type ATPase expressed in cultured mammalian cells. *J.Biol.Chem.*, **274**:22008-22012.

Vulpe, C., Levinson, B., Whitney, S., Packman, S. and Gitschier, J. (1993) Isolation of a candidate gene for Menkes disease and evidence that it encodes a copper-transporting ATPase. *Nat.Genet.*, **3**:7-13.

Waldenstrom, E., Lagervist, A., Dahlman, T., Westermarck, K. and Landegren, U. (1996) Efficient detection of mutations in Wilson disease by manifold sequencing. *Genomics*. **37**:303-309

Wapnir, R.A. (1998) Copper absorption and bioavailability. *Am.J.Clin.Nutr.*, **67**:1054S-1060S.

Wei, M.L., Bonzelius, F., Scully, R.M., Kelly, R.B. and Herman, G.A. (1998) GLUT4 and transferrin receptor are differentially sorted along the endocytic pathway in CHO cells. *J.Cell Biol.*, **140**:565-575.

Weiner, A.L. and Cousins, R.J. (1980) Copper accumulation and metabolism in primary monolayer cultures of rat liver parenchymal cells. *Biochim.Biophys.Acta*, **629**:113-125.

Westin, G. and Schaffner, W. (1988) A zinc-responsive factor interacts with a metal-regulated enhancer element (MRE) of the mouse metallothionein-I gene. *EMBO J.*, **7**:3763-3770.

Wu, J., Forbes, J.R., Shiene-Chen, H. and Cox, D.W. (1994) The LEC rat has a deletion in the copper transporting ATPase gene homologous to the Wilson disease gene. *Nat.Genet.*, **7**:541-545.

Wyler-Duda, P. and Solioz, M. (1996) Phosphoenzyme formation by purified, reconstituted copper ATPase of *Enterococcus hirae*. *FEBS Lett.*, **399**:143-146.

Yamada, S. and Ikemoto, N. (1980) Reaction mechanism of calcium-ATPase of Sarcoplasmic Reticulum. Substrates for phosphorylation reaction and back reaction, and further resolution of phosphorylated intermediates. *J.Biol.Chem.*, **255**:3108-3119.

Yamada, T., Agui, T., Suzuki, Y., Sato, M. and Matsumoto, K. (1993a) Inhibition of copper incorporation into ceruloplasmin leads to the deficiency in serum ceruloplasmin activity in Long-Evans cinnamon mutant rat. *J.Biol.Chem.*, **268**:8965-8971.

Yamada, T., Kim, J-K., Suzuki, Y., Agui, T. and Matsumoto, K. (1993b) Reduced efficiency of copper transport from cytosolic to noncytosolic fractions in LEC mutant rat. *Res.Commun.Chem.Pathol.Pharmacol.*, **81**:243-246.

Yamaguchi-Iwai, Y., Dancis, A. and Klausner, R.D. (1995) AFT1: a mediator of iron regulated transcriptional control in *Saccharomyces cerevisiae*. *EMBO J.*, **14**:1231-1239.

Yamaguchi-Iwai, Y., Stearman, R., Dancis, A. and Klausner, R.D. (1996) Iron-regulated DNA binding by the AFT1 protein controls the iron regulon in yeast. *EMBO J.*, **15**:3377-3384.

Yamaguchi-Iwai, Y., Serpe, M., Haile, D., Yang, W., Kosman, D.J., Klausner, R.J. and Dancis, A. (1997) Homeostatic regulation of copper uptake in yeast via direct binding of MAC1 protein to upstream regulatory sequences of *FRE1* and *CTR1*. *J.Biol.Chem.*, **272**:17711-17718.

Yoshida, K. (1999) Clinicopathological and molecular genetic features of hereditary ceruloplasmin deficiency (aceruloplasminemia). In Sarkar, B. (ed.), *Metals in Genetics*. Plenum Publishers, New York. p. 301-311.

Yoshimizu, T., Omote, H., Wakabayashi, T., Sambongi, Y. and Futai, M. (1998) Essential Cys-Pro-Cys motif of *Caenorhabditis elegans* copper transport ATPase. *Biosci.Biotechnol.Biochem.*, **62**:1258-1260.

Yuan, D.S., Dancis, A. and Klausner, R.D. (1997) Restriction of copper export in *Saccharomyces cerevisiae* to a late Golgi or post-Golgi compartment in the secretory pathway. *J.Biol.Chem.*, **272**:25787-25793.

Yuan, D.S., Stearman, R., Dancis, A., Dunn, T., Beeler, T. and Klausner, R.D. (1995) The Menkes/Wilson disease gene homologue in yeast provides copper to a ceruloplasmin-like oxidase required for iron uptake. *Proc.Natl.Acad.Sci.USA*, **92**:2632-2636.

Zhou, B. and Gitschier, J. (1997) hCTR1: a human gene for copper uptake identified by complementation in yeast. *Proc.Natl.Acad.Sci.USA*, **94**:7481-7486.

Zubenko, G.S., Mitchell, A.P. and Jones, E.W. (1980) Mapping of the proteinase b structural gene *PRB1* in *Saccharomyces cerevisiae* and identification of nonsense alleles within the locus. *Genetics*, **96**:137-146.

**APPENDIX.****Table A-1: Primers used for amplification of *ATP7B* cDNA.**

<b>DNA fragment amplified (nucleotide)</b>	<b>Primer Sequence</b>
<b>1-975</b>	5'-TATCGGATCCATGCCTGAGCAGGAGAGACAG-3' 5'-ACTGGGATCCTCAAACCTTAAAATTCCCAGGTGG-3'
<b>792-1946</b>	5'-GGAATGCATTGTAAGTCTTGGCG-3' 5'-ACTTGTCGACTCACTGCTTTATTCCATTTTG-3'
<b>1615-2847</b>	5'-CCCCTCGAGATAGCTCAGTTC-3' 5'-AACACCAAATCGATAAAACC-3'
<b>2800-3967</b>	5'-TGACGTTGGTGGTATGGATTG-3' 5'-ATGCGTATCCTTCGGACAGT-3'
<b>3922-4395+52</b>	5'-TGGCTAGCATTACCTTTCCA-3' 5'-GCTTGTGGTGAGTGGAGG-3'

**Table A-2: Primers used for amplification of *ATP7B* fusion protein DNA constructs.**

<b>Polypeptide</b>	<b>Primer Pairs</b>
<b>Pept1</b>	5'-ATCGCATATGAGCAACCAAGAGGCCGTCATC-3' 5'-ATCGGGATCCTCTCAGTTGGAGGGTGACCAC-3'
<b>Pept2</b>	5'-ATCGCATATGGAGAACAACAACTGCCCAAGTA-3' 5'-ATCGGGATTTCGGCAATCAGAGTGGTACTGCA-3'
<b>Pept3</b>	5'-ATCGCATATGTATAAGAAGCCTGACCTGGAG-3' 5'-ATCGGGATTCTCAGATGTACTGCTCCTCATC-3'

**Table A-3: Mutagenic primers used to create WD mutant *ATP7B* cDNA constructs.**

<b>WD Mutation</b>	<b>Mutagenic primers</b>
<b>D765N</b>	5'-CCTGTGACATTCTTCAACACGCCCCCATG-3' 5'-CATGGGGGGCGTGTGTTGAAGAATGTCACAGG-3'
<b>M769V</b>	5'-CGACACGCCCCCGTGCTCTTTGTGTTC-3' 5'-GAACACAAAGAGCACGGGGGGCGTGTCG-3'
<b>L776V</b>	5'-GTGTTCAATTGCCGTGGGCGGTGGCTG-3' 5'-CAGCCACCGGCCACGGCAATGAACAC-3'
<b>R778Q</b>	5'-CATTGCCCTGGGCCAGTGGCTGGAAC-3' 5'-GTTCCAGCCACTGGCCCAGGGCAATG-3'
<b>R778L</b>	5'-CATTGCCCTGGGCCTGTGGCTGGAAC-3' 5'-GTTCCAGCCACAGGCCACAGGGCAATG-3'
<b>G943S</b>	5'-GGTATGGATTGTAATCAGTTTTATCGATTTTGGTG-3' 5'-CACCAAAATCGATAAAACTGATTACAATCCATACC-3'
<b>T977M</b>	5'-CCAGACGTCCATCATGGTGCTGTGCATTG-3' 5'-CAATGCACAGCACCATGATGGACGTCTGG-3'
<b>P992L</b>	5'-GCTTGGCCACGCTCACGGCTGTCATG-3' 5'-CATGACAGCCGTGAGCGTGGCCAGC-3'
<b>V995A</b>	5'-CGCCCACGGCTGCCATGGTGGGCACC-3' 5'-GGTGCCCACCATGGCAGCCGTGGGCG-3'
<b>CPC/S</b>	5'-GCTGTGCATTGCCTCCCCCTCCTCCCTGGGGC-3' 5'-GCCCCAGGGAGGAGGGGGAGGCAATGCACAGC-3'

**Table A-4: Mutagenic primers used to create *ATP7B* copper-binding domain cDNA constructs.**

Mutation	Mutagenic primers
Cu1C/S	5'-CTTGGGCATGACTAGCCAGTCAAGTGTGAAGTCCATTG-3' 5'-CAATGGACTTCACACTTGACTGGCTAGTCATGCCCAAG-3'
Cu2C/S	5'-GGAGGGCATGACCAGCCAGTCCAGTGTGTCAGCTCC-3' 5'-GGAGCTGACACTGGACTGGCTGGTTCATGCCCTCC-3'
Cu3C/S	5'-GATGGAATGCATAGTAAGTCTAGCGTCTTGAATAATGAAG-3' 5'-CTTCAATATTCAAGACGCTAGACTTACTATGCATTCCATC-3'
Cu4C/S	5'-GCCGGCATGACCAGTGCATCCAGTGTCCATTCC-3' 5'-GGAATGGACACTGGATGCACTGGTTCATGCCGGC-3'
Cu5C/S	5'-CAAAGGCATGACCAGTGCATCCAGTGTGTCTAACATAG-3' 5'-CTATGTTAGACACACTGGATGCACTGGTTCATGCCTTTG-3'
Cu6C/S	5'-CAGGGATGACCAGCGCGTCCAGTGTCCACAAC-3' 5'-GTTGTGGACACTGGACGCGCTGGTTCATCCCAG-3'

**Table A-5: Primers used for construction of *ATP7B* deletion constructs.**

DNA fragment amplified (nucleotide)	Primer sequence
1-189	5'-TATCGGATCCATGCCTGAGCAGGAGAGACAG-3' 5'-CTCACTCGAGCCTGACTGTGCTGGTGGCCAC-3'
1797-2847	5'-ACTGCTCGAGGCCACCAGCAAAGCCCTTGTT-3' 5'-AACACCAAATCGATAAAACC-3'
1-555	5'-TATCGGATCCATGCCTGAGCAGGAGAGACAG-3' 5'-ACTGCTCGAGGATGACGGCCTCTTGGTTGCT-3'
1-888	5'-TATCGGATCCATGCCTGAGCAGGAGAGACAG-3' 5'-CATGCATCCTCGAGTACTTGGGCAGTTTTGTTCTC-3'